# Proteomic and functional deregulations in Philadelphia negative Myeloproliferative Neoplasms

Nuria Socoro Yuste

UNIVERSITÉ GRENOBLE ALPES

# THÈSE

Pour obtenir le grade de

## DOCTEUR DE L'UNIVERSITÉ GRENOBLE ALPES

Spécialité : **BIS - Biotechnologie, instrumentation, signal et imagerie pour la biologie, la médecine et l'environnement**

Arrêté ministériel : 7 août 2006

Présentée par

## « Nuria SOCORO YUSTE »

Thèse dirigée par **« Pascal MOSSUZ »**

préparée au sein du **Laboratoire TIMC-IMAG - Techniques de l'Ingénierie Médicale et de la Complexité - Informatique, Mathématiques et Applications, Grenoble – UMR 5525 CNRS** dans **l'École Doctorale Ingénierie Pour La Santé, La Cognition et L'environnement**

# « Dérégulations protéomiques et fonctionnelles des Syndromes Myéloprolifératifs Philadelphia négatifs »

Thèse soutenue publiquement le **« 17 décembre 2015 »**,
devant le jury composé de :

**Mme Isabelle PLO**
DR-INSERM, Université Paris Diderot-Paris 7 (Rapporteuse)
**Mr Wassim EL NEMER**
CR1-INSERM, Université Paris Diderot-Paris 7 (Rapporteur)
**Mr Jean-Yves CAHN**
PU-PH, Université Grenoble Alpes, CHU Grenoble (Examinateur)
**Mme Valérie UGO**
PU-PH, Université d'Angers, CHU Angers (Examinatrice)
**Mme Marie Claire DAGHER**
CR-CNRS, Université Grenoble Alpes (Examinatrice)
**Mr Pascal MOSSUZ**
PU-PH, Université Grenoble Alpes, CHU Grenoble (Directeur de thèse)

# INDEX

# ABBREVIATIONS

AML: Acute Myeloid Leukemia

CALR: Calreticulin

CML: Chronic Myeloid Leukemia

DMSO: Dimethyl Sulfoxide

EPO: Erythropoietin

EpoR: Erythropoietin receptor

ET: Essential Thrombocythemia

GDP: Guanosine diphosphate

GTP: Guanosine Triphosphate

Hb: Hemoglobin

HSC: Hematopoietic Stem Cell

HU: Hydroxyurea

IFN: Interferon

IL: Interleukin

IPA: Ingenuity Pathway Analysis

iTRAQ: Isobaric tags for relative and absolute quantitation

JAK2: Janus Kinase 2

LC: Liquid Chromatography

Lu/BCAM: Lutheran and basal cell adhesion molecule

MDS: Myelodysplastic Syndromes

MF: Myelofibrosis

MPN: Myeloproliferative Neoplasm

MS: Mass Spectrometry

Mut0: Non mutation

$m/z$: mass / charge

Ph: Philadelphia

PMF: Primary Myelofibrosis

PV: Polycythemia Vera

RBC: Red Blood Cell

ROS: Reactive Oxygen Species

SELDI: Surface-enhanced laser desorption/ionization

TOF: Time of Flight

TPO: Thrombopoietin

WB: Western Blot

WBC: White Blood Cells

WHO: World Health Organization

WT: wild type

# BACKGROUND

## MYELOPROLIFERATIVE NEOPLASMS

The myeloproliferative neoplasms (MPNs), are a group of hemopathies characterized by a clonal proliferation of hematopoietic stem cells that results in an augmentation of mature blood cells.

According to the World Health Organization (WHO), among the myeloid neoplasms we can distinguish, (1, 2):

1. Myeloproliferative Neoplasms
   - – Chronic myelogenous leukemia, (CML);
   - – Polycythemia Vera, (PV);
   - – Primary myelofibrosis, (PMF);
   - – Essential thrombocythemia, (ET);
   - – Chronic neutrophilic leukemia;
   - – Chronic eosinophilic leukemia, not otherwise specified;
   - – Mastocytosis,
   - – Unclassifiable MPNs,
2. Myeloid and lymphoid neoplasms associated with eosinophilia and abnormalities of PDGFRA, PDGFRB, or FGFR1.
3. Myelodysplastic/myeloproliferative neoplasms (MDS/MPN)
   - – Chronic myelomonocytic leukemia
   - – Atypical chronic myeloid leukemia, *BCR-ABL1*-negative
   - – Juvenile myelomonocytic leukemia
   - – Myelodysplastic/Myeloproliferative neoplasm unclassifiable
4. Myelodisplastic syndrome (MDS)

The only MPN with a specific gene abnormality is CML, which is characterized by the presence of the Philadelphia (Ph) chromosome which is a chromosomal translocation, t(9;22)(q34;q11) that fuses the *abl* gene from chromosome 9 with the *bcr* gene from chromosome 12 leading to the *BCR-ABL1* fusion gene (3, 4). The other subtypes are known as Philadelphia negative (Ph-) MPNs. The most frequent are PV (35%) and ET (40% of total MPN patients). CML represents 16% of MPN cases and PMF just 5%. The rest are rare

diseases. The global incidence of Ph- MPNs is about 3 per 100,000 people newly diagnosed with any form of MPN.

## *POLYCYTHEMIA VERA*

Polycythemia Vera is also known as the Osler-Vaquez disease in honor of the first ones to characterize it. Louis Henri Vaquez was a French physician who described for the first time a PV patient in 1892. This patient presented chronic cyanosis (congestion or ruddiness), vertigo, dyspnea, palpitations, hepatosplenomegaly and marked erythrocytosis. He thought that raised red blood cell count had to be due to an increased activation of hematopoiesis. The Osler term came out thanks to the first PV review by William Osler in 1903: "Chronic cyanosis, with polycythemia and enlarged spleen: a new clinical entity". In Osler's review, he included his own patients and other cases that had been previously reported (5, 6).

In those days, PV was defined by chronic cyanosis, polycythemia, moderate splenomegaly, weakness, constipation, headache and vertigo. Nowadays it is characterized by clonal overproduction of mature erythrocytes and, moreover variable overproduction of leukocytes and platelets. The erythroid stem cells present erythropoietin (EPO) independence and hypersensitivity. EPO independence means that these cells are capable of going on with their cell cycles without the EPO stimulation. EPO hypersensitivity is referred to as the increased reaction of myeloid stem cells to very low concentrations of this cytokine (7). Clinically, it is characterized by splenomegaly, thrombohemorrhagic complications and pruritus. The average age in patients is 60 years. Usually, survival rate is about 15 years for older patients, excepting for cases with grave thrombohemorrhagic complications such as aggressive phlebotomy where the survival average is shortened. Life-expectancy rises to 24 years in patients under 60 years old (8, 9). In addition, 5 to 15 % of patients evolve to Acute Myeloid Leukemia or to myelofibrosis (10).

### *Diagnosis*

According to the 2008 World Health Organization (1, 2), the diagnosis of PV needs the presence of both major criteria and one minor criterion or the presence of one major criterion and two minor criteria:

Major criteria

1. Hemoglobin > 18.5 g/dL in men, > 16.5 g/dL in women or other evidence of increased red cell volume. *(Hemoglobin or hematocrit > 99th percentile of method-specific reference range for age, sex, altitude of residence or hemoglobin > 17 g/dL in men, 15 g/dL in women if associated with a documented and sustained increase of at least 2 g/dL from baseline that cannot be attributed to correction of iron deficiency or elevated red cell mass >25% above mean normal predicted value).*

2. Presence of *JAK2V617F* or other functionally similar mutation such as JAK2 exon 12 mutation.

Minor criteria

1. Bone marrow biopsy showing hypercellularity for age with trilineage growth (panmyelosis) with prominent erythroid, granulocytic, and megakaryocytic proliferation.

2. Serum erythropoietin level below the reference range for normal.

3. Endogenous erythroid colony formation in vitro.

## *ESSENTIAL THROMBOCYTHEMIA*

This disease was described in 1934 by Emil Epstein and Alfred Goedel, two Australian pathologists; but it wasn't until 1960 that two reviews regrouped the first diagnostic criteria for what they named "primary hemorrhagic thrombocythemia": a history of thrombohemorrhagic events. These criteria included: splenomegaly or normal-size spleen; thrombocytosis without either erythrocytosis or leukocytosis; bone marrow panmyelosis with megakaryocytic hyperplasia without leukemic infiltration (6).

Nowadays, it is named "Essential Thrombocythemia" and it is defined as a myeloproliferative neoplasm characterized by high count of platelets in peripheral blood with tendency to thrombosis and hemorrhage. The typical clinical signs are predisposition to vascular occlusive events such as cerebrovascular, coronary or in peripheral circulation; and hemorrhages. Some patients are asymptomatic whereas others may present headaches, visual disturbances, distal paresthesia, lightheadedness, erythromelalgia, chest pain, and thrombotic or hemorrhagic problems (like hematomas, bruising, ecchymosis, epistaxis, melena or hematemesis). It is a disease that may occur at any age although the median age at diagnosis is 65-70 years. The incidence is twice higher in women (ratio 2:1 females:males)

and the prevalence is about 30/100,000. The median survival is about 20 years for older patients and 33 for younger ones (under 60). The only risks that can cause mortality in these patients are hematologic complications like arterial and venous thrombosis, platelet mediated occlusions of the microcirculation and hemorrhages. Sometimes it can evolve to myelofibrosis, acute myeloid leukemia or PV reducing patients' life expectancy (9, 11, 12).

*Diagnosis*

According to the WHO (1, 2), the diagnosis of ET must meet these four criteria:

1. Sustained platelet count ≥ 450 x $10^9$/L

2. Bone marrow biopsy specimen showing proliferation mainly of the megakaryocytic lineage with increased number of enlarged, mature megakaryocytes. No significant increase or left-shift of neutrophil granulopoiesis or erythropoiesis.

3. Not meeting WHO criteria for polycythemia vera, primary myelofibrosis, *BCR-ABL1*–positive CML, or myelodysplastic syndrome, or other myeloid neoplasm.

4. Demonstration of *JAK2 V617F* or other clonal marker, or in the absence of *JAK2 V617F*, or no evidence of reactive thrombocytosis.

## *PRIMARY MYELOFIBROSIS*

Primary myelofibrosis (PMF) is the last one of the three most important Ph- MPNs. Older terms used to name PMF were "*agnogenic myeloid metaplasia*"; "*chronic idiopathic myelofibrosis*" (used in the 2001 WHO on the classification of tumors of hematopoietic and lymphoid tissues); and "*myelofibrosis with myeloid metaplasia*". It was in 2006 when the International Working Group for Myelofibrosis Research and Treatment reached a consensus to exclusively use the term of Primary Myelofibrosis.

It was Gustav Heuck (a German surgeon) who gave the first description of PMF in 1879, under the title of "Two cases of leukemia with peculiar blood and bone marrow findings". His young patients presented massive splenomegaly, circulating nucleated red blood cells, and increased number of morphologically abnormal leukocytes. He realized that these patients differed from those described for CML because of the presence of marrow fibrosis and extensive extramedullary hematopoiesis. From that date, many other cases of PMF have been described in literature (6).

PMF is predominantly present in males and the age at diagnosis is usually over 60. Patients are characterized by the presence of anemia, high splenomegaly, leukoerythroblastosis, dacryocytosis, increased levels of serum lactate dehydrogenase (LDH), excess circulating blasts and stromal changes in the bone marrow such as collagen and reticulin fibrosis, osteosclerosis and angiogenesis. According to the Dynamic International Prognostic Scoring System for primary myelofibrosis (DIPSS-plus), risk factors measured at diagnosis include age over 65 years, hemoglobin levels under 10 g/dL, leukocyte count more than $25x10^9$/L, number of circulating blasts ≥1%, presence of constitutional symptoms, red cell transfusion need, platelet count lower than $100x10^9$/L and unfavorable karyotype (including complex karyotype or sole or two abnormalities that comprised +8, -7/7q-, i(17q), inv(3), -5/5q-, 12p-, or 11q23 rearrangement; all other cytogenetic abnormalities were considered favorable). These risk factors are used to define low (no risk factors), intermediate-1 (1 risk factor), intermediate-2 (2 or 3 risk factors), and high (4 risk factors) risk groups. Leukemic transformation risk was higher in the presence of unfavorable karyotype or platelet count under $100x10^9$/L and in intermediate and high risk groups. Overall survival in low risk patients was around 17.5 years, 7.8 for the intermediate-1 risk group, 3.6 for the intermediate-2 and 1.8 for high risk patients. In young patients (aged under 60), the overall survival rises to 20 years in low risk patients and 14 in the intermediate-1 risk group (13, 14).

Generally PMF patients have poorer prognosis than PV or ET patients. PMF is clinically indistinguishable from the fibrotic transformation of polycythemia vera or essential thrombocythemia. Some patients who are diagnosed of PMF probably are in the accelerated phase of previously unrecognized PV or ET (15).

*Diagnosis*

According to the WHO (1, 2), the diagnosis of PMF must meet the three major criteria and at least two minor criteria:

Major criteria

1. Presence of megakaryocyte proliferation and atypia, (*small to large megakaryocytes with an aberrant nuclear/cytoplasmic ratio and hyperchromatic, bulbous, or irregularly folded nuclei and dense clustering*), usually accompanied by either reticulin or collagen fibrosis, or, in the absence of significant reticulin fibrosis, the megakaryocyte changes must

be accompanied by an increased bone marrow cellularity characterized by granulocytic proliferation and often decreased erythropoiesis.

2. Not meeting WHO criteria for polycythemia vera, *BCR-ABL1*–positive chronic myelogenous leukemia, myelodysplastic syndrome, or other myeloid disorders.

3. Demonstration of *JAK2V617F* or other clonal marker (e.g. *MPLW515K/L*), or, in the absence of the above clonal markers, no evidence that bone marrow fibrosis is secondary to infection, autoimmune disorder or other chronic inflammatory condition, hairy cell leukemia or other lymphoid neoplasm, metastatic malignancy, or toxic (chronic) myelopathies.

Minor criteria

1. Leukoerythroblastosis
2. Increase in serum lactate dehydrogenase level.
3. Anemia.
4. Palpable splenomegaly

## *GENETIC COMPLEXITY OF MPNs*

Myeloproliferative neoplasms are clinical entities genetically complex. In fact, more than one mutation is usually present in these patients. Furthermore, there are not exclusive mutations for one type of MPN, but rather mutations that exclude the presence of other ones. Patients could be classified according to their genetic profile (number and description of mutations and order of appearance) to determine their diagnosis, prognostic and treatment.

The most important mutations in MPNs are grouped in four types depending on the action affected: signaling pathways, epigenetic regulation, splicing regulation and checkpoints, Figure 1.

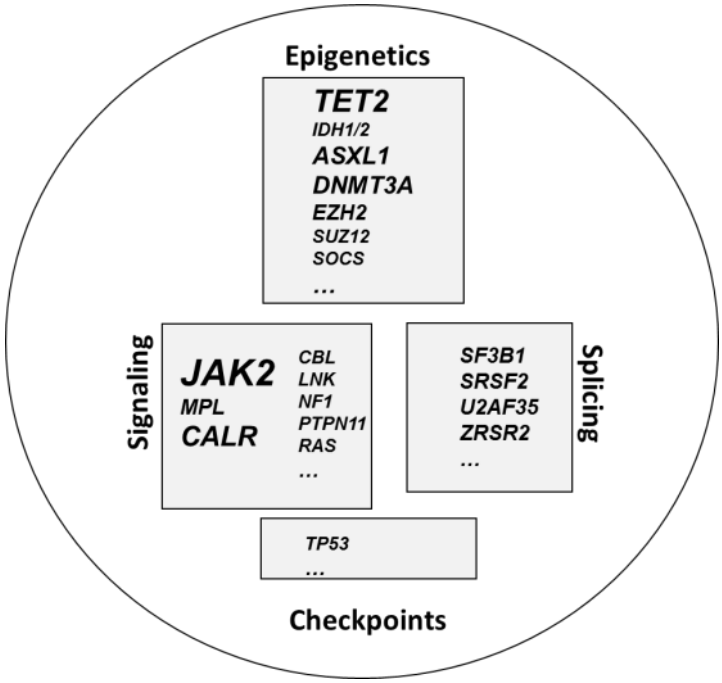


**Figure 1**. Somatic mutations in MPNs affect four major processes: Signaling, epigenetics, splicing and checkpoints.

### *Mutations implicated in signaling pathways*

JAK2 (16-20)

Mutation in *JAK2* exon 14 is the most frequent in MPNs. It is present in more than 95% of PV patients and 50 to 60% of ET and PMF patients. It consists on the nucleotide change from Guanine to Thymine at position 1849. This causes the substitution of valine by phenylalanine at codon 617 in the Janus Kinase 2 (JAK2) protein.

The JAK family is formed by 4 kinases, JAK1, 2, 3 and TYK2. They are attached to cytokine receptors. JAK2 is formed by up to seven JAK homology domains (JH1-JH7). The most important ones are the active kinase domain, JH1 and JH2, the catalytically inactive pseudokinase domain that negatively regulates JH1 (21).

In a normal cell, erythropoietin binds its receptor which activates JAK2. It phosphorylates itself and also the erythropoietin receptor what initiates a cascade of erythroid-specific signaling promoting erythroid proliferation and differentiation by activation of STATs. This cascade is controlled thanks to a negative feedback by JAK2 itself. The key role of *JAK2* in erythropoiesis is shown in *JAK2* deficient mice that died at embryonic day 12.5 with complete absence of erythropoiesis (22).

The *JAK2V617F* mutation affects to the JH2 domain. This conversion implicates an autoinhibition of JH2 domain and thus, an inhibition of the downregulation of the erythropoietin signal. Due to this mutation; *JAK2V617F* progenitor cells become erythropoietin independent and can form erythropoietin-independent erythroid colonies. It also causes cytokine-independent activation of different pathways such as JAK-STAT, PI3K, AKT, MAPK and ERK which affect to gene transcription, apoptosis, cell cycle and differentiation (Figure 2) as it was showed in Ba/F3 EpoR and Ba/F3 EpoR *JAK2V617F* murine cells (17, 19, 23) and in gamma-2A human fibrosarcoma cells (17).

Among the STATs, the STAT5 activation is compulsory for MPN establishment. Recent approaches suggest that STAT3 activation opposes thrombocytosis and promotes inflammation whereas STAT1 is associated with thrombocytosis. Conformingly, STAT1 activation has been shown to be specifically activated in ET erythroid colonies but not in PV ones (21). Chen E *et al.* (24) showed that STAT1 inhibition in stem cells promoted erythropoiesis and reduced megakaryopoiesis. Thus, STAT1 activation via JAK2 promotes ET acquisition but not PV. The mechanisms why sometimes STAT1 is phosphorylated and sometimes it is not are not yet elucidated.

In conclusion, *JAK2V617F* is directly related to MPN pathogenesis by promoting spontaneous proliferation of stem cells (15). However, the main issue remains incompletely solved: why the same mutation can lead to three different phenotypes.

On the one hand, in PV patients, its presence is associated with higher hemoglobin levels, increased granulocytes, leukocytosis, endogenous erythroid colony formation, higher spleen size, higher bone marrow cellularity and inversely to lower platelet counts. On the other hand, it is also related to leukocytosis, higher spleen size and higher levels of hemoglobin in ET subjects besides older age at diagnosis and lower platelet count. In PMF, *JAK2V617F* patients require less red cell transfusion and present higher leukocyte counts than *JAK2* wild type (25-27).

According to Alshemmari *et al.* (28), ET patients had lower *JAK2V617F* allele burden (<50% of *JAK2V617F* cells) whereas for PV patients the allele burden average was 40%. High allele burden levels are related to myelofibrotic evolution, leukocytosis and high hemoglobin levels. Low allele burden is associated with high platelet counts. Furthermore, 25% of PV patients are homozygous for *JAK2V617F* whereas ET patients are mostly heterozygous or present the wild type suggesting that higher levels of mutated *JAK2* are related to an erythroid phenotype and lower ones to a megakaryocytic phenotype. Besides

this allele-burden-dependent mechanism, the presence of other acquired somatic mutations play very probably a role in these phenotypic variations, as well as in genetic background.

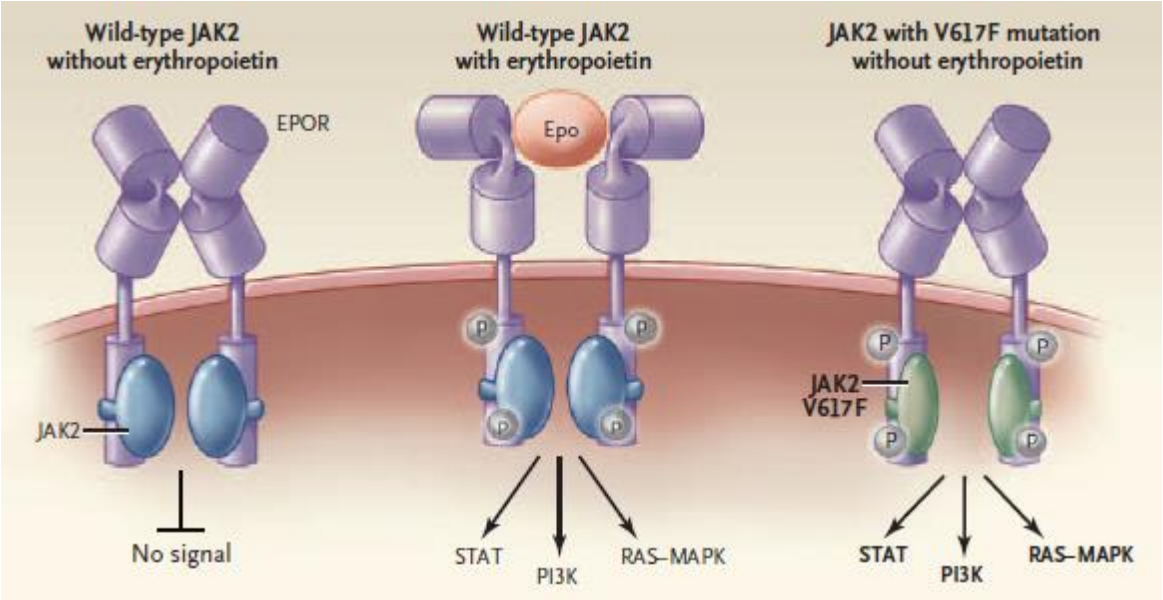


**Figure 2.** Left, wild-type JAK2 is inactivated without erythropoietin stimulation. Center, wild-type *JAK2* is phosphorylated and activated by erythropoietin action; it can then activate some pathways such as STAT, PI3K and RAS-MAPK. Right, *JAK2 V617F* is autophosphorylated in absence of EPO signal and is capable to activate the same signaling pathways as the non-mutated receptor in presence of EPO. Figure taken from Campbell *et al.*(15).

*JAK2* exon 12 mutations were identified in *JAK2V617F* negative PV patients. (Its presence is rare in ET or PMF patients). These mutations are thought to modify the JH2 structure and thus to alter its negative feedback function inducing a constitutive phosphorylation of JAK2 and STAT5 (29). These patients are characterized by erythroid myelopoiesis, lower serum erythropoietin levels, younger age at diagnosis and the possibility of progression to a secondary myelofibrosis (21, 27).

MPL mutations (9, 21, 27)

*MPL* is the Myeloproliferative Leukemia virus oncogene. It encodes for the thrombopoietin (TPO) receptor. Gain-of-function mutations have been discovered in exon 10 with the substitution of a tryptophan at codon 515 to a leucine (*MPLW515L*), lysine (*MPLW515K*), asparagine (*MPLW515N*) or alanine (*MPL W515A*). At this position, there is

a group of 5 amino acids that are responsible for the cytosolic conformation of the *MPL* protein, (transmembrane protein). This receptor possesses an amphipathic domain R/KWQFP between the transmembrane and the cytosolic domains preventing JAK2 activation in the absence of TPO. Mutations in this group of amino acids cause the spontaneous activation of the receptor, resulting in constitutive JAK-STAT activation as well as MAP-kinase ERK1, 2. This activation leads to megakaryocytic proliferation and thus thrombocytosis.

These patients are associated with older age, female sex, higher platelet count, lower hemoglobin level, splenomegaly, myelofibrosis and an increased risk of thrombosis. They are found in about 3-5% of ET patients and in 10% of PMF ones. Their presence is rare in PV. Other mutations of this exon have been reported, (*MPLW515S or MPLS505N*) but at very low frequencies.

*CALR* (30-34)

Calreticulin is a $Ca^{2+}$ binding chaperone located in the lumen of the endoplasmic reticulum (ER) that contributes to calcium homeostasis. Together with calnexin (another chaperone), and ERp57, they form the "calreticulin/calnexin cycle" responsible for the folding control of newly-synthesized proteins. When calnexin and calreticulin recognize misfolded proteins, they bind them to prevent their export to the Golgi apparatus and consequently, guaranteeing proper folding of newly synthesized glycoproteins. Calreticulin can also be found outside the ER, at the cell surface, in the cytoplasm or in extracellular compartments where it is suggested to play a role in proliferation, antigen presentation and complement activation, apoptosis and immunogenic cell death (35).

*CALR* mutations are located in exon 9 and they are present in about 15 to 30% of ET and PMF subjects. Predominantly, 80% of these mutations are classified in two groups: type 1 mutations which correspond to a 5-base-pair (bp) deletion and type 2 to 5-bp insertions. All mutations result in a novel amino acid sequence at the C-terminal. This new mutated peptide contains an important number or positively charged amino acids, whereas the native C-terminal peptide is principally negatively charged. Moreover, the new C-terminal part has lost the KDEL motif (lysine, aspartic acid, glutamic acid and leucine amino acid sequence). KDEL motif allows calreticulin to anchor to the ER. Consequently, mutant calreticulin is thought to modify its cellular location and to lose its $Ca^{2+}$binding function.

*CALR* mutations are suggested to activate the *JAK2(-)*STAT pathway in myeloid stem cells as it was suggested by Ba/F3 *CALR* cell mutants (33). Moreover, *JAK2(-)*STAT activation was shown to have the same transcriptional signature in *JAK2V617F* and mutated *CALR* peripheral blood granulocytes suggesting a common transformation (Rampal *et al.* (36)). Nonetheless, Lau *et al.* (37) argued Rampal results as theirs showed completely different signatures of STAT activation in *JAK2(+)* and *CALR(+)* ET megakaryocytes. In addition, MARIMO cell line approaches showed that *JAK2(-)*STAT activation was not activated by calreticulin (Kollman *et al*. (38)).

Generally, compared with *JAK2V617F* patients, *CALR* mutations arecorrelated with younger age, male predominance and high allele burden. They are also associated with higher platelet counts and serum erythropoietin, lower Hb and leukocyte levels and lower thrombosis risk. In addition, there is no significant difference in overall survival compared with *JAK2V617F* patients. Furthermore, phenotypical differences between both types of calreticulin mutations show that type 2 mutations are connected with younger patients and higher platelet counts whereas type 1 are linked to male sex. In these patients, there is no risk of polycythemic transformation (whereas the cumulative risk for *JAK2V617F* patients it is about 30%). In PMF, results on overall survival demonstrated differences between type 1 and type 2 mutations but are contradictory (Cabagnols *et al*. 2015, (39) vs Tefferi *et al.* 2014, (30, 40)). In addition, Cabagnols *et al.* study on 572 *JAK2(-)* MPN patients suggested that high *CALR* allele burdens and type 2 *CALR* mutations correlated with MF whereas low allele burdens with ET phenotypes.

Vannuchi *et al.* 2014 (41) showed, using immunohistochemistry labelling of bone marrow biopsy, that calreticulin expression (mutated and non-mutated) was higher in megakaryocytes than in myeloid or erythroid lineages suggesting an important role for calreticulin in platelet function. They suggested that *CALR* mutations might use the JAK-STAT signaling to contribute to the high platelet production in MPNs. This special link between *CALR* and megakaryocytes was confirmed by the study of Mondet *et al.* (42) who showed that endogenous megakaryocytic colonies (EMC) were more frequent in mutated *CALR* than in *JAK2V617F* or "triple negative" (*JAK2(-), MPL-* and *CALR(-)*) patients and among *CALR* mutated patients, type 2 induced more EMC than type 1.

*CBL* (21, 27, 43)

The casitas B-cell lymphoma family (CBL) is composed by 3 proteins: CBL, CBL-b and CBL-c. The CBL gene is located at 11q23.3 and it encodes for a protein that principally is involved in negative regulation of the receptor tyrosine kinase mediated by E3 ubiquitin ligase activity. Mutations in this gene directly affect the region that is necessary for its E3 ubiquitin ligase function. It appears to be mutated in about 6% of PMF patients and in some myeloid malignancies as juvenile monomyelocytic leukemia or chronic monomyelocytic leukemia but it is rare in PV and ET patients. It's related to myelofibrosis with poor prognosis or in AML post MPN.

*LNK* (21, 44)

This gene is located at chromosome 12 at 12q24 loci. The lymphocyte adaptor protein (LNK) is part of the SH2B family. It negatively regulates TPO-MPL and EPO receptor signaling, thus it inhibits the JAK/STAT signaling. Furthermore, it negatively regulates JAK2 thanks to its SH2 domain. These loss-of-function mutations cover codons 208 to 234 and can affect the C-terminal region; the SH2 domain or the PH domain. They seem to be involved in disease progression because they are not found in chronic states. In fact, some *LNK* mutations are found in about 13% of leukemic transformation of MPNs and in about 3 to 6% in ET and PMF subjects. A recent study by Benton *et al.* (45) showed that PV patients with mutations in this chromosome (Ch12) are more likely for myelofibrosis progression. In general, patients with this mutation are classified as poor prognosis.

*SOCS 1, 2 and 3* (21)

Suppressor of cytokine signaling (SOCS) proteins are negative regulators of JAK signaling. Loss of their activity results in an excess of signaling by cytokines. *SOCS1* gene is located at 16p13.2; *SOCS2* at 12q22 and *SOCS3* at 17q23.3. Mutations in *SOCS* genes are rare in MPNs. Nevertheless, hypermethylation of CpG sites in these genes together with a decrease in their expression was found in PV and ET mutated and non-mutated *JAK2*. The frequencies of these methylations in PV patients are: 11-13% for *SOCS1* gene; 28% for *SOCS2* and 22% for *SOCS3,* in ET patients: 14-25% for *SOCS1* gene; 28% for *SOCS2* and 10% for *SOCS3,* and in PMF patients: 17% for *SOCS1* gene; 28% for *SOCS2*.

*NRAS/KRAS* (21)

The RAS family is a group of membrane proteins associated with GTPases that controls numerous signaling pathways and cellular processes. The most common mutations are found in *KRAS* and *NRAS* genes at codons 12, 13 and 61. They involve the inhibition of the GTPase activity that avoids the inhibition of these proteins and thus, the continue activation of the effector pathways. It is not clear if these mutations promote the initiation or the progression of MPNs to acute leukemia.

*PTPN11* (46)

*PTPN11* is the protein tyrosine phosphatase non-receptor type 11. It encodes for src homology 2 domain-containing protein-tyrosine phosphatase 2 (SHP2). It regulates proliferation, apoptosis, and differentiation.

Mutations in this gene are rare in ET and PV. Nonetheless, they have been described in PMF.

*NF1* (47)

The tumor suppressor gene Neurofibromatosis-1 is located in the 17q11.2 chromosome. It is a negative regulator of the RAS pathway. Loss of *NF1* may progress into a myeloproliferative neoplasm. It is related to an enhance risk of developing myeloid leukemia in some tumors, however, it is not yet clear if this is the case for MPNs and leukemic transformation. It is a rare mutation in MPNs.

***Mutations implicated in epigenetics regulation***

*TET2* (21, 27, 48-50)

*TET* "ten-eleven-translocation" genes are a group of three homologous human proteins (TET1, 2 and 3). *TET2* gene comprises 11 exons and is located on chromosome 4q24. It encodes for a 2-oxoglutarate and Fe(II)-dependent hydroxylase whose function is to hydroxylate methylated cytosine. Therefore, *TET2* mutations result in decreased 5-hydroxymethylcytosine and thereby affect levels of DNA methylation.

*TET2* appears to be mutated in 16% of PV patients, 5 to 11% of ET and 18% of PMF ones. These mutations consist on nonsense, missense, insertions and deletions which lead to loss of function. They are associated with leukocytosis, splenomegaly, extra medullary hematopoiesis, poor overall survival, leukemic transformation and older patients. The order

in which *TET2* loss and *JAK2V617F* appear seems to be important. When *JAK2* is acquired before *TET2* mutations, it is more likely that patients develop PV; however, when *TET2* goes first, it seems that it reduces the ability of JAK2 to up-regulate proliferation genes. Actually, mice studies revealed that *TET2* loss increased self-renewal capacities of hematopoietic stem cells contrary to *JAK2V617F* which promotes proliferation and hardly reduces self-renewal of these cells. When these two mutations appeared together, *TET2* competes with *JAK2V617F* for restoring self-renewal and quieting cell proliferation. In fact, *TET2*-loss-induced self-renewal is thought to be a first event on disease initiation and progression (51) that produces a pre-leukemic state with clonal expansion of HSC that, depending on the secondary molecular events, would evolve to a MPN or other myeloid malignancies.

*IDH* (21, 27, 49)

*IDH* gene encodes for isocitrate dehydrogenases (IDH1 and IDH2). They are $NADP^+$ dependent enzymes that catalyze the oxidative decarboxylation of isocitrate to α-ketoglutarate. When mutated, they lose their affinity to isocitrate and catalyze the reduction of α-ketoglutarate (2HK) to 2-hdroxyglutatate (2HD), leading to an overproduction of 2HG instead of 2HK, which has been proposed to affect the function of some enzymes such as TET2 which are α-ketoglutarate-dependent. IDH1 an IDH2 are mutually exclusive mutations and are rare in PV and ET patients. Nonetheless they can be present in about 4% of PMF. One study has reported that the incidence of these two mutations is increased in blast transformation of MPNs (~22%) compared with its low incidence in chronic phase (1.9% in PV and 0.8% in ET). They are associated with decreased survival.

*ASXL1* (21, 27, 49, 52)

*ASXL1* gene is located on chromosome 20q11.1 and is similar to the *Drosophila megalogaster* additional sex combs gene. It is associated with the Polycomb repressive complex 2 (PRC2). The protein disrupts chromatin in localized areas, activating or suppressing the transcription activity. It is thought to have a soft role in hematopoiesis of myeloid stem cells.

This protein appears in most hematopoietic cell types and its mutated homologue is related to MPNs (19 to 40% mutated cases in PMF). Nevertheless, it is just found in less

than 7% of PV patients and in 5 to 8% in ET patients. However, it is significantly associated with acute leukemia post MPN (15-20%) and thus considered as a poor prognostic factor.

*DNMT3A* (49, 53)

This gene is implicated in DNA methylation. Even though *DNMT3A* mutations are more common in AML and post-MPN AML, it also appears in chronic phase MPNs. In PV patients, it is mutated in 5 to 7% of patients.

*EZH2* (21, 49)

EZH1 and EZH2 proteins are the catalytic members of the PRC2, which is implicated in some cellular processes such as proliferation or differentiation. It is a methyltransferase of histone H3 at lysine 27. In MPNs, these mutations are associated with loss of activity. They are found in 3 % of PV and 13% of PMF.

*SUZ12* (54)

*SUZ12* gene is located on chromosome 17q and encodes for a protein of the PRC2 as EZH2. Mutations and deletions in this region cause a dysfunction on PRC2 which seems to enhance hematopoietic stem cell activity. Mutations in this gene are not frequent in PV or ET patients.

***Mutations implicated in splicing regulation***

Some mutations have been discovered in MPNs in genes implicated on the RNA splicing machinery: *SF3B1, SRSF2, U2AF65 and ZRSR2*. They are thought to alter pre-mRNA splicing although the mechanisms remain to be elucidated.

They are rare in PV and ET; however, they are more frequent in PMF.

SRSF2 is related to bad prognosis by promoting leukemic transformation of MPNs (55).

***Mutations implicated in checkpoints***

*TP53* (21)

The *TP53* gene encodes for p53, a tumor suppressor protein that controls (among others) cell cycle and apoptosis. *TP53* mutations are found in a big amount of cancers. They

are not associated with the chronic phase of MPNs but seem to play an important role in leukemic transformation of MPNs as they are found in 20-30% of leukemic transformations.

***Other gene mutations implicated in leukemic progression***

Some gene mutations are thought to be involved in leukemic transformation of MPNs. To be classified in this way, these mutations must be detected in blast cells but not in most of cells from the precursory MPN clone. These mutations are found in less than 10% of MPN patients in chronic phases.

The most important genes implicated in leukemic transformation are: ASXL1, EZH2, IDH, TP53 and SRSF2, (already developed) IKZF1 and RUNX1.

*IKZF1* (21, 27)

*IKZF1*, Ikaros family zinc finger 1 gene is located at chromosome 7p12. It encodes for the Ikaros transcription factor, which regulates lymphoid differentiation of B and T cells. *IKZF1* deletions are prevalent in acute lymphoblastic leukemia (ALL), above all in *BCR-ABL* positive cases. In leukemic transformation of MPNs they are described as late events in the progression of MPN to AML.

*RUNX1* (21, 56)

The *RUNX1* gene, also known as *AML-1* or *CBFA2* encodes for a transcription factor with an important role in the development of normal hematopoiesis. It is believed to be one of the most common mutations in the leukemic transformation.

Generally these mutations are associated with bad prognosis (46). Nevertheless not all mutations have a prognostic value. What we can affirm is that the more mutations a patient has, the worse.

*Phenotypic and clinical impact of genetic modifications*

*JAK2* and *MPL* mutations are known to be drivers of MPN disease in mice. Actually, the presence of only one of these mutations in HSC leads to PV or ET development whereas co-existence of more than one mutation predominantly produces PMF. Nevertheless, *JAK2* and *MPL* mutations may not be the first genetic alterations in MPNs. *TET2*, *ASXL1* and

*EZH2* can precede *JAK2V617F* mutations. Even, they can appear separately from *JAK2* mutations (21). When *JAK2V617F* is acquired before *TET2* mutations, patients are more likely to develop PV (48). Moreover, *CALR* mutations are thought to be an early genetic event in MPNs (57). In addition, Lundberg *et al*. (57) showed, in a study of 197 MPN patients, that mutations in *DNMT3A* could also be acquired before *JAK2V617F* or coexisted as separate clones. They also found that *IDH1* mutations occurred exclusively after *JAK2V617F*.

Recently, a study on induced pluripotent stem cells and primary cells from patients showed that the overexpression of *ATG2B* and *GSKIP* genes induced spontaneous formation of colony forming unit-megakaryocytes (CFU-MK) enhancing hematopoietic progenitor differentiation by increasing sensitivity to thrombopoietin. The overexpression of these genes was demonstrated to cooperate with classical mutations (*JAK2, MPL* and *CALR*) to generate MPN phenotypes, predominantly ET. Moreover, they are also associated with myelofibrosis or AML progression (58).

Mutations display a remarkable influence in clinical phenotypes of patients. In general, an increased number of somatic mutations is correlated with reduced overall survival, increased leukocyte counts and risk of leukemic transformation whereas patients that don't present any detectable somatic mutation or only one mutation in *JAK2*, *CALR*, or *MPL* genes present good prognosis and low risk of leukemic transformation. The *TP53* mutation is associated with AML transformation and decreased in overall survival as well as *TET2*. *ASXL1* mutations are related to lower hemoglobin levels and *EZH2* with leukocytosis (57). *JAK2V617F* is present in almost all PV patients whereas ET and PMF are characterized by the presence of *JAK2* mutation or other genetic abnormalities such as *MPL*, *CALR* or *TET2* mutations.

## *VASCULAR COMPLICATIONS*

PV and ET are chronic diseases in which global survival is weakly decreased (PV) or not (ET) compared with healthy patients. Nevertheless, they are characterized by a significant increase of vascular events. These consist on hemorrhagic events as well as arterial and venous thrombosis that usually are first signs that lead to diagnosis. They are the principal causes of morbidity and mortality in these hemopathies. In general,

thrombotic events are more frequent in PV patients than in ET ones and in older patients compared with younger ones. The annual incidence of these events varies from 1 to 10%.

Some of the thrombohemorrhagic events are arterial thrombosis, (ischemic stroke, myocardial infarction, unstable angina pectoris, peripheral and visceral thromboembolism), venous thrombosis (deep venous thrombosis in legs and arms, pulmonary embolism, unusual sites venous thrombosis – mainly splanchnic vein thrombosis – superficial venous thrombosis) as well as microcirculatory disturbances (mainly in ET patients) such as erythromelalgia, ischemic attacks, visual or hearing defects, headache and peripheral paresthesia. Venous thrombosis at unusual sites are the most common in these patients. In fact, one of the most characteristic venous complications is abdominal venous thrombosis in splanchnic or portal veins, including Budd–Chiari syndrome affecting young women principally. Controversially, the prevalence of cerebral venous thrombosis is not well defined in MPNs. Some studies point that they are usual among MPN patients but recently, Dentali *et al* (59) concluded that these events are rarely found in MPN patients (60-62).

*Risk factors*

– Cardiovascular factors: Principally they are hypercholesterolemia, hypertension, smoking, and diabetes. They are present in about one third of PV patients with vascular complications. More precisely, smoking has been associated with an increased risk of arterial thrombotic events such as myocardial infarction, and hyperlipidemia was also related to arterial events in one clinical study (63).

– Age and sex: younger patients (under 65) have less vascular complications than >65-year-old patients, and these last ones, less than >75-year-old ones. Male patients are associated with arterial thrombotic events such as myocardial infarctions and females with thrombosis in unusual sites such as splenic or portal veins.

– Number of blood cells: In PV patients, control of hematocrit under 45% is necessary so as to reduce blood hyperviscosity that is related to vascular complications. Hyperviscosity enhances erythrocyte aggregation, what apart from disturbing blood flow; it also facilitates platelet activation and aggregation by easing platelets to interact with endothelial cells or other platelets that are more activated

in MPN patients. Furthermore, erythrocytosis linked to leukocytosis increases leukocyte proteases that could affect the integrity of endothelial cells. In fact, some abnormalities in the endothelium have been described in MPN patients such as increased expression of adhesion molecules in these modified endothelial cells that favors platelet and leukocyte arrest causing the secretion of procoagulant particles (61). In addition, PV erythrocytes have also been reported to hyperexpress adhesive molecules that could adhere to the endothelium and act in thrombotic events. In PV patients participating in the ECLAP study (European Collaboration on Low-Dose Aspirin in Polycythemia Vera), leukocytosis higher than $15x10^9$/L was associated with an increased risk of major thrombosis as myocardial infarction. Similarly, in ET, arterial and venous thrombosis were associated with leukocytosis but not with platelet count or hemoglobin level. Conversely, extreme thrombocytosis (>$1500x10^9$/L) seems to reduce the risk of arterial thrombosis in ET. It may be caused by the fact that this excessive thrombocytosis could be secondary to an acquired von Willebrand Factor (vWF) deficiency. It is suggested that increased platelet binding to vWF facilitates platelet activation and promotes vWF multimer proteolysis consuming vWF and causing erratic vWF activity (60, 61, 64, 65).

– Microparticles: They are 0.1-1μm membrane fragments released by activated cells especially from platelets and endothelial cells. They are increased in thrombotic ET patients. Additionally, these microparticles are associated with thrombin generation potential that causes a thrombo-modulin-resistant phenotype in PV and ET patients (61, 66).

– Neutrophil Extracellular Traps (NETs): These are a mixture of DNA fibers including histones and antimicrobial proteins such as myeloperoxidase, neutrophil elastase and cathepsin G released as defense mechanisms against pathogens by dying neutrophils. They are capable of killing both Gram-positive and Gram-negative bacteria, fungi and of sequester viruses (67). Fuchs *et al*. 2007 (68), proved that NET production needed NADPH oxidase activation and ROS production. NETs have been strongly associated with thrombosis risk as they are shown to promote platelet adhesion, activation, and aggregation. Their correlation with deep vein thrombosis is

explained as they can recruit red blood cells promoting fibrin deposition forming a red thrombus usually in deep veins (Fuchs *et al.* 2010 (69)). Demers *et al*. 2013 (70), showed that the stimulation of isolated neutrophils from mice with chronic myelogenous leukemia resulted in high levels of NET formation. They thought that the granulocyte colony-stimulating factor (G-CSF) could be a priming factor for NET generation. Furthermore, they also associated NET formation with thrombosis.

– APC resistance: PC is a serine protease known to be a potent anticoagulant. It is activated by thrombin bound to the thrombomodulin receptor in the endothelium. APC complexes protein S (PS) so as to reduce clotting activation by proteolytic inactivation of coagulation factors V and VIII. APC resistance is thought to be caused by a decrease in free PS level. In fact, one study showed that ET patients presented higher thrombocytosis and PS cleavage than normal ones. Actually, a platelet protease is thought to be responsible for PS cleavage. In agreement, treatment with hydroxyurea decreased platelet and PS cleavage levels. It has been reported that ET and PV patients present high APC resistance, particularly mutated *JAK2* ones and ET ones with a history of thrombosis. In fact, some studies have revealed a decrease in natural anticoagulants concentration in MPN patients.

Both, elevated levels of microparticles and APC resistance are related to an increased risk of thrombosis. These both factors were especially increased in *JAK2V617F* PV and ET patients (61, 66).

– *JAK2 V617F*: The role of this mutation in vascular complications is not well defined as clinical studies differ in their conclusions. For instance, Passamonti *et al.* (26), did not find a connection between *JAK2V617F* allele burden and risk of thrombosis in PV patients. They just concluded that advanced age is the only well-known significant predictor of thrombosis. Kuriakose *et al*. 2012 (71), also reported that even though the thrombotic events were decreased in patients treated with pegylated interferon (IFN), *JAK2V617F* allele burden barely changed after treatment. Kittur *et al*. (72), also concluded that there is no significant bond between mutated *JAK2* and arterial thrombosis (at diagnosis or post-diagnosis) or venous thrombosis at diagnosis; but there was a positive correlation in post-diagnosis venous thrombosis events. On the contrary, Vannucchi *et al.* 2007 (73), concluded that the

risk of cardiovascular events was higher in *JAK2V617F* PV patients. According to them, *JAK2V617F* ET patients are also associated with higher risk of vascular complications. Similar results were obtained by Takata *et al.* 2014 (74). Moreover, Borowczyk *et al.* 2015 (65), also associated *JAK2V617F* allele burden (>20%) with thrombohemorrhagic episodes as venous thromboembolisms and principally deep vein thrombosis.

– CALR mutation: Rumi *et al.* (31), reported that thrombosis was twofold higher in *JAKV617F* PV and ET patients than in *CALR* mutated. Furthermore, the incidence of thrombosis at diagnosis in *JAKV617F* PV patients was also higher than in *CALR* mutated ET patients. In a similar study, Rotunno *et al.* (75) also concluded that *CALR* patients presented lower risk of thrombosis than those with *JAK2* or *MPL* mutations. Therefore, *CALR* patients present low thrombotic risk.

### *LEUKEMIC PROGRESSION*

Despite progresses in MPN management, 1% of ET and 4% of PV patients after 10-year diagnosis and 4 to 8% after 18-years diagnosis evolve to secondary acute myeloid leukemia with an awful outcome: median survival of less than 6 months.

Leukocytosis (WBC count over $15x10^9$/L), advanced age and exposure to chemotherapy are poor prognostic factors for AML progression. Nevertheless, the mechanisms of leukemic transformation are not well defined yet.

In general, *JAK2/MPL*-positive patients can evolve to *JAK2*-positive AML associated with the acquisition of additional genetic alterations but they can progress to *JAK2* negative AML as well. This suggests that the leukemic clone could emerge from a "pre *JAK2V617F* cell" that has acquired secondarily the *JAK2V617F* mutation leading to the chronic phases, or that the leukemic cells developed from an independent clone that do not participate in the chronic phase. Passamonti *et al.* 2010 (26) showed that *JAK2V617F* allele burden is not connected to AML evolution.

Some of the potential gene mutations that are thought to play a role in AML transformation are *MYC, ETV6*, and *RUNX1*, as well as high frequent mutations in post-AML such as *TET2*, *ASXL1, SRSF2*, *IDH1/2* and *TP53. TP53* loss has been shown to be

strongly associated with leukemic transformation. Rampal *et al.* (76) demonstrated that the combination of *JAK2V617F* and loss of *TP53* can cause leukemic transformation in mice. However, *TP53* mutation is not frequently related to *CALR* mutations. Abdel-Wahab *et al.* 2010 (77) studied the most frequent mutations in leukemic transformation and yielded that *TET2* mutations were usually acquired at AML transformation. On the opposite, *ASXL1* mutations were detected in both MPN and AML states in most of the cases. The presence of more than one somatic mutation was also associated with poor prognosis and leukemic progression as well as *TET2* presence (57). However, the mechanism of leukemic transformation remains poorly elucidated. Knowledge from new sequencing technologies might probably bring out the effects that other genetic alterations may have in this progression.

Another well documented factor of leukemic transformation is the impact of chemotherapy. Finazzi *et al.* (10) reported the largest randomized trial in PV: The European Collaboration on Low-dose Aspirin in Polycythemia Vera (ECLAP) prospective project of 1638 patients. In this study they demonstrated that treatment with the cytoreductive molecules pipobroman, busulfan or chlorambucil alone or combined with other drugs significantly increased the risk of leukemic and fibrotic transformation. Treatment with hydroxyurea alone did not increase this risk compared with patients treated with phlebotomy or interferon (the reference treatment with no influence in leukemic progression) but it did when combining hydroxyurea with cytoreductive agents. Nevertheless, this trial was criticized as the follow-up time was short (2.8 years). Furthermore, Kiladjian *et al.* (78) reported the results of a randomized trial initiated in 1980 from the French Polycythemia Study Group (FPSG) in 285 PV patients with a median follow-up of more than 12 years. They concluded that the use of pipobroman significantly reduced overall survival as well as it increased leukemic or dysplastic evolution. Therefore this drug should be reserved for second-line treatment. Concerning hydroxyurea, they suggested that it could have an impact in dysplastic or leukemic evolution as the number of patients evolving to AML was 5.9% against 1.5% in those ones receiving phlebotomy as treatment. They stressed the role of the time of exposure since in the second overview they showed that the frequency of AML was significantly increased in comparison with their first analysis (median follow-up of 12 versus 2.8 years). In addition, they found a higher number

of patients treated with hydroxyurea that evolved to myelofibrosis compared with those treated with pipobroman. These patients are more likely to develop AML (79).

### *MYELOFIBROTIC EVOLUTION*

The risk of myelofibrotic evolution in MPN is 6% after 15 years of diagnosis. Nevertheless, patients' survival after myelofibrotic state and prognostic factors are not well defined nowadays.

A clinical study of PV patients by Passamonti *et al.* 2008 (80) concluded that leukocytosis over $15x10^9$/L at PV diagnosis was significantly correlated with myelofibrotic evolution. They sought that 96% of patients with myelosuppressive agents developed post-PV myelofibrosis (MF). They also remarked that all post-PV myelofibrotic patients had high circulating CD34+ cell counts and high levels of serum lactate dehydrogenase (LDH). They developed a prognostic model to predict survival in PV patients that evolve to MF. This model is based on the fact that leukocyte count (more than $30x10^9$/L), hemoglobin levels less than 100g/L and platelet count less than $100x10^9$/L at diagnosis are useful markers to predict survival in these patients. Another clinical study of Passamonti *et al.* 2010 (26) highlighted that MPN patients that evolved to MF had high *JAK2V617F* allele burden (>50%) and that patients with homozygous *JAK2V617F* are more likely to develop myelofibrosis. Another study by Benton *et al.* (45), revealed that PV patients with chromosome 12 mutations such as those in loci 12q15 (*HMGA2*) and 12q24 (*SH2B3 (LNK)*), were more likely for myelofibrotic progression.

A recent clinical approach of PV patients that evolved to MF (81), found that patients that followed this pathway were characterized by higher leucocyte count ($12.4\pm4.4x10^9$/L) and splenomegaly (mean size 1.6±3.3 cm). Other facts such as Hb levels, platelet count, diabetes, hypertension, LDH values or clinical facts such as advanced age, thrombocytosis or cardiovascular risk factors weren't correlated with myelofibrotic evolution in this study.

Summing up, leukocytosis at diagnosis is a risk factor to evolve into MF (as well as for leukemic transformation).

## *TREATMENT*

Despite clinical researches with new drugs, the only curative approach that exists nowadays for MPN patients is allogenic stem cell transplantation. It is reserved for intermediate-2 or high-risk myelofibrosis or patients that already have transformed to acute leukemia or myelodysplasia. In these cases, patients present a 3-year overall survival from 39 to 67%. However, stem cell transplantation is also associated with morbidity due to GVHD (Graft versus host disease). Bad outcomes of allogenic stem cell transplantation are older age, AML diagnosed at transplant time and unrelated donor (82).

In general, MPN treatment strategy is based on reducing the risk of vascular events which are the principal actors of mortality and morbidity and on the control of cardiovascular risk factors as smoking, hypertension, dyslipidemia or diabetes.

First of all, PV and ET patients are classified as high vascular risk if they are over 60 years old or/and have a history of vascular events. Low risk patients are under 60 and with no history of vascular events.

Treatment is founded on the use of cytoreductive molecules. Hydroxyurea (HU) is the "historical" molecule commonly used. It blocks the ribonucleotide reductase inactivating DNA synthesis and thus producing cell death in S phase. It reduces myeloproliferation and displays a good efficacy and tolerability. It also reduces significantly thrombotic complications. However, it is lightly associated with leukemic progression (78).

### *Interferon alfa*

The study of pegylated IFNα in both PV and ET is the aim of actual clinical researches in MPN treatment. It has been demonstrated that it is capable of normalizing platelet counts and leukocytosis; of reducing erythrocytosis (avoiding phlebotomies in PV patients) and splenomegaly. Furthermore, it is non leukemogenic. Interestingly, pegylated IFNα treated patients show a complete molecular response after 21 to 31 months in some patients. It is also remarkable that the pegylated form inhibits colony formation from *JAK2* mutated CD34+ cells from MPN patients (83, 84). On the contrary, in a clinical study by Kuriakose *et al.* (71), they didn't observe any reduction of *JAK2V617F* allele burden when treating with peg-IFN. They suggested that it could be due to the fact that they used higher

doses resulting in clinical and hematologic responses but not in molecular ones. Moreover, *JAK2* mutant erythroblasts from PV patients reduced STAT1 phosphorylation after IFNα treatment which may explain thrombocytosis reduction (24).

Even it is a promising drug in MPN therapy, long-term treatments are usually required till complete remission and the adverse effects of this drug are fatigue, depression, weight loss and nausea. Lu *et al.* (85) proposed a combination of peg-IFNα with a MDM2 antagonist, the RG7112 as IFN effects are associated with the activation of p53 pathway. On the one hand, IFNα stimulates p53 transcription through the activation of JAK1-STAT1/2 and IRF-9 (interferon regulatory factor-9). On the other hand, in *JAK2V617F* cells through PI3K/Akt/mTOR pathway, it increases MDM2 expression degrading the p53 protein. Therefore, Lu *et al.* 2014 (85) proposed an MDM2 antagonist combined with IFNα for MPN treatment that would raise p53 expression in IFNα treatments. Their results were encouraging; however no *in vivo* studies have been done for the moment (86).

First approaches to determine the effects of IFN in *CALR* patients were studied by Cassinat *et al.* (87). Even though they could just treat two patients, their results showed a reduction in mutated *CALR* allele burden coupled to hematologic complete response (reduction of thrombocytosis) for more than 60 and 18 months (patients 1 and 2). Concluding, pegylated forms of interferon alfa represent a potential effective drug for *JAK2* and *CALR* mutated MPNs.

*JAK2 inhibitors* (43)

Since its discovery in 2005, JAK2 became a potential target to treat these diseases. Controlling its activation is the main purpose of new drug design. The principal problem is that there aren't any specific drugs that target specifically mutated JAK2 so their use will disrupt normal hematopoiesis causing anemia or thrombocytopenia. These drugs are Adenosine Tri-Phosphate (ATP) mimetic JAK inhibitors binding to the active form of JAKs. Nowadays, ruxolitinib is the only *JAK2* inhibitor approved by the U.S. Food and Drug Administration (FDA) in 2011 and the European Commission in 2012 based on two clinical trials. It was approved for intermediate-2 and high risk myelofibrosis (primitive or

secondary) as it proved to reduce splenomegaly and to ameliorate disease-related symptoms (88). It is also proposed in PV patients with intolerance to Hydroxyurea.

Despite these advances and their potential efficacy; JAK inhibitors show little reduction of allele burden and myelofibrosis. In addition, they don't seem to be capable of eliminating MPN-initiating cells as a mouse model showed (89). Thus they cannot be considered as effective treatment for disease eradication as peg-IFNα suggested. Moreover, they should be taken continuously to be effective as curative treatment.

Finally, it seems that their impact is mainly mediated by their action on cytokine levels via JAK regulation. Ruxolitinib showed a large and rapid downregulation of cytokine levels in PMF patients (90) and murine models (91). In addition, the interruption on Ruxolitinib administration causes a huge increased in cytokines associated with a withdrawal syndrome (92). Furthermore, splenomegaly and symptom reduction were correlated with reductions of IL-1ra, MIP-1β, IL-6 and TNF-α (90).

Another problem of these drugs is resistance. Deshpande *et al*. (93) showed that some JAK2 mutations presented resistance to these drugs in Ba/F3 cell models.

Other clinical approaches studied SAR302503 (TG101348, fedratinib; Sanofi) which targets preferentially JAK2. Results showed that it improved myelofibrosis related symptoms, reduced spleen size and *JAK2V617F* allele burden. Nevertheless, the appearance of Gayet-Wernicke encephalopathy in some cases ended with its development.

CEP701 (lestaurtinib; Cephalon) is a multikinase inhibitor. In a clinical phase II study, it displayed little reduction in spleen volume, myelofibrosis related symptoms, and leukocytosis, but it didn't reduce either *JAK2V617F* allele burden or proinflammatory cytokine levels. In another clinical study of the same molecule, PV or ET patients showed a reduction of spleen size but not of thromboembolic events.

CYT387 (Gilead Sciences) another JAK1/JAK2 inhibitor also exhibited reduction of spleen size, anemia, and myelofibrosis related symptoms in almost 50% of patients. It is remarkable that CYT387 was also effective in patients in whom ruxolitinib or SAR302503 treatment had failed.

SB1518 (pacritinib; SBio) is a pyrimidine-based JAK2/FLT3 inhibitor. A phase II clinical trial presented reduction of spleen size and general symptoms with low frequency of myelosuppression.

Moreover, other JAK inhibitors (LY2784544, NS018, AZD1480, BMS911543, tasocitinib, NVP-BSK805, INCB16562) are being studied in preclinical or clinical approaches.

*Other strategies* (43)

Targeting Heat-shock protein (HSP) 90 is an alternative to classic JAK inhibitors. This protein belongs to the HSP family proteins that control correct folding, intracellular disposition and proteolytic turnover of key regulators of cell growth and survival. It presents folding and chaperone activity in molecules such as JAK2. Therefore, Hsp-90 inhibitors aim to destabilize JAK2 and promote its proteolytic degradation. Some of these candidates are 17-AGG, PU-H71, SNX5422 and NVP-AUY922.

Previous approaches presented a decrease in JAK2 protein and inhibition of cell growth of *JAK2V617F* or *MPLW515L*-positive cell lines and *JAK2V617F*-positive primary MPN cells by PU-H71 treatment. These results weonal similar to the ones obtained with NVP-AUY922 in primary MPN cells and cell lines. Moreover, they can be used alone or in combination with JAK2 inhibitors such as TG101348 and PU-H71 which seemed to resolve the resistance problem and presented an additive antiproliferative effect in cell lines when used together.

Hsp90 proteins are regulated by acetylation/deacetylation of their lysine residues. This process is controlled by histone acetyltransferases and HDACs. Next therapy strategies are then based on HDACs inhibitors. Several inhibitors of HDAC are already known such as givinostat (ITF235), panabinostat (LBH589), vorinostat (MK-0683), pracinostat (SB939), and abexinostat. First essays with givinostat showed a decreased in JAK2 protein level, its signaling pathways and growth inhibition in *JAK2V617F*-positive cell lines and primary MPN cells. The use of panabinostat gave similar results and showed more efficacy when combined with the JAK2 inhibitor TG101348.

Future strategies will target JAK2 effectors such as STAT5, MAPK/ERK, or PI3K/Akt/mTOR molecules or even their effectors such as Bcl-xl.

*Antioxidant strategies* (43)

The radical oxygen species (ROS) have been demonstrated to be increased in Ba/F3 cells overexpressing *JAK2V617F*; in *JAK2V617F*-positive primary cells from PV and MF patients and in the progenitor compartment of *JAK2V617F* knock-in mouse model. ROS augmentation causes an increase in cell proliferation by promoting the G1/S transition, DNA double-strand damage and genomic instability. The use of the ROS scavenger agent, the N-acetylcysteine, in *in vivo* studies restored blood parameters and reduced DNA damage. Furthermore, it also reduced spleen size by decreasing *JAK2V617F*-positive hematopoietic progenitors in bone marrow. This strategy should be used combined with previous ones to avoid *JAK2V617F* MPN development.

***Main recommendations for therapeutic decisions in Ph- MPN treatment***

*Polycythemia Vera treatment* (83)

Low risk patients will receive antiplatelet therapy by low-dose aspirin (100 mg/day) to reduce the risk of cardiovascular events and phlebotomy to maintain hematocrit levels under 45% to decrease blood viscosity.

High risk patients will receive, as first line of choice, cytoreductive therapy, hydroxyurea or interferon alfa (IFNα). Hydroxyurea presents good efficacy and tolerance although it also may cause skin toxicity, resistance and risk of disease transformation in long periods of treatment. Related to IFNα, nowadays it is its pegylated forms that are used due to its better tolerance, (it has been well studied in hepatitis treatment). It presents high efficacy as it reduces *JAK2V617F* burden. *JAK2* mutated patients are more sensitive to IFN-alfa than those with *TET2* mutations which could be resistant. The disadvantages of this drug are its toxicity and contraindications and that it is not approved for PV treatment yet.

As second line therapy, there is another approved myelosuppressive drug for PV treatment. The use of busulfan, an alkylating agent, may be an option although it is thought to increase leukemic transformation.

The Janus Kinase (JAK) 1 and 2 inhibitor Ruxolitinib can be chosen when patients are intolerant or resistant to hydroxyurea. Clinical essays show well tolerance, well control of hematocrit levels (under 35%), reduction of spleen levels, hematologic remission and decrease on PV related symptoms. The adverse events related to ruxolitinib are thrombocytopenia, dyspnea, anemia, asthenia, herpes zoster infection; basal-cell and squamous-cell carcinomas; non-melanoma skin cancer or precancerous skin conditions (94).

*Essential thrombocythemia treatment* (83)

Low risk patients will only receive low-dose aspirin if they present *JAK2V617F* or cardiovascular risk factors. If aspirin-resistance appears, anti-platelet agents can be considered as clopidogrel or even platelet-lowering agents as hydroxyurea in extreme cases of aspirin resistance. Antiplatelet drugs have been shown to decrease microvascular circulation disturbances in cerebral, coronary and peripheral circulation (61). If extreme thrombocytosis (more than $1500x10^9$/L) is present, patients could suffer von Willebrand's syndrome and they will receive cytoreductive therapy previous to antiplatelet one.

For high risk patients, the use of hydroxyurea combined to aspirin is chosen as first line. It's been demonstrated that together they reduce the rate of thrombosis. It is remarkable that *JAK2V617F* patients require lower doses of hydroxyurea. Anagrelide can be used in specific patients who are resistant or intolerant to hydroxyurea.

Management of both diseases is resumed in Table 1.

| | **PV** | **ET** |
|---|---|---|
| **All patients** | Management of cardiovascular risk factors | |
| **Low-Risk Patients** | Aspirin | Aspirin |
| | Phlebotomy | |
| **High-Risk Patients** | | |
| First line | HU or IFN-α | HU (±aspirin) |
| Second line | Switch HU or IFN-α | Anagrelide |
| | Ruxolitinib | IFN-α |
| **Other** | Busulfan | Busulfan |

**Table 1.** ET and PV treatment. Table modified from Kiladjian JJ 2015 and Tefferi *et al.* 2015 (9, 83).

*Primary Myelofibrosis treatment* (83, 95)

The only curative treatment for this hemopathy is allogeneic hematopoietic stem cell transplantation which ends with bone marrow fibrosis, reaches molecular remission and restores nonmalignant hematopoiesis. It is the choice in intermediate-2 and high risk PMF groups.

Therapy strategies treat anemia or other cytopenias, reduce splenomegaly and possible symptoms such as fever, fatigue, pruritus or weight loss. They also focus on reducing risk of leukemic transformation, thrombotic and bleeding complications.

-Anemia: Usually PMF patients present hemoglobin values under 10 g/dL. First line of treatment will manage iron, vitamin B12 and folic acid deficiency if present, but transfusion remains the base of these patients with the inherent iron overload complications due to polytransfusion. Patients with low levels of endogenous erythropoietin (under 125 mU/mL) can be treated with recombinant human EPO. The use of androgens such as danazol has also been proved to reduce anemia. Other alternatives are immunomodulators such as low-dose thalidomide combined with prednisolone that are first choice in patients with thrombocytopenia and lenalidomide combined with prednisone (first choice in 5q deletion patients). Finally, patients in whom anemia treatments are refractory to any therapy and are transfusion dependent, splenectomy may be their choice.

-Splenomegaly: Hydroxyurea is the usual drug to reduce spleen size. However the remarkable impact of JAK2 inhibitors have lead this therapeutic class as a treatment of choice of splenomegaly and symptoms associated with PMF (or secondary myelofibrosis). Therefore, hydroxyurea is usually combined with JAK inhibitors. Other alternatives are splenectomy (related to significant mortality 25-30%) and splenic irradiation but it presents high risks of cytopenias. Low-dose irradiation is also used for symptomatic extramedullary hematopoiesis in other sites than spleen and liver such as skin or the central nervous system.

-JAK2 inhibitors: Ruxolitinib is the only approved JAK2 inhibitor for PMF therapy and for treatment of myelofibrosis secondary to PV or ET. It reduces spleen size, common symptoms and increases overall survival when compared with patients taking placebo or

best available therapy. However, Ruxolitinib benefits are dose dependent and any stops in treatment will bring the symptoms back as well as splenomegaly. Common side effects are thrombocytopenia and anemia. Other JAK2 inhibitors currently in phase III studies are pacritinib (without megakaryocytic toxicity so avoids the thrombocytopenic risk of Ruxolitinib); or momelotinib which is thought to be useful in patients with transfusion-dependent anemia.

*Management of possible complications in MPN treatment* (95)

– Acute thrombotic events: They should be treated as normal patients by an anticoagulant therapy. To prevent them, phlebotomy and low-dose aspirin are the main recommendations respectively. In severe cases such as acute cerebrovascular complications, acute platelet apheresis or erythropheresis can be performed coupled to cytoreductive therapy preferably hydroxyurea. Treatment by anticoagulants and antiplatelet drugs is advised as prevention.

– Bleeding: It is mostly caused by acquired von Willebrand's syndrome associated with high platelet counts (>1,500x$10^9$/L). Thus hydroxyurea is recommended as a platelet reduction agent. (Platelet apheresis is also accepted in cases of extreme thrombocytosis).

– Pruritus: Antihistamines are the first choice. It can also be managed by selective serotonin re-uptake inhibitors or phototherapy combined with psoralen.

– Leukemic transformation: These patients need to be treated in clinical specialized units and are currently included in the therapeutic protocol for secondary AML (post MPN/MDS). As said, the only curative treatment in leukemic progression is allogenic stem cell transplantation. However, Rampal *et al.* (76) showed that ruxolitinib and decitabine were effective drugs on post-acute leukemia murine models as well as the Hsp90 inhibitor PU-H71 suggesting that these new drugs may have an interest in combination with induction or consolidation of chemotherapy.

## *PREVIOUS REPORTED DYSFUNCTIONS IN MPNs*

As explained in the first part of the manuscript, molecular alterations drive the transformation of HSC leading to myeloproliferation. One important issue is to know if these molecular alterations could cause deregulations in protein expression (inducing proteome deregulations) or functional alterations of proteins that could contribute to the phenotype and the evolution of the disease. In this sense, several studies have reported alterations of proteome profiles in MPN patients correlated or not with their molecular status.

*In serum*

One "historical" example of these protein deregulations is the modification of erythropoietin serum value in PV patients. MPNs are physiopathologically characterized by an EPO independent proliferation of erythroid progenitors inducing a decrease on the secretion of EPO by renal cells. This protein modification has been validated as a marker of PV allowing, with good specificity and sensitivity, the discrimination between PV and secondary erythrocytosis (96). Even though some contradictory results exist in some patients, Tefferi *et al.* (97) suggested that serum erythropoietin levels were expected to be decreased in PV regardless of *JAK2* mutation. Moreover, Hong *et al.* (98) also reported that patients with primary erythrocytosis or primary familial congenital polycythemia presented low serum EPO levels due to a defect on the hematopoietic progenitors.

After *JAK2V617F* discovery, studies focused on the impact of *JAK2V617F* on MPN serum proteome in comparison with *JAK2* wild type (wt). Mossuz *et al.* (99) demonstrated that a 28 kDa protein (Apolipoprotein A-1) was associated with the presence of the *JAK2V617F* mutation in PV patients, and that Apo-A1 levels were correlated with allele burden. Apo-A1 expression was higher in homozygous patients and in patients with an allele burden greater than 75%. Apolipoprotein A1 is the main component of high density lipoproteins (HDL) in plasma which are in charge of carrying lipids as cholesterol. Interestingly, they also correlated higher cholesterol levels with ≥75% *JAK2* mutant allele suggesting that some metabolic alterations might be related to the presence of mutated *JAK2*.

Similar studies with ET serum did not provide the same results. Serum proteome of both *V617F*-positive and *V617F*-negative ET shared >85% of their protein profiles and did not display significant differences. Moreover, Apo-A1 levels were not impacted by the presence and allele burden of *JAK2* mutation in ET patients. Nevertheless, there were significant differences between ET and PV serum proteomes (49% of serum proteins differed between *JAK2V617F*-PV and *JAK2V617F*-ET and 48% between *JAK2(-)* and PV) (100).

Recently, other serum protein alterations concerning cytokines have been highlighted. Tefferi *et al.* (101) found significant elevated serum levels of twenty cytokines in PMF patients compared with controls and only one underexpressed cytokine, the IFN-γ. In addition, some of these increased cytokine levels were associated with prognosis factors. For instance, IL-8 was correlated with leukemia-free survival, constitutional symptoms and 1% circulating blasts. IL-2R, IL-12 were related to the need of transfusion; IL-2R and IL-8 with leukocytosis; IP-10 with thrombocytopenia and HGF, MIG and IL-1RA with splenomegaly. Moreover, high levels of seven of these cytokines were associated with *JAK2V617F* mutation (IL-1RA, IL-2R, IL-6, IL-12, HGF, IP-10, and MIG). Pourcelot *et al.* (102) showed that variations also occurred in PV and ET with a significant increase of cytokine levels compared with normal range values. Altogether, these data suggested that alteration of protein expression do exist in the serum of MPN patients and that the molecular status could impact in these alterations depending on the nature of the mutations and the type of MPN.

*In endothelial cells*

Endothelial cells may be the first activators of blood cells if there is any injure in the endothelium. It has been found high levels of P- and E-selectin in plasma from ET thrombotic patients. These two proteins are adhesion molecules expressed by endothelial cells. The fact that they are hyperexpressed suggests that they may have a role in the pathogenesis of thrombosis in ET. Furthermore, one research showed that plasma levels of Nitric Oxide (NO) were reduced in ET patients compared with controls. This study agreed with previous ones that showed that MPN patients with thrombotic complications had NO production impaired. NO is normally released by endothelial cells and acts as a platelet inhibitor to prevent thrombus formation. The fact that it is underexpressed in ET patients may contribute to thrombosis. In addition, treatment with hydroxyurea increased plasma

levels of NO. On the opposite, PV patients presented high plasmatic levels of NO compared with controls and they didn't vary after hydroxyurea treatment. Actually, NO is associated with high hematocrit levels as it may be a compensatory mechanism for thrombotic risk situations (61).

*In white blood cells*

Thanks to Protein Pathway Array, Hui *et al.* (103) screened 15 proteins in peripheral blood neutrophils differently expressed between ET and control patients implicated in apoptosis and inflammatory pathways. They also found differences in protein expression in cycle signaling pathways when comparing ET patients with and without *JAK2V617F* mutation suggesting that this mutation contributes to malignant proliferation and cell cycle progression. Finally, they selected two proteins that could predict thrombosis in ET patients, the estrogen receptor beta and STAT3.

Falanga *et al.* (104) studied the involvement of neutrophils in the pathogenesis of thrombotic predisposition of PV and ET. They showed that neutrophils presented high levels of CD11b, which is a maker of activation. Neutrophils also presented high levels of leukocyte alkaline phosphatase which suggested the idea of neutrophil degranulation raising plasma concentrations of elastase and myeloperoxidase. Moreover, activated neutrophils can bind platelets, what originates the formation of platelet-leukocyte complexes which are thought to be the cause of pro-thrombotic condition. Arellano-Rodrigo *et al.* (105) also found that ET patients presented higher expression of CD11b in neutrophils but not in patients with thrombosis. CD11b expression was also associated with *JAK2V617F* presence. Nevertheless, they found that CD11b expression was increased in monocytes from thrombotic patients as well as the monocyte tissue factor which may be involved in blood coagulation. In general, CD11b expression promotes leukocyte adherence to the endothelium, phagocytosis, aggregation, adhesion-dependent respiratory burst and degranulation.

*In platelets*

Abnormalities in MPN platelets such as reduced functionality or abnormal aggregation have been suspected since a long time. Recently, these data have been improved

showing reduced levels of membrane adhesion molecules such as glycoprotein Ib, IIb-IIIa, IV and VI; acquired storage pool disease and defective metabolism (61). In contrast, Arellano-Rodrigo *et al*. (105) found that in ET thrombotic patients, platelets presented increased expression on their surface of P-selectine in normal conditions and after stimulation by arachidonic acid but not after stimulation by ADP or collagen. P-selectine expression was also higher in mutated *JAK2* patients. Moreover, ET patients also had more platelet-neutrophil and platelet-monocyte complexes and higher platelet counts. However, Falanga *et al*. (61) reported that platelet response to in vitro stimulation was decreased compared with healthy control platelets. Thus, even if these platelets showed activate-state makers, the fact of being constantly activated may decrease their functions.

It has also been reported that platelets of *JAK2* mutated MPN patients showed higher capacity of thrombin generation (which is associated with higher platelet activation). It was also related to *JAK2V617F* allele burden. This effect was reduced by hydroxyurea (61).

*In red blood cells*

Studies focused on red blood cell dysfunctions are rare but very informative. Lutheran and basal cell adhesion molecule, Lu/BCAM is part of red blood cell (RBC) membrane antigens. It is formed by two glycoproteins of the immunoglobulin family expressed toward the end of erythropoiesis that are directly connected to the αI-spectrin from the spectrin-based skeleton. Lu/BCAM is the erythroid receptor of Laminin 511/521. It is overexpressed on sickle RBCs where it adheres to laminin α5-chain what causes vaso-occlusive crises, the main complication in this disease. It has also been related to metastasis in some cancers (106). Moreover, Murphy *et al.* (107) showed that this adhesiveness was mediated by an increase in cAMP that activated the GTPase Rap1 which, in turn activated Lu/BCAM and caused enhanced laminin adhesion in sickle cell disease. It can also be activated by phosphorylation via Phosphokinase A (PKA) on serine 621. Similar events were described in hereditary spherocytosis (HS) by El Nemer *et al.* (108) who showed that splenectomized patients with HS presented dissociation of Lu/BCAM to the spectrin-based skeleton that resulted in increased cell adhesion to laminin.

Wautier *et al.* (109) studied whether these processes may take place in PV RBCs being the cause of thrombotic complications such as cerebrovascular events which are frequent in PV. First, they showed that Lu/BCAM was constitutively phosphorylated in PV erythrocytes

and that these cells presented increased adhesion to human umbilical vein endothelial cells. (Figure 3). Moreover, they demonstrated that *JAK2V617F* in K562 cells enhanced Lu/BCAM expression and phosphorylation suggesting a possible link between this common mutation in PV and abnormal adhesion of RBCs via Lu/BCAM phosphorylation.

To carry on with those findings, De Grandis *et al.* (110) (same study group) studied the relationship between the mechanisms of increased RBC adhesion via activated Lu/BCAM and *JAK2V617F* in PV. Using Ba/F3 *JAK2* wild-type, Ba/F3 *JAK2V617F* and HEL cells, they showed that *JAK2* mutation was the responsible for cell laminin adhesion via Lu/BCAM phosphorylation on serine 621. Furthermore, they demonstrated that Lu/BCAM phosphorylation was mediated by Rap1/Akt signaling and independent of EpoR expression. Altogether, their results suggested that increased adhesion of PV RBCs could be mediated by laminin-Lu/BCAM activation via an EpoR-independent Rap1/Akt signaling pathway activated by *JAK2V617F* (Figure 4).

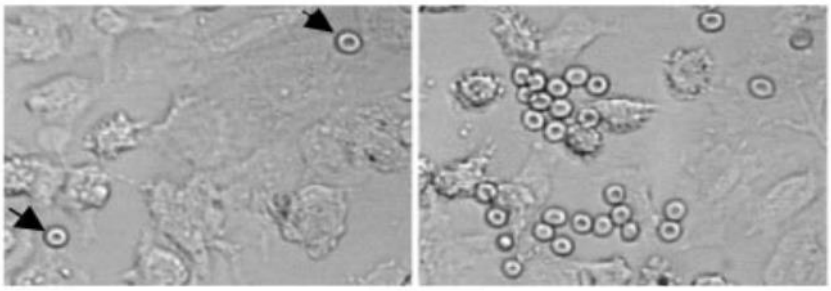


**Figure 3.** Microscopic image that shows that RBCs adhere more in PV patients than in normal subjects. (Wautier *et al.* (109))

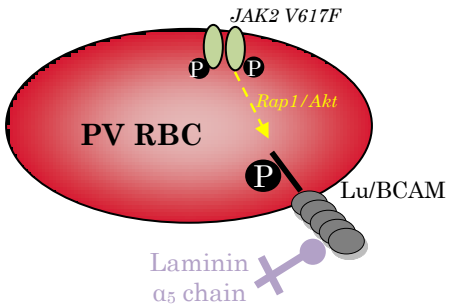


**Figure 4.** Diagram showing Lu/BCAM phosphorylation through *JAK2 V617F* – Rap1/Akt signaling pathway and its adhesion to laminin.

## PROTEOMICS, the proteome study

According to Wilkins *et al.* (111), the proteome is the ensemble of proteins expressed in a cell or a biological fluid and the term proteomics refers to the deep analysis of these proteins. Proteomic studies include detection, identification, quantification, and functional and structural characterization of proteins (112). It is an emerging strategy in the study of many human diseases because of its dynamic nature. Up to now, proteomic researches have been improving genomic studies which provide the analysis of more than 20,000 genes that constitute the human genome. Nevertheless, genomics just takes into account DNA information. It's a fixed view of cells that reflects their activated genes at a defined time. In addition, from one gene we can encounter various protein species due to post translational modifications and all different among them. Therefore, proteomics reveals information missed in genome analysis such as alternative splicing, allelic variations and post-translational modifications like phosphorylation, oxidation, ubiquitination and glycosylation. The proteome study better represents the impact of the environment on the function of cells than the picture of active genes.

### *PROTEOMIC METHODS*

Assuming that Western blotting or immunodetection still represent choice methods for investigation of a small number of proteins, nowadays, mass spectrometry has established itself as the standard method to identify and quantify, in the same run, very high number of proteins from a biological sample.

This technology, in continuous evolution, has provided tremendous results in the characterization of diverse proteomes thanks to the concomitant improvement of data processing tools.

It was in 1988 when Tanaka *et al.* (113) first could achieve a mass spectrum. Since then, different techniques have evolved to improve accuracy, sensitivity and specificity to identify and quantify the different molecules (114).

Mass spectrometry is based on the ionization of chemical compounds such as proteins, to generate gaseous charged molecules/fragments and to detect them depending on their

mass-charge ratio ($m/z$). This technique lets determine the molecule masses of free ions. Meanly, it is used to find out masses of particles or the composition of a sample.

A mass spectrometer analyzer is formed by three main elements (Figure 5):

-The **ion source**: where it takes place the gaseous ion formation. There are many types that differ on the ionization method. For instance, bombarding the sample by photons as the LDI technique (laser desorption/ionization), or by electron impact (EI) or ESI (Electro Spray Ionisation) where samples are sprinkle into an electrical field.

-The **mass analyzer**: where ions are separated according to their $m/z$ ratio. Analyzers can be coupled for tandem mass spectrometry (MS/MS) where the first analyzer will separate ions that then will pass through a collision cell that will fragment them. Finally, ion fragments will cross the second analyzer that will separate the ion fragments. Some of these analyzers are based on ion traps; magnetic and electric fields; or flight time as the Time-Of-Flight (TOF) spectrometers.

-The **detector**: It detects ion arrival and measures the quantity of ions providing data for calculating the abundances of each ion. These data are transformed into a spectrum where each pick represents the mass and quantity (intensity) of an ion.

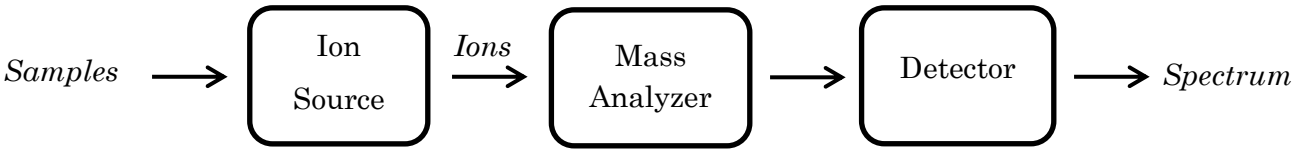


**Figure 5.** Mass spectrometer analyzer schema. Samples enter the ion source where they are ionized and throw to the mass analyzer that is coupled to the detector that will give a spectrum with the results.

In this research, two different mass spectrometers were used: SELDI-TOF MS and LC-MS/MS coupled to LTQ Orbitrap.

*SELDI TOF MS* (115)

Surface-enhanced laser desorption/ionization mass spectrometer (SELDI-TOF MS) is composed by three main instruments: protein chip arrays, mass analyzer and data analysis software. It is based on the principle that proteins are captured on a solid-phase protein chip surface and ionized with a nitrogen laser to measure their molecular masses according to their times-of-flight; (Figure 6).

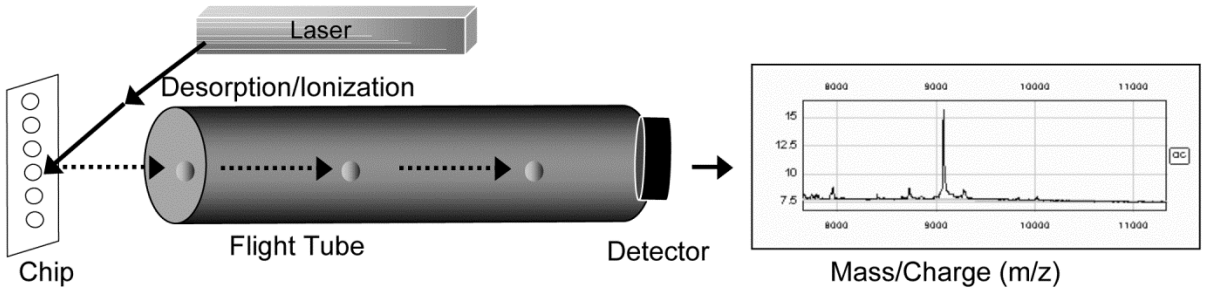


**Figure 6.** Schema of SELDI-TOF MS process: proteins are placed on chips, ionized and detected on the MS. Molecular masses are calculated according to their times-of-flight.

*Protein chip arrays*

They are active surfaces that retain all classes of proteins. These arrays are made of aluminum strip with spots composed of a chemically or biochemically modified active surface, Figure 7. These surfaces are specially designed to retain proteins according to a general or specific physicochemical property of proteins.

For example, in our study we used a weak anionic surface called: ProteinChip® CM10 array that is known to interact with cationic proteins.

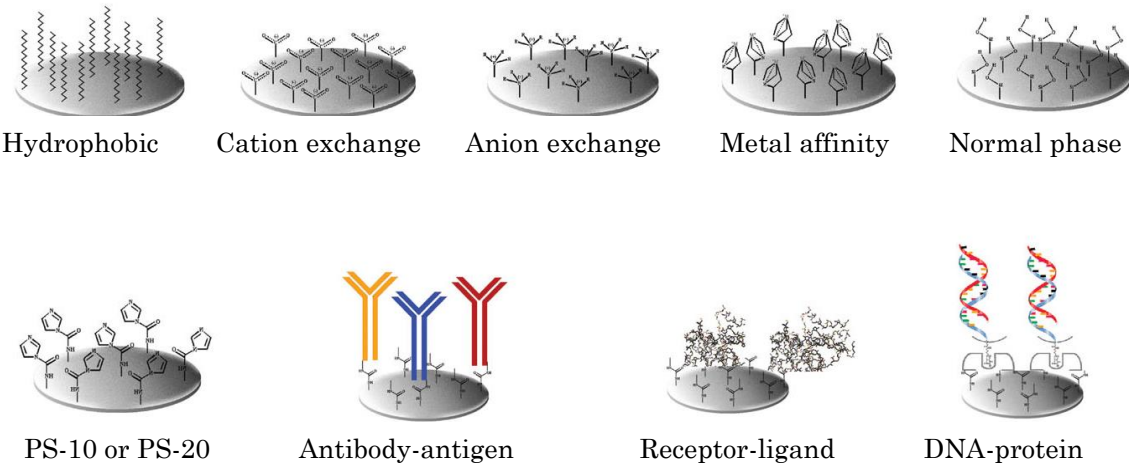


**Figure 7.** Different types of SELDI surfaces.

*Mass analyzer*

Once proteins are retained on the chip surface, a matrix solution is added and proteins can be then desorbed/ionized by a pulsed, UV, nitrogen laser. These ions are accelerated by an electro-static field during a short laser pulse. They leave the source and pass through a field-free drift region under vacuum where they are separated depending on their $m/z$ ratio towards the ion detector. This occurs because of the fact that ions are accelerated with different velocities according to their mass-charge values. Therefore, knowing the acceleration voltage and the length of the drift region, the $m/z$ ratio can be determined by measuring the flight time. Large ions with high $m/z$ values, reach the detector later than smaller ones. Ions with identical masses start with a certain energy spread which affects to the peak width.

*LC MS/MS* (116)

Liquid chromatography-tandem mass spectrometry consists of two mass filters in tandem separated by a collision cell. The sample is ionized in the source. The most typical ionization sources are electrospray ionization and atmospheric pressure chemical ionization. Ions pass into the first mass filter which continues with a collision chamber followed by the second mass filter that ends in the detector. (Figure 8)

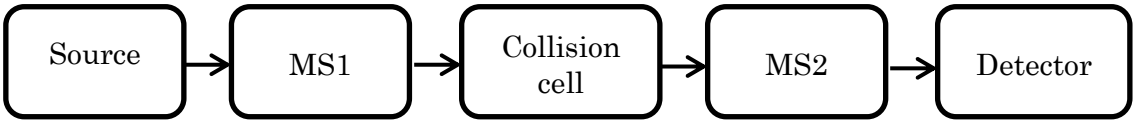


**Figure 8.** Tandem mass spectrometry schema.

LC-MS/MS provides analytical specificity and high throughput (capacity, efficiency). Nevertheless sensitivity is not its strong point. In our case, we used LC-MS/MS coupled to an LTQ-Orbitrap Velos mass spectrometer.

*LTQ-ORBITRAP*

The LTQ-Orbitrap is a mass spectrometer with two electrodes, one external and another one internal which create an electrostatic champ. Ions are produced by an electrospray ion source; then they go through the source and pass into the storage quadrupole. It is an ion accumulator that when a sufficient number of ions have been stored, the storage is opened and ions are injected into the Orbitrap with a velocity perpendicular to the long axis. It gives the ions potential energy that they use to start axial oscillations around the inner electrode. On the one hand, ions of the same $m/z$ ratio move around the inner electrode in the long axis for thousands of oscillations. On the other hand, in the radial direction, ions do not have the same oscillation magnitude. After this radial dephasing, the ion packet of a determinate $m/z$ takes a ring shape. It moves from one half of the outer electrode to the other one creating a signal which is detected and analyzed by adequate software. Figure 9.

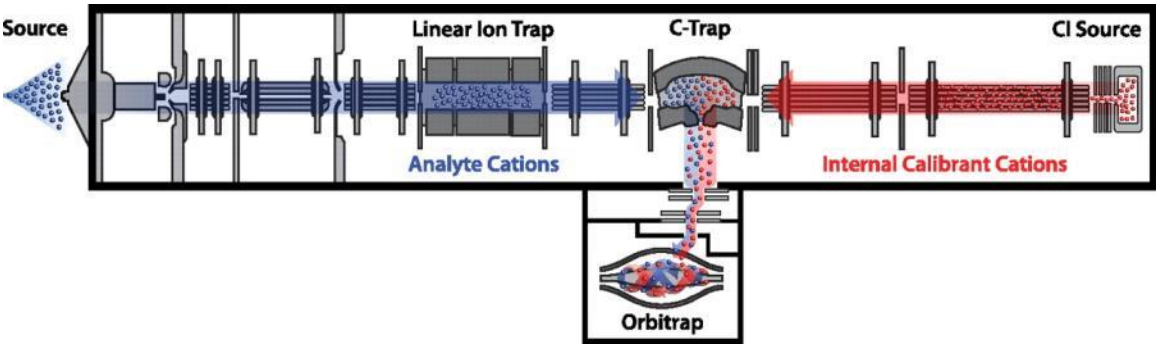


**Figure 9.** LTQ-orbitrap mass spectrometer diagram. Samples are ionized and throw through the linear ion trap where they will be separated and launched through the Orbitrap. Then they will arrive to the mass spectrometer detector.

.

Nowadays there are plenty of different types of mass spectrometers which differ on the way they ionize samples, on the method used to separate ions and the way to detect them. The choice depends on the desired result. For instance, we first used SELDI-TOF-MS as it permits to screen lots of clinical samples in a short time. It is usually used for disease biomarker identification as it generates proteome patterns from biological fluids and compares them to recognize unique biomarkers related to a particular disease with just few amounts of sample. Nevertheless, this technique has not yet been successful in studying high-molecular-weight proteins and it does not have enough specificity. Therefore, we used it as a screening tool so as to classify samples according to their content of proteins of different masses (proteome profile).

Once samples were analyzed by SELDI-TOF MS, we selected the richest ones to be analyzed by LC-MS/MS which provides more specificity.

## ERYTHROCYTE PROTEOME

Red blood cells or erythrocytes are myeloid mature blood cells specialized on carrying oxygen from lungs to all tissues. They are biconcave disks that remain around 120 days in blood circulation. In the bone marrow, pluripotent hematopoietic stem cells differentiate to create common myeloid progenitors that evolve to megakaryocytic/erythroid progenitors. These ones, thanks to specific growth factors, differentiate into erythroid burst forming units (BFU-E) and erythroid colony forming units (CFU-E) which evolve to intermediate forms of proerythroblasts and then to early and late erythroblasts. Finally, enucleation yields to reticulocytes which leave from the bone marrow to the peripheral blood and end in mature erythrocytes. At last stages of maturation, they have already lost some organelles such as mitochondrias; however large amounts of RNA assure the complete synthesis of hemoglobin to assure the main function of RBCs, the oxygen transport (117, 118).

Despite hemoglobin (Hb) is well known to be the main protein in these cells, the study of all the proteins that remain in RBCs, even if they are inactivated because of useless, represents a curiosity. Indeed, many proteins are expressed in red blood cells to assure various mandatory functions for RBC integrity as initiation and maintenance of glycolysis, cation pumping against electrochemical gradients, synthesis of glutathione and other metabolites, nucleotide catabolism reactions, maintenance of Hb iron in its ferrous state, protection of enzymatic and structural proteins from oxidative denaturation and preservation of membrane phospholipid asymmetry. In this context, the investigation of this "hidden proteome" should be clearly informative. Actually, the study of RBC proteome is a challenge as hemoglobin comprises 97% of whole proteins and it masks many low abundant proteins. First attempts to characterize the RBC proteome could identify a total of 181 proteins (half from the membrane and half from the cytoplasm) using ion trap tandem mass spectrometry coupled to liquid chromatography (119). Nevertheless, a huge amount of proteins remained hidden by hemoglobin. Thus, next approaches pre-fractionated RBC samples to deplete hemoglobin and enrich lysates in low abundant proteins. Bhattacharya *et al.* (120) depleted hemoglobin by cation exchange chromatography. Using 2D gels, they showed how Hb depletion let them visualize more than 600 spots that weren't visible before the chromatography step. Ringrose *et al.* (121) took advantage of the high Nickel-hemoglobin affinity to successfully deplete Hb by nickel (II) columns. They also depleted

carbonic anhydrase-1, which represents 1% of total erythrocyte proteome, by ion exchange chromatography. Coupling both techniques let them identify 677 proteins by LTQ-FT-ICR MS/MS.

Some commercial kits for hemoglobin depletion are available such as Hemoglobind™ and HemoVoid™. Hemoglobind™ is based on a solid-phase that specifically binds hemoglobin. Alvarez Llamas *et al.* (122) could identify a total of 34 proteins from the cytosolic fraction of RBCs thanks to this method coupled to LC-MS/MS. HemoVoid™ is a silica-based matrix support that has multiple surfaces: hydrophobic, ionic, aromatic and polymer combinations. These ligands bind a huge range of proteins and whereas high abundant proteins such as hemoglobin fast saturate their binding sites, low abundant ones continue binding other ligands. Thanks to this depletion, Walpurgis *et al.* (123) could identify a total of 189 proteins by down-stream 2D PAGE analysis coupled to Orbitrap MS.

Another method, the ProteoMiner™, consists on beads coupled to a library of either amino-terminal hexapeptides or carboxylated peptides. This technique is based on the fact that each porous bead contains billions of copies of a unique hexapeptide ligand on its surface and each hexapeptide of each bead differs from the other ligands (of the other beads). The result is a library of millions of beads, each one with a different hexapeptide. Proteins theoretically have affinity for one or more beads. Therefore, high abundant proteins will soon saturate their binding sites meanwhile low abundant proteins will have their binding sites available. Once the excess of non-bound proteins is eliminated, samples result in an enrichment of low abundant proteins (Figure 10) (124). Thereby, Roux-Dalvai *et al.* (117) could identify a total of 1524 proteins by LC-MS/MS coupled to LTQ-Orbitrap from RBC lysates that had previously been treated by ProteoMiner™.

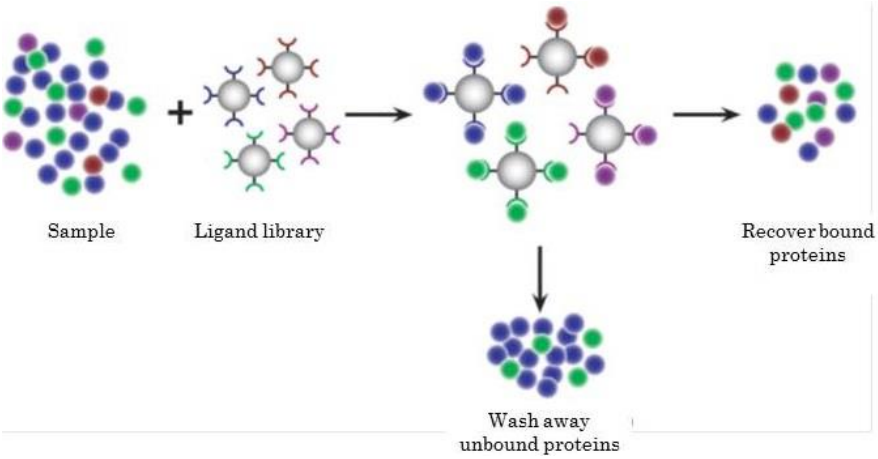


**Figure 10.** Sample enrichment in low abundant proteins. Samples are incubated with beads coupled to different ligands. Washes remove unbound proteins. Elution will let recover bound proteins (125).

Recently, a new technique has been validated by Zaccaria *et al.* (126) for the enrichment of low-abundant proteins in RBC lysates. This method, derived from the ProteoMiner™, is founded on magnetic nanoparticles (10-200 nm) with a chemical surface which will interact with the proteins in the biological samples depending on the nature of the proteins. For instance, nanoparticle surfaces may be modified by varying porosity, surface charges and functional chemical groups such as hydrophobic residues or acids) (127). As a result of this interaction between proteins and chemical surface a "corona" is formed around the nanobeads.

Thanks to the preanalytical treatment of RBC lysates with these magnetic nanoparticles, Zaccaria *et al.* (126) could identify 909 proteins by nano-LC-MS/MS from erythrocyte lysates. They showed how the proportion of high abundant proteins, and specifically Hb, had decreased in their samples as long as the proportion of low abundant proteins rose. The big advantage of this approach in comparison with ProteoMiner is its huge efficiency in low volume samples (they used 200 µL = 1 mg of RBC lysate whereas Roux-Dalvai *et al.* (117) used 200 mg). Other advantages are easy suspension, large surface area, slow sedimentation and uniform distribution of the particles in the suspension media. Moreover, thanks to their multi-domain core, they can be easily isolated by an external magnet. Another advantage is the possibility to make quantitative comparison of clinical samples after enrichment in minor proteins with high reproducibility (126).

As hemoglobin depletion technique in this research, I chose the magnetic nanoparticle fluidMAG-Q from Chemicel GmbH (Berlin, Germany) (Figure 11). It is a 200 nm particle in aqueous suspension with a positive surface. Its principal characteristics are summarized in Table 2.

| *NP* | *FluidMAG-Q* |
|---|---|
| **Application** | Strong anion exchanger |
| **Core** | Magnetite |
| **Matrix** | Poly (diallyldimethil-ammonium chloride) |
| **Functional group** | Quaternary amine group ($R_4N^+$) |

**Table 2.** Principal characteristics of fluidMAG-Q

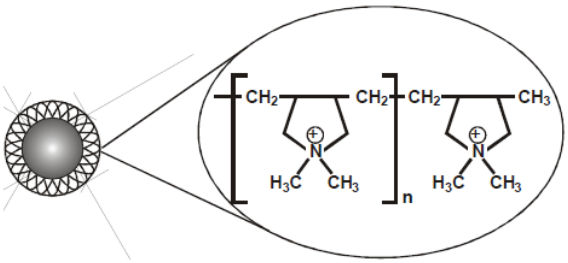


**Figure 11.** FluidMAG-Q

# OBJECTIVE

## OBJECTIVE

The main objective of my work was to perform an investigation of protein alterations associated with Ph- MPNs. To fulfil this goal, we developed an integrative proteomic strategy based on high output mass spectrometry together with specific protein identification by western blotting. These approaches let us characterize and quantify proteome variations leading to functional alteration of pathways that could be involved in MPN pathogenesis.

We explored the three "classical" Ph- MPNs in comparative analysis to identify either common alterations associated with MPNs or specific abnormalities of each MPN. We also integrated our data according to patient's genotype so as to better characterize protein dysfunctions related to the two main driver mutations *JAK2V617F* and *CALR* (ins/del).

This strategy was applied on two types of cells being directly impacted by clonal proliferation of hematopoietic stem cells, the erythrocytes and the granulocytes.

Finally, we evaluated the results of Ph- MPN red blood cell deregulation of IQGAP1/Rho GTPase signaling in a model of transfected Ba/F3 cell lines expressing high levels of JAK2 (wild type or V617F) to investigate the specific impact of *JAK2* mutations and the interest of therapies targeting JAK-STAT signaling for the regulation of this pathway.

# CHAPTER I

# Ph-negative MPN red blood cells display deregulation of IQGAP1-Rho GTPase signaling depending on *CALR/JAK2* status

## BACKGROUND

Red blood cells remain the "poor relation" of MPN researches. In absence of nuclear and nucleic acids, they avoid molecular investigations and consequently we lack information about these cells even though they represent the ultimate cells accumulating from clonal erythroid progenitors in MPNs. Hyperviscosity consequences due to their increased number in PV, clearly illustrates their pathogenic potential. Moreover, as red blood cells are the main cellular component of blood, they represent a huge "sponge" that is able to interact with and to adsorb plasma proteins released by damaged tissues giving biomolecular information about peripheral disturbances as inflammation or cell lysis. Therefore, they could be considered as witnesses of serum proteome modifications associated with diseases (126, 128).

In this context, we tried to characterize protein deregulations in erythrocytes of Ph-MPN patients and to identify functional alteration of specific pathways that could be involved in MPN pathogenesis. High amounts of hemoglobin in RBCs, being a huge impediment, we used a validated new-published technique based on ferromagnetic particles covered by chemical surfaces that permits the enrichment in low-abundance proteins and hemoglobin depletion (126).

## MATERIALS AND METHODS

### *Patients*

All patients came from the clinical hematology department of the Grenoble University Hospital (CHU Grenoble) and were classified according to the 2008 WHO criteria (2) including molecular investigation of *JAK2* (*V617F, exon 12*); *MPL* and *CALR* mutations and endogenous colony formation (erythroid and megakaryocytic colonies).

For the quantitative mass spectrometry (MS) analysis, a first set of samples (training set) was selected including 10 PV, 9 ET and 12 control samples. In order to validate by Western blotting (WB) the data obtained by quantitative MS analysis, we selected a new independent set of 14 MPN samples comprised of 7 PV (PV1 to PV7) and 7 ET (ET1 to ET7). This set was referred to as the "retrospective set". Samples from the training and the retrospective set were erythrocytes that had been cryoconserved at diagnosis (after ficoll gradient centrifugation for separation of granulocytes) in the center of biological resources of the CHU Grenoble with informed consent of patients. Next, to validate WB data obtained on the retrospective set and to avoid the possible bias induced by cryoconservation of red blood cells before lysis for protein extraction, we prospectively performed, on new patients with a suspicion of MPN, a special collection of erythrocyte lysates of fresh red blood cells obtained at the initial diagnosis consultation and lysed by hypotonic shock; (for the procedure of RBC preparation see below). Thereby, after diagnosis confirmation, we could select a prospective set of 16 samples including 8 PV (PV8 to PV15), 7 ET (ET8 to ET14) and 1 primary myelofibrosis (PMF). 12 samples were *JAK2V617F* and 4 *JAK2* wild type (WT) (ET8, ET11, ET14 and PV15). At the same time, when we collected the prospective set, we also selected a group of 10 control patients called control set and named C1 to C10. Finally, for the investigation of *CALR* mutations, we selected an additional set of 6 ET patients positive for this mutation (insertions or deletions). This set was referred to as the "calreticulin set".

### *Erythrocyte and Protein Preparation*

RBCs from peripheral blood were separated from polynuclear and mononuclear cells by ficoll gradient centrifugation. Cryoconserved erythrocyte samples from the training,

retrospective and calreticulin sets were lysed by repetitive freeze/thaw cycles followed by centrifugation at 36,000 g for 10 min to separate the red cell pellet. Supernatants containing the protein extracts were cryoconserved at -80°C before MS or WB analysis. All these samples were lysed at the same time to limit inter-experiment bias. Concerning RBCs of the control and prospective sets, the lysis was directly performed on fresh cells obtained after separation by ficoll gradient centrifugation of peripheral blood. RBCs were lysed by hypotonic shock with distilled water in the presence of protease and phosphatase inhibitors (cOmplete, EDTA-free and phospho-STOP, Roche). After centrifugation at 36,000 g for 10 min, the protein extract of the supernatant was stored at -20ºC before WB. All protein extracts were quantified by BIORAD DC™ protein assay.

### *Magnetic Nanoparticle Hemoglobin Depletion*

FluidMAG-Q (4112) was obtained from Chemicell GmbH, Berlin, Germany. RBC lysates from the training, retrospective and calreticulin sets were incubated with magnetic nanoparticles immediately after thawing. Nanoparticle incubation of the RBC lysates from the prospective and control sets was performed directly after the last centrifugation of fresh blood cells. Incubation was done as previously described by Villanueva *et al.* (129) (Figure I-1). Briefly, samples (500 µL) were mixed with 500 µg of nanoparticles (20 µL) and 500 µL of 1x PBS buffer solution (137 mM sodium chloride, 10 mM sodium phosphate, 2.7mM potassium chloride and 1.8 mM potassium phosphate, pH 7.4). The mix was incubated for 1 hour at room temperature in movement up and down. Then, samples were centrifuged 2 minutes at 9,500 g and supernatants were removed putting the tubes in a magnetized grille (MagnetoPURE, Chemicell GmbH, Berlin, Germany). Pellets were washed twice with buffer solution 1x PBS and twice with distilled water. Elution was carried out by 50µL of 2X Laemmli sample buffer (4 % SDS, 20 % glycerol, 10 % 2-mercaptoethanol, 0.004 % bromophenol blue, 0.125 M Tris HCl) and incubated one hour under gentle agitation. Samples were centrifuged and put on the magnetized grille to recover the supernatants.

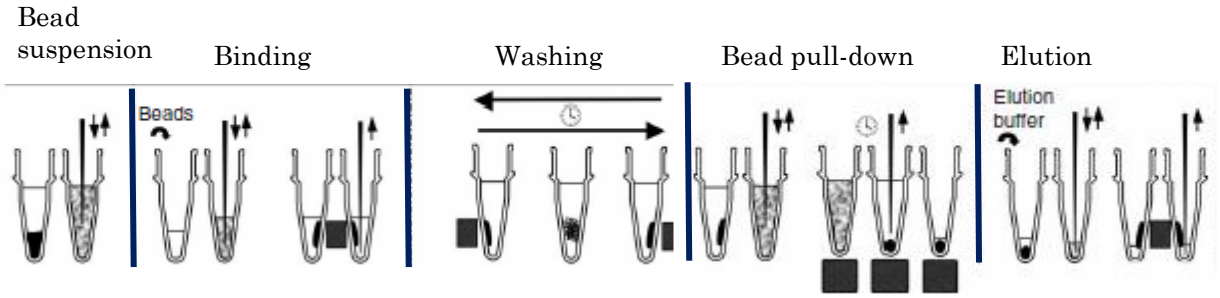


**Figure I-1.** Nanoparticle incubation schema. Samples are incubated with magnetic nanoparticles for one hour. After centrifugation and thanks to a magnetized grille, supernatants are removed and discarded. Then, beads are washed three times before incubation with elution buffer for one hour. Finally, samples are centrifuged and supernatants are recovered.

### *Proteomic Analysis*

Quantitative proteomic analysis was made by LC MS/MS (LTQ Orbitrap). Ten micrograms of RBC lysates were run on SDS-PAGE gel electrophoretic migration. The stacking bands were cut and washed in 100 mM ammonium bicarbonate. Cysteines were reduced and alkylated by 10 mM DTT (Dithiothreitol) for 35 min at 56 °C followed by 55mM iodoacetamide for 30 min at room temperature in the dark. Additional washing cycles were then performed and proteins were digested by modified sequencing grade trypsin (Promega) in ammonium bicarbonate overnight at 37°C. The resulting peptides were extracted from the gel by incubation in ammonium bicarbonate followed by two incubations in 10 % formic acid, acetonitrile (1:1). The three extracts were pooled with the initial supernatant, dried in SpeedVac, and resuspended with 5 % acetonitrile, 0.05 % trifluoroacetic acid. Peptide mixtures were analyzed by nano-LC-MS/MS using an ultimate3000 system (Dionex, Amsterdam, The Netherlands) coupled to an LTQ-Orbitrap Velos mass spectrometer (Thermo Scientific, Bremen, Germany). Samples were loaded on a C18 precolumn (300 µm inner diameter X 5 mm; Dionex) at 20 µl/min in 5 % acetonitrile, 0.05 % trifluoroaetic acid. After desalting, the precolumn was switched on line with the analytical C18 column (75 µm inner diameter X 15 cm; PepMap C18, Dionex) equilibrated in 95 % solvent A (5 % acetonitrile, 0.2 % formic acid) and 5 % solvent B (80 % acetonitrile, 0.2 % formic acid). Peptides were eluted using a 5-50 % gradient of solvent B during 80 min at a 300 nL/min flow rate. The LTQ-Orbitrap was operated in data-dependent acquisition mode with the Xcalibur software. Survey scan MS spectra (m/z mass range 300-2000) were acquired in the

Orbitrap with the resolution set to a value of 60,000 at m/z 400 (AGC target value of $1x10^6$ charges). The five most intense ions per survey with a charge state greater than one were selected for collision-induced dissociation (CID) fragmentation, and the resulting fragments were analyzed in the linear trap (LTQ). Collision energy was set to 35% for MS/MS. Dynamic exclusion was used within 60 s to prevent repetitive selection of the same peptide.

*Protein identification and quantification*

Data were searched against all entries in the International Protein Index (IPI) human v3.34 protein. For protein quantification, we used Mascot File parsing and Quantification (MFPaQ) version 4.0. Protein hits were validated when they satisfied one of the following criteria:

A) Identification with at least one top ranking peptide of a minimal length of 5 amino acids and with a Mascot score higher than the identity threshold at p=0.001 (99.9 % probability),

B) or at least two top ranking peptides each of a minimal length of 5 amino acids with a Mascot score higher than the identity threshold at p=0.05 (95 % probability).

When several proteins matched exactly the same set of peptides, only one of them was reported in the final protein lists. Furthermore, homologous Mascot protein hits were validated and included in the final list only if they were additionally assigned to a specific top ranking peptide with Mascot score higher than the identity threshold at p=0.001.

Quantification of peptide ions was based on calculated extracted ion chromatogram (XIC) areas values. To compare the abundance of different proteins or to represent the abundance profile of one protein in different samples, a protein abundance index (PAI) was calculated defined as the average of XIC area values for three intense reference tryptic peptides identified for this protein.

*Biomarker selection*

After protein identification and quantification, means of the area values from the same peptide were compared using *student's t* tests. Means were defined as significantly

different when unequal T-test was lower than the t references for a confidence interval=95% and the ratio between the two means was above 2 or below 0.5.

*Functional analysis*

LC-MS/MS results were loaded on *Ingenuity Pathway Analysis* (*IPA*) software. It enabled us to identify, analyze and understand the whole data. It helped us to know in which biological pathways the identified proteins participate; which of the proteins interact with each other directly or through intermediate molecules; which upstream regulators can explain their expression pattern; which downstream diseases or processes are likely increased or decreased by the increase or decrease of the abundance of these proteins and the effects of possible protein modifications.

*Statistical analysis*

Mean comparison was performed by *student's t* test by GraphPad Prism software with a confidence interval of 95 %.

### *Western-Blotting*

Samples were heated 5 minutes at 95°C. Next, they were run on SDS-PAGE gels and transferred to nitrocellulose membranes for 1 hour. Blocking was carried out with TBS-Tween 20 - 5% skimmed milk for 1 hour at room temperature and incubated with primary antibodies diluted in TBS-Tween 20 - 1% skimmed milk overnight at 4°C. Then, membranes were incubated with Horseradish peroxidase (HRP) labeled secondary antibodies during 90 minutes at room temperature. Development was made with ECL (enhanced chemiluminescent) Western Blotting Substrate from Pierce. β-actin was used as loading control.

### *Immunoprecipitation*

250 µL of RBC lysates were incubated 1 hour at 4°C under gentle agitation with the corresponding primary antibodies. Later, 50 µL of protein A/G PLUS agarose beads or

protein A agarose beads (Santa Cruz Biotechnology) were added and incubated 1 hour at 4°C under agitation. Three washes were done with lysis buffer (1 % NP-40, 10 mM KCl, 10 mM HEPES, 0.1 mM EDTA + protease and phosphatase inhibitors) and centrifuged 1 minute at 4°C at 800 g. Supernatants were discarded and beads were eluted with 50 µL of 2x Laemmli Buffer with 2-mercaptoethanol heating 5 minutes at 95°C. After centrifugation, supernatants were recovered and analyzed by western blotting. Rac1, Cdc42 and Rho protein activation was determined by pull-down assays incubating with GST-PAK-PBD beads or GST-Rhotekin-RBD beads (Cytoskeleton, Inc.). GST-PAK-PBD contains residues 67-150 of PAK, which corresponds to the CRIB motif - required for the high affinity interaction with GTP-Rac and GTP-Cdc42. GST-Rhotekin-RBD contains residues 7-89 of Rhotekin needed for the interaction with GTP-Rho. Control RhoA, Rac1, Cdc42 and Rho-GDI were produced as described by Ligeti *et al.* (130).

### *Antibodies*

-Primary antibodies: rabbit polyclonal anti-IQGAP1 (H-109) antibody (sc-10792) and mouse monoclonal anti-β-Actin-HRP (C4) antibody (sc-47778) were from Santa Cruz Biotechnology; mouse IgG1 anti-Cdc42 (610928) and mouse IgG2b anti-Rac1 (610651) were from BD Biosciences; rabbit monoclonal anti-JAK2 (D2E12) XP® antibody (#3230), rabbit monoclonal anti-phospho-JAK2 (Tyr1007/1008) (C80C3) antibody (#3776), rabbit monoclonal anti-phospho-PAK1 (Thr423)/PAK2 (Thr402) antibody (#2601) and rabbit monoclonal anti-PAK1 antibody (#2602) were from Cell Signaling Technology. Mouse monoclonal anti-IQGAP1 antibody, clone AF4 (#05-504) and rabbit monoclonal anti-calreticulin antibody, clone EPR3924 (#MABT145) were from EMD Millipore.

-Secondary antibodies: Goat anti-mouse IgG-HRP antibody (sc-2005) and goat anti-rabbit IgG-HRP antibody (sc-2004) were from Santa Cruz Biotechnology. Protein A full-length protein (Ab7456) was from Abcam.

### *Rac1Q61L-GST Protein Production*

*E. coli* cells transformed with pGEX-Rac1Q61L plasmid were cultured in Luria Broth medium with 100 µg/mL ampicillin at 37°C. The lac operon was activated by adding 0.5 µM

of IPTG (Isopropyl β-D-1-thiogalactopyranoside) during 3 hours at 37°C under gentle agitation. Cell suspension was centrifuged 10 minutes at 2,000 g at 4°C. Supernatant was discarded and the cell pellet was washed and resuspended in 1x PBS (with protease inhibitors). Cell lysis was done by 3 cycles of 10 seconds of sonication at 60W at 4°C followed by ultracentrifugation (40 minutes at 100,000 g at 4°C). The recombinant protein was harvested in the supernatant. Next, it was incubated with Glutathione Sepharose beads (GE Healthcare) for one hour at 4°C, washed three times with 1x PBS, centrifuged at 500 g for 5 minutes and stored in a solution of 1x PBS-10% glycerol 1:1.

### *KG1 and K562 Lysates*

K562 cells are an erythroleukemia cell line derived from a chronic myeloid leukemia patient in blast crisis. KG1 cells are also a cell line that comes from a bone marrow patient with erythroleukemia evolving to acute myelogenous leukemia. Cell lines were washed three times in 1x PBS, lysed with lysis buffer (20 µL/million cells) (50 mM HEPES - pH 7.5, 5 mM $MgCl_2$, 1 % Triton X-100, 10 µg/µl Leupeptine and protease inhibitors) for 20 minutes at 4°C, centrifuged 10 minutes at 1,000 g and quantified by BIORAD DC™ protein assay.

# RESULTS

## *1-RBC proteome of MPN patients display specific alterations of protein expression*

Quantitative analysis by LC MS/MS – LTQ Orbitrap let us identify and quantify a total of 1019 proteins. S*tudent's t* tests were calculated to ascertain if there were significant differences in protein expression between the different groups of patients. Results showed that:

-51 proteins were overexpressed in PV patients compared with controls.

-85 proteins were overexpressed in ET patients compared with controls.

-15 proteins were overexpressed in controls compared with PV patients.

-50 proteins were overexpressed in controls compared with ET patients.

-2 proteins were overexpressed in PV compared with ET patients.

-14 proteins were overexpressed in ET compared with PV patients.

In all cases, we considered a ratio > 2 with *student's t* test p-values lower than 0.05. Moreover, we also compared protein profiles of *JAK2(+)* PV and ET patients with *JAK2(-)* ET patients. We found 17 proteins overexpressed in *JAK2* positive PV patients compared with *JAK2* negative ET ones; and 11 overexpressed in *JAK2* negative ET patients compared with *JAK2* positive PV ones (ratio>2; p-value<0.05). We also found 9 proteins overexpressed in *JAK2* positive ET patients compared with *JAK2* negative ones; and only 2 proteins were overexpressed in *JAK2* negative ET patients compared with *JAK2* positive ET ones (ratio>2; p-value<0.05). The list of all proteins is accessible in Supplemental Data I-1.

Thanks to *IPA* software, we could evaluate which functional pathways were more affected by the deregulated proteins. (Lists of all deregulated pathways in Supplemental Data I-2). In general, examining PV vs controls and ET vs controls analysis; we remarked that the most deregulated proteins belonged to the RAS superfamily of GTPase signaling pathways; specially the Rho subfamily of GTPases (Table I-1). RABGGTA, RABEP-1 and IQGAP1 were the three proteins the most significantly overexpressed in both PV and ET patients compared with controls that belonged to the RAS GTPase family (Table I-2).

| PV vs Control | | | ET vs Control | | |
|---|---|---|---|---|---|
| Ingenuity Canonical Pathways | -log(p-value) | Ratio | Ingenuity Canonical Pathways | -log(p-value) | Ratio |
| RAN Signaling | 8,62E00 | 0.25 | Actin Cytoskeleton Signaling | 1,58E01 | 0.10 |
| Actin Cytoskeleton Signaling | 8,35E00 | 0.05 | Integrin Signaling | 9,41E00 | 0.07 |
| Integrin Signaling | 7,87E00 | 0.06 | VEGF Signaling | 8,17E00 | 0.11 |
| Regulation of Actin-based Motility by Rho | 4,63E00 | 0.07 | Regulation of Actin-based Motility by Rho | 7,77E00 | 0.11 |
| Protein Ubiquitination Pathway | 4,5E00 | 0.05 | ILK Signaling | 7,67E00 | 0.07 |
| Ephrin Receptor Signaling | 4,4E00 | 0.04 | RhoA Signaling | 7,65E00 | 0.10 |
| VEGF Signaling | 4,23E00 | 0.06 | RAN Signaling | 7,5E00 | 0.3 |
| Rac Signaling | 3,95E00 | 0.05 | Sertoli Cell-Sertoli Cell Junction Signaling | 7,12E00 | 0.07 |
| RhoA Signaling | 3,95E00 | 0.05 | Signaling by Rho Family GTPases | 6,74E00 | 0.05 |
| Axonal Guidance Signaling | 3,84E00 | 0.03 | Germ Cell-Sertoli Cell Junction Signaling | 6,7E00 | 0.07 |
| fMLP Signaling in Neutrophils | 3,75E00 | 0.05 | Rac Signaling | 6,61E00 | 0.08 |
| Signaling by Rho Family GTPases | 3,68E00 | 0.03 | RhoGDI Signaling | 6,4E00 | 0.06 |
| CD28 Signaling in T Helper Cells | 3,63E00 | 0.05 | Tight Junction Signaling | 6,18E00 | 0.07 |
| Corticotropin Releasing Hormone Signaling | 3,57E00 | 0.04 | Clathrin-mediated Endocytosis Signaling | 5,92E00 | 0.06 |
| Synaptic Long Term Potentiation | 3,49E00 | 0.05 | α-Adrenergic Signaling | 5,91E00 | 0.09 |
| Apoptosis Signaling | 3,37E00 | 0.05 | Protein Kinase A Signaling | 5,83E00 | 0.04 |
| Cdc42 Signaling | 3,37E00 | 0.03 | Coagulation System | 5,71E00 | 0.16 |
| ERK/MAPK Signaling | 3,36E00 | 0.03 | Cellular Effects of Sildenafil (Viagra) | 5,43E00 | 0.07 |
| Protein Kinase A Signaling | 3,3E00 | 0.02 | Mechanisms of Viral Exit from Host Cells | 5,28E00 | 0.01 |
| CD27 Signaling in Lymphocytes | 3,27E00 | 0.07 | FAK Signaling | 5,21E00 | 0.08 |
| Fcγ Receptor-mediated Phagocytosis in Macrophages and Monocytes | 3,19E00 | 0.05 | NRF2-mediated Oxidative Stress Response | 5,2E00 | 0.06 |

**Table I-1.** Top canonical deregulated pathways in PV or ET patients compared with controls. Pathways are ordered according to their p-value. Ratio means the number of molecules of the pathway that were found in our analysis (thus deregulated) in relation with the total number of proteins that belong to that pathway. Analysis was performed by *IPA* software.

| Protein ID | Gene name | Protein name | Ratio | p-value |
|---|---|---|---|---|
| IPI00022664 | RABGGTA | Rab geranylgeranyltransferase, alpha subunit | PV-ET/Control: ∞ | PV/C: 0.0001<br>ET/C: 0.0001 |
| IPI00412712 | RABEP1 | Rab GTPase-binding effector protein 1 or Rabaptin-4 or Rabaptin-5 or Rabaptin-5alpha | ET/Control: 2.2 | ET/C: 0.014<br>PV/C: 0.95 |
| IPI00009342 | IQGAP1 | Ras GTPase-activating like protein 1 | PV/Control: 2.2<br>ET/Control: 2.5 | PV/C: 0.047<br>ET/C: 0.0008 |
| IPI00299048 | IQGAP2 | Ras GTPase-activating like protein 2 | ET/Control: 1.8<br>ET/PV: 1.9 | ET/C: 0.0019<br>ET/PV: 0.003 |

**Table I-2.** Overexpressed proteins of the RAS family of GTPases.

### *2-IQGAP1 is overexpressed in MPN patients according to their JAK2 status*

In a first time, in order to verify mass spectrometry results, we tried to confirm LC/MS-MS data by western blotting of RABGGTA and RABEP-1 but we failed to confirm deregulation of these two proteins in MPN samples. However, according to *IPA* analysis, Rho GTPase pathways were the most disturbed among this big family so we chose to dig deeply on the overexpression of IQGAP1 due to its role as a scaffold protein among this subfamily.

We first performed western blot analysis of IQGAP1 expression in red blood cells of samples previously cryoconserved (the retrospective set) and, in a second time, to avoid bias potentially induced by cryoconservation we analyzed, as described in material and methods, fresh red blood cells from a new independent set of patients (the prospective and control sets). As shown in Figure I-2, IQGAP1 was expressed in almost all MPN patients at different levels in PV and ET patients without obvious variations between PV and ET. IQGAP1 was also found in globally all controls. In order to compare IQGAP1 expression between MPN patients and controls, IQGAP1/β-actin ratios were used to normalize IQGAP1 concentrations. Using *student's t* test, we confirmed that IQGAP1/β-actin ratios were significantly higher in MPN patients compared with controls. IQGAP1/β-actin mean ratio of all ET and PV patients (from both retrospective and prospective sets) was significantly higher compared with controls (p-value<0.01) (Figure I-3A and Supplemental Data I-3A).

When considering separately PV and ET, we didn't find significant differences between them but we remarked that IQGAP1 was also overexpressed in PV and ET patients compared with controls (respectively PV vs control set, $p<0.01$ and ET vs control set, $p<0.05$).

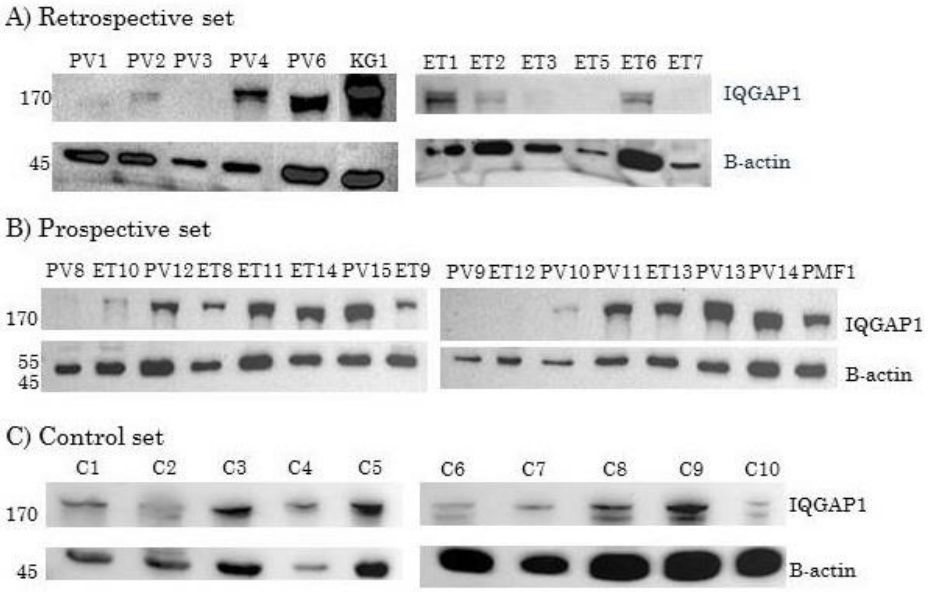


**Figure I-2.** IQGAP1 expression in retrospective, prospective and control samples. Samples were submitted to nanoparticle incubation followed by WB. B-actin acts as loading control and KG1 acts as positive control. Molecular weights of target proteins: IQGAP1 189kDa, β-actin 42 kDa. Patients: A) Retrospective set: PV1, PV2, PV3, PV4, PV5, PV6 and ET1, ET2, ET3, ET5, ET6 and ET7. B) Prospective set: *JAK2(+)*: PV8, PV9, PV10, PV11, PV12, PV13, PV14, ET9, ET10, ET12, ET13 and PMF1. *JAK2(-)*: ET8, ET11, ET14 and PV15. C) Control set: C1, C2, C3, C4, C5, C6, C7, C8, C9, and C10.

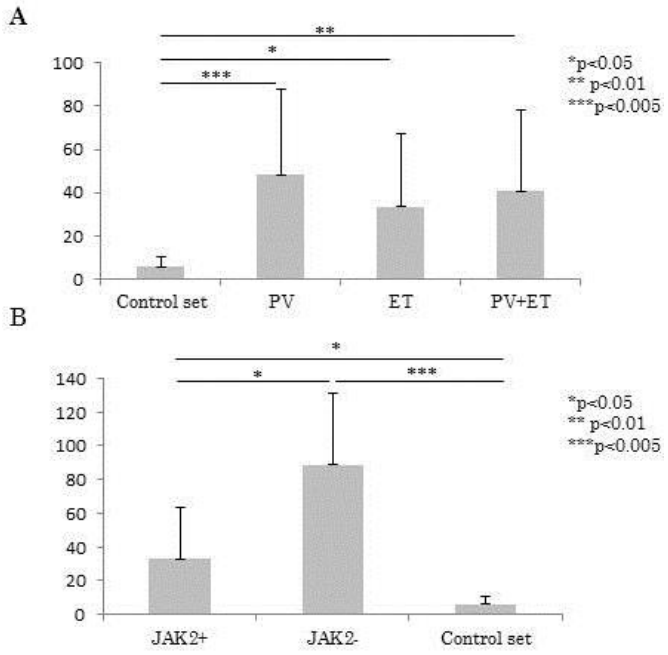


**Figure I-3. A)** Comparison of IQGAP1/β-actin ratio means according to different sets of patients. IQGAP1/β-actin ratio means are represented by bars with their respective standard deviations denoted by error bars. Comparative analysis is made by *student's t* test; (*p<0.05, ** p<0.01, ***p<0.005). **B)** Comparison of IQGAP1/β-actin rate means according to patients' genotype. IQGAP1/β-actin ratio means are represented by bars with their respective standard deviations denoted by error bars. Comparative analysis is made by *student's t* test; (* p<0.05, **p<0.01, **** p<0.0001). Patients: *JAK2(+)*: Retrospective set: PV1, PV2, PV3, PV4, PV5, PV6 and ET1, ET2, ET3, ET5, ET6 and ET7. Prospective set: PV8, PV9, PV10, PV11, PV12, PV13, PV14, ET9, ET10, ET12 and ET13. *JAK2(-)*: Prospective set: ET8, ET11, ET14 and PV15. Control set: C1, C2, C3, C4, C5, C6, C7, C8, C9, and C10.

Furthermore, we looked at IQGAP1 expression according to patient's genotype. MPN patients were regrouped as: *JAK2(+)* and *JAK2(-)* and differences of IQGAP1 levels were evaluated by s*tudent's t test* on IQGAP1/β-actin ratios. Figure I-3B showed that there were significant differences in IQGAP1 expression between *JAK2(+)* and control patients (p<0.01) as well as between *JAK2(-)* and control patients (p=0.0001). We highlighted that *JAK2(-)* patients expressed significantly higher levels of IQGAP1 than *JAK2(+)* ones (p<0.05). (Figure I-3B and Supplemental Data I-3B).

### *3-IQGAP1 interacts selectively with Rho GTPase proteins in MPN RBCs*

IQGAP1 is a scaffold protein known to interact with small GTPase proteins of the Rho family of GTPases. (131-138). Therefore, we checked if these interactions took place in red blood cells from MPNs. To this end, we immunoprecipitated RBC lysates of MPNs with IQGAP1 followed by western blotting using antibodies against Rac1, Cdc42, RhoA and RhoGDI, an inhibitor that binds Rho family GTPases.

Figure I-4 shows that IQGAP1 could form a complex with Rac1, Cdc42 and RhoA but not with RhoGDI in most of MPN samples independently of ET and PV diagnosis. In controls, immunoprecipitation assays showed that IQGAP1 was also able to co-precipitate with Rac1, Cdc42 and RhoA suggesting that IQGAP1 interaction with small Rho GTPase proteins is a functional pathway in normal erythrocytes.

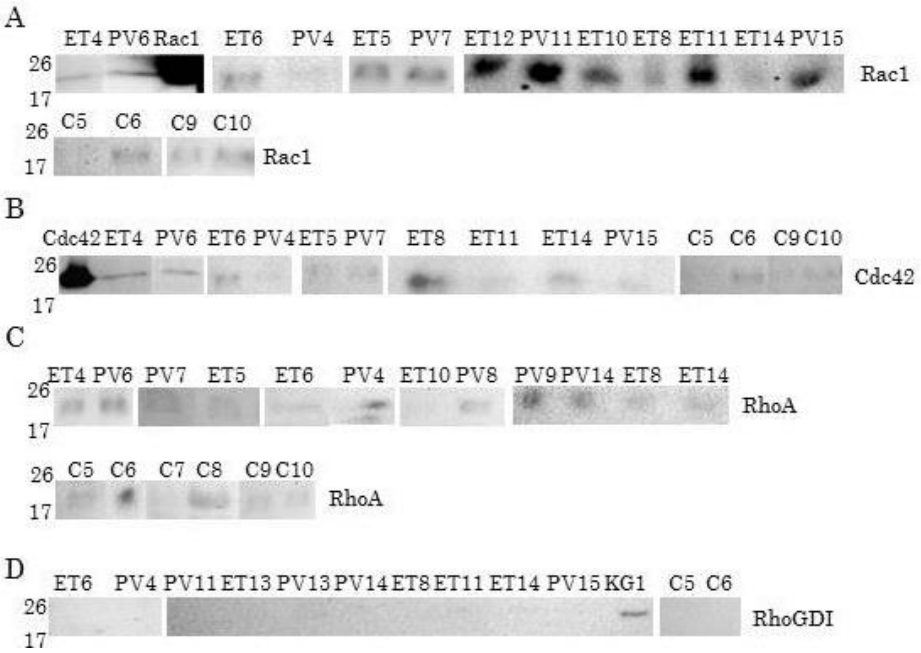


**Figure I-4.** IQGAP1 binding proteins in retrospective and prospective sets. RBC lysates were immunoprecipitated with IQGAP1 followed by WBs processed by Rac1 **(A)**, Cdc42 **(B)**, RhoA **(C)** or RhoGDI **(D)** antibodies. Molecular weights of targeted proteins: Rac1 21 kDa, Cdc42 21 kDa, RhoA 22 kDa, RhoGDI 23 kDa. Patients: Retrospective set: PV4, PV6, PV7, ET4, ET5 and ET6. Prospective set: *JAK2(+)*: PV9, PV11, PV13, PV14, PV8, ET10, ET12 and ET13. *JAK2(-)*: ET8, ET11, ET14 and PV15. Control set: C1, C2, C3, C4, C5, C6, C7, C8, C9, and C10.

When interacting with Rho GTPase proteins, IQGAP1 is known to prevent their inactivation (133), thus we verified the activated state of Rho GTPase proteins in our RBC lysates. To this end, we pulled-down RBC lysates from a small subset of ET and PV patients (n=2) with GST-Rhotekin-RBD and GST-PAK-PBD agarose beads so as to detect activated RhoA (GTP-RhoA) and activated proteins Rac1 and Cdc42 respectively. As shown in Figure I-5A, Rac1 is activated in both MPNs (ET and PV) but neither RhoA nor Cdc42. As these results suggested a particular link between IQGAP1 and activated Rac1, we used the recombinant protein Rac1Q61L-GST, which is constitutively activated, coupled to Sepharose beads to pull-down proteins that bind activated Rac1 protein (GTP-Rac1). This test corroborated IQGAP1/GTP-Rac1 bond as IQGAP1 precipitated with Rac1Q61L-GST in PV, ET and control samples (Figure I-5B).

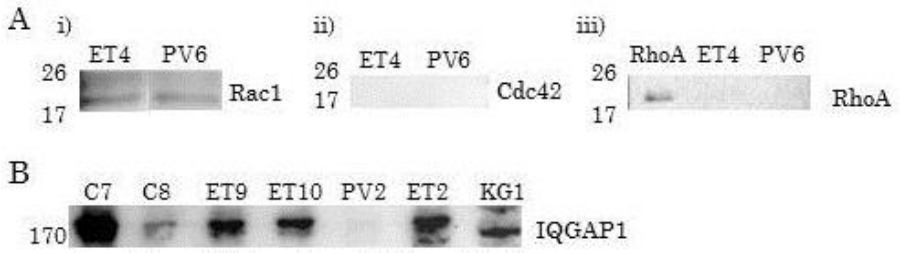


**Figure I-5.** Pull-down assays of activated proteins of the Rho family. **A)** Ras activated proteins. RBC lysates were immunoprecipitated with GST-PAK-PBD (Rac and Cdc42) or GST-Rhotekin-RBD (RhoA) agarose beads and eluted by Laemmli buffer. WBs were developed with Rac1, Cdc42 and RhoA antibodies. **i)** Rac1 is activated in ET and PV samples. **ii)** Cdc42 is not activated. **iii)** Samples are negative for activated RhoA. RhoA was used as positive control. Molecular weights of targeted proteins: Rac1 21 kDa, Cdc42 21 kDa, RhoA 22 kDa. **B)** GTP-Rac1 complexes. Rac1Q61L-GST coupled to Sepharose beads was used to precipitate proteins that bind GTP-Rac1. IQGAP1 was detected in all patients after Rac1Q61L-GST precipitation. Molecular weight of IQGAP1: 189 kDa. Patients: Retrospective set: PV2, PV6, ET2 and ET4. Prospective set: *JAK2(+)*: ET9 and ET10. Control set: C7 and C8.

P21-activated kinase 1 (PAK1) has been described as a Rac1 effector and it is upregulated in some cancers (139, 140). Hence, we were interested in studying its connection with Rac1 in MPNs. First, RBC lysates were incubated with fluidMAG-Q followed by western blotting so as to check PAK1 presence in erythrocytes. As seen in

Figure I-6A, PAK1 was detected in all MPN samples. Then, we treated RBC lysates with Rac1Q61L-GST Sepharose beads. Rac1Q61L-GST-Sepharose-bead blots showed that both PAK1 and phosphorylated-PAK1 bound GTP-Rac1 (Figure I-6B). Moreover, we showed that both Rac1 and IQGAP1 co-precipitated with PAK1 when using PAK1 antibody to immunoprecipitate RBC proteins (Figure I-6C). Therefore, these data demonstrated the presence of P-PAK1-Rac1 and PAK1-IQGAP1 complexes in MPN RBCs.

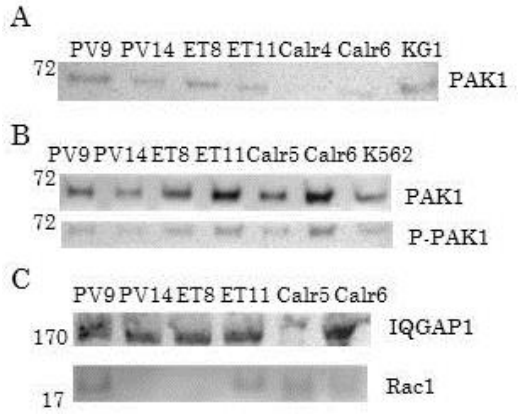


**Figure I-6. A)** PAK1 expression in MPN patients. RBC lysates were submitted to nanoparticle incubation followed by WB assays. Patients: MPN *JAK2(+)*: 12-27; *JAK2(-)*: 4-11, Calreticulin+ 4-6. KG1 acts as positive control. Molecular weights of target proteins: PAK1 60 kDa. **B)** GTP-Rac1 complexes with PAK1 and P-PAK1. Rac1Q61L-GST coupled to Sepharose beads was used to precipitate proteins in RBC lysates. It was followed by western blotting developed by PAK1 and Phosphorylated PAK1 (P-PAK1). **C)** PAK1 immunoprecipitations. RBC lysates were immunoprecipitated with PAK1 and labeled by IQGAP1 or Rac1 antibodies. Patients: Prospective set: *JAK2(+)*: PV9 and PV14; *JAK2(-)*: ET8 and ET11. Calreticulin+ set: Calr4, Calr5 and Calr6. Molecular weights of targeted proteins: PAK1 and P-PAK1: ~60 kDa, IQGAP1 189 kDa, Rac1 21 kDa. K562 and KG1 cells were used as positive controls.

### *4-Calreticulin but not JAK2 protein is expressed by MPN RBCs*

Recently, *CALR* mutations have been discovered in ET and PMF patients, (32, 33) and calreticulin (CALR) protein has been shown to be expressed in granulocytes (32, 141). However, any data exists about CALR expression in MPN red blood cells. In this context, we took advantage of our quantitative MS analysis of erythrocyte proteome to explore CALR

expression in our samples. We thereby found that CALR was effectively present in red blood cells without any significant differences in concentrations between controls, PV and ET patients according to MS results, (PV vs Controls, p=0.89; ET vs controls, p=0.65; PV vs ET, p=0.53). To confirm these data, we performed western blot assays in controls and MPN patients including *CALR* mutated (all ET patients, n=6) and *CALR* non mutated ones, (16 MPNs and 10 controls). These latter ones were PV and ET patients either *JAK2V617F* positive or *JAK2* wild type. Figure I-7A showed that CALR could be detected in almost all MPN patients independently of the presence or not of *CALR* mutation. *CALR(+)* patients seemed to express the highest levels of CALR protein but we could not see any double band in western blots, which theoretically appear in calreticulin-mutated samples and denote calreticulin insertions or deletions. *JAK2* positive and *JAK2* WT patients seemed to harbor the same profile of CALR expression. Finally, we found that control patients also expressed CALR protein (Figure I-7B).

To quantify and compare Calreticulin expression, we used β-actin to normalize Calreticulin concentrations and, in similarity with IQGAP1 blots, Calreticulin/β-actin ratios were calculated between different subsets of patients. As shown in Supplemental Data I-4, Calreticulin expression was not found to differ significantly between MPNs and controls (p=0.8). Among MPNs, we did not observe significant differences between *JAK2(+)* and *JAK2(-)* patients (p=0.35), nor between *JAK2(+)* or *JAK2(-)* and *CALR(+)* (p=0.81 and p=0.08) respectively. Our only finding was that Calreticulin expression differed almost significantly in ET patients between *CALR(+)* and *CALR(-)* (p=0.0560).

As JAK2 is one of the most important proteins implicated in unregulated cell proliferation in MPNs, we also verified its presence in RBC lysates but MS results didn't present any data for JAK2 expression which was confirmed by JAK2 western blots of RBC lysates (Figure I-7C).

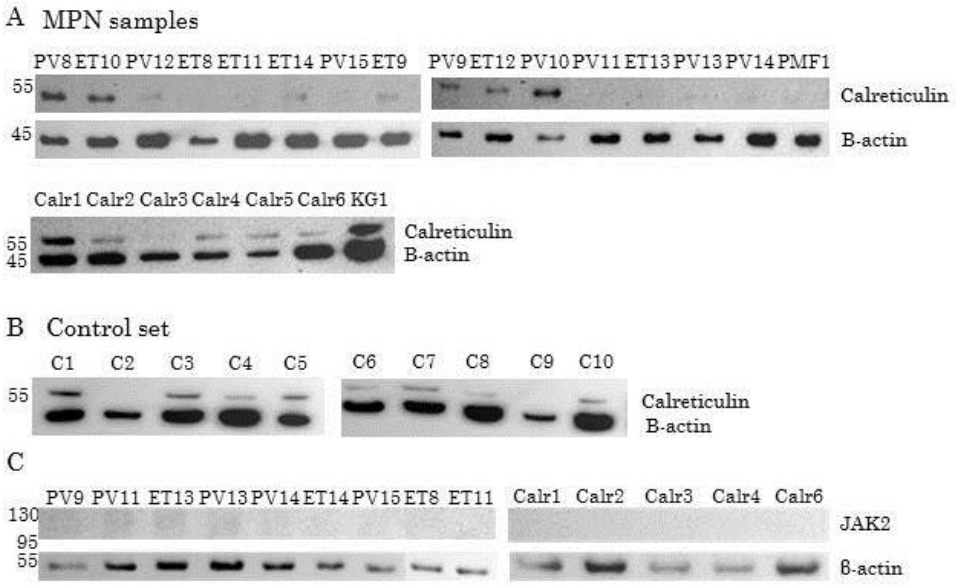


**Figure I-7.** Calreticulin expression in MPN and control patients. **A)** MPN samples. **B)** Control set of patients. B-actin acts as loading control. Molecular weights of target proteins: Calreticulin 48 kDa, β-actin 42 kDa. Patients: Prospective set: *JAK2(+)*: PV8, PV9, PV10, PV11, PV12, PV13, PV14, ET9, ET10, ET12, ET13 and PMF1. *JAK2(-)*: ET8, ET11, ET14 and PV15. Calreticulin + set: Calr1, Calr2, Calr3, Calr4, Calr5 and Calr6. **C)** JAK2 expression in MPN patients. B-actin acts as loading control. Molecular weights of target proteins: JAK2 130 kDa, β-actin 42 kDa. Patients: Prospective set: *JAK2(+)*: PV9, PV11, PV13, PV14 and ET13. *JAK2(-)*: ET8, ET11, ET14 and PV15. Calreticulin + set: Calr1, Calr2, Calr3, Calr4 and Calr6.

### *5-CALR mutated patients displayed distinct IQGAP1/Rho GTPase protein interactions compared with JAK2V617F ones*

Since the study of IQGAP1 expression showed different levels of expression according to the presence of the *JAK2V617F* mutation, we carried out an investigation of IQGAP1 expression in *CALR* mutated patients by western blotting. As shown in Figure I-8, IQGAP1 signals showed a heterogeneous pattern and they were quite low in *CALR* mutated patients, similar to what was observed in controls. Indeed, there were no significant differences of IQGAP1/β-actin ratio between *CALR(+)* and control patients ($p=0.523$) but there were between *CALR(+)* vs *JAK2(+)* ($p<0.05$) and *CALR(+)* vs *JAK2(-)* ($p=0.001$).

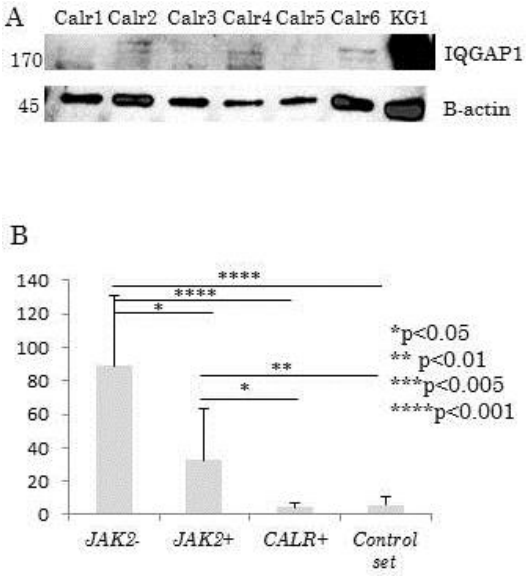


**Figure I-8.** IQGAP1 expression in *CALR(+)* samples. **A)** Samples were submitted to nanoparticle incubation followed by WB. B-actin acts as loading control and KG1 cell lysate acts as positive control. Molecular weights of target proteins: IQGAP1 189kDa, β-actin 42 kDa. **B)** IQGAP1/β-actin ratio means are represented by bars with their respective standard deviations. *Student's t* tests (*p<0.05, ** p<0.01, ***p<0.005, ****p<0.001). Patients: *JAK2(+):* Retrospective set: PV1, PV2, PV3, PV4, PV5, PV6 and ET1, ET2, ET3, ET5, ET6 and ET7. Prospective set: PV8, PV9, PV10, PV11, PV12, PV13, PV14, ET9, ET10, ET12, ET13. *JAK2(-):* Prospective set: ET8, ET11, ET14 and PV15. Calreticulin+ set: Calr1, Calr2, Calr3, Calr4, Calr5 and Calr6. Control set: C1, C2, C3, C4, C5, C6, C7, C8, C9, and C10.

Then, we looked at potential links between IQGAP1 and CALR in RBCs by immunoprecipitation assays. Apparently, as shown in Figure I-9B, calreticulin mutated protein did not seem to be a partner of IQGAP1 since over 6 *CALR(+)* tested patients, only one showed a co-precipitation of CALR protein with IQGAP1. Similarly, in non-mutated *CALR* patients, we did not highlight any interaction (either direct or indirect) of both proteins (Figure I-9A). Interestingly, in control patients, CALR protein clearly co-precipated with IQGAP1 (Figure I-9C), suggesting that in non MPN subjects, CALR and IQGAP1 proteins could interact with each other.

Immunoprecipitation assays in *CALR* mutated patients between IQGAP1 and Rho GTPases showed that IQGAP1 gathered RhoA and Cdc42 in some patients but oddly no complexes were detected between IQGAP1 and Rac1 unlike what was observed in *JAK2V617F* patients (Figures I-10B to I-10D). We also found that Rac1 was not in an

activated state in *CALR(+)* samples (Figure I-10A). One other major observation was that in all *CALR* mutated samples, the Rho family inhibitory protein RhoGDI co-precipitated with IQGAP1 conversely to what was observed in all MPN patients without *CALR* mutation (Figure I-10E).

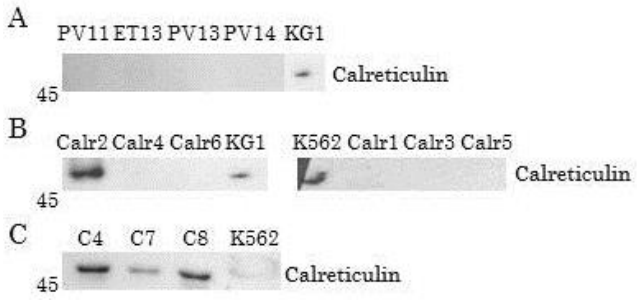


**Figure I-9.** IQGAP1-Calreticulin relationship. RBC lysates were immunoprecipitated with IQGAP1 followed by WB revealed by Calreticulin antibodies. **A)** *JAK2(+)* patients. **B)** Calreticulin mutated samples. **C)** Control set. Patients: Prospective set: *JAK2(+)*:PV11, PV13, PV14 and ET13; Calreticulin+ set: Calr1, Calr2, Calr3, Calr4, Calr5 and Calr6; Control set: C4, C7, C8. KG1 and K562 were used as positive controls.

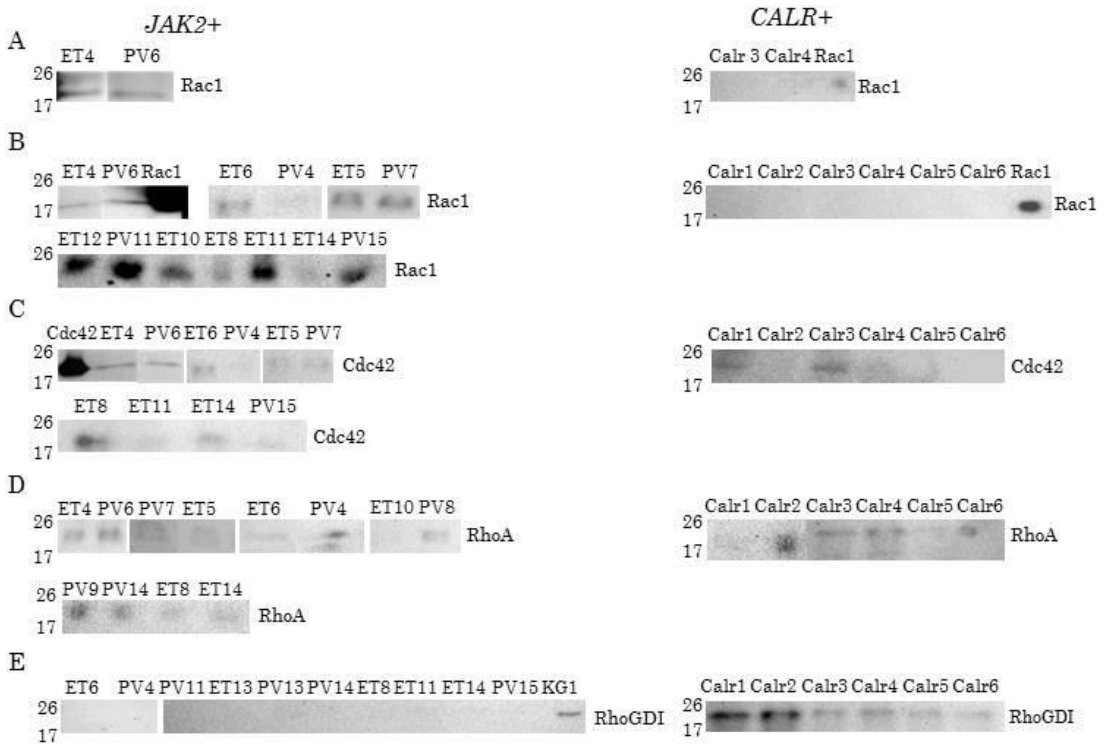


**Figure I-10.** Rho GTPase protein recruitment profile in *JAK2(+)/CALR(+)* patients. **A)** RBC lysates were pulled-down with GST-PAK-RBD agarose beads and developed by Rac1 antibody. **B to E)** RBC lysates were immunoprecipitated with IQGAP1, eluted by Laemmli buffer and followed by WBs developed by Rac1, Cdc42, RhoA or RhoGDI antibodies. Patients: Retrospective set: PV4, PV6, PV7, ET4, ET5 and ET6. Prospective set: *JAK2(+)*: PV8, PV11, PV13, PV14, ET10 and ET13. *JAK2(-)*: ET8, ET11, ET14 and PV15. Calreticulin + set: Calr1, Calr2, Calr3, Calr4, Calr5 and Calr6. Molecular weights of targeted proteins: Rac1 21 kDa, Cdc42 21 kDa, RhoA 22 kDa, RhoGDI 23 kDa.

## DISCUSSION

This work aimed to characterize the RBC proteome of PV and ET compared with controls by an integrative proteomic approach using quantitative mass spectrometry analysis coupled to functional study of pathways targeted by protein deregulations. Indeed, functional alterations of blood cells play an important role in the pathogenesis of these diseases. However, the erythrocyte proteome has not yet been deeply studied in MPNs.

We firstly found that RBCs of MPN patients expressed more than 1000 proteins and displayed significant deregulations of many protein levels. Consequently, several functional pathways were affected by these alterations. In particular, we underlined a deregulation of several members of the RAS superfamily of GTPases in RBCs suggesting that those pathways could play a significant role in MPN pathogenesis. The RAS GTPases constitute a big family composed by over 150 human proteins divided in 5 subfamilies: Ras, Rho, Rab, Ran and Arf (142) (Figure I-11). These members are capable of switching between an activated state when bound to GTP and an inactivated state when bound to GDP. These switches are regulated, on the one hand, by Guanine-Nucleotide-Exchange-Factors (GEFs) that promote the formation of the GTP form and then activate these proteins. On the other hand, GTPase-activating proteins (GAPs) promote the intrinsic GTPase activity of these proteins to convert bound GTP into GDP determining the GDP inactive form (143) (Figure I-12).

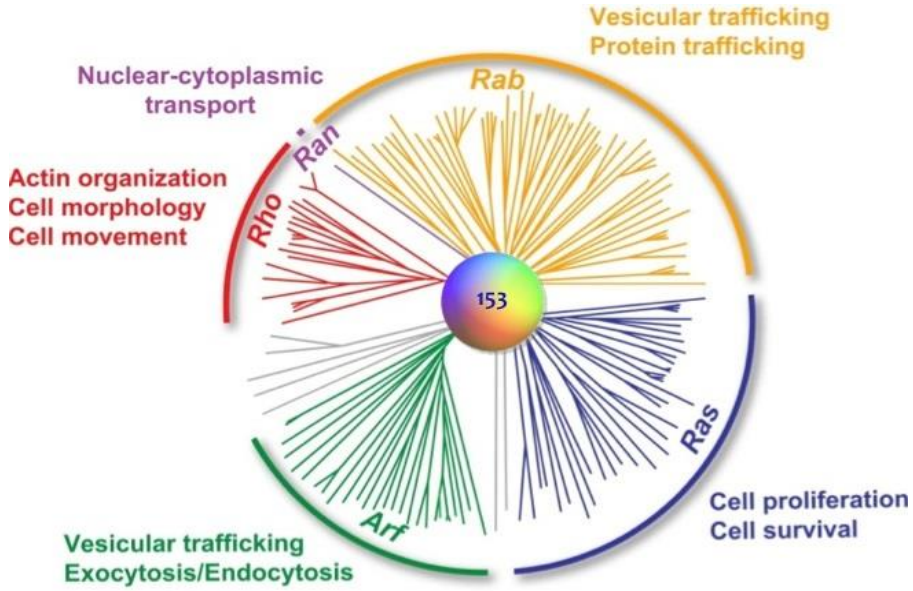


**Figure I-11**: The RAS superfamily of GTPases. It comprises 153 human protein members and is subdivided in 5 subfamilies: Ras, Rho, Rab, Ran and Arf. Their principal functions are signaled on the figure.

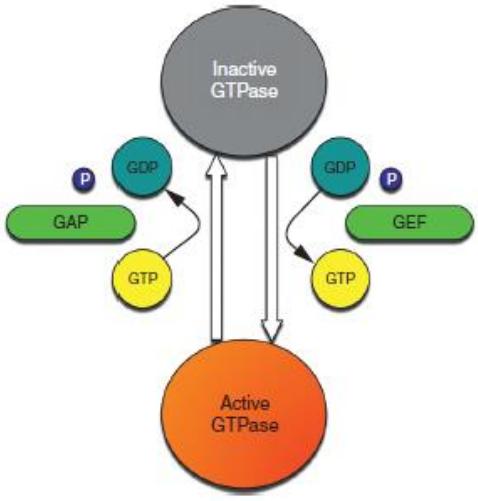


**Figure I-12**: RAS activation and inactivation. The switch between the inactive form (GDP linked) to the active form (GTP linked) is promoted by GEFs and the switch to the inactive form by GAPs.

### *RAS subfamilies*

- *The Ras subfamily* (142, 143)

  The Ras proteins or Ras sarcoma oncoproteins are involved in multiple processes including control gene expression and regulation of cell growth, differentiation and survival. Some of their principal effector pathways are the Raf/MEK/ERK pathway and the PI3K which are also activated by *JAK2V617F* (15).

- *The Rho subfamily* (142)

  The Ras homologous (Rho) proteins regulate actin cytoskeleton remodeling, cellular movement, cell cycle progression and gene expression. Among the principal members we find RhoA, Rac1 and Cdc42. These two last ones are direct effectors of IQGAP1. Cdc42 binding to IQGAP1 has been implicated in modulation of cell architecture, exocytosis and cell growth (144).

- *The Rab subfamily* (142)

  The Ras-like proteins in brain (Rab) are regulators of vesicular and membrane trafficking. They ease vesicle formation and budding from the donor compartment, transport, vesicle fusion and release of vesicle content. They are specifically localized in relation to their function. This localization depends on their grade of prenylation which is facilitated by RABGGTA.

- *The Ran subfamily* (142)

  The Ras-like nuclear family (Ran) principally controls nucleocytoplasmic transport.

- *The Arf subfamily* (142)

  The ADP-ribosylation factor (Arf) family regulates vesicular transport in endocytic and exocytic pathways, intracellular trafficking and actin remodeling.

The Rab geranylgeranyltransferase alpha subunit – RABGGTA, the Rab GTPase-binding effector protein 1 or Rabaptin-4 or Rabaptin-5 or Rabaptin-5alpha – RABEP1 and the Rho GTPase-activating-like protein IQGAP1 were the three potential candidates as MPN RBC biomarkers.

RABGGTA, which is absent in control samples, is a protein in charge of Rab protein prenylation that is needed for their function as it provides some hydrophobicity to Rab molecules to improve their insertion to membranes (145, 146). To accomplish this function, it makes a complex with Rab escort protein (REP). Pereira-Leal *et al.* (147) suggested that mutations in this gene and thus diminution of Rab proteins prenylation resulted in the Hermansky-Pudlak syndrome (HPS) with immunodeficiency and hypopigmentation. Detter *et al.* (148) have also discovered a mutation in RABGGTA gene which reduced its activity an 80%; and resulted in gunmetal mice characterized by prolonged bleeding, thrombocytopenia and reduced platelet α- and δ- granule contents. These mice also presented hypopigmentation and altered platelet biogenesis (149). Therefore, gunmetal mouse models are considered a model for HPS characterized by albinism, bleeding and platelet deregulations (150).

The protein Rabep1 which is the Rab GTPase-binding effector protein 1 also knew as Rabaptin-4 or Rabaptin-5 or Rabaptin-5-alpha is part of the Rab subfamily of GTPases which are involved in vesicular and membrane trafficking. Rabep1 interacts with the active form of Rab5 (GTP-linked), which is a small GTPase implicated in membrane docking or fusion of vesicles and early endosomes (151). This union stabilizes Rab5 in a GTP-bound (active) form by down-regulating GTP hydrolysis (152). Successive studies discovered that Rabex-5, a Rab5 nucleotide exchange factor is also implicated in this complex of Rab5 activation. The association of Rabep1 to Rabex-5 stimulated GEF activity of Rabex-5 what increases Rabep1-Rabex-5 and Rab5 complex formation (153).

Among these three proteins, IQGAP1 was chosen due to its role as a scaffold protein among the subfamily of Rho GTPases. Western blot analysis of IQGAP1 expression confirmed in two independent sets of patients that IQGAP1 was upregulated in both PV and ET compared with controls. In laboratory experiences, Wang *et al.* (144) showed that when in western blots IQGAP1 signal presents a double band; the upper one corresponds to phosphorylated IQGAP1 and thus, to the active form. Unexpectedly, in our experiences, almost all normal patients had double band, whereas just some MPN patients presented this double band. The double band appeared in Calreticulin mutated patients as well. Further investigations about its activation and phosphorylation should be done.

IQGAP1 belongs to the IQGAPs family besides IQGAP2 and IQGAP3. They regulate diverse processes such as cytokinesis, cell migration, vesicle trafficking and cytoskeletal dynamics. IQGAP1 is formed by several domains (Figure I-13): the calponin homology domain (CHD); IQGAP repeats; polyproline binding region (WW); IQ domain containing four IQ motifs; Ras GTPase-activating protein-related domain (GRD) and RasGAP C-terminus (RGCT) (154). Even though IQGAP1 presents a domain similar to GTPase activating proteins (GAPs), IQGAPs don't own any GAP activity. On the contrary, they are capable to bind GTP-bound Ras-like proteins of the Rho subfamily and keep them in their activated state (131). IQGAP1 is generally regulated by the calcium-binding protein calmodulin via the IQ motifs (154). This binding brings a conformational alteration that inhibits the binding of other targets to IQGAP1. It is also documented that Ca2+ regulation via calmodulin alters the subcellular localization of IQGAP1 influencing its functions (131, 155). Interestingly, our mass spectrometry results showed that calmodulin is under-expressed in ET samples comparing with controls (See Supplemental Data I-1); that could explain one part of IQGAP1 upregulation. It can also be regulated via phosphorylation. Growth factor receptors including EGFR (Endothelial growth factor receptor) and VEGFR (vascular endothelial growth factor receptor), when activated, they can phosphorylate IQGAP1 thanks to their tyrosine kinase activity, or induce IQGAP1 phosphorylation at $Ser^{1443}$ through protein kinase C. Furthermore, IQGAP1 is required for EGFR phosphorylation after EGF stimuli (154). IQGAP1 phosphorylation via EGF-EGFR-PKC activates Cdc42 which seems to promote cell division.

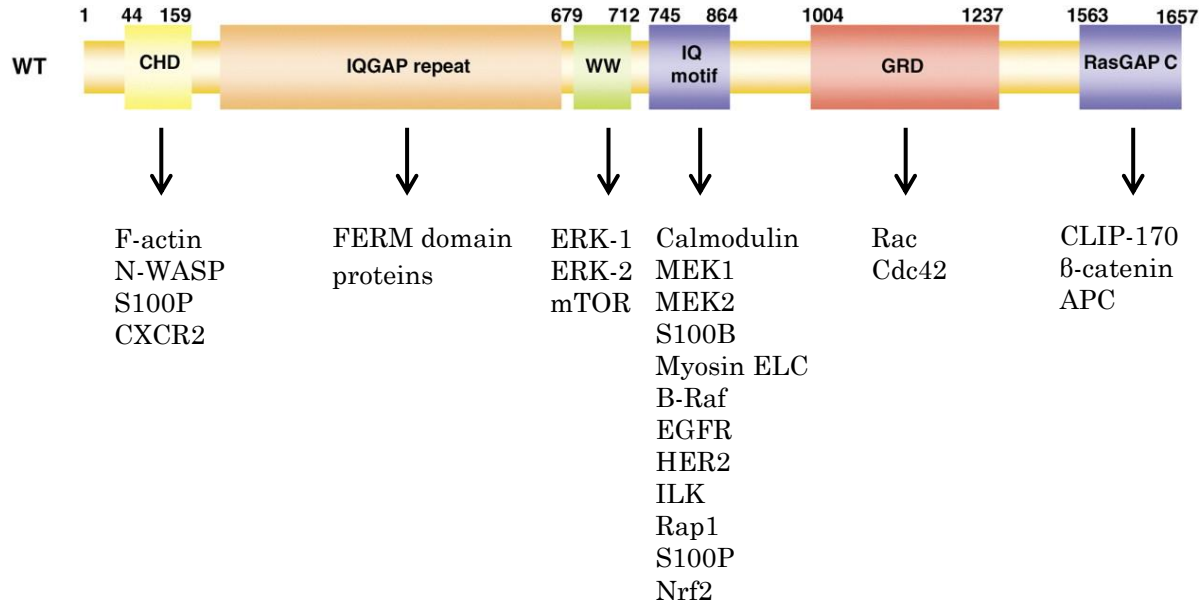


**Figure I-13.** IQGAP1 domains and its effector proteins. It shows the different domains of IQGAP1 and the principal molecules that bind each domain. CHD: calponin homology domain; WW: polyproline binding region; IQ motif: calmodulin binding repeat; GRD: RasGAP related domain; RGCT: RasGAP C terminus (154).

One could hence hypothesize that deregulation of IQGAP1 in MPNs may be directly linked to *JAK2V617F* mutation. In favor, we showed that *JAK2V617F* patients had effectively greater ratios of IQGAP1 expression (expressed as IQGAP1/β-actin ratios) than controls. However, we also observed that *JAK2* WT patients displayed greater levels of IQGAP1 compared with controls and with *JAK2V617F* ones. In fact, the highest levels of IQGAP1 were observed in *JAK2* WT patients. One explanation of these unexpected results might be that the overexpression of IQGAP1 was not directly linked to the presence of *JAK2V617F* mutation but probably to JAK2 protein itself, either WT or mutated. Nevertheless, JAK2 expression falls down as hematopoietic cells differentiate (and is not expressed anymore in RBCs). Moreover, the Erythropoietin receptor (EpoR) is present on immature cells of the erythroid line from BFU-E cells (Burst-Forming Unit-Erythroid cells) to erythroblasts and it has already disappeared in reticulocytes, the previous maturation state to RBC (156, 157). As JAK2 is directly bound to the EpoR, the disappearance of the receptor should affect JAK2 protein as well. In fact, we confirmed this disappearance by our

mass spectrometry analysis and western blot results: erythrocytes of MPNs and controls were devoid of JAK2.

Since its discovery in ET and PMF patients, many studies have been carried out to understand how *CALR* mutation is involved in MPN pathogenesis. However, up to now, no study was made either on CALR expression in red blood cells of MPN patients or on the relationship between *CALR* status and IQGAP1. We firstly found that unlike JAK2 protein, CALR protein is present in the erythrocytes of most MPN patients. Interestingly, we also showed that CALR is present in non MPN erythrocytes at similar levels as in MPN ones (expressed as CALR/β-actin ratios). These data suggest that CALR protein is constitutively expressed in red blood cells and that its expression is not significantly altered in MPNs. However, we highlighted another remarkable different behavior of IQGAP1 protein in MPNs compared with controls. As seen in our experiments, no complexes were formed between CALR and IQGAP1 in MPN patients (apart from one over ten), whatever their molecular status were including triple negative patients. Conversely, we observed in all controls tested, that these two proteins co-precipitated suggesting that in non-MPN patients this interaction between CALR and IQGAP1 could occur physiologically. The fact that *CALR(-)*IQGAP1 interaction is altered in both *JAK2(+)* and *CALR(+)* although IQGAP1 is overexpressed only in *JAK2(+)* but not in *CALR(+)* patients suggests that high levels of IQGAP1 in MPNs are not the cause (or the only cause) of this defect of interaction. Qualitative alteration of IQGAP1 might impede IQGAP1/CALR interaction in MPNs.

Concerning IQGAP1 expression in mutated *CALR* patients, our results showed that there were significant differences between *JAK2(+)* and *CALR(+)* ($p<0.05$); *JAK2(-)* and *CALR(+)* ($p<0.005$) but not between controls and *CALR(+)* ($p=0.523$). In fact, *CALR(+)* patients displayed the same levels of IQGAP1 as controls. Taking into account the whole data about IQGAP1 expression according to *JAK2* and *CALR* status, we showed that its levels were dependent on patient's genotype (*JAK2* WT / *CALR* WT>*JAK2V617F*>*CALR(+)*) but seemed not or only partially linked to these two main driver mutations. The fact that *JAK2 WT/CALR WT* patients are those harboring the highest levels of IQGAP1 argues for the impact of an unknown molecular event on its expression.

IQGAP1 is overexpressed in several cancers such as colorectal carcinoma, breast cancer, astrocytoma and squamous cell carcinoma of head and neck (136). This upregulation may have consequences in effector pathways such as the MAPK/ERK kinases that are related to apoptosis, cell proliferation, survival, invasion and metastasis (136, 154, 158-160). Furthermore, previous studies have shown that IQGAP1 could bind the active form of Cdc42 and Rac1 (131-138). A whole review of all IQGAP1 interacting proteins is done by White *et al.* 2012 (154). Thereby IQGAP1/Cdc42 complex could promote mechanisms implicated in tumorigenesis such as cytokinesis, cell proliferation and migration (144, 161). To evaluate this hypothesis, we investigated if IQGAP1 could form a complex with Cdc42 and Rac1 in our MPN patients. Our data demonstrated that IQGAP1 could actually form a complex with Rac1, Cdc42 and also RhoA, which all belong to the Rho subfamily of RAS GTPases. That is in agreement with Jacquemet *et al.* (133) and Ory *et al.* (162), who had previously reported the existence of IQGAP1-RhoA complex in tumor cells. We also disclosed that only Rac1 was present in its activated state in MPN samples but that both Cdc42 and RhoA weren't activated, at least to a detectable level by our protocol. Our data also showed that IQGAP1 did not interact with the Rho inhibitory protein RhoGDI which could explain the fact that Rac1 was in an activated state in its complex with IQGAP1.

To decipher the consequence of this IQGAP1/Rac1 interaction, we also investigated the p-21-activated kinase 1 (PAK1). PAK1 belongs to group I of PAK family and it is related to the Rho family of GTPases (139, 140). It can be activated by binding to activated GTPases such as Cdc42 and Rac1 which promote autophosphorylation and activation of PAK1 and release its autoinhibitory conformation (139, 163-165). Our experiments confirmed the interaction of Rac1 with PAK1 and they also showed that PAK1 bound IQGAP1, a connection that had already been described by Malarkannan *et al.* (166). This fact argued for a direct recruitment of PAK1 in the IQGAP1/Rac1 complex through its interaction with activated Rac1 in red blood cells. Indeed, in Rac1Q61L-GST-Sepharose-bead pull-down assays, both PAK1 and phosphorylated-PAK1 bound GTP-Rac1. Moreover, DerMardirossian *et al.* (167) found that the Rho GTPase dissociation inhibitor RhoGDI, which forms an inhibitory complex with Rac1, RhoA and Cdc42 (168), can be phosphorylated by PAK1 resulting in dissociation of Rac1-RhoGDI complex and allowing Rac1 activation.

These data demonstrated, for the first time, to our knowledge, that in MPN red blood cells, IQGAP1 is able to recruit Rac1 and PAK1. The fact that IQGAP1 is overexpressed in most MPN patients provides a new molecular mechanism potentially implicated in MPN pathogenesis through an abnormal recruitment and activation of Rac1 and PAK1. Rho GTPases and in particular Rac1 are crucial for normal hematopoiesis. More precisely, Rac (and Cdc42) are necessary for hematopoietic stem and progenitor cell survival and proliferation and are also required for self-renewal and for cell cycle entry of quiescent ($G_0$) (169). Rac1 is also a regulator of ROS production which has been shown to play a particular role in MPN signaling. Indeed, the presence of 8-oxo-guanines and DNA double-strand-breaks that denote DNA oxidative damage, were reported as consequence of increased ROS production in PV and PMF CD34+ cells and Ba/F3-EpoR-*JAK2V617F* cells by Marty *et al.* (170). Moreover, they also showed that PI3K/Akt activation via *JAK2V617F* negatively regulated the Forkhead Box-O (FoxO3) transcription factor (an oxidative stress regulator) leading to a reduced expression of anti-oxidant enzymes in bone marrow cells of knock-in mice, that could cause a myeloproliferative syndrome in Foxo3-/- mice sensitive to the ROS scavenger N-acetyl-cysteine (171).

Taking into account that red blood cells represent the terminal maturation stage of erythroid progenitors, their functional alterations are very probably evidence of genetic deregulations occurring in erythroid progenitors. Hence, our results about Rac1 deregulation in red blood cells provide new original data about the mechanism of the oncogenic potential of Rac1 in MPNs that could occur through the imbalance of RhoA signaling associated with IQGAP1 disturbance. The fact that Rac1 is necessary for enucleation of erythroblasts (169), also suggest that abnormalities of red blood cell maturation could occur in MPNs.

The p-21-activated kinases are a family of serine/threonine protein kinases which are part of several signaling pathways such as gene transcription or apoptosis important in oncogenesis. In fact, PAK1 upregulation has already been described in some cancers (139, 140). PAK1 is also implicated in cell morphology and membrane cell motility. Similarly, Rho GTPases are important for actin organization and polymerization. Furthermore, Focal Adhesion Kinase (FAK) Pathways, which are activated by RhoA, also appeared deregulated in ET vs Controls (Table I-1). Altogether, these results suggest that disruption of the Rho

GTPases and PAK1 in red blood cells could lead to the alteration of membrane motility and adhesion which might participate to vascular complications frequently observed in MPNs.

However, we showed that IQGAP1 was not overexpressed in *CALR(+)* patients suggesting that IQGAP1 could impact MPN pathogenesis through different molecular mechanisms depending on the driver mutation. Indeed, when exploring IQGAP1-Rho GTPases relationship in *CALR* mutated patients, we showed different results than the ones obtained in *CARL(-)/JAK2V617F* MPNs. Firstly, in *CALR(+)* patients, we showed that IQGAP1 immunoprecipitated with RhoGDI. The fact that RhoGDI formed a complex with IQGAP1 was not unexpected since Liu *et al.* (172) had already suggested that this Rho GTPase inhibitor could bind IQGAP1 thanks to its FERM domain. However, they couldn't prove that these two proteins interact directly in mouse kidney cell lysates. We also hypothesized that there could be a link between mutated calreticulin and RhoGDI but these two proteins didn't co-immunoprecipitate in calreticulin set. Moreover, we did not find any activated Rho protein in *CALR(+)* patients (Supplemental Data I-5) and CALR failed to bind activated Rac1 as well. The fact that when we added activated Rac1 to *CALR(+)* samples, GTP-Rac1 could pull-down IQGAP1 (Supplemental Data I-6) but that both proteins didn't co-precipitate with IQGAP1 antibodies, could imply that Rac1 couldn't bind IQGAP1 because it was in a deactivated state in *CALR(+)* samples. This hypothesis was reinforced by the demonstrated interaction between IQGAP1 and RhoGDI in *CALR(+)* patients different from *JAK2(+)* ones. This fact strongly suggested that alternative recruitment of RhoGDI could explain differences in Rac1 activation between *JAK2*(+) and *CALR(+)* patients. We therefore supposed that in *CALR* mutated patients, although IQGAP1 was not overexpressed, it could recruit RhoGDI and that this complex may interfere with the activation of Rho GTPases. The link between *CALR* mutation and the recruitment of RhoGDI by IQGAP1 remains to be investigated.

Taking all results together, we noticed that some remarkable differences arose between *CALR* mutated and *JAK2V617F* patients. In consequence, we grouped some results depending on the molecular status *JAK2(+)* or *CALR(+)* (Figure I-10). As IQGAP1/β-actin rate comparison indicated, IQGAP1 is overexpressed in *JAK2(+)* patients compared with calreticulin mutated ones ($p<0.05$). It is also outstanding that no difference in IQGAP1

expression was found between *CALR(+)* and normal patients ($p>0.05$). Thus, we can conclude that IQGAP1 is overexpressed in *JAK2(+)* MPNs but not in *CALR(+)* ones. Regarding IQGAP1 effectors, Rac1, Cdc42 and RhoA bound IQGAP1 in *JAK2(+)* patients but RhoGDI didn't. On the contrary, in *CALR(+)* samples, IQGAP1 didn't co-immunoprecipitate with activated Rac1 but it did with RhoGDI. Moreover, Rac1 was activated in *JAK2(+)* subjects but not in *CALR(+)* ones.

# CONCLUSION AND PERSPECTIVES

In conclusion, our results demonstrated a deregulation of the Rho family of GTPases, specifically alterations of IQGAP1/Rac1 signaling in red blood cells of MPNs depending on *JAK2* and *CALR* status. *JAK2V617F* patients displayed an up regulation of IQGAP1 that consequently recruited and activated Rac1 and the cytoskeleton motility protein PAK1. In *CALR(+)* patients, IQGAP1 was not overexpressed but it recruited RhoGDI which consequently impeded the activation of Rac1 and PAK1. These alterations may participate in vascular complications via alterations of erythrocyte adhesion due to deregulation of PAK1 activation or Rac1 dependent actin organization. The differential activation of IQGAP1/Rac1/PAK1 observed between *JAK2(+)* and *CALR(+)* patients could explain differences in vascular complications observed among these subgroups. These data demonstrate that, IQGAP1/Rac1/PAK1 signaling is implicated in MPN red blood cell pathogenesis and should be considered as a target for therapy.

These results also stress out two issues:

### *1-Does a link between JAK2 and IQGAP1 exist?*

According to JAK2 connection with IQGAP1 we couldn't look into it as JAK2 was not present in our RBC lysates. As previously said, IQGAP1 could be phosphorylated via activation of EGFR either thank to its tyrosine kinase activity or via PKC at $Ser^{1443}$ (154). Yamauchi *et al.* (173) reported that JAK2 phosphorylates EGFR activating it. As a result, the MAPK pathway is activated. Moreover, Brown *et al.* (131) also reported the activation of MAPK/ERK pathway by IQGAP1 as a consequence of EGFR activation. We could therefore hypothesized that *JAK2V617F* could indirectly phosphorylate IQGAP1 activating it and the effector pathways including MAPK pathway via *JAK2 V617F* dependent phosphorylation of EGFR.

### *2-Is there any link between JAK2 and IQGAP1/Rho GTPase signaling?*

Once seen the different recruitment of the Rho GTPases by IQGAP1 depending on the molecular status either *JAK2(+)* or *CALR(+)*, we wonder what role *JAK2V617F* plays on the control of IQGAP1/Rho GTPase signaling. It would also be interesting to decipher if there

are any differences between *JAK2(+)* and *JAK2(-)* on this pathway and which mechanisms are the responsible for IQGAP1/Rho GTPase signaling activation in MPNs.

Altogether, our results and these issues suggest a new theoretical model of Rho GTPase signaling alterations in MPN erythrocytes (Figure I-14).

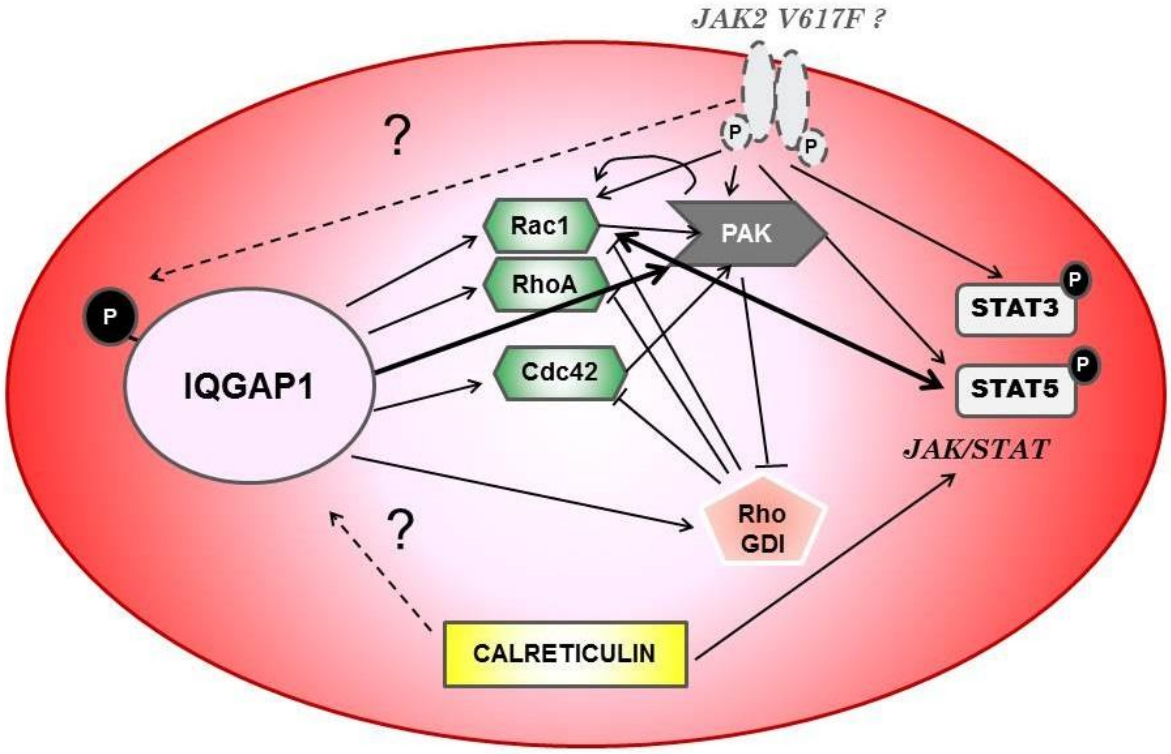


**Figure I-14**. IQGAP1/Rho GTPase signaling alterations in MPN erythrocytes.

## RESUME DU CHAPITRE I

Dans cette première partie, nous avons sélectionné et validé une technique pour la déplétion indirecte d'hémoglobine basée sur la capture de protéines par des nanobilles magnétiques présentant de surfaces chimiques particulières (126). Cette déplétion a été utilisée pour une analyse quantitative et qualitative par LC-MS/MS (LTQ Orbitrap) du protéome érythrocytaire de patients SMP. Cette étude a montré des dérégulations de la famille des Rho GTPases qui étaient significativement plus fortement exprimées chez les patients PV et TE. Plus particulièrement, la protéine IQGAP1, (Ras GTPase-activating like protein IQGAP1), était surexprimée chez les sujets TE-*JAK2V617F* et PV-*JAK2V617F* par rapport aux contrôles. Nous avons pu confirmer par western blot cette surexpression d'IQGAP1 entre les sujets PV-TE et les contrôles ($p<0.05$), et en plus, que des différences existaient en fonction du statut moléculaire des patients (*JAK2 ou CALR*).

Par la suite, nous avons approfondi la nature des interactions entre IQGAP1 et des protéines Rho GTPases en montrant qu'IQGAP1 pouvait coprécipiter avec certaines de ces protéines mais de façon différente selon le statut des patients (*JAK2(+) / CALR(+)*). Pour aller plus loin, nous avons aussi étudié la protéine PAK1 qui est un effecteur des Rho GTPases, et ainsi confirmé ses liens avec Rac1 activé et IQGAP1 dans les globules rouges des patients.

En conclusion, nos travaux mettent à jour la présence de dérégulations protéiques dans les érythrocytes des patients PV et TE. Ces résultats mettent en évidence le rôle potentiel des protéines GTPases dans la physiopathologie des SMP et leurs implications potentielles dans les dérégulations fonctionnelles du GR. Les différences entre les patients *JAK2* mutés et les patients *CALR* mutés renforcent l'hypothèse de dérégulations protéiques induites par les anomalies moléculaires, qui pourraient expliquer les différences phénotypiques et cliniques observées entre les patients *JAK2(+)* et *CALR(+)*.

# CHAPTER II

# Proteomic study of granulocytes in Ph-negative MPNs

## BACKGROUND

The study of the erythrocyte proteome in Ph- MPNs let us quantify more than 1000 proteins and to highlight an important deregulation of the RAS GTPase family, more precisely, an upregulation of the Ras activated protein IQGAP1. We saw how the recruitment of the Rho GTPases by IQGAP1 varied according to patient's genotype.

Apart from erythrocyte deregulations, other protein disruptions have also been reported in other blood cells such as granulocytes in these hemopathies. For instance, Hui *et al.* (103), thanks to Protein Pathway Array, could screen 15 proteins in peripheral blood neutrophils differently expressed between ET and control patients implicated in apoptosis and inflammatory pathways. They also found differences in protein expression in cycle signaling pathways when comparing ET patients with and without *JAK2V617F* mutation suggesting that this mutation contributes to malignant proliferation and cell cycle progression.

Falanga *et al.* (104) studied the involvement of neutrophils in PV and ET pathogenesis of thrombotic predisposition. They showed that neutrophils presented high levels of CD11b, which is a maker of neutrophil activation. These cells also presented high levels of leukocyte alkaline phosphatase which suggested the idea of neutrophil degranulation. This fact raises plasma concentrations of elastase and myeloperoxidase. Moreover, activated neutrophils can bind platelets, what originates the formation of platelet-leukocyte complexes which are thought to be the cause of pro-thrombotic condition. Arellano-Rodrigo *et al.* (105) also found that ET patients presented higher expression of CD11b in neutrophils but not in patients with thrombosis. CD11b expression was also associated with *JAK2V617F* presence. Nevertheless, they found that CD11b expression was increased in monocytes from thrombotic patients as well as the monocyte tissue factor which may be involved in blood coagulation. In general, CD11b expression promotes leukocyte adherence to the endothelium, phagocytosis, aggregation, adhesion-dependent respiratory burst and degranulation.

Furthermore, Gallardo *et al.* (174) found three upregulated proteins in PV compared with ET patients (HSP70, LTA4H and SERPINB1) besides other 58 proteins through 2D-DIGE and mass spectrometry analysis. Moreover, using an HSP70 inhibitor they could

show that this protein had a potential role in the *JAK2(-)*STAT signaling pathway in the erythroid lineage.

With this background and to go further in the characterization of the MPN proteome, we performed a proteomic study of Ph- MPN granulocytes. In order to improve proteomic data, we performed a comparative quantitative proteomic analysis using iTRAQ labeling method. In parallel, a transcriptomic analysis was performed on each sample through collaboration with the Institute of Medical Research in Belgrade, (Serbia). In order to deep on the impact of *JAK2V617F*, we analyzed patients harboring different allele burdens, from 0 (non-mutated patients) to more than 80% (high allele burden). Finally, this analysis would let us compare the granulocyte and erythrocyte proteomes in order to see if there are any common deregulations that could be linked to MPN pathogenesis.

## MATERIAL AND METHODS

### *Patients*

A total of 24 patients were used for this study. All patients agreed to be part of the study and signed the informed consent. Patients were grouped according to their diagnosis: 6 patients were diagnosed as PV with *JAK2V617F* with high mutant allele burden over 88% (range 88-93%; mean 92%); 5 ET patients with *JAK2V617F* mutation (allele burden between 35 and 50%, mean 40.5%); 6 PMF patients with *JAK2V617F* mutation (allele burden between 38 and 94%, mean 63%) and 7 patients diagnosed as ET or PMF but with no *JAK2V617F* mutation, (group named Mut0). (Table II.1)

| No | Diagnosis | *JAK2V617F* allele burden |
|---|---|---|
| 6 | PV | [88-93%], mean 92% |
| 5 | ET | [35-50%], mean 40.5% |
| 6 | PMF | [38-94%], mean 63% |
| 7 | ET/PMF Mut0 | 0% |

**Table II.1.** Patients' features for the proteomic study of granulocytes.

### *Sample Preparation*

Thirty milliliters of peripheral blood were collected in 10% sodium citrate tubes. The maximum time interval between venipuncture and arrival in the laboratory was 2 hours. Lymphocytes were separated adding on top 15 ml of lymphocyte separation medium (PAA Laboratories GmbH, Pasching, Austria). After centrifugation (400 g, 20 min, 20°C), the pellet, which is composed of erythrocytes and granulocytes that migrated through the gradient, was submitted to erythrocyte lysis with lysing solution (0.15 M $NH_4Cl$, 0.1 mM $Na_2EDTA$, 12 mM $NaHCO_3$). High quality of purified granulocytes was confirmed by cytospin preparations and Wright–Giemsa staining. Viability was measured with trypan-blue (BioWhittaker). Granulocytes were washed twice with PBS and resuspended in 10ml cold PBS with 2 mM EDTA and 1 mM Na-orthovanadat and centrifuged 10 min at 1,000 g. The cell pellet was dried by inversion over paper towel, vortexed and placed on ice. Then, granulocytes were lysed with cold lysis buffer (50 mM Tris pH 7.5, 150 mM NaCl, 1% NP-40, 2 mM EDTA, 50 mM NaF) with protease inhibitors (1 mM phenylmethylsulfonyl

fluoride PMSF, 10 mM ε-aminocaproic acid, 2 µg/ml aprotinin, 50 µg/ml leupeptin, 1 µM pepstatin A) and phosphatase inhibitors (1 mM Na-orthovanadat) for 30 minutes at 4ºC. Cell suspensions were centrifuged at 10,000 g for 15 min at 4ºC. The supernatant was transfered in cold eppendorfs, mixed and aliquoted into precolded small eppendorfs and frozen at -70ºC.

### *iTRAQ Labeling*

Next, the same amount of protein was taken from each patient to form four groups (PV, ET, PMF and Mut0) containing 250 µg of protein each. Proteins were precipitated with acetone and digested according to Applied Biosystems digestion protocol for iTRAQ marking: protein pellets were suspended in triethylammonium bicarbonate buffer (TEAB) 500 mM 0.1% SDS pH 8.5. Cysteines were reduced with TCEP (tris(2-carboxyethyl)phosphineand), alkylated with MMTS (methyl methanethiosulfonate) and proteins were digested by trypsin overnight. Then, groups were splitted in two subgroups of 100 µg and marqued during 2 hours by an specific iTRAQ marquer (113 and 117 for the group Mut0; 115 and 119 for PV; 116 and 121 for ET and 114 and 118 for PMF). Then, samples were combined together and desalted in Sep-Pak C18 Cartridges (Waters®). Prefractionation of peptides prior to LC-MS/MS was done thanks to the 3100 off-gel fractionator (24 wells). The resulted fractions were desalted using C18 micro spincolumns Harvard Apparatus®.

### *Protein Identification*

For the LC-MS/MS analysis, about 200 ng of each fraction were injected. Peptides were separated thanks to nano LC-MS/MS (Ultimate 3000, Dionex®, Amsterdam, The Netherlands) coupled to LTQ Orbitrap Velos mass spectrometer (Thermo Scientific®, Bremen, Germany). The LTQ-Orbitrap operated with the Xcalibur software. Survey scans MS spectra were acquired in the Orbitrap on the 300-2000 m/z range with 60,000 as value resolution. The five most intense ions per survey were selected for collision-induced dissociation (CID) fragmentation to be analyzed in the linear trap (LTQ). Dynamic exclusion was used within 60 seconds to prevent repetitive selection of the same peptide.

For protein analysis, we selected Mascot Daemon software (version 2.3.0, Matrix Science, London, UK). The following parameters were set for creation of the peak lists: parent ions in the mass range 400–4500, no grouping of MS/MS scans and threshold at 1000. A peak list was created for each analyzed sample and individual Mascot searches were performed. Protein identification was performed comparing data with *homo sapiens* entries in Uniprot protein database (http://www.uniprot.org/). Protein hits were automatically validated if they satisfied one of the following criteria: identification with at least one top ranking peptide with a Mascot score of more than 39 (p-value < 0.001) or at least two top ranking peptides each with a Mascot score of more than 22 (p-value < 0.05). When several proteins matched exactly the same set of peptides, only one member of the protein group was reported in the final list. To evaluate the false positive rate in these experiments, all the initial database searches were performed using the "decoy" option of Mascot.

### *Protein Quantification*

For peptide quantification, the intensity of the different ions (m/z: 114; 115; 116; 118; 119 and 121) was divided by the intensity of the reporter ion (m/z: 117 – Mut0) for each measured compound. All ratios were normalized against the median intensity of reporters. Only proteins quantified with at least two peptide ratios for each condition were validated. Ratios were transformed into natural logarithms and plotted against the number of peptides subjected to MS/MS analysis. Proteins with natural log-transformed ion ratios differing by at least 2×SD (95% confidence) were considered significantly different from the random variation (ratio range between 0.76 and 1.24). *Student's t* test was performed for ratio comparison corresponding to each replicate (i.e. 116/117 vs. 121/117). Only proteins without a significant difference between the replicates were maintained for comparison between subgroups of patients.

### *Statistical Analysis*

Mean comparison was performed by *student's t* test by GraphPad Prism software with a confidence interval of 95%.

### *Functional Analysis*

MS results were loaded on *Reactome* software (http://www.reactome.org/). It enabled us to identify, analyze and understand the whole data. It helped us to know in which biological pathways the identified proteins participate; which of the proteins interact with each other directly or through intermediate molecules; which upstream regulators can explain their expression pattern; which downstream diseases or processes are likely up or down regulated by the increase or decrease of the abundance of these proteins and the effects of possible protein modifications.

# RESULTS

## *1-Granulocyte proteome of Ph- MPN patients displays alterations in protein expression*

Thanks to LC-MS/MS analysis we could identify 1048 proteins from Ph- MPN granulocytes. To quantify the differences of expression in these proteins, we calculated the ratios and the p-values (*student's t* test) between the means of expression of each protein group. Table II.2 shows the number of proteins differently expressed between the four groups (PV, ET, PMF and Mut0).

| | PV vs Mut0 | ET vs Mut0 | PMF vs Mut0 | PV vs PMF | ET vs PMF | PV vs ET |
|---|---|---|---|---|---|---|
| **N proteins p<0.01** | 54 | 75 | 77 | 62 | 67 | 39 |
| **N proteins p<0.05** | 22 | 22 | 69 | 15 | 34 | 7 |
| **Total** | 76 | 97 | 146 | 79 | 101 | 46 |
| **Ratio** | 1.01±0.17 | 1.01±0.19 | 1.02±0.12 | 1.00±0.19 | 0.99±0.21 | 1.06±0.35 |
| **Median** | 0.94 | 0.94 | 0.96 | 0.97 | 0.94 | 0.93 |
| **Range** | [0.74-1.56] | [0.36-1.60] | [0.63-1.55] | [0.64-1.69] | [0.54-2.23] | [0.66-2.85] |
| **Ratio>1** | 30 | 40 | 62 | 34 | 42 | 21 |
| **Ratio<1** | 46 | 57 | 84 | 43 | 59 | 25 |

**Table II.2.** Protein expression comparison between PV, ET, PMF and Mut0.

In order to reinforce statistical analysis and to avoid technical bias, we calculated medians and standard deviations of ratios (i.e. 115/117 and 119/117 for PV). Thereby we obtained a range of ratios from 0.76 to 1.24 corresponding to ±2 SD of the ratio value. Therefore, we defined as high significant difference between two peptides when the ratio of the two values was under 0.76 or over 1.24 and the *student's t* test under 0.01; and low significant difference when the ratio was between 0.76 and 1.24 but the statistical p-value was under 0.05.

Proteins expressed with high significant differences are presented as a comparative histogram in Figure II.1. Interestingly, among this proteins, we found that the protein

Calreticulin was overexpressed in all *JAK2(+)* Ph- MPNs compared with Mut0: ET vs Mut0 (ratio 1.28, p-value<0.001), PV vs Mut0 (ratio 1.29, p-value<0.001) and PMF vs Mut0 (ratio 1.22, p-value<0.001). The list of all deregulated proteins is accessible in Supplemental Data II-1).

Among the proteins expressed with low significant differences we found some Rho GTPase proteins that we had previously observed in erythrocytes, such as Rho-related GTP-binding protein RhoG (ratio 0.88, p-value 0.001 in PMF vs Mut0); Rho GDP-dissociation inhibitor 1 (ratio 0.95, p-value 0.01 in PMF vs Mut0); and Rho GDP-dissociation inhibitor 2 (ratio 0.93, p-value 0.001 in PMF vs Mut0). These two last proteins were also upregulated in our proteomic study of MPN RBCs. The Rho GDP-dissociation inhibitor 1 was twofold more expressed in RBCs of ET patients than in controls and 1.7 times in PV than in non-mutated patients. The Rho GDP-dissociation inhibitor 2 was 2.7 times more expressed in RBCs of ET patients than in controls and 2.5 times more than in non-mutated patients.

The Ras GTPase-activating-like protein IQGAP1, which was overexpressed in MPN RBCs, was surprisingly found lightly down-regulated when comparing ET vs PMF patients (ratio 0.95, p-value<0.01) and PV vs PMF patients (ratio 0.93, p-value<0.001). We also highlighted that the IQGAP1 regulatory protein calmodulin was highly downregulated in ET vs PMF patients (ratio 0.76, p-value<0.01) and in PV vs PMF patients (ratio 0.80, p-value<0.01).

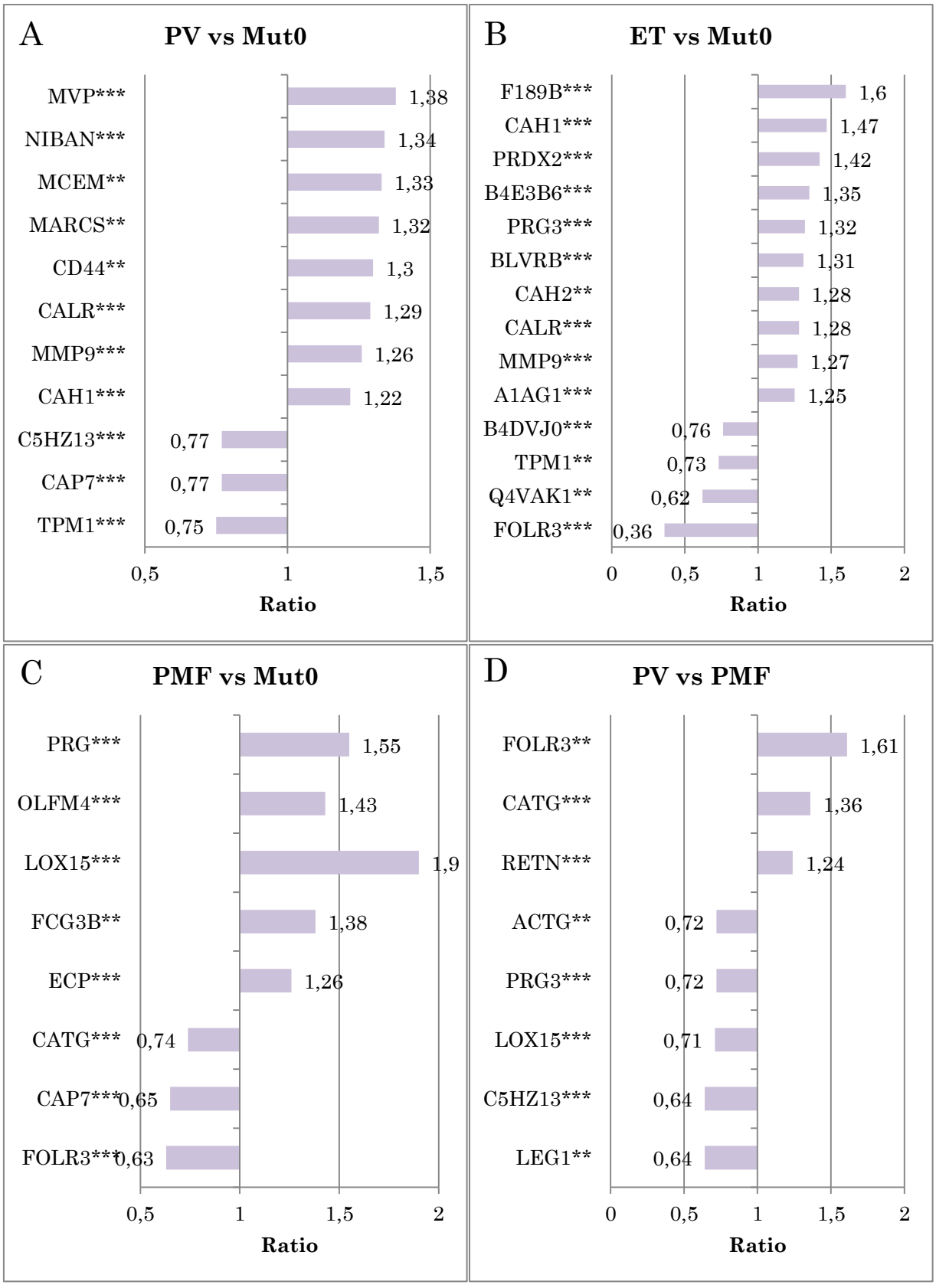
A
PV vs Mut0
MVP*** 1,38
NIBAN*** 1,34
MCEM** 1,33
MARCS** 1,32
CD44** 1,3
CALR*** 1,29
MMP9*** 1,26
CAH1*** 1,22
C5HZ13*** 0,77
CAP7*** 0,77
TPM1*** 0,75
0,5 1 1,5
Ratio
B
ET vs Mut0
F189B*** 1,6
CAH1*** 1,47
PRDX2*** 1,42
B4E3B6*** 1,35
PRG3*** 1,32
BLVRB*** 1,31
CAH2** 1,28
CALR*** 1,28
MMP9*** 1,27
A1AG1*** 1,25
B4DVJ0*** 0,76
TPM1** 0,73
Q4VAK1** 0,62
FOLR3*** 0,36
0 0,5 1 1,5 2
Ratio
C
PMF vs Mut0
PRG*** 1,55
OLFM4*** 1,43
LOX15*** 1,9
FCG3B** 1,38
ECP*** 1,26
CATG*** 0,74
CAP7*** 0,65
FOLR3*** 0,63
0,5 1 1,5 2
Ratio
D
PV vs PMF
FOLR3** 1,61
CATG*** 1,36
RETN*** 1,24
ACTG** 0,72
PRG3*** 0,72
LOX15*** 0,71
C5HZ13*** 0,64
LEG1** 0,64
0 0,5 1 1,5 2
Ratio

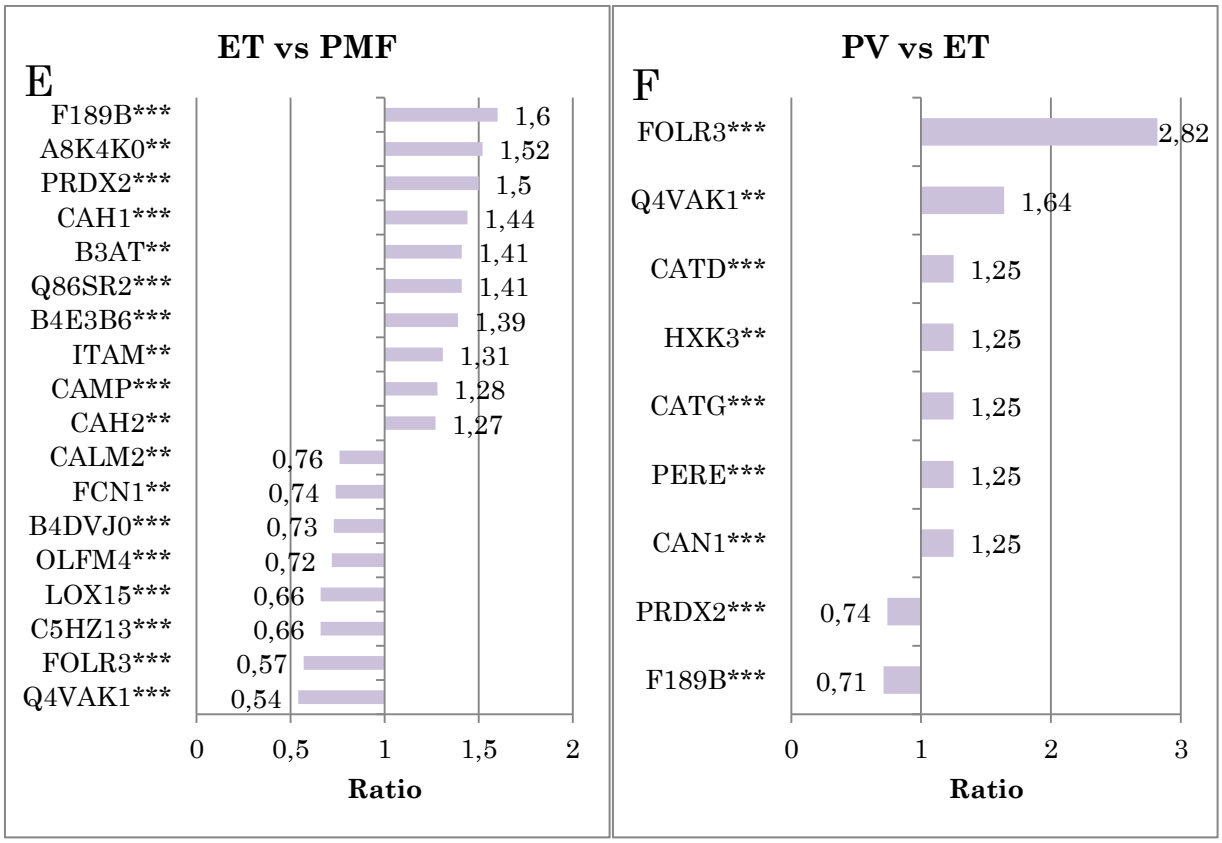


**Figure II.1.** Proteins expressed with high significant differences between **A)** PV and Mut0, **B)** ET and Mut0, **C)** PMF and Mut0, **D)** PV and ET, **E)** PV and PMF, **F)** ET and PMF. Names of proteins: A1AG1: Alpha-1-acid glycoprotein 1, A8K4K0: cDNA FLJ75006, highly similar to Homo sapiens CD177, ACTG: Actin cytoplasmic-2, B3AT: Band 3 anion transport protein, B4DVJ0: Glucose-6-phosphate isomerase, B4E3B6: Heat shock 70 kDa protein, BLVRB: Flavin reductase, C5HZ13: Galectin-10, CAH1: carbonic anhydrase 1, CAH2: carbonic anhydrase 2, CALM2: calmodulin 2, CALR: calreticulin, CAMP: cathelicidin antimicrobial peptide, CAN1: Calpain-1 catalytic subunit, CAP7: azurocidin, CATD: Cathepsin D, CATG: cathepsin G, CD44: CD44 antigen, ECP: Eosinophil cationic protein, F189B: protein FAM189B, FCG3B: Low affinity immunoglobulin gamma Fc region receptor II-B, FCN1: Ficolin-1, FOLR3: folate receptor gamma, HXK3: Hexokinase-3, ITAM: Integrin alpha-M - CD11b, LEG1: Galectin-1, LOX15: arachidonate 15-lipoxygenase, MARCS: Myristoylated alanine-rich C-kinase substrate, MCEM: Mast cell-expressed membrane protein 1, MMP9: matrix metalloproteinase-9, MVP: Major vault protein, NIBAN: Protein Niban, OLFM4: olfactomedin 4, PERE: eosinophil peroxidase, PRDX2: peroxiredoxin 2, PRG3: proteoglycan 3, Q4VAK1: integrin, alpha M, Q86SR2: AZU1 protein, RETN: Resistin, TPM1: tropomyosin alpha-1chain. P-values: **p<0.01, ***p<0.001.

Looking at these deregulated proteins, we noticed that some of them appeared in more than one comparison, meaning that they were commonly altered in at less two subgroups of patients (Table II.3).

| | PV vs Mut0 | ET vs Mut0 | PMF vs Mut0 | PV vs PMF | ET vs PMF | PV vs ET |
|---|---|---|---|---|---|---|
| B4DVJ0 | | ↓ | | | ↓ | |
| C5HZ13 | ↑ | | | ↓ | ↓ | |
| CAH1 | ↑ | ↑ | | | ↑ | |
| CAH2 | | ↑ | | | ↑ | |
| CALR | ↑ | ↑ | | | | |
| CAP7 | ↓ | | ↓ | | | |
| CATG | | | ↓ | ↑ | | ↑ |
| F189B | | ↑ | | | ↑ | ↓ |
| FOLR3 | | ↓ | ↓ | ↑ | ↓ | ↑ |
| LOX15 | | | ↑ | ↓ | ↓ | |
| MMP9 | ↑ | ↑ | | | | |
| OLFM4 | | | ↑ | | ↓ | |
| PRDX2 | | ↑ | | | ↑ | ↓ |
| PRG3 | | ↑ | ↑ | ↓ | | |
| Q4VAK1 | | ↓ | | | ↓ | ↑ |
| TPM1 | ↓ | ↓ | | | | |

**Table II.3**. Common proteins between the different comparisons and their status of expression either over-expressed (↑) or under-expressed (↓).Names of proteins: B4DVJ0: Glucose-6-phosphate isomerase; C5HZ13: Galectin-10, CAH1: carbonic anhydrase 1, CAH2: carbonic anhydrase 2, CALR: calreticulin, CAP7: azurocidin, CATG: cathepsin G, F189B: protein FAM189B, FOLR3: folate receptor gamma, LOX15: arachidonate 15-lipoxygenase, MMP9: matrix metalloproteinase-9, OLFM4: olfactomedin 4, PRDX2: peroxiredoxin 2, PRG3: proteoglycan 3, Q4VAK1: integrin, alpha M, TPM1: tropomyosin alpha-1chain.

Moreover, as shown in Figure II.2, when comparing *JAK2(+)* patients (PV, ET and PMF) versus the *JAK2(-)* (ET and PMF patients), we could identify several proteins that were selectively different between mutated and non-mutated patients. Interestingly, when we compared the spectrum of these proteins, we highlighted that there were four proteins commonly overexpressed in PV and ET *JAK2(+)* (vs *JAK2(-)),* two common in both mutated ET and PMF and one in both PV and PMF patients. However, we failed to found any protein significantly modified in all subtypes of *JAK2(+)* MPNs.

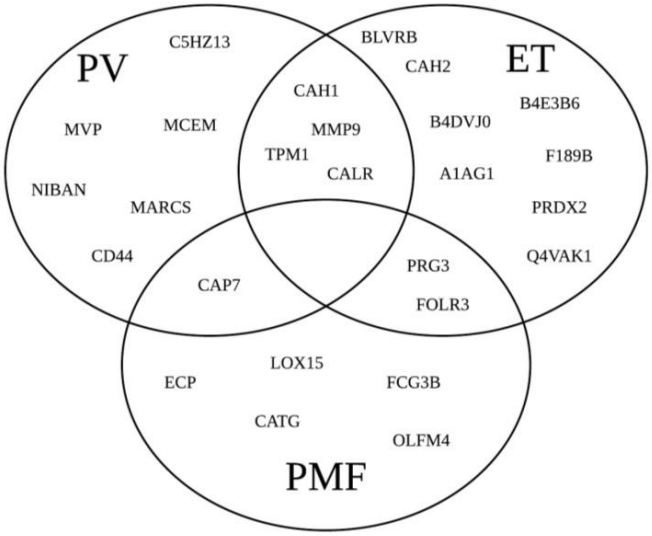


**Figure II.2.** Venn diagram of high differently expressed proteins in *JAK2(+)* vs *JAK2(-)* (Mut0) MPNs.

Regarding proteins expressed with low significant differences, Figure II.3 shows the number of them that rose when comparing two subgroups.

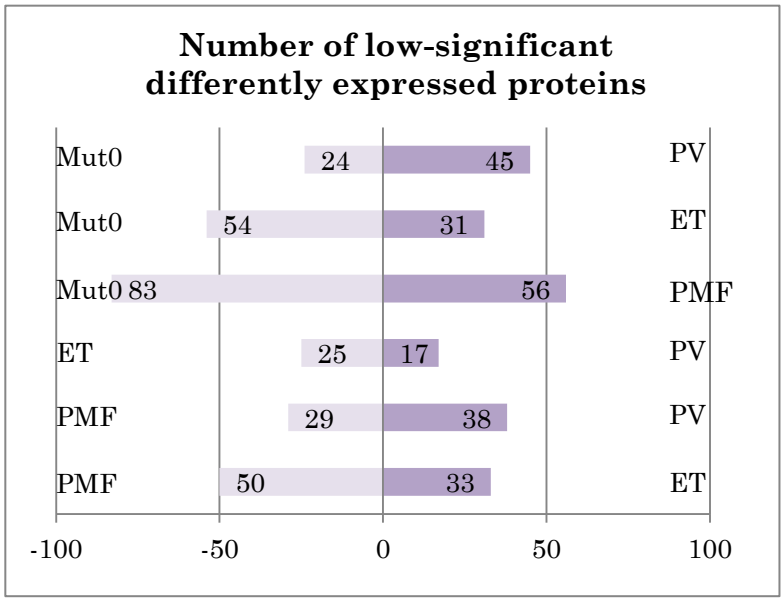


**Figure II.3.** Number of proteins expressed with low-significant differences between the different subgroups.

### *2-Impact of JAK2V617F allele burden in granulocyte protein expression*

The level of *JAK2V617F* expression in PV has been shown to be directly associated with hemoglobin concentration, leukocytosis, splenomegaly, age-adjusted bone marrow cellularity but inversely to platelet count. Moreover, patients with the highest amounts of J*AK2V617F* were more likely to develop myelofibrotic evolution (26). In addition, a link between the allele burden and thrombotic complications has also been suggested but remains controversial.

Taking into account that *JAK2V617F* allele burden is assessed on purified neutrophils from peripheral blood, we aimed to study the influence of *JAK2V617F* allele burden in granulocyte protein expression. Therefore, we performed another comparative analysis of proteome between subgroups of patients classified according to their levels of *JAK2V617F*. We hence compared the ratios of the proteins expressed with significant differences in ET vs Mut0 patients (allele burden <50%) and PV vs Mut0 patients (allele burden >88% (88-93%)), (Table II.4).

| | **JAK2 <50%** | **JAK2 >88%** |
|---|---|---|
| **No of proteins** | 111 | 83 |
| **Ratio>1** | 48 | 32 |
| **Ratio<1** | 63 | 51 |

**Table II.4.** Impact of *JAK2V617F* allele burden in protein expression. No: Number of proteins significantly altered.

As shown in Table II.4, the number of deregulated proteins was higher at low allele burden than at higher ranges of allele burden (over 88%). Table II.5 shows the particular influence of mutated *JAK2* allele burden in some proteins. Interestingly, the expression of some proteins rose in parallel with mutated *JAK2* allele burden. It is the case of the mast cell-expressed membrane protein 1, the major vault protein, the protein Niban or the resisitin. On the contrary, even though the Flavin reductase and the carbonic anhydrase 1 are overexpressed in *JAK2V617F* granulocytes, their overexpression decreased when the *JAK2V617F* allele burden rose. Furthermore, the protein Peroxiredoxin 2, that was highly

expressed in low-*JAK2(-)*allele-burden granulocytes (ratio=1.42), hugely decreased its expression when the allele burden increased (ratio=0.94). It is remarkable that the folate receptor gamma is strongly under-expressed at low ranges of allele burden and, even being always highly under-expressed, its expression increases at higher charges of *JAK2V617F*.

| Protein group | Description | JAK2 <50% | JAK2 38-94% | JAK2 >88% |
|---|---|---|---|---|
| A8K9E4_HUMAN | cDNA FLJ76459, highly similar to Homo sapiens matrix metallopeptidase 8 (neutrophil collagenase) (MMP8) | 1.13 | 1.10 | 1.24 |
| ANXA1_HUMAN | Annexin A1 | 1.09 | 1.05 | |
| B4DV10_HUMAN | cDNA FLJ59142, highly similar to Epididymal secretory protein E1 | 0,79 | | 0.84 |
| BLVRB_HUMAN | Flavin reductase | 1.31 | | 1.18 |
| BPI_HUMAN | Bactericidal permeability-increasing protein | 0.81 | 0.94 | 0.84 |
| C5HZ13_HUMAN | Galectin-10 | 0.78 | 1.21 | 0.77 |
| CAH1_HUMAN | Carbonic anhydrase 1 | 1.47 | | 1.22 |
| CALR_HUMAN | Calreticulin | 1.28 | 1.22 | 1.29 |
| CAP7_HUMAN | Azurocidin | 0.86 | 0.65 | 0.77 |
| CATG_HUMAN | Cathepsin G | 0.81 | 0.74 | |
| FLNA_HUMAN | Filamin-A | 0.94 | 0.94 | 0.94 |
| FOLR3_HUMAN | Folate receptor gamma | 0.36 | 0.63 | |
| HPT_HUMAN | Haptoglobin | 1.14 | | 1.17 |
| MCEM1_HUMAN | Mast cell-expressed membrane protein 1 | | 1.19 | 1.33 |
| MMP9_HUMAN | Matrix metalloproteinase-9 | 1.27 | 1.14 | 1.26 |
| MVP_HUMAN | Major vault protein | | 1.22 | 1.38 |
| NIBAN_HUMAN | Protein Niban | | 1.15 | 1.34 |
| PRDX2_HUMAN | Peroxiredoxin-2 | 1.42 | 0.94 | |
| RETN_HUMAN | Resistin | 1.07 | | 1.22 |

**Table II.5.** Impact of *JAK2V617F* allele burden in protein expression.

CALR protein keeps its presence significantly increased in all MPN granulocytes but independently of *JAK2V617F* allele burden suggesting that only the presence of the mutation but not the amount of mutation present any influence on CALR regulation.

### *3-Pathway alterations in Ph-MPN granulocytes*

In order to discover the pathways that could be altered due to the deregulation of many proteins, we used the Reactome. It is an online site that analyzes data and compares them to their pathway database. Thanks to this software, we remarked an important deregulation of the Rho GTPase pathways among the most deregulated pathways in *JAK2V617F* MPN granulocytes as well as pathways in relation with ROS detoxification (highly deregulated in PMF vs Mut0 comparison), MAPK-ERK pathways or mTOR among others. (Lists of all altered pathways are accessible in Supplemental Data II-2).

### *4-Rho GTPase deregulations in Ph-MPN granulocytes*

We have previously reported important alterations of the Rho family of GTPases in red blood cells. More specifically, we highlighted an upregulation of the Ras GTPase-activating-like protein IQGAP1 in RBCs of MPNs compared with controls. This protein also appeared in our proteomic study of granulocytes. Interestingly, we observed variations on its levels of expression among MPN patients in these cells. More concretely, IQGAP1 was lightly down-regulated in ET and PV vs PMF patients thus overexpressed in PMF patients. However, we cannot certify its overexpression in MPN granulocytes since iTRAQ analysis did not include non-MPN controls. Similarly to what we had observed in erythrocytes, *JAK2(-)* patients harbored higher levels of IQGAP1 as compared with *JAK2(+)* ones. Indeed, in the comparison between PV vs Mut0 patients in granulocytes we found a weak but highly significant decrease (ratio 0.96, p-value<0.01).

We also remarked that the IQGAP1 regulatory protein calmodulin was highly downregulated in ET vs PMF patients (ratio 0.76, p-value<0.01) and in PV vs PMF patients (ratio 0.80, p-value<0.01). Calmodulin is thus upregulated in PMF patients compared with PV and ET ones providing an explanation for IQGAP1 levels modification at least in ET patients. Altogether, these data suggest that alterations of IQGAP1 regulation are dependent, at least partially, of *JAK2* mutation and take place in both granulocytes and erythrocytes and could be considered as a hallmark of MPNs.

Interestingly, among the deregulated proteins in granulocytes we also found some Rho GTPases as well as some of the big family of RAS GTPases. Table II.6 summarizes RAS GTPase protein deregulations in granulocytes.

| Protein description | Comparison | Ratio | p-value |
|---|---|---|---|
| GDI2 protein | PMF vs Mut0 | 0.94 | 0.0063 |
| | PV vs Mut0 | 0.92 | 0.0172 |
| GTP-binding nuclear protein Ran | ET vs Mut0 | 0.92 | 2.21E-04 |
| Rab GDP dissociation inhibitor alpha | ET vs PMF | 1.09 | 0.0192 |
| Ras-related C3 botulinum toxin substrate 2, (RAC2) | PMF vs Mut0 | 0.85 | 0.0386 |
| | ET vs Mut0 | 0.74 | 0.0147 |
| Ras-related protein Rab-11B | PV vs Mut0 | 0.88 | 5.96E-04 |
| Ras-related protein Rab-31 | PMF vs Mut0 | 0.93 | 0.0043 |
| Ras-related protein Rab-35 | PMF vs Mut0 | 0.95 | 0.0041 |
| Rho GDP-dissociation inhibitor 1 | PMF vs Mut0 | 0.95 | 0.0017 |
| Rho GDP-dissociation inhibitor 2 | PMF vs Mut0 | 0.93 | 0.0007 |
| | PV vs Mut0 | 0.86 | 2.99E-06 |
| | PV vs PMF | 0.94 | 0.0180 |
| Rho-related GTP-binding protein RhoG | PMF vs Mut0 | 0.88 | 9.30E-05 |
| | ET vs Mut0 | 0.85 | 0.0080 |
| Transforming protein RhoA | PV vs PMF | 0.95 | 0.0059 |

**Table II.6**. RAS GTPase protein deregulations in granulocytes.

Rho GDP-dissociation inhibitors 1 and 2 were also upregulated in our proteomic study of MPN RBCs. The first one was twofold more expressed in RBCs of ET patients than in controls and 1.7 times in PV than in non-mutated patients. The second one was 2.7 times more expressed in RBCs of ET patients than in controls and 2.5 times more than in non-mutated patients. On the contrary, both proteins were under-expressed in *JAK2(+)* MPN granulocytes compared with *JAK2(-)* ones. In addition, the protein Rab-11B that was also under-expressed in PV RBCs when compared with ET (ratio 0.3) was also under-expressed in PV vs Mut0 granulocytes.

Altogether these results show a deregulation of the RAS family of GTPases and, more concretely, the Rho family of GTPases in MPN granulocytes that reinforce similar results observed in erythrocytes.

### *5-Oxidative stress in granulocytes*

Neutrophils are well-known cells to produce high levels of free radicals, the reactive oxygen species (ROS). These ions can cause significant damages in the environment. Fortunately, cells are gifted with machinery that helps them to battle this harmful oxidative stress. Many of these proteins that control ROS were found deregulated in our proteomic analysis, (Table II.7).

| Description | Comparison | Ratio | p-value |
|---|---|---|---|
| Flavin reductase | PMF vs Mut0 | 1.09 | 1.97E-02 |
| | ET vs Mut0 | 1.31 | 2.68E-06 |
| | PV vs Mut0 | 1.18 | 1.49E-04 |
| | PV vs PMF | 1.09 | 8.27E-03 |
| | ET vs PMF | 1.21 | 1.28E-05 |
| Catalase | PV vs ET | 0.93 | 7.55E-04 |
| | PMF vs Mut0 | 0.94 | 1.55E-06 |
| | ET vs Mut0 | 0.97 | 1.63E-01 |
| | PV vs Mut0 | 0.90 | 1.91E-08 |
| Superoxide dismutase [Cu-Zn] | ET vs PMF | 1.09 | 8.73E-03 |
| | PMF vs Mut0 | 0.97 | 1.97E-02 |
| Glutathione reductase, mitochondrial | PMF vs Mut0 | 1.04 | 2.42E-02 |
| Glutathione S-transferase omega-1 | PMF vs Mut0 | 0.93 | 4.37E-05 |
| | PV vs Mut0 | 1.09 | 2.37E-03 |
| | PV vs PMF | 1.17 | 2.99E-05 |
| | ET vs PMF | 1.10 | 1.02E-02 |
| Glutathione S-transferase P | PMF vs Mut0 | 0.91 | 1.04E-07 |
| | ET vs Mut0 | 0.94 | 9.37E-04 |
| | PV vs PMF | 1.00 | 1.35E-02 |
| Protein disulfide-isomerase | ET vs Mut0 | 0.99 | 2.11E-01 |
| Eosinophil peroxidase | ET vs PMF | 0.88 | 7.90E-04 |
| Myeloperoxidase | PMF vs Mut0 | 0.80 | 2.53E-15 |
| | ET vs Mut0 | 0.96 | 8.32E-03 |
| | PV vs Mut0 | 0.94 | 1.69E-03 |
| | PV vs PMF | 1.21 | 1.69E-09 |
| | ET vs PMF | 1.22 | 1.82E-09 |
| Peroxiredoxin-2 | PMF vs Mut0 | 0.94 | 9.70E-03 |
| | ET vs Mut0 | 1.42 | 7.53E-08 |
| | ET vs PMF | 1.50 | 3.38E-09 |
| | PV vs ET | 0.74 | 2.24E-05 |

| Description | Comparison | Ratio | p-value |
|---|---|---|---|
| Thioredoxin-dependent peroxide reductase, mitochondrial | PMF vs Mut0 | 0.92 | 2.18E-02 |
| NAD(P)H dehydrogenase, quinone 2 | ET vs Mut0 | 1.23 | 1.84E-02 |
| Sulfhydryl oxidase 1 | ET vs Mut0 | 1.17 | 4.96E-03 |
| Thioredoxin | PMF vs Mut0 | 0.97 | 8.32E-03 |
| Glutaredoxin | PMF vs Mut0 | 1.08 | 1.24E-02 |
| | PV vs PMF | 0.91 | 9.49E-03 |
| | ET vs PMF | 0.89 | 5.82E-03 |

**Table II.7**. Oxidative stress protein deregulations in granulocytes.

### *6-Transcriptomic analysis*

The transcriptomic analysis of CD34+ cells and granulocytes is detailed on the published article of Čokić *et al*. (175) (Supplemental Data II-3). They showed that in CD34+ cells, the number of differently expressed genes was twofold larger compared with granulocytes. Thirty-six genes were persistently highly expressed in both CD34+ cells and granulocytes and forty-two genes persistently highly down-regulated. Interestingly, they showed that, among upregulated genes, there were genes that control myeloid differentiation such as runt-related transcription factor 1 (*RUNX1*) or hematopoietic cell-specific Lyn substrate 1 (*HCLS1)*; as well as genes that stimulate cell proliferation as signal transducer and activator of transcription 1 (*STAT1*), MAS1 oncogene (*MAS1*) or the ras-related C3 botulinum toxin substrate 2 (*RAC2*). There were also upregulated some genes that control cell proliferation such as retinoic acid receptor responder 3 (*RARRES3*) and transducer of ERBB2 1 (*TOB1*); and apoptotic genes such as S100 calcium binding protein A8 (*S100A8*) and tumor necrosis factor receptor superfamily 19 (*TNFRSF19*). Apoptotic inhibitor genes such as NLR family apoptosis inhibitory protein (*NAIP*, absent in PMF) and tumor necrosis factor alpha-induced protein 3 (*TNFAIP3*) were also upregulated.

Interestingly, it was shown that some of the upregulated genes belonged to the PI3K/AKT/mTOR pathway such as ribosomal protein S6 kinase, 90kDa, polypeptide 1 (*RPS6KA1*), Ras-related GTP binding A (*RRAGA*) or the phosphatase and tensin homolog (*PTEN*) and the protein kinase C ß (*PRKCB*). Phosphoinositide-3-kinase, catalytic, α polypeptide (*PIK3CA*), regulatory subunit 1 (*PIK3R1*) and *MAPK1* were only overexpressed

in PV subjects while hypoxia inducible factor α (*HIF1α*) was significantly more expressed in *JAK2* positive ET and PMF subjects. It was also reported that some of the upregulated genes could activate this apoptotic pathway (the PI35/AKT pathway) such as the coiled-coil domain containing 88A (*CCDC88A*) and coronin 1A (*CORO1A*) genes, while it could be inhibited by up-regulated Kruppel-like factor 13 (*KLF13*). Similarly, MAPK pathway could be activated by up-regulated chemokine (C-X-C motif) receptor 4 (*CXCR4*), growth arrest and DNA-damage-inducible, beta (*GADD45B*) and *MAPK10* gene expression. This pathway plays a critical role in regulation of cell proliferation. In addition, it could be inhibited by up-regulated dual specificity phosphatase 1 (*DUSP1*) and protein tyrosine phosphatase, receptor type J (*PTPRJ*) genes. Altogether these data showed an important deregulation on the genome of MPN granulocytes and CD34+ cells.

### *7-Comparison between transcriptomic and proteomic analysis*

We took in advantage that for some patients we had both, transcriptome and proteome results to link genetic deregulations with protein alterations in granulocytes. Indeed, in the literature, data about any correlation between transcripts and proteins stressed out that all cases were possible. Čokić *et al.* (175), in their report, found that the upregulation of certain genes resulted in an augmentation of some protein expression and the opposite. For instance, they reported an upregulation in *JAK2* positive MPN subjects of the following genes and proteins: annexin A1 (*ANXA1*) in ET and PMF; carbonic anhydrase 1 (*CAI*), ficolin 1 (*FCN1*), major vault protein (*MVP*) in PV; formin binding protein 1 (*FNBP1*) and *S100A4* in PMF; as well as in *JAK2* negative MPN subjects: tropomyosin 3 (*TPM3*), actin related protein 2/3 complex subunit 2 (*ACTR2*), leukotriene A4 hydrolase (*LTA4H*) and oxidative stress related catalase (*CAT*). Finally, the proteins Ras-related C3 botulinum toxin substrate 2 (*RAC2*), myeloid cell nuclear differentiation antigen (*MNDA*), S100A8/9, coronin 1A (*CORO1A*) and the guanine nucleotide binding protein α inhibiting activity polypeptide (*GNAI2*) were deregulated in both analysis (transcriptomic and proteomic).

## DISCUSSION

The LC-MS/MS analysis allowed us to identify more than 1000 proteins expressed by granulocytes. Quantification of these proteins allows establishing the picture of the relative variations (expressed as protein ratios between two conditions) of the granulocyte proteome according to clinical and *JAK2V617F* presence. Globally, we found that a small part of the proteome varied among the different subtypes of MPNs. The variation ranged from 4.4% (PV vs ET) to 9.6% (ET vs PMF). A significant number of proteins were also altered in mutated *JAK2* MPN granulocytes compared with non-mutated (76 in PV, 97 in ET and 146 in PMF). This represents the variation of the proteome from 7.3% (*JAK2(+)* PV vs *JAK2* WT MPNs) to 13.9 % (*JAK2(+)* PMF vs *JAK2* WT MPNs). Several conclusions raise from these data: i) MPNs are associated with significant variations of the proteome of mature blood cells originated from clonal progenitors; ii) alterations of protein levels could participate to phenotypic differences observed among Ph- MPNs; II) mutations could induce proteome variations; iv) the number of proteins found differently expressed among MPNs or according to *JAK2* mutation is quite low. This last point is of importance because it suggests that probably, a relatively low number of pathways play a critical role in MPN physiopathology.

The approach presented in the first part of the manuscript about the erythrocyte proteome reinforces these data since when comparing with non-MPN controls, we observed variations of the erythrocyte proteome of PV and ET ranging from 6.5 to 13.4% respectively.

Another interesting issue that allows the proteome analysis is the variation of the proteins directly targeted by driver mutations. Indeed, molecular analysis of DNA doesn't inform about the levels of JAK2 or CALR and their variations according to the presence of the mutation. Interestingly, in this study we were able to analyze CALR expression and variation in different subgroups of patients. We showed that Calreticulin was effectively present in granulocytes as previously reported, but that it was overexpressed in *JAK2V617F/CALR(-)* granulocytes compared with *JAK2(-)/CALR(-)* ones (ET vs Mut0 ratio 1.28, p-value<0.001, PV vs Mut0 ratio 1.29, p-value<0.001 and PMF vs Mut0 ratio 1.22, p-value<0.001). The fact that this protein is upregulated in these cells even though they are non-*CALR(-)*mutated, may suggest that CALR could play a role in the MPN pathogenesis due to its upregulation (in non- *CALR(-)*mutated patients) or to its molecular alteration (mutated *CALR* ones). The higher values observed in *JAK2(+)* patients suggest that CALR

levels could be impacted by *JAK2* mutation in granulocytes. We did not observe a similar impact of *JAK2V617F* in red blood cells; however, in the absence of gene activity in erythrocytes, it is quite logical that *JAK2V617F* did not play a significant role.

The fact that calreticulin is overexpressed in MPNs, and particularly in granulocytes from *JAK2* mutated patients without *CALR* mutation, raised the hypothesis that normal CALR protein by itself could have an oncogenic role potentially dependent of *JAK2V617F*. In fact, CALR has already been suggested to take part in pancreatic cancer development and progression through MEK/ERK signaling pathway and independently of p53 (176). On the contrary, calreticulin overexpression has been related to increase apoptosis sensitivity to some drugs in calreticulin-inducible HeLa cells (177), as well as in human MCF-7 breast cancer cells (178).

Unfortunately, our LC MS/MS analysis failed to quantify JAK2 protein so we were not able to analyze the impact of JAK2 protein levels. In addition, the transcriptomic analysis didn't highlight any up-regulation of *JAK2* in granulocytes. Nonetheless, the mRNA analysis of CD34+ cells showed an important up-regulation of *JAK2* transcription in PV (4.02 times), ET (3.54 times) and PMF (3.01 times).

Calreticulin is also well-known to be a regulator of calcium homeostasis. Thus its deregulation linked to the deregulation of calcium binding proteins S100 also observed in MPNs (see Supplemental Data II-1) could imply possible calcium alterations in MPN granulocytes that influence their homeostasis. In fact, S100 alterations have already been described in other cancers such as breast, melanoma, head and neck or colorectal tumors (179). In addition, the protein S100A8 was identified as a marker of poor prognosis in AML patients (180). Moreover, IQGAP1 functions are known to be modified by $Ca^{2+}$ regulation via calmodulin (131, 155) thus these Ca2+ alterations could also influence IQGAP1 state.

As seen in the first part of this manuscript, we found that the Ras GTPase-activating-like protein IQGAP1 and the Rho family of GTPases were deregulated in MPN erythrocytes. Regarding granulocyte deregulations, IQGAP1 was found lightly upregulated in PMF patients compared with ET ones and in PV compared with non-mutated ET and PMF. Moreover, calmodulin, an IQGAP1 regulatory protein, was highly upregulated in PMF. Generally, calmodulin causes a conformational change in IQGAP1 that avoids its bound to the Rho GTPases (159). Therefore, we could hypothesize that alteration of the activation of

some Rho GTPases could occur in PMF granulocytes. In the same sense, we also found that the expression of the RhoGDI-dissociation inhibitors 1 and 2 was reduced in *JAK2V617F* PMF and PV compared with *JAK2* WT. Altogether these data suggested that the specific alteration of IQGAP1 and some of its effector proteins could take place in the clinical diversity of MPNs. In particular, PMF patients seemed characterized by a moderate increase of IQGAP1 levels together with calmodulin overexpression and decreased levels of RhoGDI that were globally decreased in all *JAK2(+)* patients compared with *JAK2 WT*.

Thanks to pathway analysis software, we could confirm the deregulation of the Rho GTPases, also observed in RBCs, in *JAK2V617F* granulocytes. In RBCs, this alteration was related to both PV and ET patients compared with controls. Therefore, we could relate Rho GTPase deregulations to *JAK2V617F* MPNs. Furthermore, the fact that Rho GTPase pathways are deregulated in both *JAK2V617F* MPN granulocytes and erythrocytes suggests a deregulation on this family that could take place on a common myeloid progenitor and affect to the entire myeloid lineage. Rho GTPases are principally involved in actin cytoskeleton remodeling, cellular movement, cell cycle progression and gene expression (142). The fact that these functions are altered in granulocytes could explain that leukocyte levels above $15x10^9$/L were associated with an increased risk of major thrombosis as myocardial infarction in PV patients (181) as well as in ET (182, 183) Moreover, leukocytes can contribute to the pathogenesis of thrombosis in ET and PV through their interaction with platelets, endothelial cells, and coagulation factors. They can also participate in inflammatory processes in atherosclerotic plaques increasing thrombotic risk. In addition, neutrophil activation involves ROS production, proteolytic enzymes such as elastase and cathepsin G and higher expression of CD11b on their cell surface. All of these molecules can alter the hemostasis and induce a prothrombotic condition (61). Interestingly, we highlighted that CD11b was deregulated in our proteomic results. It was significantly overexpressed in *JAK2V617F* ET granulocytes compared with non-mutated ones (ratio 1.15, p-value<0.01); in ET vs PMF (ratio 1.31, p-value<0.001); in PV vs PMF (ratio 1.16, p-value<0.01), in PV vs ET (ratio 1.68, p-value<0.01) and PMF vs Mut0 (ratio 0.90, p-value<0.05) thus overexpressed principally in *JAK2V617F* PV and ET granulocytes and down-expressed in PMF ones. These data agree with Arellano-Rodrigo *et al.* (105) that related this molecule to *JAK2V617F* ET neutrophils but not to thrombotic risk. Nevertheless, CD11b expression in monocytes was indeed associated with thrombosis.

We also remarked some deregulations of the MAPK, ERK and mTOR pathways (see Supplemental Data II-2). Interestingly, Čokić *et al.* (175) had already described that some of the upregulated genes belonged to the PI3K/AKT/mTOR pathway such as ribosomal protein S6 kinase, 90kDa, polypeptide 1 (*RPS6KA1*), Ras-related GTP binding A (*RRAGA*) or the phosphatase and tensin homolog (*PTEN*) and the protein kinase C ß (*PRKCB*). The PI3K/Akt pathway plays a crucial role in cancer progression due to its capacity of regulating apoptotic processes. In fact, Akt has already been shown to be activated in many types of cancer (184) inhibiting apoptosis and promoting cell cycle progression and differentiation. Grimwade *et al.* (185) showed how Akt as well as STAT-5 were highly activated in *JAK2V617F* megakaryocytes of ET and PV patients compared with healthy donors and *JAK2(-)* ones. Interestingly, there was no such difference in *JAK2* exon 12 patients. Furthermore, the PI3K/Akt effector: the mammalian target of rapamycin (mTOR) has been shown to be activated by the thrombopoietin receptor in human megakaryocytes. This protein is present in two different complexes: mTORC1 and mTORC2. The mTOR pathway is necessary for proliferation of primary human megakaryocyte progenitors and MO7E cells (a human magakaryoblastic cell line) (186). In addition, Vicari *et al.* (187) showed that mTOR phosphorylation was higher in ET and PMF megakaryocyte cells, derived from CD34+ progenitors, compared with healthy donors. Finally, Khan *et al.* (188) confirmed that the PI3K/Akt pathway is activated in both *JAK2V617F* and *MPLW515L* MPN cells.

These investigations suggested this pathway as a new target for new therapy strategies in Ph- MPNs. Some studies have already tested the effects of mTOR inhibitors alone and in combination with JAK2 inhibitors. Bogani *et al.* (189) showed that both the RAD001, also known as Everolimus, (an allosteric mTOR inhibitor of mTORC1) and the PP242 (an ATP mTOR inhibitor that targets both mTORC1 and 2) were able to inhibit cell proliferation in a dose-dependent manner as well as the inhibition of CD34+ cells and the formation of hematopoietic colonies from MPN patients. They also proved the synergic effect of using mTOR and JAK2 inhibitors together in cell proliferation and colony formation inhibition in Ba/F3 cell lines. Bartalucci *et al.* (190) studied the effects of a dual mTOR/PI3K inhibitor, BEZ235 in mouse and human cells expressing *JAK2V617F*. They showed that this molecule caused cell cycle arrest, proliferation inhibition, apoptosis induction (at higher concentrations) and inhibited cytokine-induced clonogenic growth of MPN progenitors as well as endogenous erythroid colony formation. They also evidenced the enhanced effect

when combining mTOR inhibitors with Ruxolitinib (JAK inhibitor). This synergy provided more survival, reduced splenomegaly and cell production in *JAK2V617F* mouse models. Similar results were obtained by Fiskus *et al.* (191) combining the BEZ235 with the JAK inhibitors TG101209 and SAR302503 in Ba/F3 cells presenting *JAK2V617F* mutation. Another strategy to block this pathway is the one taken by Khan *et al.* (188) that investigated the effects of an Akt inhibitor, the MK-2206. They showed that this drug hugely reduced megakaryocyte colony formation from PMF CD34+ cells (and also from healthy donors unfortunately). Nonetheless, using an *MPLW515L* murine model with myelofibrosis, they could show that the MK-2206 reduced extramedullary hematopoiesis, megakaryocyte expansion and reticulin fibrosis in the bone marrow without peripheral cytopenias and without any effect on the hematopoiesis of healthy mice.

In addition, the protein IQGAP1, which appeared to have a crucial role in MPN RBCs, is tightly linked to this pathway as it interacts with the mTOR protein through is N-terminus domain enhancing cell size and division. The phosphorylated form of IQGAP1 could be implicated in these alterations as it was shown to directly activate the mTOR/Akt signaling pathway (144, 161). We could hypothesized that mutated *JAK2* could also phosphorylate IQGAP1 and then activate the mTOR/Akt signaling pathway amplifying the PI3K/Akt/mTOR signal.

High levels of oxidative stress have already been associated with thrombosis in PV and ET patients (192) and with myelofibrotic evolution in PV patients (193). Furthermore, Hurtado-Nedelec *et al.* (194) described an increased production of reactive oxygen species in MPN neutrophils in *JAK2V617F* patients compared with non-mutated ones together with an increased phosphorylation of p47phox and ERK1/2. In agreement with those results, Marty *et al.* (170) reported increased ROS production in PV and PMF CD34+ cells and Ba/F3-EpoR-*JAK2V617F* cells that lead to an increase of DNA oxidative damage (8-oxo-guanines and DNA double-strand-breaks). In our proteomic research, we also found a big deregulation of ROS related proteins that involved an alteration of oxygen detoxification pathways (see Table II.7). For instance, the protein myeloperoxidase (MPO) was overexpressed in non-*JAK2* mutated granulocytes compared with mutated ones and particularly we observed an increased under-expression in mutated PMF granulocytes compared with *JAK2V617F* PV, ET and *JAK2(-)* ones. Peroxiredoxin 2 was highly

upregulated in *JAK2V617F* ET granulocytes compared with *JAK2V617F* PV, PMF and non-mutated ones. Moreover, the analysis of genomic analysis confirmed the implication of oxidative stress in the pathophysiology of MPNs. We highlighted that the oxidative stress related catalase (*CAT*) was under-regulated due to a decreased on the expression of the *CAT* gene in *JAK2V617F* MPN subjects.

In addition, catalase gene expression was also reduced in PV and PMF CD34+ cells. Concerning the catalase protein, unfortunately, we couldn't confirm a decrease expression in granulocytes of patients compared with normal ones since we did not explore control granulocytes. However, we observed a significant variation of the catalase expression among MPN subtypes and particularly lower levels were found in *JAK2(+)* MPNs vs *JAK2* WT. This latter observation could suggest that *JAK2V617F* induces a decrease of catalase expression participating to the oncogenic role of this mutation. Indeed, Marty *et al.* (170) had already reported a decreased of the catalase expression in mouse models that showed that the PI3K/Akt activation via *JAK2V617F* negatively regulated the Forkhead O transcription factor leading to a reduced expression of anti-oxidant enzymes such as the catalase in bone marrow cells of knock-in mice. Moreover, the protein RAC2, which was under-regulated in *JAK2V617F* ET and PMF patients compared with non-mutated ones, is directly linked to the NADPH complex. It has been related to ROS production as it is capable of altering the mitochondrial membrane potential and electron flow producing high levels of ROS in CML in chronic phase cells and primitive leukemia stem cells (195). Altogether, our data confirmed, in clinical samples, the prominent role of ROS balance in MPN physiopathology.

Apart clinical aspects associated with *JAK2V617F* expression in PV granulocytes such as hemoglobin concentration, leukocytosis or splenomegaly, as well as *JAK2V617F* value as poor prognostic factor (myelofibrotic evolution) (26), *JAK2V617F* allele burden has also been correlated with high expression of CD11b in ET neutrophils (105). In our proteomic analysis, we reported (Table II.5) that some proteins could be directly impacted by the amount of mutated *JAK2*. The protein Galectin-10 (C5HZ13) was more overexpressed in ET granulocytes than in PMF and in these ones more than in PV ones and those ones more than in non-mutated granulocytes suggesting a positive *JAK2V617F* allele burden impact. Conversely, the protein azurocidin (CAP7), an antibacterial granule of neutrophils with a cytotoxic action against Gram-negative bacteria and tropomyosin alpha-1 chain (TPM1) a

protein with a central role on the stabilization of cytoskeleton actin filaments, appeared overexpressed in non-mutated granulocytes alluding a negative impact of the *JAK2V617F* allele burden. Finally, some proteins like folate receptor gamma (FOLR3), cathepsin G (CATG) and proteoglycan 3 (PRG3) were equally expressed in PV and non-mutated granulocytes and their expression was higher than in PMF and ET suggesting that *JAK2* allele burden did not influence their levels of expression.

## CONCLUSION AND PERSPECTIVES

The collaboration with the Institute of Medical Research in Belgrade, (Serbia), let us perform a proteomic and transcriptomic study of granulocytes in Ph- MPNs. The cDNA microarray analysis was done by the research group of Alan N. Schechter and their results can be found in their article (Supplemental Data II-3). In this paper, it is principally developed the genomic deregulations in granulocytes and CD34+ cells in MPNs. To complete this analysis, the proteomic study of granulocytes allowed us to identify important protein alterations associated with transcriptomic data (see the article).

Our data showed that important proteomic deregulations existed between *JAK2V617F* MPNs and non-mutated ones as well as between PV, ET and PMF mutated patients. Moreover, some of these proteins seemed to be impacted by the *JAK2V617F* allele burden. Moreover, it was remarkable that the protein CALR, whose gene is mutated in some cases of Ph- MPNs, was up-regulated in *JAK2V617F* MPN granulocytes independently of this mutation allele burden.

Our results also showed an important deregulation of the RAS GTPase pathways that had also been found altered in MPN RBCs suggesting a myeloid alteration of this family of proteins. Moreover, the mTOR pathways, linked to cell growth, were also deregulated in MPN granulocytes.

Finally, the stress conditions to which *JAK2V617F* cells are exposed could be the reason that brings to $Ca^{2+}$ as well as ROS deregulation presented in MPN granulocytes.

Altogether these data showed that, apart from genetic well-known alterations such as *JAK2V617F* and *CALR* exon 9, proteome alterations play a critical role in MPNs.

Considering this common alterations in granulocytes and RBCs, it could be useful to perform a proteomic analysis of progenitors to better understand proteome alterations that take place in HSC and their link with the main genotypes.

## RESUME DU CHAPITRE II

L'analyse quantitative et qualitative par LC-MS/MS couplée au LTQ Orbitrap des granulocytes des patients atteintes des syndromes myéloprolifératifs Philadelphia négatifs nous a permis de montrer des dérégulations importantes des protéines selon le statut moléculaire des patients (*JAK2V617F* vs *JAK2 WT*), leur diagnostic (*JAK2V617F* PV, ET ou PMF) voir pour certaines protéines comme la Peroxiredoxine 2 selon la charge allélique en JAK2V617F.

En plus, nous avons retrouvé dans les polynucléaires des dérégulations de la famille des Rho GTPases qui étaient aussi altérées chez les globules rouges des SMP (cf part I), confirmant l'importance des dérégulations de cette voie dans la physiopathologie des SMP Ph-. Outre les protéines GTPases, nous avons retrouvé des dérégulations de la signalisation mTOR, de protéines de régulation de l'homéostasie du calcium, et d'importante dérégulation de protéines régulatrices du stress oxydatif, pouvant altérer à la fois les mécanismes de protection contre le stress oxydatif (i.e. diminution de la catalase) ou au contraire favoriser la production d'espèces réactives de l'oxygène comme la MPO. Ces dérégulations de l'activité peroxydasique renforcent l'hypothèse du possible rôle de l'activation des PNN sur des complications thrombotiques si fréquentes chez les patients SMP. Enfin, nous avons montré que la protéine Calréticuline, connue pour son potentiel myéloprolifératif quand elle est mutée, se trouve hyper-exprimée chez les granulocytes des patients SMP *JAK2V617F* en comparaison avec les *JAK2 WT* de façon indépendant à la charge allélique de *JAK2V617F*. Ce résultat suggère un potetiel oncogénique de la protéine CALR native en dehors de ses formes mutées.

En conclusion, ces résultats mettent en évidence la présence de dérégulations protéiques dans les granulocytes, certaines communes avec les érythrocytes des patients SMP suggérant qu'elles prennent leur origine dans un d'un progéniteur clonale commun. En outre, ces altérations protéiques différentes selon le diagnostic des patients pourraient expliquer les différences phénotypiques trouvées chez les sous-groupes des SMP Ph-.

# CHAPTER III

# Ba/F3 and HEL cells as models on the study of MPN deregulations

## BACKGROUND

Our results on RBC proteome highlighted the implication of Rho GTPases in protein alterations. At this point, two questions arise: i) Are these Rho GTPase deregulations specific of RBCs or do they occur in other MPN cell lineages? ii) Is there a link between *JAK2V617F* and these deregulations?

To answer these questions, Ba/F3 EpoR, Ba/F3 EpoR JAK2 wild-type (WT), Ba/F3 EpoR JAK2V617F and HEL cells were selected as MPN cell models. Hence, the objective of this third chapter was to validate in these cell models the previous reported deregulations of Rho GTPases and to evaluate the influence that JAK2 inhibitors and hydroxyurea may have on them.

Ba/F3 cell lines are interleukin 3 (IL-3) dependent hematopoietic cells. They are very used in the study of cytokines; mutations, downstream signaling pathways and inhibitors. The fact that they are used for kinase-related drug discovery lets researchers evaluate drug potential; effects and the screening of possible resistant mutations to these kinase inhibitors. Their high utilization emerges because these Ba/F3 are suspension cells that grow very quickly facilitating rapid experimental procedures. Secondly, they are easily transfected by electroporation and susceptible to infection by retro and lentiviral expression systems. Finally, they can proliferate independently from IL-3 when they express constitutively active tyrosine kinases or other growth oncogenes. They have already been proved for the study of multiple kinases such as NPM-Alk, Flt3 mutants and JAK2 (196).

First studies of *JAK2* mutations in Ba/F3 cells by James *et al.* (17) showed that *JAK2V617F* EpoR increased cell sensitivity to erythropoietin stimulation compared with Ba/F3 wild type EpoR. In addition, mutated *JAK2* Ba/F3 presented growth-factor independent growth and increased STAT5 signaling as well as PI3K and ERK pathways. Similar experiences in Ba/F3 cells were carried out in other JAK2 cytokine receptors such as thrombopoietin and granulocyte-colony stimulating factor receptors with analogous results (197).

In addition, another human cell line also presents the *JAK2V617F* mutation: the leukemia cell line HEL (19). It expresses constitutively tyrosine-phosphorylated *JAK2* as well as its downstream effectors STAT5 and ERK. When treated with JAK2 inhibitors,

these cells showed a dose-dependent inhibition of proliferation due to reduced JAK2 phosphorylation as wells as apoptosis. Therefore, Ba/F3 EpoR cell lines: normal EpoR, EpoR JAK2 wild-type (overexpressing JAK2) and EpoR mutated JAK2 (*JAK2V617F*) are well stablished cell lines in MPN researches.

In this study, I used the three Ba/F3 cell lines as well as the leukemia cell line HEL to go on with my investigations of MPN protein deregulations and to evaluate the possible effects of JAK2 inhibitors on the IQGAP1/Rho GTPase signaling.

Nowadays, the only approved JAK2 inhibitor for MPN treatment is Ruxolitinib; (approved by the U.S. Food and Drug Administration in 2011 and the European Commission in 2012) for its use in intermediate-2 and low risk PMF and secondary myelofibrosis post-PV or ET. It can also be given in PV treatment as third line when hydroxyurea and IFNα have already been discarded (43). In my research, I used Ruxolitinib (INCB018424), which inhibits JAK1 and JAK2; as well as AZD1480 that inhibits JAK2. Both are Adenosine Tri-Phosphate (ATP) mimetic JAK inhibitors that bind to the active form of JAKs.

I also selected hydroxyurea, a first line chemotherapy of high risk MPN to test its possible effects on the Rho family of GTPases in my cell models. HU blocks the dihydrophosphate reductase, an enzyme needed for nucleotide reduction inhibiting DNA synthesis and inducing cell death in S-phase. It is used for treating both ET and PV patients as first choice in high risk patients (83).

# MATERIAL AND METHODS

### *Cell Lines*

Ba/F3 EpoR, Ba/F3 EpoR JAK2 wild-type (WT) and Ba/F3 EpoR JAK2V617F were provided by Dr Isabelle Plo from (INSERM U1009 "*Hématopoïèse et cellules souches*," "Institut Gustave Roussy" Villejuif, Pr Solary E). They were cultured in DMEM culture with 1% penicillin/streptomycin, 1% glutamine, 10% fetal bovine serum (FBS) and 1UI Erythropoietin (EPO).

HEL cells were cultured in RPMI culture with 1% penicillin/streptomycin, 1% glutamine, 10% FBS at 37°C with 5% $CO_2$.

All cell lines (Ba/F3 and HEL) were washed three times in cold 1x PBS, lysed with lysis buffer (20 µL/million de cellules) (1% NP-40, 10 mM KCl, 10 mM HEPES, 0.1 mM EDTA + protease (cOmplete, EDTA-free, Roche) and phosphatase inhibitors (phospho-STOP, Roche)) during 20 minutes vortexing vigorously each five minutes at 4°C and quantified by BIORAD DC™ protein assay. Cell viability was measured using trypan blue as cell death marker.

### *Western-Blotting*

(See Material and Methods of Chapter I)

### *Immunoprecipitation*

(See Material and Methods of Chapter I)

### *Antibodies*

(See Material and Methods of Chapter I)

### *Inhibitors*

Ruxolitinib (INCB018424) a JAK1 and JAK2 inhibitor was provided by Novartis. AZD1480 an ATP-competitive JAK2 inhibitor was from Selleckchem®. Both drugs were diluted in dimethyl sulfoxide (DMSO).

Hydroxyurea (HU) was purchased at Sigma-Aldrich® and diluted in water.

### *Cell cycle analysis by Flow Cytometry*

Flow cytometry was used to measure cell cycles of HEL cells under the influence of the different inhibitors. To explore cell cycleS we chose propidium iodide (PI) which is a DNA intercalant agent that will let us quantify the quantity of DNA in each cell. How cell cycle is shown by flow cytometry is explain in Figure III.1.

One million cells were washed twice in cold 1x PBS and resuspended in 300 µL of PBS. Then, 700 µL of cold ethanol (70%) was drop-wise and left at 4°C overnight. Next, cells were washed twice in cold PBS and resuspended in 250 µL of PBS. 5 µL of 10 mg/mL RNAse A were carefully added and samples were incubated at 37°C for 1 hour. Finally, 10 µL of 1 mg/mL of propidium iodide stain were added and samples were analyzed on Fluorescence-activated cell sorting, (FACS) on cytometer at 488 nm. We measured a minimum of 30,000 cells if possible.

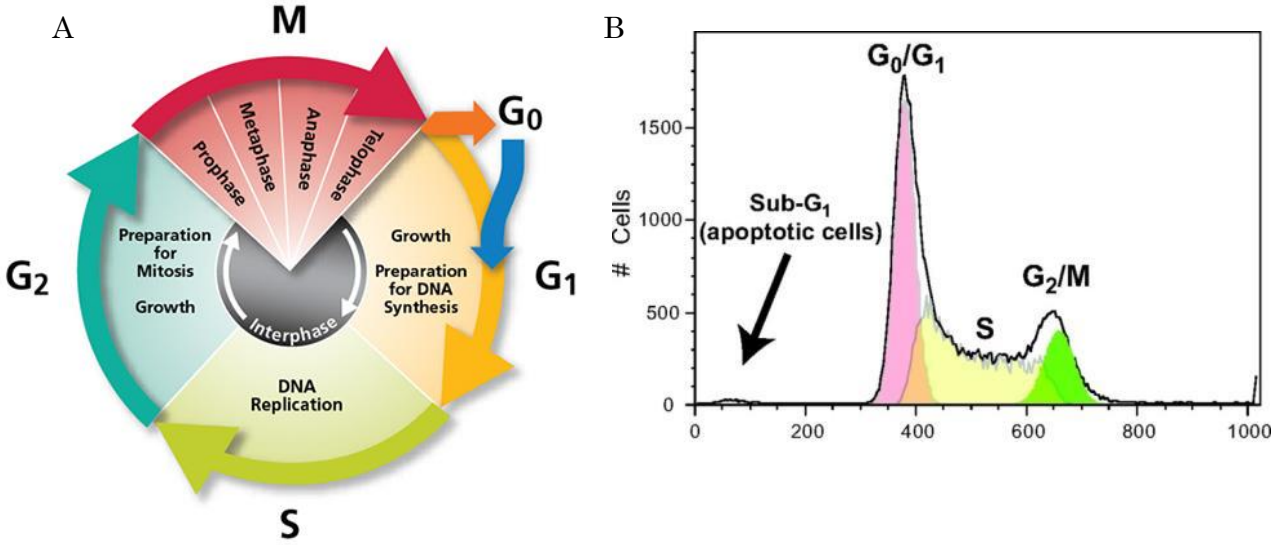


**Figure III.1. A)** Cell cycle of normal cells. **B)** Image of cell cycle analyzed by flow cytometry. To read the cryptogram, if we go from left to right the amount of DNA increases and from down to up the number of cells rises. When cells are in G0/G1 phase they have a quantity of DNA. If they pass to S phase they start replicating their DNA so the quantity of DNA increases and finally, cells in G2/M phase have the biggest quantity of DNA (they have doubled it) just before they split in two. In this case we can see that most of the cells are in G0/G1 phase followed by G2/M phase and there are fewer cells in S phase. Cells that appear on the left represent death cells (Sub-$G_1$).

# RESULTS

## HEL CELLS

### *1-Effects of JAK2 inhibitors and hydroxyurea on cell concentration and cell viability*

The objective of this part was to determine HEL cell sensibility to some inhibitors (Ruxolitinib, AZD1480 and Hydroxyurea) to select an ideal concentration balanced between toxicity and no effect. These concentrations would be used to study the effects of these inhibitors on protein expression, specifically on the Rho family of GTPases.

In order to fulfil this objective, HEL cells were cultured for 24, 48 and 72 hours with inhibitors at different concentrations. A control with DMSO was used to measure cell death caused by this toxic agent as Ruxolitinib and AZD1480 are diluted on it. DMSO final concentration was always ≤ 1%.

As seen in Figure III.2, cell death was correlated with increased concentrations of hydroxyurea. We could observe that concentrations above 250 μM of HU completely blocked cell growth and induced apoptosis. Both Ruxolitinib and AZD1480 also inhibited cell growth when comparing with controls but less markedly than HU.

After 24h of incubation, cell viability hardly changed in all cases; however, it decreased together with time and rising inhibitor concentrations. We observed that HU caused more apoptosis than Ruxolitinib or AZD1480 at the concentrations tested.

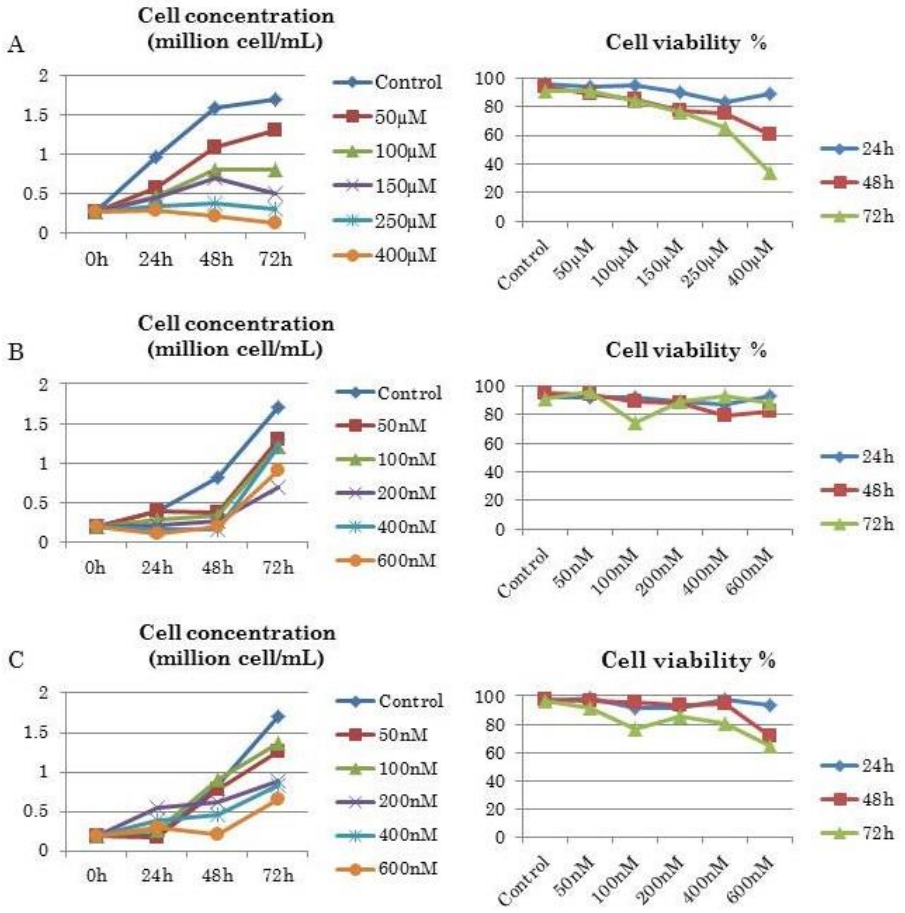


**Figure III.2**. Effects of Hydroxyurea **(A)**, Ruxolitinib **(B)** and AZD1480 **(C)** on HEL cells. Graphics on the left show cell concentration after 24, 48 and 72 hours of incubation at different inhibitor concentrations. Those on the right represent cell viability after 24, 48 and 72 hours of incubation at different inhibitor concentrations.

### *2-Cell cycle analysis*

Cell cycle analysis by flow cytometry was determined at 24 and 48 hours after treatment with HU, Ruxolitinib or AZD1480 at different concentrations (Figure III.3 to III.8 and Tables III.1 to III.6). Results show that after 24 hours of drug incubation, hydroxyurea blocked cells on the S phase and cells on the G0/G1 and G2/M phases decreased dose-dependently. Ruxolitinib effects were similar at all conentrations. However, AZD1480 caused a light decreased of cells on the G0/G1 phase while the proportion of cells on S and G2/M phases raised blocking cells on the S phase. After 48 hours of drug incubation, we saw that the number of cells decreased on S phase and increased on G2/M phase under HU

treatment. AZD1480 turned cells into apoptosis and Ruxolitinib decreased number of cells on S and G2/M phases as the number of cells on G0/G1 phase was more or less stable.

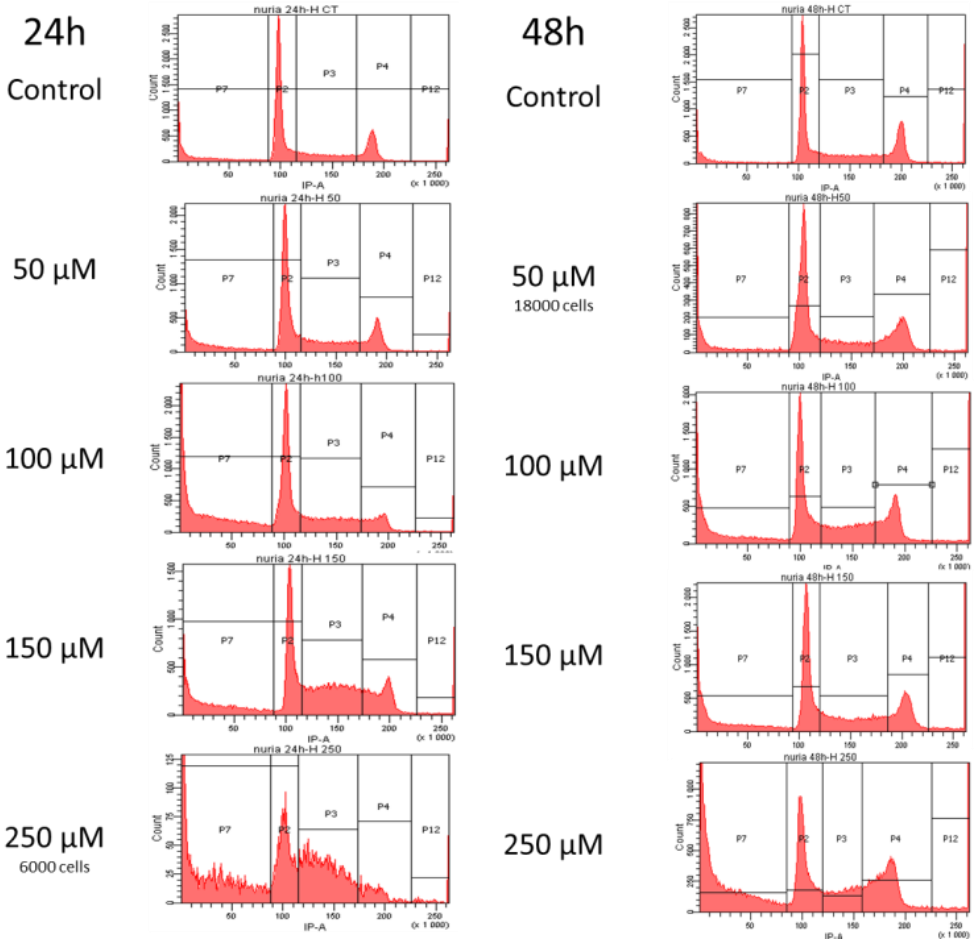


**Figure III.3.** DNA fluorescence profiles of HEL cells with +/- Hydroxyurea. The x axis shows PI intensity and y axis number of cells. More than 30,000 cells were measured apart from those where it is noted.

| Hydroxyurea 24h | Control | 50 µM | 100 µM | 150 µM | 250 µM |
|---|---|---|---|---|---|
| G0/G1 Phase | 44.9 | 42.6 | 30.7 | 26.3 | 20.3 |
| S Phase | 18.1 | 20.4 | 18.2 | 33.2 | 30.8 |
| G2/M Phase | 17.3 | 16.5 | 9.7 | 17.6 | 6.5 |
| Apoptotic cells | 16.2 | 17.8 | 39.7 | 19.3 | 40.3 |
| Double cells | 3.5 | 2.6 | 1.7 | 3.5 | 2.2 |
| Total population | 100 | 100 | 100 | 100 | 100 |

**Table III.1.** Cell cycle analysis by flow cytometry. It shows the percentage of cells in each phase at different concentrations of HU after 24 hours.

| Hydroxyurea 48h | Control | 50 µM | 100 µM | 150 µM | 250 µM |
|---|---|---|---|---|---|
| G0/G1 Phase | 37.7 | 36.7 | 27.4 | 26.4 | 19.7 |
| S Phase | 21.6 | 13.8 | 18.9 | 19.5 | 11.5 |
| G2/M Phase | 22 | 20.9 | 18.5 | 15.9 | 21.3 |
| Apoptotic cells | 10.3 | 15.5 | 21.2 | 19.5 | 34.8 |
| Double cells | 8.4 | 13 | 14 | 18.7 | 12.6 |
| Total population | 100 | 100 | 100 | 100 | 100 |

**Table III.2.** Cell cycle analysis by flow cytometry. It shows the percentage of cells in each phase at different concentrations of HU after 48 hours.

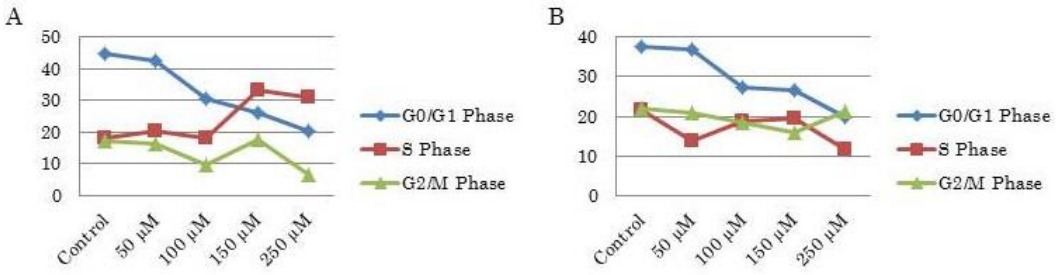


**Figure III.4.** Analysis of cell cycle of HEL cells with +/- hydroxyurea. Graphics show the percentage of cells in each phase at different hydroxyurea concentrations after 24 **(A)** or 48 hours **(B)** of drug incubation.

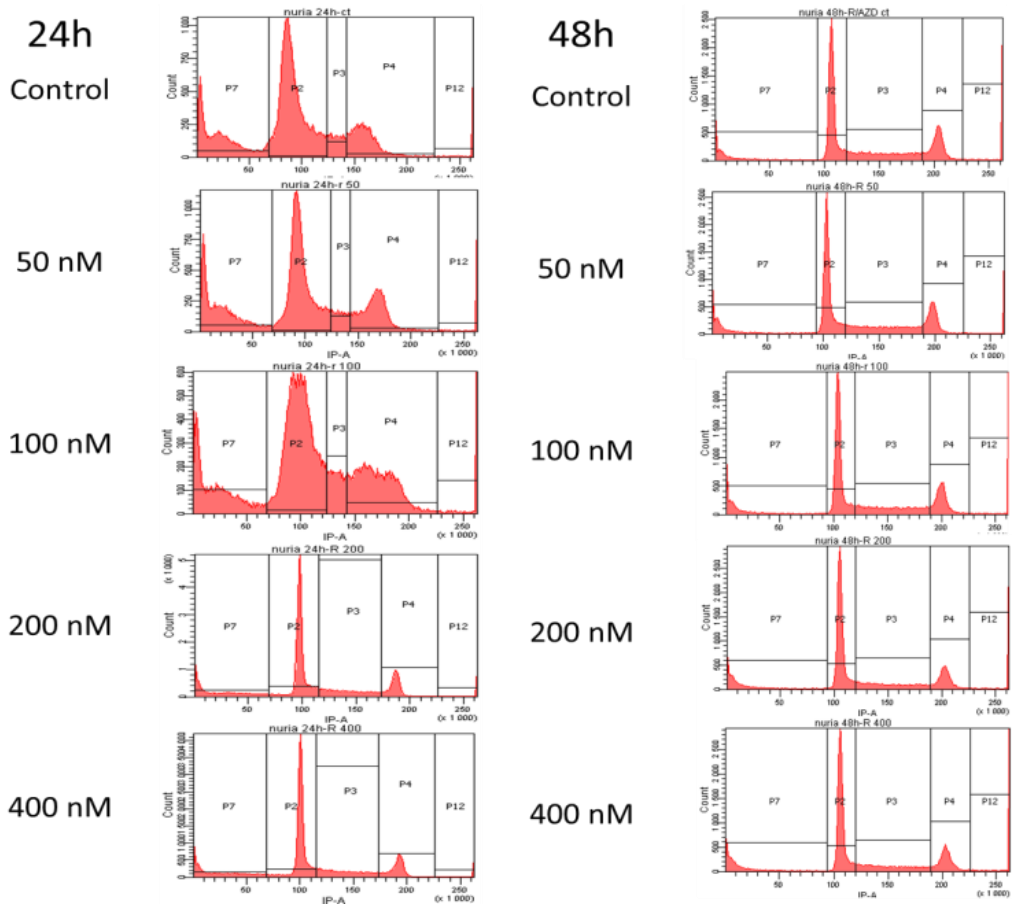


**Figure III.5.** DNA fluorescence profiles of HEL cells with +/- Ruxolitinib. The x axis shows PI intensity and y axis number of cells. More than 30,000 cells were measured each time.

| Ruxolitinib 24h | Control | 50 nM | 100 nM | 200 nM | 400 nM |
|---|---|---|---|---|---|
| G0/G1 Phase | 52.5 | 45.9 | 46.6 | 51.6 | 52.2 |
| S Phase | 6.5 | 6 | 7.7 | 5.9 | 5.8 |
| G2/M Phase | 16.6 | 20.7 | 24.7 | 22.7 | 23 |
| Apoptotic cells | 22.1 | 24.5 | 17.8 | 17.7 | 17.3 |
| Double cells | 2.3 | 3 | 3.3 | 2.1 | 1.7 |
| Total population | 100 | 100 | 100 | 100 | 100 |

**Table III.3.** Cell cycle analysis by flow cytometry. It shows the percentage of cells in each phase at different concentrations of Ruxolitinib after 24 hours.

| Ruxolitinib 48h | Control | 50 nM | 100 nM | 200 nM | 400 nM |
|---|---|---|---|---|---|
| G0/G1 Phase | 38.7 | 41.5 | 39.1 | 43.9 | 39.3 |
| S Phase | 22.9 | 23.6 | 20.6 | 18.2 | 17.3 |
| G2/M Phase | 19.8 | 16.9 | 17 | 15.5 | 15.5 |
| Apoptotic cells | 9.7 | 12.6 | 11.8 | 13.3 | 13.6 |
| Double cells | 8.8 | 5.4 | 11.5 | 9 | 14.3 |
| Total population | 100 | 100 | 100 | 100 | 100 |

**Table III.4.** Cell cycle analysis by flow cytometry. It shows the percentage of cells in each phase at different concentrations of Ruxolitinib after 48 hours.

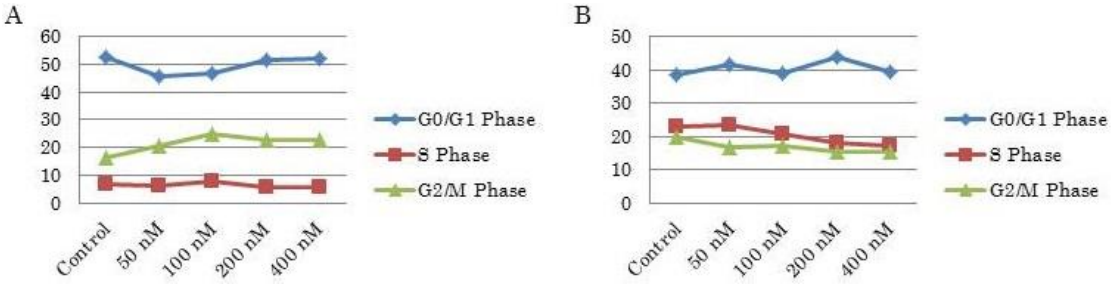


**Figure III.6.** Analysis of cell cycle of HEL cells with +/- Ruxolitinib. Graphics show the percentage of cells in each phase at different inhibitor concentrations after 24 **(A)** or 48 hours **(B)** of drug incubation.

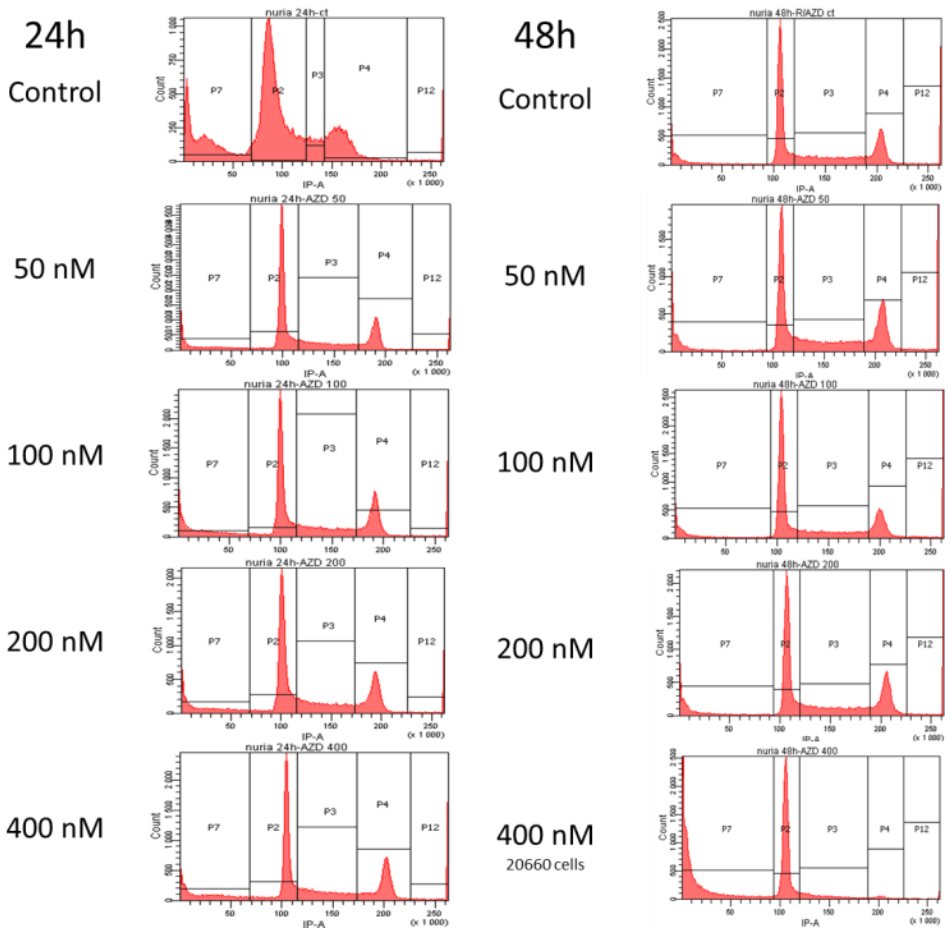


**Figure III.7.** DNA fluorescence profiles of HEL cells with +/- AZD1480. The x axis shows PI intensity and y axis number of cells. More than 30,000 cells were measured apart from those where it is noted.

| AZD1480 24h | Control | 50 nM | 100 nM | 200 nM | 400 nM |
|---|---|---|---|---|---|
| G0/G1 Phase | 52.5 | 46.7 | 38.9 | 42.1 | 36.7 |
| S Phase | 6.5 | 19.5 | 18.9 | 19.7 | 18.6 |
| G2/M Phase | 16.6 | 18.3 | 20.7 | 21 | 22.7 |
| Apoptotic cells | 22.1 | 12.6 | 16.6 | 13.4 | 15.4 |
| Double cells | 2.3 | 2.9 | 5 | 3,9 | 6.8 |
| Total population | 100 | 100 | 100 | 100 | 100 |

**Table III.5.** Cell cycle analysis by flow cytometry. It shows the percentage of cells in each phase at different concentrations of AZD1480 after 24 hours.

| AZD1480 48h | Control | 50 nM | 100 nM | 200 nM | 400 nM |
|---|---|---|---|---|---|
| G0/G1 Phase | 38.7 | 30.1 | 42.7 | 37.2 | 39.5 |
| S Phase | 22.9 | 22 | 19 | 21.4 | 7.6 |
| G2/M Phase | 19.8 | 20.9 | 17.6 | 20.9 | 1.6 |
| Apoptotic cells | 9.7 | 10.2 | 9.6 | 11.1 | 50.8 |
| Double cells | 8.8 | 16.8 | 11.1 | 9.3 | 0.5 |
| Total population | 100 | 100 | 100 | 100 | 100 |

**Table III.6.** Cell cycle analysis by flow cytometry. It shows the percentage of cells in each phase at different concentrations of AZD1480 after 48 hours.

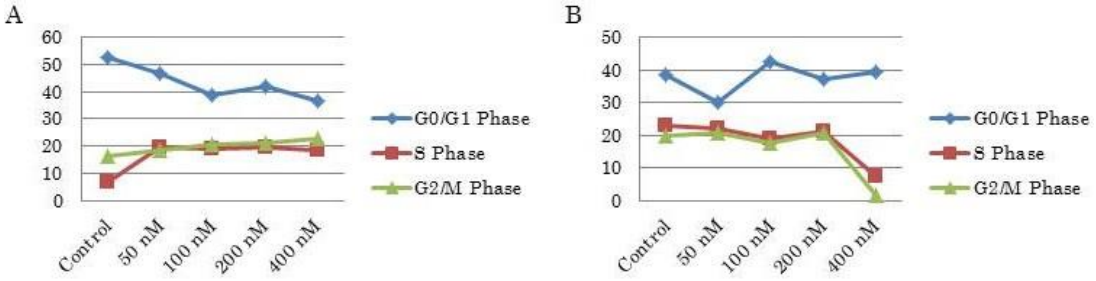


**Figure III.8.** Analysis of cell cycle of HEL cells with +/- AZD1480. Graphics show the percentage of cells in each phase at different AZD1480 concentrations after 24 **(A)** or 48 hours **(B)** of drug incubation.

### *3-IQGAP1 and Rho GTPases expression in HEL cells*

We first verified by western blotting the expression of the following proteins: IQGAP1, PAK1, P-PAK1, Rac1, Cdcd42, RhoA and RhoGDI in HEL lysates. As seen in Figure III.9 all the proteins tested except for phosphorylated PAK-1 were present in HEL lysates.

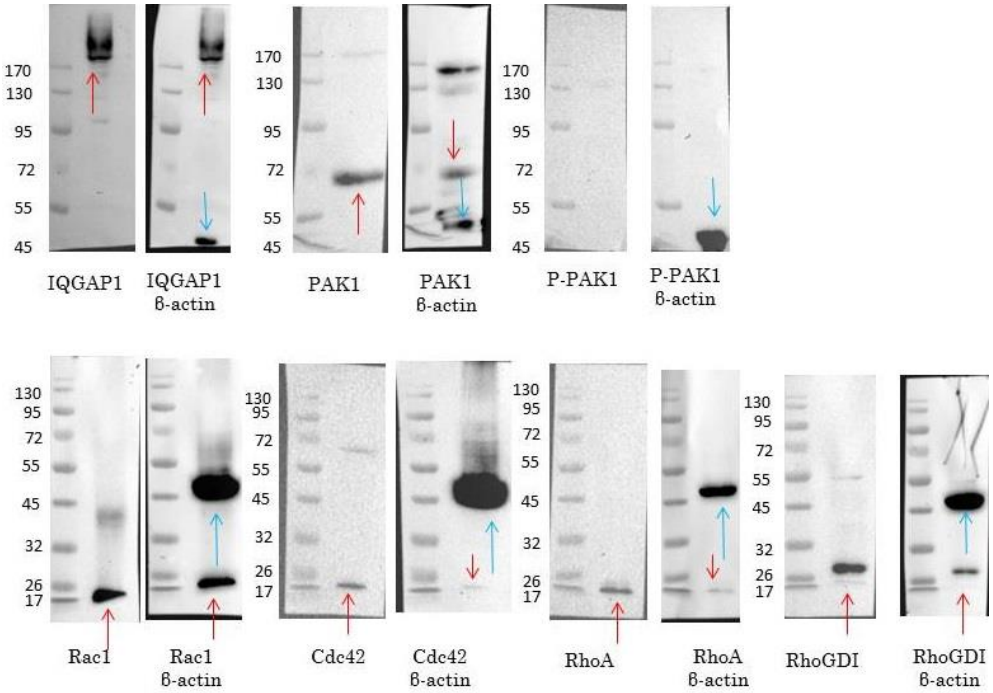


**Figure III.9.** Western blot analysis of HEL lysates. 20 µg of HEL lysates were loaded on SDS-PAGE gels and transferred to nitrocellulose membranes to be revealed with suitable antibodies: IQGAP1, PAK1, P-PAK1, Rac1, Cdc42, RhoA, RhoGDI and β-actin. Red arrows point to the correspondent proteins. Blue arrows point to β-actin. Molecular weights of targeted proteins: IQGAP1: 189 kDa, PAK1 and P-PAK1: 61 kDa, Rac1 21 kDa, Cdc42 21 kDa, RhoA 22 kDa, RhoGDI: 22 kDa, ß-actin: 42 kDa.

Secondly, we measured inhibitor effects on protein expression in HEL cells. Equal amounts of protein were loaded to be analyzed by western blotting using the specific antibodies (Figures III.10 to III.15).

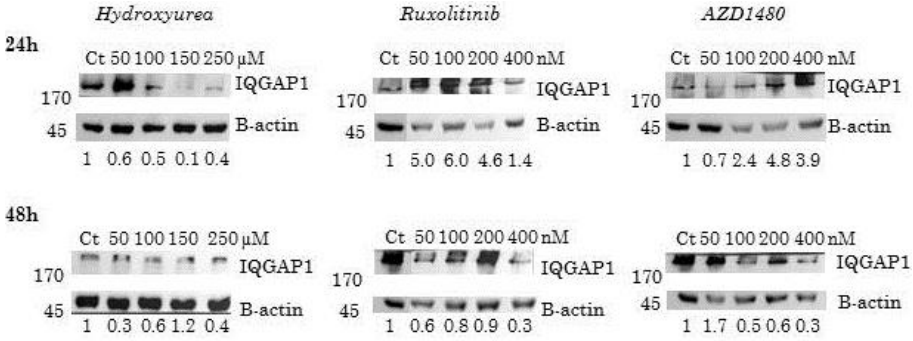


**Figure III.10.** IQGAP1 expression in HEL cells. Western blots of HEL lysates under hydroxyurea, Ruxolitinib or AZD1480 conditions and at 24 or 48 hours. ß-actin was used as loading control. Numbers indicate IQGAP1/ß-actin ratios relative to Control ratios. Ct: Control. Molecular weights: IQGAP1: 189 kDa, ß-actin: 42 kDa.

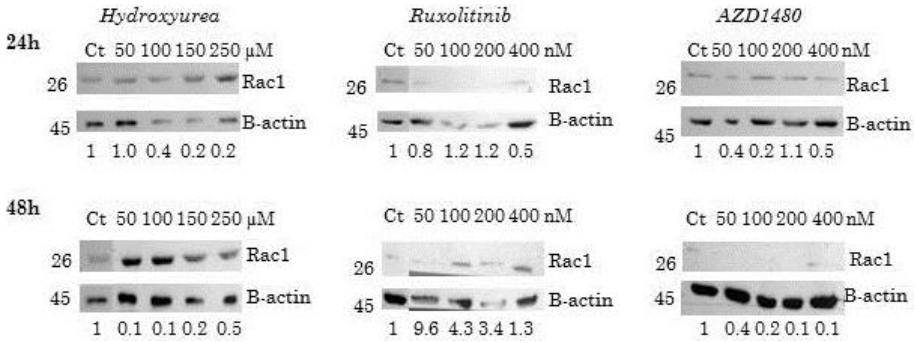


**Figure III.11.** Rac1 expression in HEL cells. Western blots of HEL lysates under hydroxyurea, Ruxolitinib or AZD1480 conditions and at 24 or 48 hours. ß-actin was used as loading control. Numbers indicate Rac1/ß-actin ratios relative to Control ratios. Ct: Control. Molecular weights: Rac1; 21 kDa, ß-actin: 42 kDa.

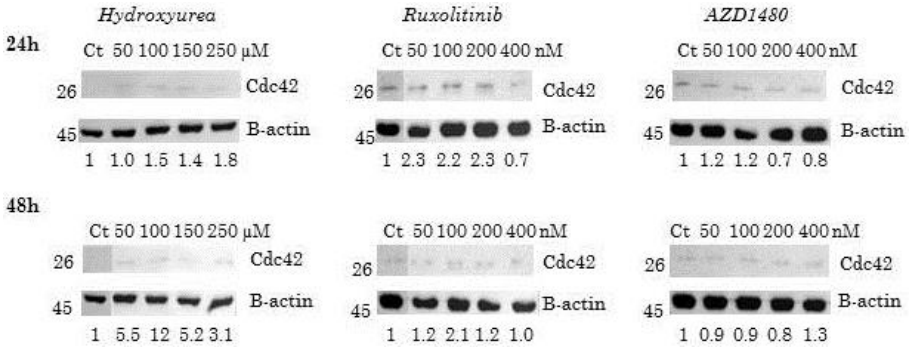


**Figure III.12.** Cdc42 expression in HEL cells. Western blots of HEL lysates under hydroxyurea, Ruxolitinib or AZD1480 conditions and at 24 or 48 hours. ß-actin was used as loading control. Numbers indicate Cdc42/ß-actin ratios relative to Control ratios. Ct: Control. Molecular weights: Cdc42: 21 kDa, ß-actin: 42 kDa.

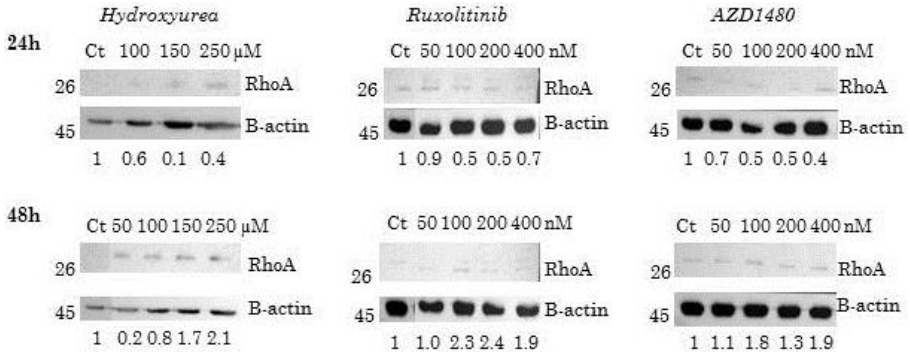


**Figure III.13.** RhoA expression in HEL cells. Western blots of HEL lysates under hydroxyurea, Ruxolitinib or AZD1480 conditions and at 24 or 48 hours. ß-actin was used as loading control. Numbers indicate RhoA/ß-actin ratios relative to Control ratios. Ct: Control. Molecular weights: RhoA: 22 kDa, ß-actin: 42 kDa.

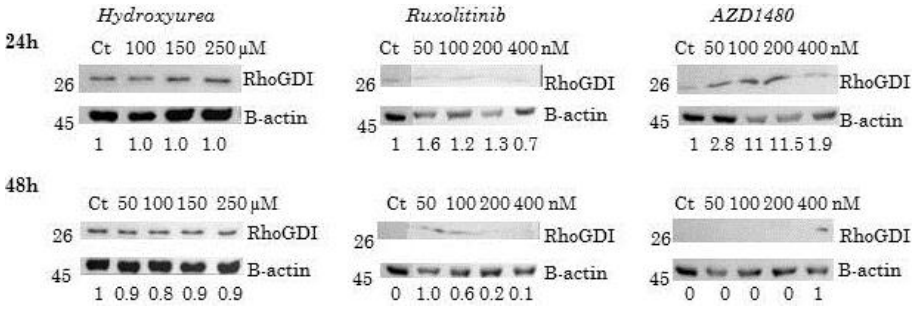


**Figure III.14.** RhoGDI expression in HEL cells. Western blots of HEL lysates under hydroxyurea, Ruxolitinib or AZD1480 conditions and at 24 or 48 hours. ß-actin was used as loading control. Numbers indicate RhoGDI/ß-actin ratios relative to Control ratios. Ct: Control. Molecular weights: RhoGDI: 22 kDa, ß-actin: 42 kDa.

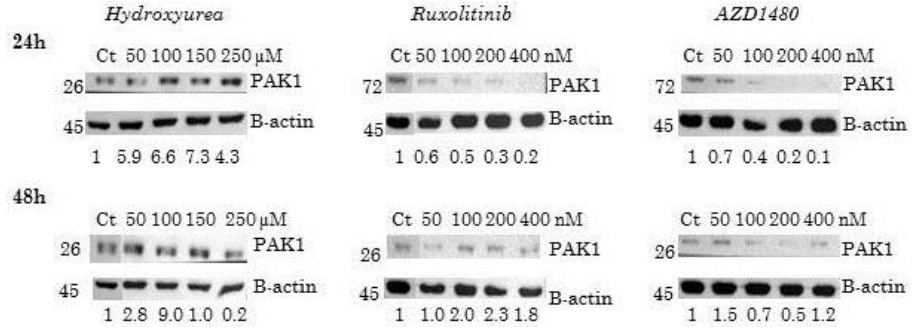


**Figure III.15.** PAK1 expression in HEL cells. Western blots of HEL lysates under hydroxyurea, Ruxolitinib or AZD1480 conditions and at 24 or 48 hours. ß-actin was used as loading control. Numbers indicate PAK1/ß-actin ratios relative to Control ratios. Ct: Control. Molecular weights: PAK1: 61 kDa, ß-actin: 42 kDa.

As shown in Figures III.10 to III.15, and as resumed in Table III.7, IQGAP1 expression was reduced by increasing concentrations of HU at both 24h and 48h of incubation and after 48h with Ruxolitinib and AZD1480. On the opposite, IQGAP1 expression was increased after 24h of AZD1480 and Ruxolitinib treatment. Rac1 decreased it expression under hydroxyurea and AZD1480 influence but not with Ruxolitinib (increased expression). Surprisingly, RhoA expression decreased at higher concentrations of the three inhibitors after 24h and it increased its expression after 48h. Similar results were obtained for PAK1 expression under the effects of Ruxolitinib and AZD1480. Nevertheless, PAK1 expression was increased after 24h under rising concentrations of hydroxyurea. The signals

for Cdc42 were light but it tended to increased it expression under inhibiting conditions. We remarked that RhoGDI wasn't perturbed by hydroxyurea.

| | | Hydroxyurea | | | | | | Ruxolitinib | | | | | | AZD1480 | | | | | |
|---|---|---|---|---|---|---|---|---|---|---|---|---|---|---|---|---|---|---|---|
| | | Ct | 50 | 100 | 150 | 250 | | Ct | 50 | 100 | 200 | 400 | | Ct | 50 | 100 | 200 | 400 | |
| **IQGAP1** | 24h | 1 | 0,6 | 0,5 | 0,1 | 0,4 | ↓ | 1 | 5,0 | 6,0 | 4,6 | 1,4 | ↑ | 1 | 0,7 | 2,4 | 4,8 | 3,9 | ↑ |
| | 48h | 1 | 0,3 | 0,6 | 1,2 | 0,4 | ↓ | 1 | 0,6 | 0,8 | 0,9 | 0,3 | ↓ | 1 | 1,7 | 0,5 | 0,6 | 0,3 | ↓ |
| **Rac1** | 24h | 1 | 1,0 | 0,4 | 0,2 | 0,2 | ↓ | 1 | 0,8 | 1,2 | 1,2 | 0,5 | ≈ | 1 | 0,4 | 0,2 | 1,1 | 0,5 | ↓ |
| | 48h | 1 | 0,1 | 0,1 | 0,2 | 0,5 | ↓ | 1 | 9,6 | 4,3 | 3,4 | 1,3 | ↑ | 1 | 0,4 | 0,2 | 0,1 | 0,1 | ↓ |
| **Cdc42** | 24h | 1 | 1,0 | 1,5 | 1,4 | 1,8 | ↑ | 1 | 2,3 | 2,2 | 2,3 | 0,7 | ↑ | 1 | 1,2 | 1,2 | 0,7 | 0,8 | ≈ |
| | 48h | 1 | 5,5 | 12,0 | 5,2 | 3,1 | ↑ | 1 | 1,2 | 2,1 | 1,2 | 1,0 | ↑ | 1 | 0,9 | 0,9 | 0,8 | 1,3 | ≈ |
| **RhoA** | 24h | 1 | x | 0,6 | 0,1 | 0,4 | ↓ | 1 | 0,9 | 0,5 | 0,5 | 0,7 | ↓ | 1 | 0,7 | 0,5 | 0,5 | 0,4 | ↓ |
| | 48h | 1 | 0,2 | 0,8 | 1,7 | 2,1 | ↑ | 1 | 1,0 | 2,3 | 2,4 | 1,9 | ↑ | 1 | 1,1 | 1,8 | 1,3 | 1,9 | ↑ |
| **RhoGDI** | 24h | 1 | x | 1,0 | 1,0 | 1,0 | ≈ | 1 | 1,6 | 1,2 | 1,3 | 0,7 | ↑ | 1 | 2,8 | 11,0 | 11,5 | 1,9 | ↑ |
| | 48h | 1 | 0,9 | 0,8 | 0,9 | 0,9 | ≈ | 1 | 1,0 | 0,6 | 0,2 | 0,1 | ↓ | 0 | 0 | 0 | 0 | 1 | ↑ |
| **PAK1** | 24h | 1 | 5,9 | 6,6 | 7,3 | 4,3 | ↑ | 1 | 0,6 | 0,5 | 0,3 | 0,2 | ↓ | 1 | 0,7 | 0,4 | 0,2 | 0,1 | ↓ |
| | 48h | 1 | 2,8 | 9,0 | 1,0 | 0,2 | ↑ | 1 | 1,0 | 2,0 | 2,3 | 1,8 | ↑ | 1 | 1,5 | 0,7 | 0,5 | 1,2 | ≈ |

**Table III.7.** Protein/ß-actin ratios. This table shows the different protein/ß-actin ratios under the influence of the diverse inhibitors from western blot results (Figures III.10 to III.15). Abbreviations: Ct: Control (DMSO or water).

### *4-Both Rac1 and Cdc42 are activated in HEL cells*

We pulled-down HEL lysates with GST-PAK-PBD beads and found that both Rac1 and Cdc42 were activated in HEL lysates. On the contrary, pulled-down essays with GST-Rhotekin-RBD beads did not show any activation for RhoA. (Figure III.16)

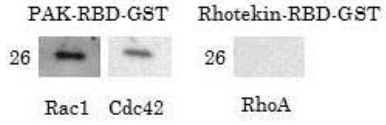


**Figure III.16.** Rho activated proteins in HEL cells. HEL lysates were pulled-down with GST-PAK-RBD and GST-Rhotekin-RBD beads followed by WB developed by Rac1, Cdc42 and RhoA. Molecular weights: Rac1: 21 kDa, Cdc42: 21 kDa, RhoA: 22 kDa.

### *5-JAK2 and Calreticulin expression in HEL cells*

Concurrently, we also studied JAK2 and CALR expressions in HEL cells as they are important actors on MPNs. Figure III.17 shows that JAK2, P-JAK2 and CALR are expressed in normal HEL lysates.

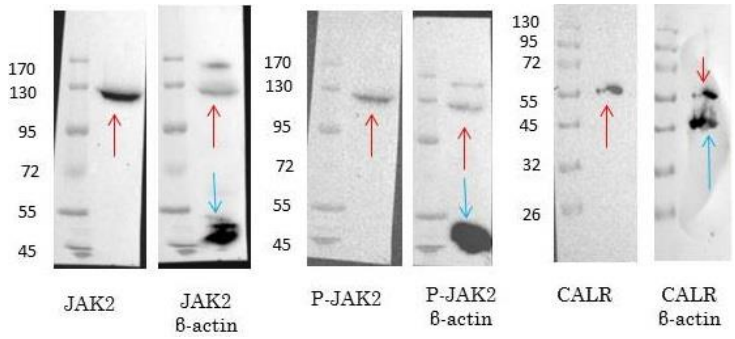


**Figure III.17.** Western blot analysis of HEL lysates. 20 µg of HEL lysates were loaded on SDS-PAGE gels and transferred to nitrocellulose membranes to be revealed with suitable antibodies: JAK2, P-JAK2, CALR and β-actin. Red arrows point to the correspondent proteins. Blue arrows point to β-actin. Molecular weights of targeted proteins: JAK2 and P-JAK2: 131 kDa, CALR: 48 kDa, ß-actin: 42 kDa.

The effects of Hydroxyurea, Ruxolitinib and AZD1480 on CALR and JAK2 protein expression were also measured as shown in Figures III.18 to III.20 and as resumed in Table III.8. In general, JAK2 and P-JAK2 signals were so light that it was difficult to observe any variation. Nonetheless, ß-actin ratios suggest that JAK2 tended to increase its expression under the influence of JAK2 inhibitors. On the opposite, P-JAK2 seemed to decrease under the effects of both JAK2 inhibitors. The levels of CALR expression didn't present any huge variation.

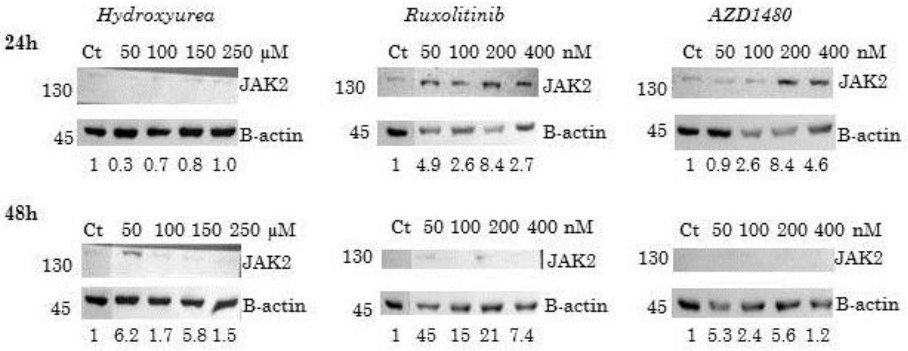


**Figure III.18.** JAK2 expression in HEL cells. Western blots of HEL lysates under hydroxyurea, Ruxolitinib or AZD1480 conditions and at 24 or 48 hours. β-actin was used as loading control. Numbers indicate JAK2/β-actin ratios relative to Control ratios. Ct: Control. Molecular weights: JAK2: 131 kDa, ß-actin: 42 kDa.

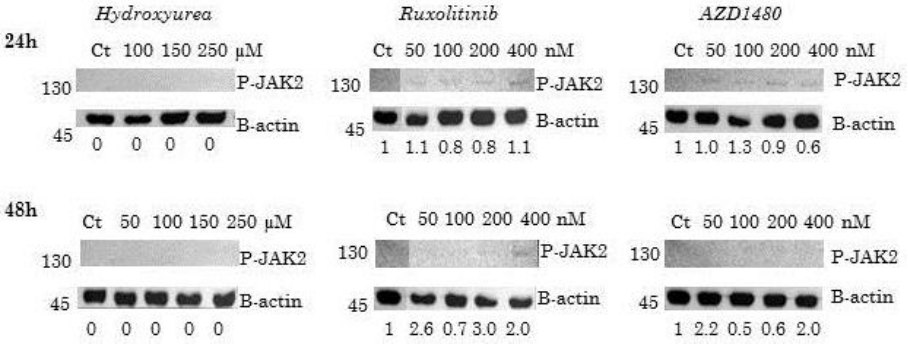


**Figure III.19.** Phosphorylated JAK2 expression in HEL cells. Western blots of HEL lysates under hydroxyurea, Ruxolitinib or AZD1480 conditions and at 24 or 48 hours. β-actin was used as loading control. Numbers indicate P-JAK2/β-actin ratios relative to Control ratios. Ct: Control. Molecular weights: P-JAK2: 131 kDa, ß-actin: 42 kDa.

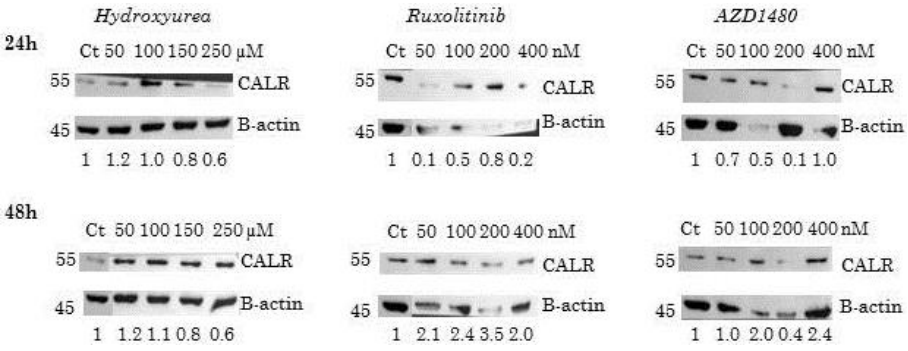


**Figure III.20.** Calreticulin expression in HEL cells. Western blots of HEL lysates under hydroxyurea, Ruxolitinib or AZD1480 conditions and at 24 or 48 hours. β-actin was used as loading control. Numbers indicate CALR/β-actin ratios relative to Control ratios. Ct: Control. Molecular weights: CALR: 48 kDa, ß-actin: 42 kDa.

| | | Hydroxyurea | | | | | | Ruxolitinib | | | | | | AZD1480 | | | | | |
|---|---|---|---|---|---|---|---|---|---|---|---|---|---|---|---|---|---|---|---|
| | | Ct | 50 | 100 | 150 | 250 | µM | Ct | 50 | 100 | 200 | 400 | nM | Ct | 50 | 100 | 200 | 400 | nM |
| **JAK2** | 24h | 1 | 0.3 | 0.7 | 0.8 | 1.0 | ↓ | 1 | 4.9 | 2.6 | 8.4 | 2.7 | ↑ | 1 | 0.9 | 2.6 | 8.4 | 4.6 | ↑ |
| | 48h | 1 | 6.2 | 1.7 | 5.8 | 1.5 | ↑ | 1 | 45 | 15 | 21 | 7.4 | ↑ | 1 | 5.3 | 2.4 | 5.6 | 1.2 | ↑ |
| **P-JAK2** | 24h | 0 | x | 0 | 0 | 0 | ≈ | 1 | 1.1 | 0.8 | 0.8 | 1.1 | ≈ | 1 | 1.0 | 1.3 | 0.9 | 0.6 | ≈ |
| | 48h | 0 | 0 | 0 | 0 | 0 | ≈ | 1 | 2.6 | 0.7 | 3.0 | 2.0 | ↑ | 1 | 2.2 | 0.5 | 0.6 | 2.0 | ≈ |
| **CALR** | 24h | 1 | 1.2 | 1.0 | 0.8 | 0.6 | ≈ | 1 | 0.1 | 0.5 | 0.8 | 0.2 | ↓ | 1 | 0.7 | 0.5 | 0.1 | 1.0 | ↓ |
| | 48h | 1 | 1.2 | 1.1 | 0.8 | 0.6 | ≈ | 1 | 2.1 | 2.4 | 3.5 | 2.0 | ↑ | 1 | 1.0 | 2.0 | 0.4 | 2.4 | ↑ |

**Table III.8.** Protein/ß-actin ratios. This table shows the different protein/ß-actin ratios under the influence of the diverse inhibitors from western blot results (Figures III.18 to III.20). Abbreviations: Ct: Control (DMSO or water).

## Ba/F3 CELLS

### *1-Effects of inhibitors on cell concentration and cell viability*

Similarly to HEL cells, the objective was to determine the sensibility to Ruxolitinib and AZD1480 of the three Ba/F3 cell lines to select an ideal concentration balanced between toxicity and no effect so as to study the effects on protein expression, specifically on the Rho family of GTPases.

The three types of Ba/F3 cells: Ba/F3 EpoR, Ba/F3 EpoR JAK2 WT and Ba/F3 EpoR JAK2V617F were cultured for 24 and 48 hours with JAK2 inhibitors at different concentrations. A control with DMSO was used to measure its toxicity (DMSO concentration ≤ 1%).

As seen in Figures III.21 to III.23, JAK2 inhibitors hampered cell proliferation after 24 hours and they induced cell death after 48 hours of incubation in the three cell lines.

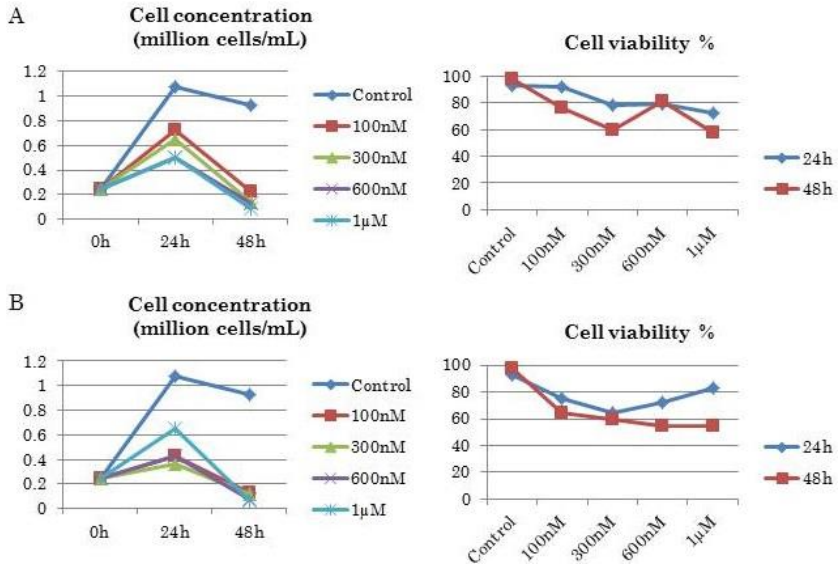


**Figure III.21.** Effects of Ruxolitinib **(A)** and AZD1480 **(B)** on cell concentration and cell viability of Ba/F3 EpoR cells. Graphics on the left show cell concentration after 24 and 48 hours of incubation at different inhibitor concentrations. Those on the right represent cell viability after 24 and 48 hours of incubation at different inhibitor concentrations.

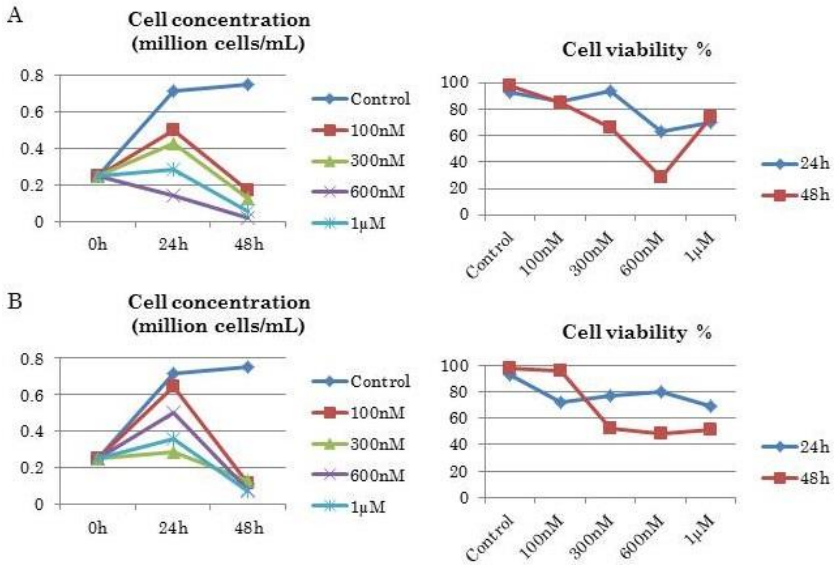


**Figure III.22.** Effects of Ruxolitinib **(A)** and AZD1480 **(B)** on cell concentration and cell viability of Ba/F3 EpoR JAK2 WT cells. Graphics on the left show cell concentration after 24 and 48 hours of incubation at different inhibitor concentrations. Those on the right represent cell viability after 24 and 48 hours of incubation at different inhibitor concentrations.

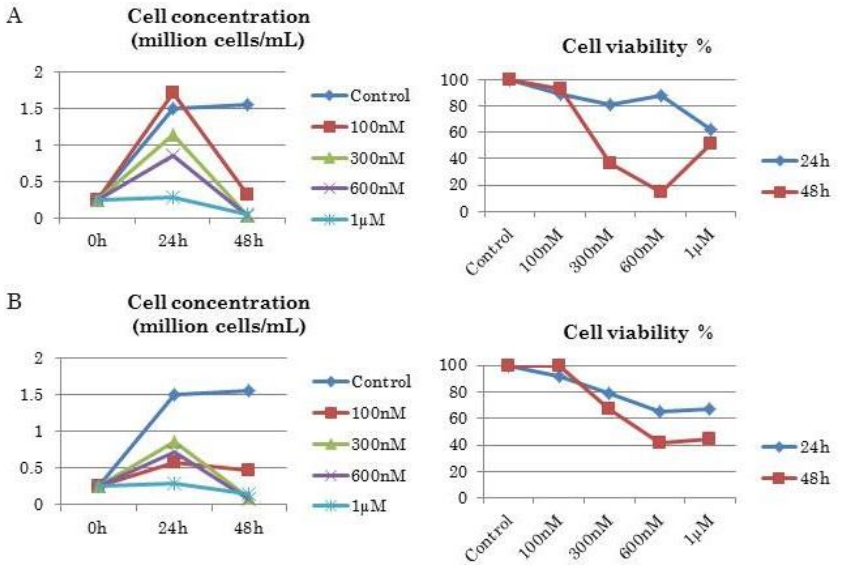


**Figure III.23.** Effects of Ruxolitinib **(A)** and AZD1480 **(B)** on cell concentration and cell viability of Ba/F3 EpoR JAK2V617F cells. Graphics on the left show cell concentration after 24 and 48 hours of incubation at different inhibitor concentrations. Those on the right represent cell viability after 24 and 48 hours of incubation at different inhibitor concentrations.

### *2-Rho GTPase family expression in Ba/F3 cells*

The expressions of IQGAP1, Rac1, RhoA and phosphorylated PAK1 were measured under different conditions. First culture conditions, (referred to as "Control"), consisted of DMEM medium with 1% penicillin/streptomycin, 1% glutamine, 10% FBS and 1UI EPO. Second one consisted of deprivation conditions without either FBS or EPO in order to see the effects of environmental distress on our protein expressions. Finally, cells were cultured under deprivation conditions with JAK2 inhibitors (500 nM Ruxolitinib and AZD1480). All cells were cultured during 6 hours and lysed for western blotting. (Figure III.24).

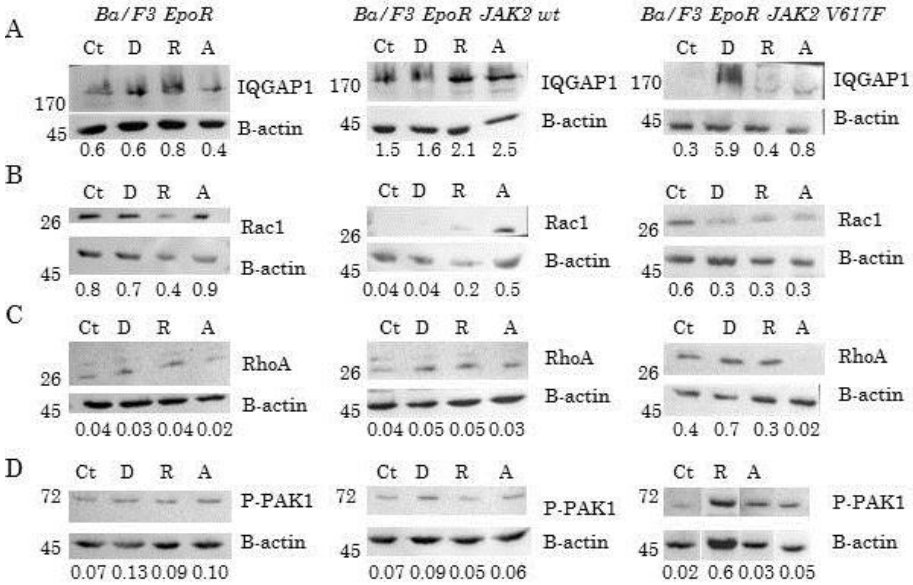


**Figure III.24.** Protein expression in Ba/F3 cells. Cells were cultured under different conditions; After 6h, cells were lysed, run on SDS-PAGE gels followed by western blotting incubated with suitable antibodies. **A)** IQGAP1 expression, **B)** Rac1 expression, **C)** RhoA expression and **D)** P-PAK1 expression. B-actin was used as loading control. Abbreviations: Ct: Control, D: Deprivation of FBS and EPO, R: Ruxolitinib 500 nM, A: AZD1480 500 nM. Molecular weights of targeted proteins: IQGAP1: 189 kDa, P-PAK1: 61 kDa, Rac1 21 kDa, RhoA 22 kDa, ß-actin: 42 kDa.

| | | EpoR | WT | V617F |
|---|---|---|---|---|
| **IQGAP1** | Control | 0.57 | 1.50 | 0.28 |
| | Deprivation | 0.61 | 1.58 | 5.87 |
| | D + Ruxolitinib | 0.79 | 2.14 | 0.37 |
| | D + AZD1480 | 0.41 | 2.50 | 0.83 |
| **Rac1** | Control | 0.76 | 0.04 | 0.55 |
| | Deprivation | 0.70 | 0.04 | 3.10 |
| | D + Ruxolitinib | 0.42 | 0.20 | 0.31 |
| | D + AZD1480 | 0.86 | 0.50 | 0.29 |
| **RhoA** | Control | 0.04 | 0.04 | 0.43 |
| | Deprivation | 0.03 | 0.05 | 0.66 |
| | D + Ruxolitinib | 0.04 | 0.05 | 0.34 |
| | D + AZD1480 | 0.02 | 0.03 | 0.02 |
| **P-PAK1** | Control | 0.07 | 0.07 | 0.02 |
| | Deprivation | 0.13 | 0.09 | 0.64 |
| | D + Ruxolitinib | 0.09 | 0.05 | 0.03 |
| | D + AZD1480 | 0.10 | 0.06 | 0.05 |

| | | EpoR | WT | V617F |
|---|---|---|---|---|
| **Control conditions** | IQGAP1 | 0.57 | 1.50 | 0.28 |
| | Rac1 | 0.76 | 0.04 | 0.55 |
| | RhoA | 0.04 | 0.04 | 0.43 |
| | P-PAK1 | 0.07 | 0.07 | 0.02 |
| **Deprivation (FBS-, EPO-)** | IQGAP1 | 0.61 | 1.58 | 5.87 |
| | Rac1 | 0.70 | 0.04 | 3.10 |
| | RhoA | 0.03 | 0.05 | 0.66 |
| | P-PAK1 | 0.13 | 0.09 | 0.64 |
| **Deprivation + Ruxolitinib (500nM)** | IQGAP1 | 0.79 | 2.14 | 0.37 |
| | Rac1 | 0.42 | 0.20 | 0.31 |
| | RhoA | 0.04 | 0.05 | 0.34 |
| | P-PAK1 | 0.09 | 0.05 | 0.03 |
| **Deprivation + AZD1480 (500nM)** | IQGAP1 | 0.41 | 2.50 | 0.83 |
| | Rac1 | 0.86 | 0.50 | 0.29 |
| | RhoA | 0.02 | 0.03 | 0.02 |
| | P-PAK1 | 0.10 | 0.06 | 0.05 |

**Table III.9 and III.10.** Protein/β-actin ratios. These tables show the different protein/β-actin ratios on the diverse conditions and cell lines from western blot results (Figure III.24). First arrow indicates ratio variations comparing WT with EpoR and second one V617F with EpoR. Abbreviations: D: Deprivation; EpoR: Ba/F3 EpoR; WT: Ba/F3 EpoR JAK2 WT; V617F: Ba/F3 EpoR JAK2V617F.

As shown in Tables III.9 and III.10, we first compared protein expressions under control conditions (presence of serum and EPO). Interestingly, over-expression in Ba/F3 cells of JAK2 WT was associated with an upregulation of IQGAP1 expression comparatively with EpoR cells which do not overexpress JAK2. In contrast, JAK2V617F cells showed a net decrease (x2) of IQGAP1 levels at steady state, (control cell culture conditions). IQGAP1 expression was the lowest in mutated *JAK2* cells compared with JAK2 WT and EpoR.

Concerning other proteins at steady state, Rac1 and RhoA were expressed at variable amounts in the different types of Ba/F3 cells. Both proteins were overexpressed in JAK2V617F cells in comparison with JAK2 WT cells, even though their levels in non-transfected cells varied. P-PAK1 levels seemed to be non-affected by overexpression of JAK2 either WT or V617F compared with control.

Dynamic evolution of IQGAP1 and Rho GTPase members was also studied using serum deprivation which allows studying the impact of *JAK2V617F*. Firstly, we observed that under these distress conditions the expression of all proteins showed a markedly increase in Ba/F3 EpoR JAK2V617F cells; x9.7; 4.4; 22 and 4.9 for IQGAP1, Rac1, RhoA and P-PAK1 respectively (compared with EpoR cells) and x3.7; 77.5; 13.2 and 7.1 compared with JAK2 WT ones. It is noteworthy that these four proteins displayed less or none significant variations in Ba/F3 EpoR and JAK2 WT when these cells were cultivated under deprivation. We also noticed that IQGAP1, which was upregulated in JAK2 WT (vs controls), did not display variation in these stress conditions.

When we combined JAK2 inhibitors with deprivation, levels of all upregulated proteins in JAK2V617F cells under distress conditions, were decreased to levels very closed to or under their steady state levels unlike RhoA which seemed less sensitive to Ruxolitinib.

Interestingly, the impact of these inhibitors on JAK2 WT cells was quite negative since we observed no decrease, even a slight increase of proteins (mainly IQGAP1).

### *3-Rac1 and Cdc42 are activated in Ba/F3 EpoR JAK2 V617F cells*

GST-Rhotekin-RBD and GST-PAK-PBD agarose beads were used to establish if Rho proteins were activated in Ba/F3 cells. As shown in Figure III.25, Rac1 and Cdc42 were activated in all 3 cell lines but not RhoA. In order to normalize the amount of protein loaded, we calculated Rac1/GST and Cdc42/GST ratios. We observed that Rac1 presented variations on its activation as it was more active in Ba/F3 EpoR cells than in those overexpressing JAK2 WT and in those ones more than in mutated ones. The effects of JAK2 inhibitors increased its activation. Similarly, Cdc42 was more active in Ba/F3 EpoR cells than in mutated ones were it was almost non-active.

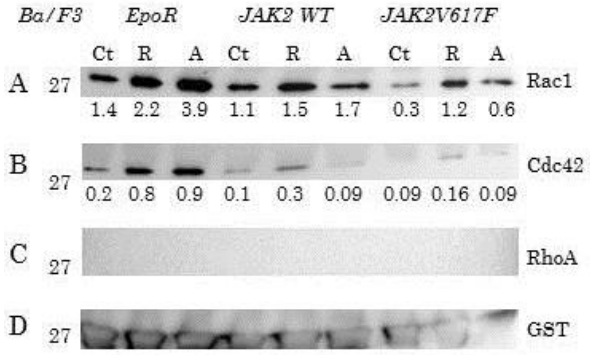


**Figure III.25.** Pull-down assays of activated proteins of the Rho family. 500 µg of protein were pulled-down with GST-PAK-PBD **(A**, **B** and **D)** and GST-Rhotekin-RBD **(C)** agarose beads. Elution was made with 60 µL of 2x Sample Buffer with ß-mercaptoethanol (5 min at 95°C) followed by western blotting revealed with anti Rac1 **(A)**, Cdc42 **(B)**, RhoA **(C)** or GST **(D)** antibodies. The ratios between Rac1 and Cdc42/GST are under the images. Abbreviations: Ct: control; R: 500 nM Ruxolitinib; A: 500 nM AZD1480. Molecular weights: Rac1: 21 kDa, Cdc42: 21 kDa, RhoA: 22 kDa, GST: 26 kDa.

### *4-JAK2 and Calreticulin expression in Ba/F3 cells*

In similarity as performed for the Rho GTPase family, we also inquired into the expression of CALR and JAK2 proteins in the same conditions as seen before (Figure III.26).

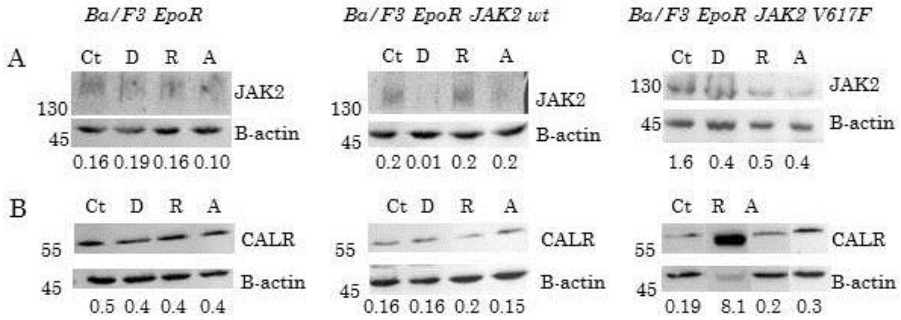


**Figure III.26.** Protein expression in Ba/F3 cells with inhibitors. Cells were cultured under different conditions; Ct: Control, D: Deprivation of FBS and EPO, R: Ruxolitinib 500nM, A: AZD1480 500nM. After 6h, cells were lysed and run on SDS-PAGE gels for western blotting. **A)** JAK2 expression and **B)** CALR expression. B-actin was used as loading control. Molecular weights of targeted proteins: JAK2: 131 kDa, CALR: 48 kDa, ß-actin: 42 kDa0.

| | | EpoR | WT | V617F |
|---|---|---|---|---|
| **JAK2** | Control | 0.16 | 0.24 | 1.63 |
| | Deprivation | 0.19 | 0.01 | 0.44 |
| | D + Ruxolitinib | 0.16 | 0.19 | 0.52 |
| | D + AZD1480 | 0.10 | 0.22 | 0.41 |
| **CALR** | Control | 0.45 | 0.16 | 0.19 |
| | Deprivation | 0.42 | 0.16 | 8.1 |
| | D + Ruxolitinib | 0.39 | 0.24 | 0.21 |
| | D + AZD1480 | 0.37 | 0.15 | 0.32 |

| | | EpoR | WT | V617F |
|---|---|---|---|---|
| **Control conditions** | JAK2 | 0.16 | 0.24 | 1.63 |
| | CALR | 0.45 | 0.16 | 0.19 |
| **Deprivation (FBS-, EPO-)** | JAK2 | 0.19 | 0.01 | 0.44 |
| | CALR | 0.42 | 0.16 | 8.1 |
| **D + Ruxolitinib (500nM)** | JAK2 | 0.16 | 0.19 | 0.52 |
| | CALR | 0.39 | 0.24 | 0.21 |
| **D + AZD1480 (500nM)** | JAK2 | 0.10 | 0.22 | 0.41 |
| | CALR | 0.37 | 0.15 | 0.32 |

**Table III.11 and III.12.** Protein/β-actin ratios. These tables show the different protein/β-actin ratios on the diverse conditions and cell lines from the western blot results (Figure III.26). Abbreviations: D: Deprivation; EpoR: Ba/F3 EpoR; WT: Ba/F3 EpoR JAK2 WT; V617F: Ba/F3 EpoR *JAK2V617F*.

As expected, JAK2 expression in control culture conditions was increased in JAK2V617F cells and at a lesser degree in Ba/F3 EpoR JAK2 WT compared with non-transfected ones. Under deprivation conditions, we observed a significant decrease of both JAK2 WT and JAK2V617F compared with control conditions. The addition of inhibitors in deprivation conditions corrected JAK2 expression in WT cells, reaching levels closed to those observed in control culture. However, in JAK2V617F cells, inhibitors partially corrected the decreased induced by deprivation.

The protein Calreticulin was globally expressed at similar levels in JAK2 WT and JAK2V617F cells but slightly lower in those JAK2 transfected cells compared with control cells (Ba/F3 EpoR cells). However, when cells were deprived of serum, we observed, in comparison with normal conditions, a very significant increase (x42) of CALR in JAK2V617F cells. In contrast, CALR levels in JAK2 WT or EpoR cells in the same deprivation conditions were not altered. As observed for Rho proteins, P-PAK1 and IQGAP1 when using JAK2 inhibitors this up-regulation was annihilated.

Unfortunately, western blot assays for phosphorylated JAK2 didn't work.

### *5-IQGAP1 effectors in Ba/F3 cells*

In order to detect IQGAP1 effectors, we immunoprecipitate Ba/F3 cell lysates with IQGAP1 followed by western blotting. Figure III.27 shows that when we revealed with anti-mouse antibodies, plenty of lines appeared on the membranes. Theoretically, Rac1 and Cdc42 should be the bands present around the band marker of 25-26 kDa. Nevertheless, after dehybridization and incubation with first antibodies followed by protein A, membranes didn't present any signal even though the protein A should emphasize heavy chains suggesting that IQGAP1 didn't immunoprecipitate with Rac1 or Cdc42.

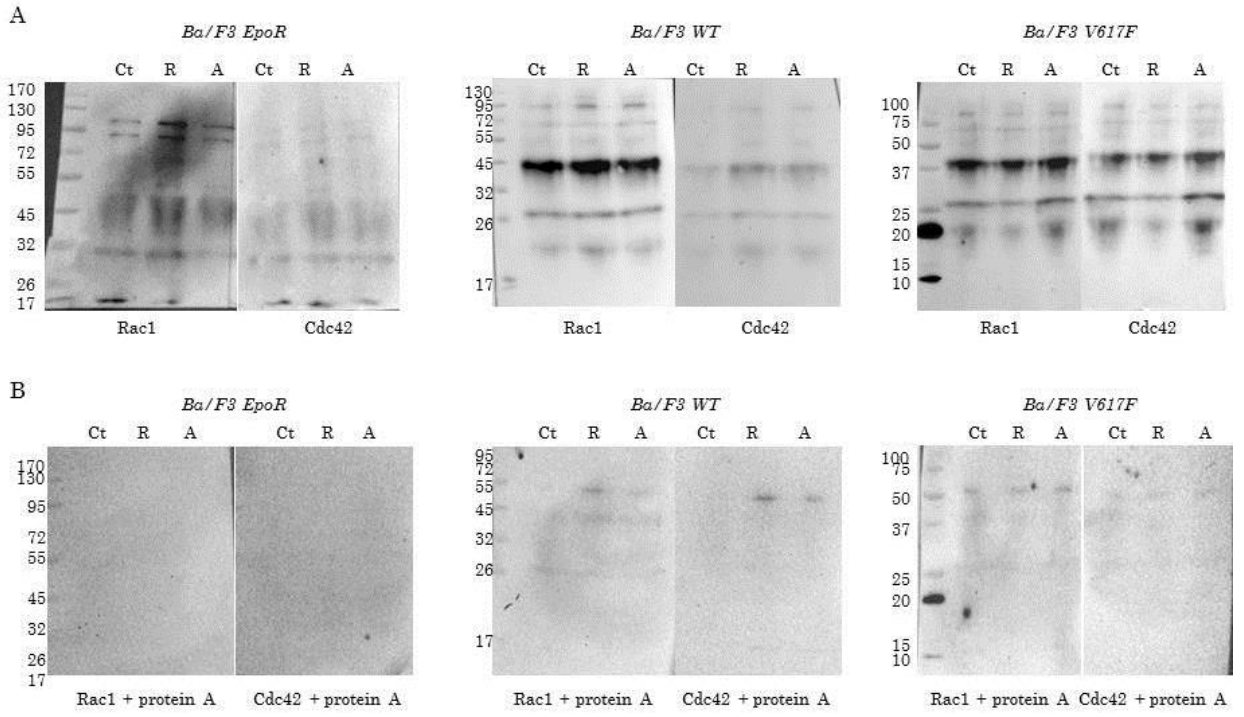


**Figure III.27.** IQGAP1 effectors. 1000 mg of protein were lysed an immunoprecipitated with rabbit polyclonal anti-IQGAP1 antibodies followed by western blotting. **A)** Western blots revealed with anti-mouse antibodies. **B)** Western blots revealed with protein A. Molecular weights of targeted proteins: Rac1: 21 kDa, Cdc42: 21 kDa.

Furthermore, we immunoprecipitated Ba/F3 cell lysates with JAK2 antibodies and revealed it with IQGAP1 antibodies to see if there could be a link between these two proteins. As shown in Figure III.28, IQGAP1 co-immunoprecipitated with JAK2 in all cell lysates independently of JAK2 inhibitors. We remarked that a band appeared around 100 kDa that could correspond to IQGAP1 degradation. Nonetheless, PAK1 didn't co-immunoprecipitate with JAK2.

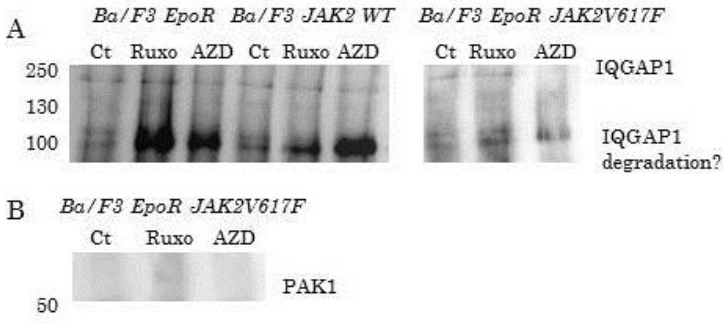


**Figure III.28.** JAK2 effectors. 1000 mg of protein were lysed an immunoprecipitated with JAK2 antibodies followed by western blotting. **A)** Ba/F3 EpoR, Ba/F3 EpoR JAK2 WT and Ba/F3 EpoR JAK2V617F cell lysates revealed with IQGAP1 antibodies under inhibiting conditions: Ct: Control; Ruxo: Ruxolitinib 600nM; AZD: AZD1480 600nM. **B)** Ba/F3 EpoR JAK2V617F cell lysates revealed with PAK1 antibodies under inhibiting conditions: Ct: Control; Ruxo: Ruxolitinib 600nM; AZD: AZD1480 600nM. Molecular weights: IQGAP1: 189 kDa, PAK1: 61 kDa.

# DISCUSSION

## *1-Effects of inhibitors on cell concentration and cell viability*

In HEL cells, as shown in results, hydroxyurea's capacity for blocking cell proliferation is stronger than Ruxolitinib's or AZD1480's at concentrations tested. We should have tried higher concentrations of Ruxolitinib and AZD1480 to see more effects. In fact, Bogani *et al.* (189) reported that the $IC_{50}$ of Ruxolitinib and AZD1480 in HEL cells after 24 hours were 0.79±0.15 μM and 0.86±0.02 μM respectively. Contrarily, Barrio *et al.* (198) also measured $IC_{50}$ of Ruxolitinib in HEL cells being 274 nM. Therefore, we just used concentrations up to 600 nM and as we couldn't observe the apoptotic effects of these drugs; our results may agree with those of Bogani *et al.* (189) and we should have used higher concentrations to see the apoptotic induction of these inhibitors. To sum up, at tested concentration ranges, hydroxyurea was more effective providing apoptosis and preventing cell division and proliferation than JAK2 inhibitors in HEL cells.

The effects of JAK2 inhibitors in Ba/F3 cells were higher than in HEL cells. As seen in Figures II.21 to II.23, in all types of Ba/F3 cells, at 48 hours of incubation, cell proliferation decreased markedly as cells were induced into apoptosis. Bogani *et al.* (189) also measured the effects of these JAK2 inhibitors on Ba/F3 cells. They obtained less viability than us after 48 hours of incubation. However, they did not incubate cells with EPO as we did. They showed that the addition of EPO to cell culture protected cells from the inhibitory effects of JAK2 inhibitors increasing their $IC_{50}$: 313±23 nM for AZD1480 in Ba/F3 *JAK2V617F* cells vs 707±11 nM with EPO and 220±20 vs 521±45 nM for Ruxolitinib in Ba/F3 *JAK2 V617F* cells without and with EPO respectively. Barrio *et al*. (198) also measured the $IC_{50}$ of Ruxolitinib in Ba/F3 cells obtaining 157.5 nM for *JAK2V617F* cells and 137.4 for the wild type. Differences in $IC_{50}$ values may be due to the fact that Barrio *et al.* (198) supplemented cell media with IL-3 and Bogani *et al*. (189) used ±EPO.

Therefore, these results suggested that Ba/F3 cells are more sensitive to Ruxolitinib and AZD1480 than HEL cells and that these drugs are capable of inducing apoptosis and inhibiting proliferation. The fact that Ba/F3 cells are supplemented with EPO reduces JAK2 effects but not when supplemented with IL-3.

### *2-Cell cycle analysis*

Cell cycle disturbances of HEL cells under drug incubation were measured by flow cytometry. After 24 hours of drug incubation, we saw how hydroxyurea blocked cells on the S phase in a dose-dependent manner whereas cells on the G0/G1 and G2/M phases decreased similarly. For Ruxolitinib, we observed similar but less marked effects. When treated with AZD1480 we remarked a huge fall of cells on the G0/G1 phase while the proportion of cells on S and G2/M phases rose; thus cell cycle was blocked on the S phase after 24 hours.

Nevertheless, after 48 hours of drug incubation, we saw that cells treated with high doses of hydroxyurea tried to repair drug effects and to continue normal cell cycles (number of cells on S phase decreased and number of cells on G2/M phase went up) but reparation mechanisms didn't work and cells turned to apoptosis, (increased proportion of death cells). These results agreed with the ones got by Gui *et al*. (199) who demonstrated how HEL cells turned to apoptosis when treated with HU. For AZD1480, at the highest dose after 48 hours, cells also turned into apoptosis as we saw a big amount of cells on the left part of the graphic and the number of cells in replication phases almost decreased to zero. Cells were blocked at G0/G1 phase with subsequent reduction of the S and G2/M phases. The effects of Ruxolitinib after 48 hours of incubation didn't vary among the different concentrations. We just observed that the amount of cells on S and G2/M phases decreased as the number of cells on G0/G1 phase was more or less stable as long as we increased drug concentrations suggesting that cells were blocked on G0/G1 phase.

### *3-Protein expression in Ba/F3 EpoR, Ba/F3 JAK2 WT, Ba/F3 EpoR JAK2V617F and HEL cells*

This model of cell lines brought out some teaching about the link between *JAK2V617F* and IQGAP1/Rho GTPase signaling.

First, we had observed in erythrocytes different levels of IQGAP1 according to *JAK2* status; *JAK2 WT* patients expressed higher levels than *JAK2V617F* ones. In Ba/F3 cells, we clearly observed that Ba/F3 EpoR JAK2 WT cells also expressed higher levels of IQGAP1

than Ba/F3 EpoR JAK2V617F. In HEL cells, we indirectly confirmed this *JAK2(-)* dependent regulation of the amount of IQGAP1 protein. Indeed, levels of IQGAP1 increased in HEL cells, which are *JAK2V617F,* when using JAK2 inhibitors which down-regulate the levels of *JAK2V617F* activity. Up-regulation of IQGAP1 levels did not seem to correlate with the amount of JAK2 protein itself (including JAK2 WT and JAK2V617F) since in our experience, higher levels of JAK2 protein were found in Ba/F3 EpoR JAK2V617F cells contrasting with the lowest levels of IQGAP1. Moreover, JAK2 inhibitors but not hydroxyurea increased JAK2 levels in HEL cells similarly to IQGAP1. We could hypothesize that in presence of JAK2 inhibitors, cells could promote JAK2 (and IQGAP1) transcription to counteract their effect.

We also underscore a particular link between JAK2 and IQGAP1 by our immunoprecipitation results. We inquired into JAK2 possible links with IQGAP1 and saw that these two proteins co-immunoprecipitated together in the three types of Ba/F3 suggesting that this co-precipitation was not affected by the mutation of the pseudo kinase domain of JAK2 protein (JH2). Liu *et al.* (172) studied IQGAP1 new binding partners through the "sequence repeats" of this protein but did not propose JAK2 as one of them. Nevertheless, JAK2 could potentially bind IQGAP1 as it presents a FERM domain comprised between JH4 and JH7 domains. Thus, our results confirmed *in cellulo* the potential link between these two proteins. The fact that this interaction was not perturbed by the addition of JAK2 inhibitors confirmed that *JAK2(-)* IQGAP1 relationship is not influenced by JAK2 mutation. Moreover, we noticed that a band appeared around 100 kDa in JAK2 immunoprecipitations. IQGAP1 antibody recognizes the sequence comprised between 314 and 422 amino acids on the N-terminal part that corresponds to the WW domain (see Figure I.13 on the chapter I of the manuscript) present next to the "sequence repeats" domain proposed to link JAK2. Therefore, even if IQGAP1 cleavage took place next to the C-terminal resulting in a ~100 kDa peptide, IQGAP1 could precipitate with JAK2.

The analysis of Ba/F3 cells demonstrated a direct link between *JAK2V617F* presence and the deregulation of the IQGAP1/Rho GTPase signaling. *JAK2V617F* is well known to induce a cytokine independent proliferation mediated by constitutive activation of the JAK-STAT pathway. This impact is better evidenced in culture conditions deprived of growth factors and serum which induce, in normal cells, a stress that could lead to apoptosis. We

therefore evaluated the impact of such conditions (referred to as deprivation in our study) on IQGAP1/Rho GTPase signaling. We hence highlighted that all tested partners of this pathway could be clearly up-regulated in such metabolic stress but only in cells expressing *JAK2V617F*. This effect was confirmed to be *JAK2V617F* dependent since using JAK2 inhibitors we were able to impede this up-regulation in JAK2V617F cells, (without any effect on JAK2 WT cells). These data strongly suggest a direct link between *JAK2V617F* and Rho signaling alteration. On the other hand, they propose that, in parallel to constitutive activation of JAK-STAT pathway, activation of IQGAP1/Rho GTPase signaling could be implicated in autonomous growth induced by *JAK2V617F*. The fact that P-PAK1 is similarly influenced by deprivation and JAK2 inhibitors is in favor of a potential role of these inhibitors on membrane homeostasis via regulation of PAK1 recruitment and activation. This highlights a potential impact of JAK2 inhibitors in thrombotic complications via P-PAK1 regulation.

The results on Rac1 and Cdc42 activation showed that both are more or less activated in all types of Ba/F3 and HEL cells in normal culture conditions. This suggests that either their activation is not dependent on *JAK2* mutation or that Ba/F3 cells have developed an internal mechanism of activation linked to EpoR expression that could activate Rac1 and Cdc42 probably linked with the protein JAK2 itself.

Results on CALR protein expression are also informative of new relationships between CALR and *JAK2V617F*. Indeed, in similar deprivation conditions that revealed *JAK2V617F* effects, we observed a very significant increase of CALR expression sensitive to JAK2 inhibitors. Of note, in granulocytes we showed that CALR amount was significantly higher in *JAK2V617F* granulocytes compared with *JAK2 WT*. We can therefore hypothesize that *JAK2V617F* mutation could induce up-regulation of CALR, at least in some cells, and thereby induce modification of cellular pathways regulated by its global chaperone activity. This hypothesis would suggest that new mechanisms complementary to JAK-STAT pathway could be deregulated via *JAK2V617F*. Finally, these data underscore a dual oncogenic potential of CALR in MPNs via its mutated form (as previously published) but also through the up-regulation of the native protein.

## CONCLUSION AND PERSPECTIVES

In this third part we confirmed, in the cell model of Ba/F3 cell lines overexpressing JAK2V617F, that there was indeed a special connection between the presence of JAK2 mutation and IQGAP1/Rho GTPases signaling alterations and emphasized a potential oncogenic role of unmutated JAK2 and CALR proteins. HEL and Ba/F3 cell models let us confirm that hydroxyurea and JAK2 inhibitors have a cell growth potential as they blocked cell proliferation leading cells to turn into apoptosis.

Altogether, these data raise some new issues:

### *1-Does JAK2V617F have any influence on the IQGAP1/Rho GTPase complexes?*

The role of *JAK2* mutation on IQGAP1/Rho GTPase signaling is remarkable as the tested members of this signaling increased their levels of expression under distress conditions in *JAK2V617F* cells. To confirm the implication of IQGAP1/Rho GTPases activation in the autonomous cell growth, it would be interesting to investigate the impact of blocking this signaling on Ba/F3 cell proliferation under deprivation conditions. Moreover, IQGAP1 links with its Rho GTPase effectors, which we have actually demonstrated in RBCs, remains to be explored in this model of Ba/F3 cells as well as the possible effects that distress conditions and JAK2 inhibitors may have on the formation of IQGAP1/Rho GTPases complexes especially in mutated *JAK2* cells.

### *2-Is there any link between STAT5/3 and IQGAP1/Rho GTPase signaling?*

*JAK2V617F* is well known to induce autonomous cell growth through activation of STAT proteins. As our results demonstrated a direct link between IQGAP1/Rho GTPase signaling and the presence of *JAK2V617F*, it is licit to ask whether STAT5/3 are implicated in IQGAP1/Rho GTPases deregulation. Phosphorylated STAT5 has been demonstrated to induce NADPH oxidase ROS production via its binding to Rac1, which is part of NADPH oxidase complex. In contrast, inactivated STAT5 has a protective effect due to the fact that it reduces Rac1 binding and ROS production (200). In addition, Rac1 was shown to

indirectly activate STAT3 by phosphorylation promoting nuclear translocation and gene expression in HeLa cells (201). It is proposed that active Rac1 leads to NF-kB activation and thus IL-6 gene induction. Then, IL-6 binds its receptor activating JAKs and subsequently tyrosine phosphorylation and activation of STAT3. Moreover, Debidda *et al*. (202) found that apart from active Rac1, active Cdc42 and RhoA could also promote tyrosine and serine phosphorylation of STAT3 independently from IL-6. However, Rho GTPases activate STAT3 in and indirect way. This activation implies nuclear translocation and regulation of cellular functions such as actin cytoskeleton reorganization, cell migration, gene activation and proliferation. Kanda *et al*. (203) showed that Rac was activated via phosphorylation of *JAK2(-)* EpoR in hematopoietic cells promoting cell adhesion.

Altogether these data from the literature strongly imply a link between IQGAP1/Rac1 and the STATs activation that remains to be explored.

### *3-Does CALR mutations induce deregulation of IQGAP1/Rho GTPase signaling?*

Our results in erythrocytes underscored differences between *CALR(+)* and *JAK2* mutated patients in the nature of IQGAP1/Rho GTPase interactions particularly concerning RhoGDI recruitment. Moreover, we observed that CALR protein displayed functional alterations in MPN erythrocytes (independently of *CALR* mutation). However, we lack of confirmation of these observations in a cellular model. The use of Ba/F3 cells expressing *CALR* mutation should answer these issues.

### *4-Does up-regulation of CALR protein participate to autonomous growth of cells?*

Our results stressed out an up-regulation of the CALR protein in JAK2V617F Ba/F3 cells cultured without serum nor growth factor. These unexpected data suggest that CALR up-regulation could participate to mechanisms implicated in autonomous growth. Hence, it would be informative to study the potential impact of CALR up-regulation in a cell model expressing high levels of CALR (mutated or not).

## RESUME DU CHAPITRE III

L'utilisation des lignées cellulaires HEL (qui possède *JAK2V617F* de façon constitutive) et des lignées Ba/F3 EpoR, surexprimant JAK2 dans sa forme native (Ba/F3 EpoR JAK2 WT) ou dans sa forme mutée (Ba/F3 EpoR *JAK2V617F*) nous a permis d'évaluer les liens entre la mutation *JAK2* et les protéines de la voie de signalisation IQGAP1/ Rho GTPases.

L'évaluation des inhibiteurs sur ces cellules a montré que l'hydroxyurée était plus effective sur les cellules HEL en favorisant l'apoptose et en empêchant la division et la prolifération cellulaires que les inhibiteurs de JAK2. Par contre, l'impact des inhibiteurs a été plus marqué sur les Ba/F3.

Dans le modèle Ba/F3 nous avons pu confirmer l'observation faite dans les globules rouges que les niveaux d'IQGAP1 se rattachent à la présence de JAK2 WT et non à la présence de JAK2V617F ni à sa quantité d'allèle muté. En outre, les inhibiteurs de JAK2 font augmenter les niveaux d'IQGAP1 ce qui supporte ces résultats.

La culture des lignées cellulaires Ba/F3 sous des conditions de stress, c'est à dire, privées de sérum et d'érythropoïétine, en comparaison avec les conditions normales, montre une augmentation très significative des protéines de la voie IQGAP1/Rho GTPases qui retournent à leurs niveaux de base quand on ajoute les inhibiteurs de JAK2. Ces résultats confirment donc une grosse influence de *JAK2V617F* dans la régulation de cette voie de signalisation. En plus, nous avons montré par co-précipitation un lien entre IQGAP1 et JAK2 qui ne dépend pas du domaine muté de JAK2.

Finalement, nos résultats mettent en lueur l'effet direct de *JAK2V617F*, sensible à l'action des inhibiteurs de JAK2, sur les niveaux d'expression de la protéine calréticuline en conditions de culture sans facteur de croissance. Tenant compte de nos observations sur les polynucléaires, ces résultats soulignent un nouveau mode d'action de la calréticuline dans la pathogenèse des SMP via la régulation de son niveau d'expression qui pourrait modifier les nombreuses voies au niveau desquelles elle intervient comme protéine chaperonne.

En conclusion, ces modèles cellulaires nous ont permis de montrer les liens particuliers entre la mutation *JAK2V617F* et la voie IQGAP1/Rho GTPases et de mettre à jour un role original de la calréticuline.

# GENERAL SYNTHESIS

The aim of my work was to characterize proteomic deregulations in Ph- MPNs that would help us better understand the mechanisms in myeloid cells that brought to uncontrolled proliferation as well as pathways implicated in some complications such as thrombotic complications.

The proteomic approach of Ph- MPN erythrocytes and granulocytes revealed more than 1000 proteins in each type of cell. Among them, we highlighted significant protein deregulations that varied not only according to the genetic status *JAK2(+)* vs *JAK2(-)* or *JAK2(+)* vs *CALR(+)* but also among *JAK2(+)* MPNs or depending on the *JAK2V617F* allele burden. Among this landscape of proteome alterations in MPNs, we stressed out 5 functional pathways that seem particularly implicated in MPN pathogenesis.

Firstly, we were able to reveal and decipher the particular role of the alterations of the IQGAP1/Rho GTPase signaling in MPNs. We highlighted that IQGAP1 was up regulated in RBCs according to *JAK2* and *CALR* status, in Ba/F3 JAK2V617F under stress conditions and in granulocytes when comparing PMF with PV and ET. Subsequently, we showed that the recruitment of the Rho GTPases by IQGAP1 in RBCs depended on *JAK2(+)* and *CALR(+)* status. We also showed the up-regulation of these proteins in Ba/F3 JAK2V617F cells under stress conditions. Altogether, these data imply a particular role of IQGAP1/Rho GTPase signaling in the autonomous growth of MPNs additionally to JAK-STAT pathway activation. The concordance and the complementarity of our data in erythrocytes, granulocytes and Ba/F3 cell line models reinforced by the impact of JAK2 inhibitors and the connection between IQGAP1 and JAK2 proteins, plead for a critical oncogenic role of this pathway in *JAK2V617F* MPNs.

We also found a big deregulation of ROS related proteins, in particular the myeloperoxidase and those involved in detoxification pathways. The Transcriptomic analysis confirmed the implication of oxidative stress in the pathophysiology of MPNs. We highlighted that the oxidative stress related catalase (*CAT*) was under-regulated due to a decreased on the expression of the *CAT* gene in *JAK2V617F* MPN subjects. Moreover, we observed a significant variation of the catalase protein expression among MPN subtypes and particularly lower levels were found in *JAK2(+)* MPNs vs *JAK2* WT. This latter observation could suggest that *JAK2V617F* induces a decrease of catalase expression

participating in the oncogenic role of this mutation. Altogether, our data confirmed, in clinical samples, the prominent role of ROS balance in MPN physiopathology.

Besides, we were able to underline a significant deregulation of proteins implicated in the membrane cytoskeleton and actin signaling closed to IQGAP1/Rho GTPase signaling. In particular, we demonstrated that PAK1 alteration was associated with IQGAP1 up-regulation in RBCs and in Ba/F3 JAK2V617F cells. Focal Adhesion Kinase (FAK) pathways, which are activated by RhoA, also appeared deregulated in ET vs Controls in RBCs. Altogether, these deregulations may play an important role on the membrane integrity of RBCs or other cell types and therefore induce alterations of cell adhesion that could be connected with thrombotic events so frequent in these patients.

Finally our data highlighted mTOR pathway deregulation in *JAK2V617F* granulocytes, which was not surprising taking into account knowledge about the implication of this pathway in oncogenesis but also in the light of promising results obtained with therapies targeting this pathway in MPNs. CALR up-regulation linked to S100 protein alterations observed in granulocytes could be the cause of $Ca^{2+}$ deregulations in *JAK2V617F* granulocytes that could play a role in MPNs even though currently no data from the literature have confirmed this hypothesis.

Regarding CALR protein expression, our data allow hypothesizing additional roles of CALR in MPN oncogenesis through its up-regulation. It must be stressed that Calreticulin appeared over-expressed in *JAK2V617F* granulocytes compared with non-mutated ones independently of *JAK2V617F* allele burden even if its expression didn't present any variation in RBCs. Moreover, when we looked for CALR expression in our cell model, we underlined that CALR levels were also positively influenced by *JAK2V617F* under stress conditions suggesting that this mutation could increase CALR expression in some MPN cells. Hence, CALR could have a dual oncogenic role through its up-regulation in *JAK2V617F* MPN or though the alteration of its function in *CALR* mutated patients.

Altogether, these data showed that proteomic deregulations in Ph- MPN cells play an important oncogenic role in uncontrolled cell proliferation and could be implicated in complication as thrombotic accidents. Differences on the proteome among genetic status,

(*JAK2(+)*, *JAK2(-)* or *CALR(+)*), and diagnosis (PV, ET or PMF), could explain some phenotypical differences found among these patients. Nevertheless, the number of deregulated proteins, compared with the total number of quantified proteins, remains quite low. Indeed, globally just 5 to 15% of the proteome displayed significant variations in MPNs. The study of the functional role of these deregulated proteins showed that a limited number of pathways were found commonly deregulated in MPNs by these proteome variations. This confirms that a little number of pathways is mandatory to maintain the control of myeloid cell proliferation, and consequently, that proteins of these pathways could play a critical role on MPN pathogenesis. This dependence on proteins may be closed to the concept of oncogene addiction and, by analogy, this protein dependence could lead to new therapeutic targets.

# BIBLIOGRAPHY

1. Vardiman JW, Harris NL, Brunning RD. The World Health Organization (WHO) classification of the myeloid neoplasms. Blood. 2002;100(7):2292-302.
2. Vardiman JW, Thiele J, Arber DA, Brunning RD, Borowitz MJ, Porwit A, et al. The 2008 revision of the World Health Organization (WHO) classification of myeloid neoplasms and acute leukemia: rationale and important changes. Blood. 2009;114(5):937-51.
3. Tefferi A, Gilliland G. Classification of chronic myeloid disorders: from Dameshek towards a semi-molecular system. Best Pract Res Clin Haematol. 2006;19(3):365-85.
4. Chopra R, Pu QQ, Elefanty AG. Biology of BCR-ABL. Blood Rev. 1999;13(4):211-29.
5. Osler W. Chronic cyanosis, with polycythaemia and enlarged spleen: a new clinical entity. 1903. Am J Med Sci. 2008;335(6):411-7.
6. Tefferi A. The history of myeloproliferative disorders: before and after Dameshek. Leukemia. 2008;22(1):3-13.
7. Chen G, Prchal JT. Polycythemia vera and its molecular basis: an update. Best Pract Res Clin Haematol. 2006;19(3):387-97.
8. Tefferi A. The diagnosis of polycythemia vera: new tests and old dictums. Best Pract Res Clin Haematol. 2006;19(3):455-69.
9. Tefferi A, Barbui T. Polycythemia vera and essential thrombocythemia: 2015 update on diagnosis, risk-stratification and management. Am J Hematol. 2015;90(2):162-73.
10. Finazzi G, Caruso V, Marchioli R, Capnist G, Chisesi T, Finelli C, et al. Acute leukemia in polycythemia vera: an analysis of 1638 patients enrolled in a prospective observational study. Blood. 2005;105(7):2664-70.
11. Harrison CN, Green AR. Essential thrombocythaemia. Best Pract Res Clin Haematol. 2006;19(3):439-53.
12. Briere JB. Essential thrombocythemia. Orphanet J Rare Dis. 2007;2:3.
13. Gangat N, Caramazza D, Vaidya R, George G, Begna K, Schwager S, et al. DIPSS plus: a refined Dynamic International Prognostic Scoring System for primary myelofibrosis that incorporates prognostic information from karyotype, platelet count, and transfusion status. J Clin Oncol. 2011;29(4):392-7.
14. Tefferi A, Lasho TL, Jimma T, Finke CM, Gangat N, Vaidya R, et al. One thousand patients with primary myelofibrosis: the mayo clinic experience. Mayo Clin Proc. 2012;87(1):25-33.
15. Campbell PJ, Green AR. The myeloproliferative disorders. N Engl J Med. 2006;355(23):2452-66.
16. Baxter EJ, Scott LM, Campbell PJ, East C, Fourouclas N, Swanton S, et al. Acquired mutation of the tyrosine kinase JAK2 in human myeloproliferative disorders. Lancet. 2005;365(9464):1054-61.
17. James C, Ugo V, Le Couedic JP, Staerk J, Delhommeau F, Lacout C, et al. A unique clonal JAK2 mutation leading to constitutive signalling causes polycythaemia vera. Nature. 2005;434(7037):1144-8.
18. Kralovics R, Passamonti F, Buser AS, Teo SS, Tiedt R, Passweg JR, et al. A gain-of-function mutation of JAK2 in myeloproliferative disorders. N Engl J Med. 2005;352(17):1779-90.
19. Levine RL, Wadleigh M, Cools J, Ebert BL, Wernig G, Huntly BJ, et al. Activating mutation in the tyrosine kinase JAK2 in polycythemia vera, essential thrombocythemia, and myeloid metaplasia with myelofibrosis. Cancer Cell. 2005;7(4):387-97.
20. Vainchenker W, Constantinescu SN. A unique activating mutation in JAK2 (V617F) is at the origin of polycythemia vera and allows a new classification of myeloproliferative diseases. Hematology Am Soc Hematol Educ Program. 2005:195-200.
21. Vainchenker W, Delhommeau F, Constantinescu SN, Bernard OA. New mutations and pathogenesis of myeloproliferative neoplasms. Blood. 2011;118(7):1723-35.
22. Neubauer H, Cumano A, Muller M, Wu H, Huffstadt U, Pfeffer K. Jak2 deficiency defines an essential developmental checkpoint in definitive hematopoiesis. Cell. 1998;93(3):397-409.
23. Staerk J, Kallin A, Demoulin JB, Vainchenker W, Constantinescu SN. JAK1 and Tyk2 activation by the homologous polycythemia vera JAK2 V617F mutation: cross-talk with IGF1 receptor. J Biol Chem. 2005;280(51):41893-9.

24. Chen E, Beer PA, Godfrey AL, Ortmann CA, Li J, Costa-Pereira AP, et al. Distinct clinical phenotypes associated with JAK2V617F reflect differential STAT1 signaling. Cancer Cell. 2010;18(5):524-35.
25. Dupont S, Masse A, James C, Teyssandier I, Lecluse Y, Larbret F, et al. The JAK2 617V>F mutation triggers erythropoietin hypersensitivity and terminal erythroid amplification in primary cells from patients with polycythemia vera. Blood. 2007;110(3):1013-21.
26. Passamonti F, Rumi E, Pietra D, Elena C, Boveri E, Arcaini L, et al. A prospective study of 338 patients with polycythemia vera: the impact of JAK2 (V617F) allele burden and leukocytosis on fibrotic or leukemic disease transformation and vascular complications. Leukemia. 2010;24(9):1574-9.
27. Tefferi A. Novel mutations and their functional and clinical relevance in myeloproliferative neoplasms: JAK2, MPL, TET2, ASXL1, CBL, IDH and IKZF1. Leukemia. 2010;24(6):1128-38.
28. Alshemmari SH, Rajaan R, Ameen R, Al-Drees MA, Almosailleakh MR. JAK2V617F allele burden in patients with myeloproliferative neoplasms. Ann Hematol. 2014;93(5):791-6.
29. Scott LM, Tong W, Levine RL, Scott MA, Beer PA, Stratton MR, et al. JAK2 exon 12 mutations in polycythemia vera and idiopathic erythrocytosis. N Engl J Med. 2007;356(5):459-68.
30. Tefferi A, Lasho TL, Finke CM, Knudson RA, Ketterling R, Hanson CH, et al. CALR vs JAK2 vs MPL-mutated or triple-negative myelofibrosis: clinical, cytogenetic and molecular comparisons. Leukemia. 2014;28(7):1472-7.
31. Rumi E, Pietra D, Ferretti V, Klampfl T, Harutyunyan AS, Milosevic JD, et al. JAK2 or CALR mutation status defines subtypes of essential thrombocythemia with substantially different clinical course and outcomes. Blood. 2014;123(10):1544-51.
32. Nangalia J, Massie CE, Baxter EJ, Nice FL, Gundem G, Wedge DC, et al. Somatic CALR mutations in myeloproliferative neoplasms with nonmutated JAK2. N Engl J Med. 2013;369(25):2391-405.
33. Klampfl T, Gisslinger H, Harutyunyan AS, Nivarthi H, Rumi E, Milosevic JD, et al. Somatic mutations of calreticulin in myeloproliferative neoplasms. N Engl J Med. 2013;369(25):2379-90.
34. Tefferi A, Wassie EA, Guglielmelli P, Gangat N, Belachew AA, Lasho TL, et al. Type 1 versus Type 2 calreticulin mutations in essential thrombocythemia: a collaborative study of 1027 patients. Am J Hematol. 2014;89(8):E121-4.
35. Gelebart P, Opas M, Michalak M. Calreticulin, a Ca2+-binding chaperone of the endoplasmic reticulum. Int J Biochem Cell Biol. 2005;37(2):260-6.
36. Rampal R, Al-Shahrour F, Abdel-Wahab O, Patel JP, Brunel JP, Mermel CH, et al. Integrated genomic analysis illustrates the central role of JAK-STAT pathway activation in myeloproliferative neoplasm pathogenesis. Blood. 2014;123(22):e123-33.
37. Lau WW, Hannah R, Green AR, Gottgens B. The JAK-STAT signaling pathway is differentially activated in CALR-positive compared with JAK2V617F-positive ET patients. Blood. 125. United States2015. p. 1679-81.
38. Kollmann K, Nangalia J, Warsch W, Quentmeier H, Bench A, Boyd E, et al. MARIMO cells harbor a CALR mutation but are not dependent on JAK2/STAT5 signaling. Leukemia. 29. England2015. p. 494-7.
39. Cabagnols X, Cayuela JM, Vainchenker W. A CALR mutation preceding BCR-ABL1 in an atypical myeloproliferative neoplasm. N Engl J Med. 2015;372(7):688-90.
40. Tefferi A, Thiele J, Vannucchi AM, Barbui T. An overview on CALR and CSF3R mutations and a proposal for revision of WHO diagnostic criteria for myeloproliferative neoplasms. Leukemia. 2014;28(7):1407-13.
41. Vannucchi AM, Rotunno G, Bartalucci N, Raugei G, Carrai V, Balliu M, et al. Calreticulin mutation-specific immunostaining in myeloproliferative neoplasms: pathogenetic insight and diagnostic value. Leukemia. 2014;28(9):1811-8.
42. Mondet J, Park JH, Menard A, Marzac C, Carillo S, Pourcelot E, et al. Endogenous megakaryocytic colonies underline association between megakaryocytes and calreticulin mutations in essential thrombocythemia. Haematologica. 100. Italy2015. p. e176-8.

43. Pasquier F, Cabagnols X, Secardin L, Plo I, Vainchenker W. Myeloproliferative neoplasms: JAK2 signaling pathway as a central target for therapy. Clin Lymphoma Myeloma Leuk. 2014;14 Suppl:S23-35.
44. Ha JS, Jeon DS. Possible new LNK mutations in myeloproliferative neoplasms. Am J Hematol. 2011;86(10):866-8.
45. Benton CB, Tanaka M, Wilson C, Pierce S, Zhou L, Cortes J, et al. Increased likelihood of post-polycythemia vera myelofibrosis in Ph-negative MPN patients with chromosome 12 abnormalities. Leuk Res. 2015;39(4):419-23.
46. Brecqueville M, Rey J, Devillier R, Guille A, Gillet R, Adelaide J, et al. Array comparative genomic hybridization and sequencing of 23 genes in 80 patients with myelofibrosis at chronic or acute phase. Haematologica. 2014;99(1):37-45.
47. Stegelmann F, Bullinger L, Griesshammer M, Holzmann K, Habdank M, Kuhn S, et al. High-resolution single-nucleotide polymorphism array-profiling in myeloproliferative neoplasms identifies novel genomic aberrations. Haematologica. 2010;95(4):666-9.
48. Vainchenker W, Plo I. TET2 loss, a rescue of JAK2V617F HSCs. Blood. 2015;125(2):212-3.
49. Kim E, Abdel-Wahab O. Focus on the epigenome in the myeloproliferative neoplasms. Hematology Am Soc Hematol Educ Program. 2013;2013:538-44.
50. Delhommeau F, Dupont S, Della Valle V, James C, Trannoy S, Masse A, et al. Mutation in TET2 in myeloid cancers. N Engl J Med. 2009;360(22):2289-301.
51. Moran-Crusio K, Reavie L, Shih A, Abdel-Wahab O, Ndiaye-Lobry D, Lobry C, et al. Tet2 loss leads to increased hematopoietic stem cell self-renewal and myeloid transformation. Cancer Cell. 2011;20(1):11-24.
52. Gelsi-Boyer V, Brecqueville M, Devillier R, Murati A, Mozziconacci MJ, Birnbaum D. Mutations in ASXL1 are associated with poor prognosis across the spectrum of malignant myeloid diseases. J Hematol Oncol. 2012;5:12.
53. Brecqueville M, Cervera N, Gelsi-Boyer V, Murati A, Adelaide J, Chaffanet M, et al. Rare mutations in DNMT3A in myeloproliferative neoplasms and myelodysplastic syndromes. Blood Cancer J. 2011;1(5):e18.
54. Brecqueville M, Cervera N, Adelaide J, Rey J, Carbuccia N, Chaffanet M, et al. Mutations and deletions of the SUZ12 polycomb gene in myeloproliferative neoplasms. Blood Cancer J. 2011;1(8):e33.
55. Lasho TL, Jimma T, Finke CM, Patnaik M, Hanson CA, Ketterling RP, et al. SRSF2 mutations in primary myelofibrosis: significant clustering with IDH mutations and independent association with inferior overall and leukemia-free survival. Blood. 2012;120(20):4168-71.
56. Klampfl T, Harutyunyan A, Berg T, Gisslinger B, Schalling M, Bagienski K, et al. Genome integrity of myeloproliferative neoplasms in chronic phase and during disease progression. Blood. 2011;118(1):167-76.
57. Lundberg P, Karow A, Nienhold R, Looser R, Hao-Shen H, Nissen I, et al. Clonal evolution and clinical correlates of somatic mutations in myeloproliferative neoplasms. Blood. 2014;123(14):2220-8.
58. Saliba J, Saint-Martin C, Di Stefano A, Lenglet G, Marty C, Keren B, et al. Germline duplication of ATG2B and GSKIP predisposes to familial myeloid malignancies. Nat Genet. 2015.
59. Dentali F, Ageno W, Rumi E, Casetti I, Poli D, Scoditti U, et al. Cerebral venous thrombosis and myeloproliferative neoplasms: results from two large databases. Thromb Res. 2014;134(1):41-3.
60. Casini A, Fontana P, Lecompte TP. Thrombotic complications of myeloproliferative neoplasms: risk assessment and risk-guided management. J Thromb Haemost. 2013;11(7):1215-27.
61. Falanga A, Marchetti M. Thrombotic disease in the myeloproliferative neoplasms. Hematology Am Soc Hematol Educ Program. 2012;2012:571-81.
62. Franchini M. Thromboembolic risk in hematological malignancies. Clin Chem Lab Med. 2015;53(8):1139-47.
63. Besses C, Cervantes F, Pereira A, Florensa L, Sole F, Hernandez-Boluda JC, et al. Major vascular complications in essential thrombocythemia: a study of the predictive factors in a series of 148 patients. Leukemia. 1999;13(2):150-4.

64. Sun T, Zhang L. Thrombosis in myeloproliferative neoplasms with JAK2V617F mutation. Clin Appl Thromb Hemost. 2013;19(4):374-81.
65. Borowczyk M, Wojtaszewska M, Lewandowski K, Gil L, Lewandowska M, Lehmann-Kopydlowska A, et al. The JAK2 V617F mutational status and allele burden may be related with the risk of venous thromboembolic events in patients with Philadelphia-negative myeloproliferative neoplasms. Thromb Res. 2015;135(2):272-80.
66. Barbui T, Finazzi G, Falanga A. Myeloproliferative neoplasms and thrombosis. Blood. 2013;122(13):2176-84.
67. Martinod K, Wagner DD. Thrombosis: tangled up in NETs. Blood. 2014;123(18):2768-76.
68. Fuchs TA, Abed U, Goosmann C, Hurwitz R, Schulze I, Wahn V, et al. Novel cell death program leads to neutrophil extracellular traps. J Cell Biol. 2007;176(2):231-41.
69. Fuchs TA, Brill A, Duerschmied D, Schatzberg D, Monestier M, Myers DD, Jr., et al. Extracellular DNA traps promote thrombosis. Proc Natl Acad Sci U S A. 2010;107(36):15880-5.
70. Demers M, Wagner DD. Neutrophil extracellular traps: A new link to cancer-associated thrombosis and potential implications for tumor progression. Oncoimmunology. 2013;2(2):e22946.
71. Kuriakose E, Vandris K, Wang YL, Chow W, Jones AV, Christos P, et al. Decrease in JAK2 V617F allele burden is not a prerequisite to clinical response in patients with polycythemia vera. Haematologica. 2012;97(4):538-42.
72. Kittur J, Knudson RA, Lasho TL, Finke CM, Gangat N, Wolanskyj AP, et al. Clinical correlates of JAK2V617F allele burden in essential thrombocythemia. Cancer. 2007;109(11):2279-84.
73. Vannucchi AM, Antonioli E, Guglielmelli P, Longo G, Pancrazzi A, Ponziani V, et al. Prospective identification of high-risk polycythemia vera patients based on JAK2(V617F) allele burden. Leukemia. 2007;21(9):1952-9.
74. Takata Y, Seki R, Kanajii T, Nohara M, Koteda S, Kawaguchi K, et al. Association between thromboembolic events and the JAK2 V617F mutation in myeloproliferative neoplasms. Kurume Med J. 2014;60(3-4):89-97.
75. Rotunno G, Mannarelli C, Guglielmelli P, Pacilli A, Pancrazzi A, Pieri L, et al. Impact of calreticulin mutations on clinical and hematological phenotype and outcome in essential thrombocythemia. Blood. 2014;123(10):1552-5.
76. Rampal R, Mascarenhas J. Pathogenesis and management of acute myeloid leukemia that has evolved from a myeloproliferative neoplasm. Curr Opin Hematol. 2014;21(2):65-71.
77. Abdel-Wahab O, Manshouri T, Patel J, Harris K, Yao J, Hedvat C, et al. Genetic analysis of transforming events that convert chronic myeloproliferative neoplasms to leukemias. Cancer Res. 2010;70(2):447-52.
78. Kiladjian JJ, Chevret S, Dosquet C, Chomienne C, Rain JD. Treatment of polycythemia vera with hydroxyurea and pipobroman: final results of a randomized trial initiated in 1980. J Clin Oncol. 2011;29(29):3907-13.
79. Silverstein MN, Brown AL, Jr., Linman JW. Idiopathic myeloid metaplasia. Its evolution into acute leukemia. Arch Intern Med. 1973;132(5):709-12.
80. Passamonti F, Rumi E, Caramella M, Elena C, Arcaini L, Boveri E, et al. A dynamic prognostic model to predict survival in post-polycythemia vera myelofibrosis. Blood. 2008;111(7):3383-7.
81. Tiribelli M, Barraco D, De Marchi F, Marin L, Medeot M, Damiani D, et al. Clinical factors predictive of myelofibrotic evolution in patients with polycythemia vera. Ann Hematol. 2015;94(5):873-4.
82. Lussana F, Rambaldi A, Finazzi MC, van Biezen A, Scholten M, Oldani E, et al. Allogeneic hematopoietic stem cell transplantation in patients with polycythemia vera or essential thrombocythemia transformed to myelofibrosis or acute myeloid leukemia: a report from the MPN Subcommittee of the Chronic Malignancies Working Party of the European Group for Blood and Marrow Transplantation. Haematologica. 2014;99(5):916-21.
83. Kiladjian JJ. Current therapies and their indications for the Philadelphia-negative myeloproliferative neoplasms. Am Soc Clin Oncol Educ Book. 2015;35:e389-96.

84. Kiladjian JJ, Cassinat B, Chevret S, Turlure P, Cambier N, Roussel M, et al. Pegylated interferon-alfa-2a induces complete hematologic and molecular responses with low toxicity in polycythemia vera. Blood. 2008;112(8):3065-72.
85. Lu M, Xia L, Li Y, Wang X, Hoffman R. The orally bioavailable MDM2 antagonist RG7112 and pegylated interferon alpha 2a target JAK2V617F-positive progenitor and stem cells. Blood. 2014;124(5):771-9.
86. Plo I. p53 at the crossroads of MPN treatment. Blood. 2014;124(5):668-9.
87. Cassinat B, Verger E, Kiladjian JJ. Interferon alfa therapy in CALR-mutated essential thrombocythemia. N Engl J Med. 2014;371(2):188-9.
88. Deisseroth A, Kaminskas E, Grillo J, Chen W, Saber H, Lu HL, et al. U.S. Food and Drug Administration approval: ruxolitinib for the treatment of patients with intermediate and high-risk myelofibrosis. Clin Cancer Res. 2012;18(12):3212-7.
89. Koppikar P, Abdel-Wahab O, Hedvat C, Marubayashi S, Patel J, Goel A, et al. Efficacy of the JAK2 inhibitor INCB16562 in a murine model of MPLW515L-induced thrombocytosis and myelofibrosis. Blood. 2010;115(14):2919-27.
90. Verstovsek S, Kantarjian H, Mesa RA, Pardanani AD, Cortes-Franco J, Thomas DA, et al. Safety and efficacy of INCB018424, a JAK1 and JAK2 inhibitor, in myelofibrosis. N Engl J Med. 2010;363(12):1117-27.
91. Kleppe M, Kwak M, Koppikar P, Riester M, Keller M, Bastian L, et al. JAK-STAT pathway activation in malignant and nonmalignant cells contributes to MPN pathogenesis and therapeutic response. Cancer Discov. 2015;5(3):316-31.
92. Tefferi A, Pardanani A. Serious adverse events during ruxolitinib treatment discontinuation in patients with myelofibrosis. Mayo Clin Proc. 2011;86(12):1188-91.
93. Deshpande A, Reddy MM, Schade GO, Ray A, Chowdary TK, Griffin JD, et al. Kinase domain mutations confer resistance to novel inhibitors targeting JAK2V617F in myeloproliferative neoplasms. Leukemia. 2012;26(4):708-15.
94. Vannucchi AM, Kiladjian JJ, Griesshammer M, Masszi T, Durrant S, Passamonti F, et al. Ruxolitinib versus standard therapy for the treatment of polycythemia vera. N Engl J Med. 2015;372(5):426-35.
95. Agarwal MB, Malhotra H, Chakrabarti P, Varma N, Mathews V, Bhattacharyya J, et al. Myeloproliferative neoplasms working group consensus recommendations for diagnosis and management of primary myelofibrosis, polycythemia vera, and essential thrombocythemia. Indian J Med Paediatr Oncol. 2015;36(1):3-16.
96. Mossuz P, Girodon F, Donnard M, Latger-Cannard V, Dobo I, Boiret N, et al. Diagnostic value of serum erythropoietin level in patients with absolute erythrocytosis. Haematologica. 2004;89(10):1194-8.
97. Tefferi A, Pardanani A. Evaluation of "increased" hemoglobin in the JAK2 mutations era: a diagnostic algorithm based on genetic tests. Mayo Clin Proc. 2007;82(5):599-604.
98. Hong WJ, Gotlib J. Hereditary erythrocytosis, thrombocytosis and neutrophilia. Best Pract Res Clin Haematol. 2014;27(2):95-106.
99. Mossuz P, Bouamrani A, Brugiere S, Arlotto M, Hermouet S, Lippert E, et al. Apolipoprotein A1: A new serum marker correlated to JAK2 V617F proportion at diagnosis in patients with polycythemia vera. Proteomics Clin Appl. 2007;1(12):1605-12.
100. Mossuz P, Arlotto M, Hermouet S, Bouamrani A, Lippert E, Girodon F, et al. Proteomic study of the impact of the JAK2-V617F mutation on the phenotype of essential thrombocythemia. Exp Hematol. 2008;36(12):1642-7.
101. Tefferi A, Vaidya R, Caramazza D, Finke C, Lasho T, Pardanani A. Circulating interleukin (IL)-8, IL-2R, IL-12, and IL-15 levels are independently prognostic in primary myelofibrosis: a comprehensive cytokine profiling study. J Clin Oncol. 2011;29(10):1356-63.
102. Pourcelot E, Trocme C, Mondet J, Bailly S, Toussaint B, Mossuz P. Cytokine profiles in polycythemia vera and essential thrombocythemia patients: clinical implications. Exp Hematol. 2014;42(5):360-8.
103. Hui W, Ye F, Zhang W, Liu C, Cui M, Li W, et al. Aberrant expression of signaling proteins in essential thrombocythemia. Ann Hematol. 2013;92(9):1229-38.

104. Falanga A, Marchetti M, Barbui T, Smith CW. Pathogenesis of thrombosis in essential thrombocythemia and polycythemia vera: the role of neutrophils. Semin Hematol. 2005;42(4):239-47.
105. Arellano-Rodrigo E, Alvarez-Larran A, Reverter JC, Villamor N, Colomer D, Cervantes F. Increased platelet and leukocyte activation as contributing mechanisms for thrombosis in essential thrombocythemia and correlation with the JAK2 mutational status. Haematologica. 2006;91(2):169-75.
106. Eyler CE, Telen MJ. The Lutheran glycoprotein: a multifunctional adhesion receptor. Transfusion. 2006;46(4):668-77.
107. Murphy MM, Zayed MA, Evans A, Parker CE, Ataga KI, Telen MJ, et al. Role of Rap1 in promoting sickle red blood cell adhesion to laminin via BCAM/LU. Blood. 2005;105(8):3322-9.
108. El Nemer W, Colin Y, Le Van Kim C. Role of Lu/BCAM glycoproteins in red cell diseases. Transfus Clin Biol. 2010;17(3):143-7.
109. Wautier MP, El Nemer W, Gane P, Rain JD, Cartron JP, Colin Y, et al. Increased adhesion to endothelial cells of erythrocytes from patients with polycythemia vera is mediated by laminin alpha5 chain and Lu/BCAM. Blood. 2007;110(3):894-901.
110. De Grandis M, Cambot M, Wautier MP, Cassinat B, Chomienne C, Colin Y, et al. JAK2V617F activates Lu/BCAM-mediated red cell adhesion in polycythemia vera through an EpoR-independent Rap1/Akt pathway. Blood. 2013;121(4):658-65.
111. Wilkins MR, Sanchez JC, Gooley AA, Appel RD, Humphery-Smith I, Hochstrasser DF, et al. Progress with proteome projects: why all proteins expressed by a genome should be identified and how to do it. Biotechnol Genet Eng Rev. 1996;13:19-50.
112. Langley SR, Dwyer J, Drozdov I, Yin X, Mayr M. Proteomics: from single molecules to biological pathways. Cardiovasc Res. 2013;97(4):612-22.
113. Tanaka K, Waki H, Ido Y, Akita S, Yoshida Y, Yoshida T, et al. Protein and polymer analyses up to m/z 100 000 by laser ionization time-of-flight mass spectrometry. Rapid Communications in Mass Spectrometry. 1988;2(8):151-3.
114. Chen CH. Review of a current role of mass spectrometry for proteome research. Anal Chim Acta. 2008;624(1):16-36.
115. Issaq HJ, Conrads TP, Prieto DA, Tirumalai R, Veenstra TD. SELDI-TOF MS for diagnostic proteomics. Anal Chem. 2003;75(7):148a-55a.
116. Grebe SK, Singh RJ. LC-MS/MS in the Clinical Laboratory - Where to From Here? Clin Biochem Rev. 2011;32(1):5-31.
117. Roux-Dalvai F, Gonzalez de Peredo A, Simo C, Guerrier L, Bouyssie D, Zanella A, et al. Extensive analysis of the cytoplasmic proteome of human erythrocytes using the peptide ligand library technology and advanced mass spectrometry. Mol Cell Proteomics. 2008;7(11):2254-69.
118. Tsiftsoglou AS, Vizirianakis IS, Strouboulis J. Erythropoiesis: model systems, molecular regulators, and developmental programs. IUBMB Life. 2009;61(8):800-30.
119. Kakhniashvili DG, Bulla LA, Jr., Goodman SR. The human erythrocyte proteome: analysis by ion trap mass spectrometry. Mol Cell Proteomics. 2004;3(5):501-9.
120. Bhattacharya D, Mukhopadhyay D, Chakrabarti A. Hemoglobin depletion from red blood cell cytosol reveals new proteins in 2-D gel-based proteomics study. Proteomics Clin Appl. 2007;1(6):561-4.
121. Ringrose JH, van Solinge WW, Mohammed S, O'Flaherty MC, van Wijk R, Heck AJ, et al. Highly efficient depletion strategy for the two most abundant erythrocyte soluble proteins improves proteome coverage dramatically. J Proteome Res. 2008;7(7):3060-3.
122. Alvarez-Llamas G, de la Cuesta F, Barderas MG, Darde VM, Zubiri I, Caramelo C, et al. A novel methodology for the analysis of membrane and cytosolic sub-proteomes of erythrocytes by 2-DE. Electrophoresis. 2009;30(23):4095-108.
123. Walpurgis K, Kohler M, Thomas A, Wenzel F, Geyer H, Schanzer W, et al. Validated hemoglobin-depletion approach for red blood cell lysate proteome analysis by means of 2D PAGE and Orbitrap MS. Electrophoresis. 2012;33(16):2537-45.
124. Boschetti E, Righetti PG. The ProteoMiner in the proteomic arena: a non-depleting tool for discovering low-abundance species. J Proteomics. 2008;71(3):255-64.

125. Thulasiraman V, Lin S, Gheorghiu L, Lathrop J, Lomas L, Hammond D, et al. Reduction of the concentration difference of proteins in biological liquids using a library of combinatorial ligands. Electrophoresis. 2005;26(18):3561-71.
126. Zaccaria A, Roux-Dalvai F, Bouamrani A, Mombrun A, Mossuz P, Monsarrat B, et al. Accessing to the minor proteome of red blood cells through the influence of the nanoparticle surface properties on the corona composition. Int J Nanomedicine. 2015;10:1869-83.
127. Geho DH, Jones CD, Petricoin EF, Liotta LA. Nanoparticles: potential biomarker harvesters. Curr Opin Chem Biol. 2006;10(1):56-61.
128. Pasini EM, Mann M, Thomas AW. Red blood cell proteomics. Transfus Clin Biol. 2010;17(3):151-64.
129. Villanueva J, Lawlor K, Toledo-Crow R, Tempst P. Automated serum peptide profiling. Nat Protoc. 2006;1(2):880-91.
130. Ligeti E, Dagher MC, Hernandez SE, Koleske AJ, Settleman J. Phospholipids can switch the GTPase substrate preference of a GTPase-activating protein. J Biol Chem. 2004;279(7):5055-8.
131. Brown MD, Sacks DB. IQGAP1 in cellular signaling: bridging the GAP. Trends Cell Biol. 2006;16(5):242-9.
132. Grohmanova K, Schlaepfer D, Hess D, Gutierrez P, Beck M, Kroschewski R. Phosphorylation of IQGAP1 modulates its binding to Cdc42, revealing a new type of rho-GTPase regulator. J Biol Chem. 2004;279(47):48495-504.
133. Jacquemet G, Humphries MJ. IQGAP1 is a key node within the small GTPase network. Small GTPases. 2013;4(4):199-207.
134. McCallum SJ, Wu WJ, Cerione RA. Identification of a putative effector for Cdc42Hs with high sequence similarity to the RasGAP-related protein IQGAP1 and a Cdc42Hs binding partner with similarity to IQGAP2. J Biol Chem. 1996;271(36):21732-7.
135. Owen D, Campbell LJ, Littlefield K, Evetts KA, Li Z, Sacks DB, et al. The IQGAP1-Rac1 and IQGAP1-Cdc42 interactions: interfaces differ between the complexes. J Biol Chem. 2008;283(3):1692-704.
136. White CD, Brown MD, Sacks DB. IQGAPs in cancer: a family of scaffold proteins underlying tumorigenesis. FEBS Lett. 2009;583(12):1817-24.
137. Yamaoka-Tojo M, Ushio-Fukai M, Hilenski L, Dikalov SI, Chen YE, Tojo T, et al. IQGAP1, a novel vascular endothelial growth factor receptor binding protein, is involved in reactive oxygen species--dependent endothelial migration and proliferation. Circ Res. 2004;95(3):276-83.
138. Erickson JW, Cerione RA, Hart MJ. Identification of an actin cytoskeletal complex that includes IQGAP and the Cdc42 GTPase. J Biol Chem. 1997;272(39):24443-7.
139. Radu M, Semenova G, Kosoff R, Chernoff J. PAK signalling during the development and progression of cancer. Nat Rev Cancer. 2014;14(1):13-25.
140. Ye DZ, Field J. PAK signaling in cancer. Cell Logist. 2012;2(2):105-16.
141. Johnson S, Michalak M, Opas M, Eggleton P. The ins and outs of calreticulin: from the ER lumen to the extracellular space. Trends Cell Biol. 2001;11(3):122-9.
142. Wennerberg K, Rossman KL, Der CJ. The Ras superfamily at a glance. J Cell Sci. 2005;118(Pt 5):843-6.
143. Johnson DS, Chen YH. Ras family of small GTPases in immunity and inflammation. Curr Opin Pharmacol. 2012;12(4):458-63.
144. Wang JB, Sonn R, Tekletsadik YK, Samorodnitsky D, Osman MA. IQGAP1 regulates cell proliferation through a novel CDC42-mTOR pathway. J Cell Sci. 2009;122(Pt 12):2024-33.
145. Gutkowska M, Swiezewska E. Structure, regulation and cellular functions of Rab geranylgeranyl transferase and its cellular partner Rab Escort Protein. Mol Membr Biol. 2012;29(7):243-56.
146. Leung KF, Baron R, Seabra MC. Thematic review series: lipid posttranslational modifications. geranylgeranylation of Rab GTPases. J Lipid Res. 2006;47(3):467-75.
147. Pereira-Leal JB, Hume AN, Seabra MC. Prenylation of Rab GTPases: molecular mechanisms and involvement in genetic disease. FEBS Lett. 2001;498(2-3):197-200.
148. Detter JC, Zhang Q, Mules EH, Novak EK, Mishra VS, Li W, et al. Rab geranylgeranyl transferase alpha mutation in the gunmetal mouse reduces Rab prenylation and platelet synthesis. Proc Natl Acad Sci U S A. 2000;97(8):4144-9.

149. Recchi C, Seabra MC. Novel functions for Rab GTPases in multiple aspects of tumour progression. Biochem Soc Trans. 2012;40(6):1398-403.
150. Seabra MC, Mules EH, Hume AN. Rab GTPases, intracellular traffic and disease. Trends Mol Med. 2002;8(1):23-30.
151. Stenmark H, Vitale G, Ullrich O, Zerial M. Rabaptin-5 is a direct effector of the small GTPase Rab5 in endocytic membrane fusion. Cell. 1995;83(3):423-32.
152. Magnusson MK, Meade KE, Brown KE, Arthur DC, Krueger LA, Barrett AJ, et al. Rabaptin-5 is a novel fusion partner to platelet-derived growth factor beta receptor in chronic myelomonocytic leukemia. Blood. 2001;98(8):2518-25.
153. Lippe R, Miaczynska M, Rybin V, Runge A, Zerial M. Functional synergy between Rab5 effector Rabaptin-5 and exchange factor Rabex-5 when physically associated in a complex. Mol Biol Cell. 2001;12(7):2219-28.
154. White CD, Erdemir HH, Sacks DB. IQGAP1 and its binding proteins control diverse biological functions. Cell Signal. 2012;24(4):826-34.
155. Briggs MW, Sacks DB. IQGAP1 as signal integrator: Ca2+, calmodulin, Cdc42 and the cytoskeleton. FEBS Lett. 2003;542(1-3):7-11.
156. Broudy VC, Lin N, Brice M, Nakamoto B, Papayannopoulou T. Erythropoietin receptor characteristics on primary human erythroid cells. Blood. 1991;77(12):2583-90.
157. Elliott S, Sinclair A, Collins H, Rice L, Jelkmann W. Progress in detecting cell-surface protein receptors: the erythropoietin receptor example. Ann Hematol. 2014;93(2):181-92.
158. Jameson KL, Mazur PK, Zehnder AM, Zhang J, Zarnegar B, Sage J, et al. IQGAP1 scaffold-kinase interaction blockade selectively targets RAS-MAP kinase-driven tumors. Nat Med. 2013;19(5):626-30.
159. Johnson M, Sharma M, Henderson BR. IQGAP1 regulation and roles in cancer. Cell Signal. 2009;21(10):1471-8.
160. Sanchez-Laorden B, Viros A, Marais R. Mind the IQGAP. Cancer Cell. 2013;23(6):715-7.
161. Tekletsadik YK, Sonn R, Osman MA. A conserved role of IQGAP1 in regulating TOR complex 1. J Cell Sci. 2012;125(Pt 8):2041-52.
162. Ory S, Gasman S. Rho GTPases and exocytosis: what are the molecular links? Semin Cell Dev Biol. 2011;22(1):27-32.
163. Jaffer ZM, Chernoff J. p21-activated kinases: three more join the Pak. Int J Biochem Cell Biol. 2002;34(7):713-7.
164. Zhao ZS, Manser E. PAK family kinases: Physiological roles and regulation. Cell Logist. 2012;2(2):59-68.
165. Rider L, Shatrova A, Feener EP, Webb L, Diakonova M. JAK2 tyrosine kinase phosphorylates PAK1 and regulates PAK1 activity and functions. J Biol Chem. 2007;282(42):30985-96.
166. Malarkannan S, Awasthi A, Rajasekaran K, Kumar P, Schuldt KM, Bartoszek A, et al. IQGAP1: a regulator of intracellular spacetime relativity. J Immunol. 2012;188(5):2057-63.
167. DerMardirossian C, Schnelzer A, Bokoch GM. Phosphorylation of RhoGDI by Pak1 mediates dissociation of Rac GTPase. Mol Cell. 2004;15(1):117-27.
168. Dovas A, Couchman JR. RhoGDI: multiple functions in the regulation of Rho family GTPase activities. Biochem J. 2005;390(Pt 1):1-9.
169. Mulloy JC, Cancelas JA, Filippi MD, Kalfa TA, Guo F, Zheng Y. Rho GTPases in hematopoiesis and hemopathies. Blood. 2010;115(5):936-47.
170. Marty C, Lacout C, Droin N, Le Couedic JP, Ribrag V, Solary E, et al. A role for reactive oxygen species in JAK2 V617F myeloproliferative neoplasm progression. Leukemia. 2013;27(11):2187-95.
171. Yalcin S, Marinkovic D, Mungamuri SK, Zhang X, Tong W, Sellers R, et al. ROS-mediated amplification of AKT/mTOR signalling pathway leads to myeloproliferative syndrome in Foxo3(-/-) mice. Embo j. 2010;29(24):4118-31.
172. Liu J, Guidry JJ, Worthylake DK. Conserved sequence repeats of IQGAP1 mediate binding to Ezrin. J Proteome Res. 2014;13(2):1156-66.

173. Yamauchi T, Ueki K, Tobe K, Tamemoto H, Sekine N, Wada M, et al. Growth hormone-induced tyrosine phosphorylation of EGF receptor as an essential element leading to MAP kinase activation and gene expression. Endocr J. 1998;45 Suppl:S27-31.
174. Gallardo M, Barrio S, Fernandez M, Paradela A, Arenas A, Toldos O, et al. Proteomic analysis reveals heat shock protein 70 has a key role in polycythemia Vera. Mol Cancer. 2013;12:142.
175. Cokic VP, Mossuz P, Han J, Socoro N, Beleslin-Cokic BB, Mitrovic O, et al. Microarray and Proteomic Analyses of Myeloproliferative Neoplasms with a Highlight on the mTOR Signaling Pathway. PLoS One. 2015;10(8):e0135463.
176. Sheng W, Chen C, Dong M, Zhou J, Liu Q, Dong Q, et al. Overexpression of calreticulin contributes to the development and progression of pancreatic cancer. J Cell Physiol. 2014;229(7):887-97.
177. Nakamura K, Bossy-Wetzel E, Burns K, Fadel MP, Lozyk M, Goping IS, et al. Changes in endoplasmic reticulum luminal environment affect cell sensitivity to apoptosis. J Cell Biol. 2000;150(4):731-40.
178. Prathyuman S, Sellappa S, Joseph S, Keyan KS. Enhanced calreticulin expression triggers apoptosis in the MCF-7 cell line. Asian Pac J Cancer Prev. 2010;11(4):1133-6.
179. Bresnick AR, Weber DJ, Zimmer DB. S100 proteins in cancer. Nat Rev Cancer. 2015;15(2):96-109.
180. Nicolas E, Ramus C, Berthier S, Arlotto M, Bouamrani A, Lefebvre C, et al. Expression of S100A8 in leukemic cells predicts poor survival in de novo AML patients. Leukemia. 2011;25(1):57-65.
181. Landolfi R, Di Gennaro L, Barbui T, De Stefano V, Finazzi G, Marfisi R, et al. Leukocytosis as a major thrombotic risk factor in patients with polycythemia vera. Blood. 2007;109(6):2446-52.
182. Carobbio A, Finazzi G, Guerini V, Spinelli O, Delaini F, Marchioli R, et al. Leukocytosis is a risk factor for thrombosis in essential thrombocythemia: interaction with treatment, standard risk factors, and Jak2 mutation status. Blood. 2007;109(6):2310-3.
183. Carobbio A, Antonioli E, Guglielmelli P, Vannucchi AM, Delaini F, Guerini V, et al. Leukocytosis and risk stratification assessment in essential thrombocythemia. J Clin Oncol. 2008;26(16):2732-6.
184. Nicholson KM, Anderson NG. The protein kinase B/Akt signalling pathway in human malignancy. Cell Signal. 2002;14(5):381-95.
185. Grimwade LF, Happerfield L, Tristram C, McIntosh G, Rees M, Bench AJ, et al. Phospho-STAT5 and phospho-Akt expression in chronic myeloproliferative neoplasms. Br J Haematol. 2009;147(4):495-506.
186. Drayer AL, Olthof SG, Vellenga E. Mammalian target of rapamycin is required for thrombopoietin-induced proliferation of megakaryocyte progenitors. Stem Cells. 2006;24(1):105-14.
187. Vicari L, Martinetti D, Buccheri S, Colarossi C, Aiello E, Stagno F, et al. Increased phospho-mTOR expression in megakaryocytic cells derived from CD34+ progenitors of essential thrombocythaemia and myelofibrosis patients. Br J Haematol. 2012;159(2):237-40.
188. Khan I, Huang Z, Wen Q, Stankiewicz MJ, Gilles L, Goldenson B, et al. AKT is a therapeutic target in myeloproliferative neoplasms. Leukemia. 2013;27(9):1882-90.
189. Bogani C, Bartalucci N, Martinelli S, Tozzi L, Guglielmelli P, Bosi A, et al. mTOR inhibitors alone and in combination with JAK2 inhibitors effectively inhibit cells of myeloproliferative neoplasms. PLoS One. 2013;8(1):e54826.
190. Bartalucci N, Tozzi L, Bogani C, Martinelli S, Rotunno G, Villeval JL, et al. Co-targeting the PI3K/mTOR and JAK2 signalling pathways produces synergistic activity against myeloproliferative neoplasms. J Cell Mol Med. 2013;17(11):1385-96.
191. Fiskus W, Verstovsek S, Manshouri T, Smith JE, Peth K, Abhyankar S, et al. Dual PI3K/AKT/mTOR inhibitor BEZ235 synergistically enhances the activity of JAK2 inhibitor against cultured and primary human myeloproliferative neoplasm cells. Mol Cancer Ther. 2013;12(5):577-88.
192. Musolino C, Allegra A, Saija A, Alonci A, Russo S, Spatari G, et al. Changes in advanced oxidation protein products, advanced glycation end products, and s-nitrosylated proteins, in

patients affected by polycythemia vera and essential thrombocythemia. Clin Biochem. 2012;45(16-17):1439-43.
193. Vener C, Novembrino C, Catena FB, Fracchiolla NS, Gianelli U, Savi F, et al. Oxidative stress is increased in primary and post-polycythemia vera myelofibrosis. Exp Hematol. 2010;38(11):1058-65.
194. Hurtado-Nedelec M, Csillag-Grange MJ, Boussetta T, Belambri SA, Fay M, Cassinat B, et al. Increased reactive oxygen species production and p47phox phosphorylation in neutrophils from myeloproliferative disorders patients with JAK2 (V617F) mutation. Haematologica. 2013;98(10):1517-24.
195. Nieborowska-Skorska M, Kopinski PK, Ray R, Hoser G, Ngaba D, Flis S, et al. Rac2-MRC-cIII-generated ROS cause genomic instability in chronic myeloid leukemia stem cells and primitive progenitors. Blood. 2012;119(18):4253-63.
196. Warmuth M, Kim S, Gu XJ, Xia G, Adrian F. Ba/F3 cells and their use in kinase drug discovery. Curr Opin Oncol. 2007;19(1):55-60.
197. Lu X, Levine R, Tong W, Wernig G, Pikman Y, Zarnegar S, et al. Expression of a homodimeric type I cytokine receptor is required for JAK2V617F-mediated transformation. Proc Natl Acad Sci U S A. 2005;102(52):18962-7.
198. Barrio S, Gallardo M, Arenas A, Ayala R, Rapado I, Rueda D, et al. Inhibition of related JAK/STAT pathways with molecular targeted drugs shows strong synergy with ruxolitinib in chronic myeloproliferative neoplasm. Br J Haematol. 2013;161(5):667-76.
199. Gui CY, Jiang C, Xie HY, Qian RL. The apoptosis of HEL cells induced by hydroxyurea. Cell Res. 1997;7(1):91-7.
200. Bourgeais J, Gouilleux-Gruart V, Gouilleux F. Oxidative metabolism in cancer: A STAT affair? Jakstat. 2013;2(4):e25764.
201. Faruqi TR, Gomez D, Bustelo XR, Bar-Sagi D, Reich NC. Rac1 mediates STAT3 activation by autocrine IL-6. Proc Natl Acad Sci U S A. 2001;98(16):9014-9.
202. Debidda M, Wang L, Zang H, Poli V, Zheng Y. A role of STAT3 in Rho GTPase-regulated cell migration and proliferation. J Biol Chem. 2005;280(17):17275-85.
203. Kanda E, Jin ZH, Mizuchi D, Arai A, Miura O. Activation of Rac and tyrosine phosphorylation of cytokine receptors induced by cross-linking of integrin alpha4beta1 and cell adhesion in hematopoietic cells. Biochem Biophys Res Commun. 2003;301(4):934-40.

# SUPPLEMENTAL DATA

# SUPPLEMENTAL DATA I

## Supplemental Data I-1

Lists of deregulated proteins in erythrocytes between the different subgroups: *JAK2V617F* PV, *JAK2V617F* ET, *JAK2(-)* ET and controls.

### *List of most upregulated proteins in JAK2V617F PV vs control patients*

| Protein name | p-value | Ratio |
|---|---|---|
| C8orf62 Phosphoserine aminotransferase | 0.022 | Infinite |
| RABGGTA Geranylgeranyl transferase type-2 subunit alpha | 0.005 | Infinite |
| PHKB Isoform 1 of Phosphorylase b kinase regulatory subunit beta | 0.009 | Infinite |
| IGHG4 Putative uncharacterized protein DKFZp686M24218 | 0.021 | Infinite |
| SMS Isoform 1 of Spermine synthase | 0.025 | 18.483 |
| MYH10 Isoform 3 of Myosin-10 | 0.009 | 13.055 |
| TRIM58 Tripartite motif-containing protein 58 | 0.038 | 11.327 |
| PSMB8 Isoform 2 of Proteasome subunit beta type-8 | 0.017 | 8.289 |
| CASP8 Isoform 4 of Caspase-8 | 0.015 | 8.236 |
| CYB5A Isoform 1 of Cytochrome b5 | 0.027 | 7.021 |
| TNPO1 Isoform 2 of Transportin-1 | 0.017 | 6.670 |
| IFIT5 Interferon-induced protein with tetratricopeptide repeats 5 | 0.020 | 5.571 |
| ANXA3 Annexin A3 | 0.044 | 5.528 |
| MYH9 Isoform 1 of Myosin-9 | 0.003 | 5.427 |
| APOA1 Apolipoprotein A-I | 0.027 | 5.401 |
| MYL4 Myosin light chain 4 | 0.003 | 5.083 |
| MYL12B Myosin regulatory light chain 12B | 0.009 | 4.947 |
| PRIC285 Isoform 2 of Peroxisomal proliferator-activated receptor A-interacting complex 285 kDa protein | 0.024 | 4.841 |
| IFI35 Isoform 2 of Interferon-induced 35 kDa protein | 0.011 | 4.229 |
| DNM1L cDNA FLJ55044, highly similar to Dynamin-1-like protein | 0.011 | 4.218 |
| TSG101 Isoform 2 of Tumor susceptibility gene 101 protein | 0.027 | 3.508 |
| S100A9 Protein S100-A9 | 0.029 | 3.448 |
| DPCD Protein DPCD | 0.024 | 3.431 |
| TTC38 Tetratricopeptide repeat protein 38 | 0.017 | 3.405 |
| ARPC5 Isoform 1 of Actin-related protein 2/3 complex subunit 5 | 0.038 | 3.378 |
| EEF1A1 Elongation factor 1-alpha 1 | 0.013 | 3.338 |
| ARPC1B cDNA FLJ57124, highly similar to Actin-related protein 2/3 complex subunit 1A | 0.038 | 3.321 |
| LAP3 Isoform 1 of Cytosol aminopeptidase | 0.045 | 3.185 |
| YARS Tyrosyl-tRNA synthetase, cytoplasmic | 0.015 | 3.058 |
| MYL6B 16 kDa protein | 0.006 | 2.854 |
| DCTN5 Dynactin subunit 5 | 0.026 | 2.824 |
| RPSAP15;RPSA 40S ribosomal protein SA | 0.048 | 2.727 |
| GCA 22 kDa protein | 0.047 | 2.621 |
| ACTN1 Alpha-actinin-1 | 0.003 | 2.543 |

| | | |
|---|---|---|
| DCTN3 Isoform 3 of Dynactin subunit 3 | 0.038 | 2.365 |
| KPNA1 Importin subunit alpha-1 | 0.010 | 2.311 |
| ACTN4 cDNA FLJ58087, highly similar to Alpha-actinin-4 | 0.045 | 2.311 |
| NIT1 Isoform 5 of Nitrilase homolog 1 | 0.006 | 2.295 |
| DHRS11 Isoform 1 of Dehydrogenase/reductase SDR family member 11 | 0.007 | 2.226 |
| AARS cDNA FLJ61339, highly similar to Alanyl-tRNA synthetase | 0.004 | 2.211 |
| GNPDA1 Glucosamine-6-phosphate isomerase 1 | 0.013 | 2.203 |
| TPT1 Tumor protein, translationally-controlled 1 | 0.003 | 2.160 |
| TSTA3 GDP-L-fucose synthetase | 0.001 | 2.156 |
| TLN2 Talin-2 | 0.012 | 2.129 |
| DCTN2 dynactin 2 | 0.026 | 2.081 |
| PCBP1 Poly(rC)-binding protein 1 | 0.032 | 2.077 |
| ANXA7 Isoform 1 of Annexin A7 | 0.004 | 2.057 |
| PPCS Phosphopantothenate--cysteine ligase | 0.014 | 2.048 |
| VPS35 Vacuolar protein sorting-associated protein 35 | 0.012 | 2.033 |
| CLIC2 Chloride intracellular channel protein 2 | 0.006 | 2.033 |
| ACTR3 Actin-related protein 3 | 0.025 | 2.030 |

### *List of most downregulated proteins in JAK2V617F PV vs Controls*

| **Protein name** | **p-value** | **Ratio** |
|---|---|---|
| LDHA Isoform 1 of L-lactate dehydrogenase A chain | 0.002 | 0.497 |
| DAK Bifunctional ATP-dependent dihydroxyacetone kinase/FAD-AMP lyase (cyclizing) | 0.003 | 0.495 |
| AK1 Adenylate kinase 1 | 0.005 | 0.494 |
| PGD 6-phosphogluconate dehydrogenase, decarboxylating | 0.021 | 0.491 |
| IDH1 Isocitrate dehydrogenase [NADP] cytoplasmic | 0.027 | 0.468 |
| BAG1 Isoform 3 of BAG family molecular chaperone regulator 1 | 0.007 | 0.464 |
| HBB Hemoglobin subunit beta | 0.015 | 0.400 |
| EIF4G3 Isoform 1 of Eukaryotic translation initiation factor 4 gamma 3 | 0.015 | 0.399 |
| ATP7A Isoform 4 of Copper-transporting ATPase 1 | 0.034 | 0.390 |
| - Similar to L-lactate dehydrogenase | 0.013 | 0.376 |
| BCL2L1 Isoform Bcl-X(L) of Bcl-2-like protein 1 | 0.011 | 0.354 |
| HBD Hemoglobin subunit delta | 0.002 | 0.311 |
| CA3 Carbonic anhydrase 3 | 0.042 | 0.280 |
| RRM1 Ribonucleoside-diphosphate reductase large subunit | 0.005 | 0.268 |
| HBG2 Hemoglobin subunit gamma-2 | 0.0003 | 0.174 |

### *List of most upregulated proteins in JAK2V617F ET vs Controls*

| **Protein name** | **p-value** | **Ratio** |
|---|---|---|
| RABGGTA Geranylgeranyl transferase type-2 subunit alpha | 0.016 | Infinite |
| PHKB Isoform 1 of Phosphorylase b kinase regulatory subunit beta | 0.036 | Infinite |
| IGHG2 Putative uncharacterized protein DKFZp686I04196 (Fragment) | 0.040 | Infinite |
| IGHG4 Putative uncharacterized protein DKFZp686M24218 | 0.036 | Infinite |
| CP cDNA FLJ58075, highly similar to Ceruloplasmin | 0.045 | Infinite |
| A2M Alpha-2-macroglobulin | 0.040 | 36.777 |
| SERPINA1 Isoform 1 of Alpha-1-antitrypsin | 0.035 | 33.341 |
| LMNB1 LMNB1 protein | 0.008 | 15.805 |
| ALB Isoform 1 of Serum albumin | 0.014 | 12.057 |
| IPO4 Isoform 2 of Importin-4 | 0.029 | 11.437 |
| APOA1 Apolipoprotein A-I | 0.027 | 10.672 |

| | | |
|---|---|---|
| ISOC1 CGI-111 protein | 0.043 | 10.363 |
| GYG1 cDNA FLJ57427, highly similar to Glycogenin-1 | 0.008 | 8.543 |
| FGG Putative uncharacterized protein FGG | 0.007 | 7.892 |
| FGA Isoform 2 of Fibrinogen alpha chain | 0.012 | 7.523 |
| PYGB Glycogen phosphorylase, brain form | 0.037 | 7.077 |
| PYGL Glycogen phosphorylase, liver form | 0.021 | 6.924 |
| CLU CLU | 0.015 | 6.889 |
| LOC653888 similar to actin related protein 2/3 complex subunit 1B | 0.019 | 6.835 |
| CORO1A 40 kDa protein | 0.005 | 6.607 |
| ANXA3 Annexin A3 | 0.010 | 6.538 |
| GYS1 glycogen synthase 1 (muscle) isoform 2 | 0.002 | 6.276 |
| HDDC3 7 kDa protein | 0.001 | 5.315 |
| F13A1 Coagulation factor XIII A chain | 0.009 | 5.045 |
| FGB Fibrinogen beta chain | 0.006 | 5.035 |
| RABEP1 Isoform 2 of Rab GTPase-binding effector protein 1 | 0.005 | 5.021 |
| MYH10 Isoform 3 of Myosin-10 | 0.024 | 4.871 |
| ARPC5 Isoform 1 of Actin-related protein 2/3 complex subunit 5 | 0.011 | 4.711 |
| DPCD Protein DPCD | 0.0003 | 4.596 |
| TTC38 Tetratricopeptide repeat protein 38 | 0.009 | 4.486 |
| CAB39 Calcium-binding protein 39 | 0.018 | 4.458 |
| TNPO1 Isoform 2 of Transportin-1 | 0.002 | 3.844 |
| CBX3 Chromobox protein homolog 3 | 0.044 | 3.758 |
| LOC646214;PAK2 Serine/threonine-protein kinase PAK 2 | 0.012 | 3.755 |
| SHPK Sedoheptulokinase | 0.005 | 3.751 |
| RTCD1 Isoform 2 of RNA 3'-terminal phosphate cyclase | 0.003 | 3.711 |
| IQGAP1 Ras GTPase-activating-like protein IQGAP1 | 0.005 | 3.684 |
| FLNA Isoform 2 of Filamin-A | 0.001 | 3.530 |
| CYB5A Isoform 1 of Cytochrome b5 | 0.012 | 3.357 |
| MYH9 Isoform 1 of Myosin-9 | 0.008 | 3.307 |
| PDIA6 Isoform 2 of Protein disulfide-isomerase A6 | 0.005 | 3.273 |
| TSG101 Isoform 2 of Tumor susceptibility gene 101 protein | 0.025 | 3.246 |
| TLN2 Talin-2 | 0.001 | 3.243 |
| PLEK Pleckstrin | 0.002 | 3.215 |
| ACTN1 Alpha-actinin-1 | 0.004 | 3.195 |
| CASP3 Caspase-3 | 0.023 | 2.899 |
| THBS1 Thrombospondin-1 | 0.045 | 2.886 |
| NIT1 Isoform 5 of Nitrilase homolog 1 | 0.011 | 2.840 |
| ARHGDIB Rho GDP-dissociation inhibitor 2 | 0.009 | 2.730 |
| COPB2 Coatomer subunit beta' | 0.044 | 2.719 |
| TPT1 Tumor protein, translationally-controlled 1 | 0.002 | 2.707 |
| PARVB parvin, beta isoform a | 0.021 | 2.685 |
| TLN1 Talin-1 | 0.001 | 2.622 |
| ZNF595 Zinc finger protein 595 | 0.002 | 2.568 |
| YARS Tyrosyl-tRNA synthetase, cytoplasmic | 0.035 | 2.542 |
| NUDCD1 Isoform 1 of NudC domain-containing protein 1 | 0.003 | 2.528 |
| PCBP1 Poly(rC)-binding protein 1 | 0.015 | 2.474 |
| MYL12B Myosin regulatory light chain 12B | 0.029 | 2.471 |
| TNPO2 Isoform 2 of Transportin-2 | 0.051 | 2.469 |
| MYL4 Myosin light chain 4 | 0.051 | 2.465 |
| EIF2S1 Eukaryotic translation initiation factor 2 subunit 1 | 0.002 | 2.455 |
| RPSAP15;RPSA 40S ribosomal protein SA | 0.026 | 2.437 |

| | | |
|---|---|---|
| ATP6V1C1 V-type proton ATPase subunit C 1 | 0.021 | 2.423 |
| FLNB Isoform 1 of Filamin-B | 0.023 | 2.381 |
| ACTR3 Actin-related protein 3 | 0.006 | 2.362 |
| CAP1 Isoform 1 of Adenylyl cyclase-associated protein 1 | 0.00001 | 2.345 |
| ANXA11 cDNA FLJ55482, highly similar to Annexin A11 | 0.035 | 2.324 |
| KPNA3 Importin subunit alpha-3 | 0.007 | 2.261 |
| MYL6B 16 kDa protein | 0.011 | 2.241 |
| OSTF1 Osteoclast-stimulating factor 1 | 0.031 | 2.230 |
| CCDC150 Isoform 1 of Coiled-coil domain-containing protein 150 | 0.002 | 2.210 |
| MDP1 Isoform 2 of Magnesium-dependent phosphatase 1 | 0.010 | 2.206 |
| CLIC2 Chloride intracellular channel protein 2 | 0.0001 | 2.177 |
| RGS10 Isoform 3 of Regulator of G-protein signaling 10 | 0.018 | 2.158 |
| ACTN4 Alpha-actinin-4 | 0.009 | 2.155 |
| GNPDA2 Isoform 1 of Glucosamine-6-phosphate isomerase 2 | 0.011 | 2.145 |
| CAP1 Adenylyl cyclase-associated protein | 0.00001 | 2.131 |
| UCHL5 Isoform 3 of Ubiquitin carboxyl-terminal hydrolase isozyme L5 | 0.006 | 2.107 |
| DHRS11 Isoform 1 of Dehydrogenase/reductase SDR family member 11 | 0.0002 | 2.099 |
| CARS Isoform 2 of Cysteinyl-tRNA synthetase, cytoplasmic | 0.005 | 2.092 |
| PPCS Phosphopantothenate--cysteine ligase | 0.001 | 2.091 |
| PRKACA Isoform 2 of cAMP-dependent protein kinase catalytic subunit alpha | 0.026 | 2.083 |
| HBQ1 Hemoglobin subunit theta-1 | 0.005 | 2.081 |
| PABPC1 cDNA FLJ37875 fis, clone BRSSN2018771, highly similar to Poly(A)-binding protein 1 | 0.040 | 2.024 |
| EEF1A1 Elongation factor 1-alpha 1 | 0.015 | 2.023 |

### *List of most downregulated proteins in JAK2V617F ET vs Controls*

| **Protein name** | **p-value** | **Ratio** |
|---|---|---|
| UBB;UBC;RPS27A 16 kDa protein | 0.021 | 0.481 |
| PRKAG1 cDNA FLJ40287 fis, clone TESTI2027909, highly similar to 5'-AMP-ACTIVATED PROTEIN KINASE, GAMMA-1 SUBUNIT | 0.047 | 0.466 |
| GAPDH Glyceraldehyde-3-phosphate dehydrogenase | 0.018 | 0.464 |
| NEDD8 Putative uncharacterized protein NEDD8 (Fragment) | 0.005 | 0.461 |
| WDR1 Isoform 1 of WD repeat-containing protein 1 | 0.003 | 0.457 |
| GAPDH 9 kDa protein | 0.009 | 0.450 |
| PPA1 Inorganic pyrophosphatase | 0.010 | 0.448 |
| GRHPR Glyoxylate reductase/hydroxypyruvate reductase | 0.023 | 0.444 |
| FAM114A2 Isoform 1 of Protein FAM114A2 | 0.012 | 0.433 |
| LTA4H Isoform 1 of Leukotriene A-4 hydrolase | 0.000 | 0.430 |
| FAM114A2 cDNA FLJ54229 | 0.014 | 0.422 |
| CFL1 Cofilin-1 | 0.0005 | 0.422 |
| LDHB L-lactate dehydrogenase B chain | 0.0001 | 0.414 |
| SELENBP1 Selenium binding protein 1 | 0.002 | 0.414 |
| CMBL Carboxymethylenebutenolidase homolog | 0.032 | 0.403 |
| AP2S1 Isoform 1 of AP-2 complex subunit sigma | 0.041 | 0.401 |
| RAB3GAP2 Isoform 2 of Rab3 GTPase-activating protein non-catalytic subunit | 0.011 | 0.400 |
| BCL2L1 Isoform Bcl-X(L) of Bcl-2-like protein 1 | 0.014 | 0.399 |
| PARK7 Protein DJ-1 | 0.006 | 0.390 |
| ADA Adenosine deaminase | 0.001 | 0.390 |
| ABHD14B Isoform 1 of Abhydrolase domain-containing protein 14B | 0.016 | 0.383 |

| | | |
|---|---|---|
| AK1 Adenylate kinase 1 | 0.001 | 0.364 |
| ACP1 Isoform 1 of Low molecular weight phosphotyrosine protein phosphatase | 0.0002 | 0.346 |
| LDHC L-lactate dehydrogenase C chain | 0.015 | 0.341 |
| IDH1 Isocitrate dehydrogenase [NADP] cytoplasmic | 0.008 | 0.335 |
| LDHA Isoform 1 of L-lactate dehydrogenase A chain | 0.0001 | 0.335 |
| ALDOA Fructose-bisphosphate aldolase A | 0.001 | 0.323 |
| 6 KDA PROTEIN | 0.034 | 0.320 |
| GLOD4 Uncharacterized protein C17orf25 | 0.014 | 0.317 |
| - Similar to L-lactate dehydrogenase | 0.005 | 0.316 |
| ALDOC Fructose-bisphosphate aldolase | 0.005 | 0.309 |
| CA3 Carbonic anhydrase 3 | 0.040 | 0.307 |
| HBA2;HBA1 Hemoglobin subunit alpha | 0.012 | 0.297 |
| GSTO1 Glutathione S-transferase omega-1 | 0.001 | 0.274 |
| MDH1 Malate dehydrogenase | 0.001 | 0.267 |
| MDH1 Putative uncharacterized protein MDH1 | 0.004 | 0.251 |
| CBR1 Carbonyl reductase 1, isoform CRA_c | 0.002 | 0.250 |
| HBA2;HBA1 Hemoglobin alpha-2 | 0.00001 | 0.232 |
| PGD 6-phosphogluconate dehydrogenase, decarboxylating | 0.000002 | 0.228 |
| HBB Hemoglobin subunit beta | 0.001 | 0.225 |
| PGD 6-phosphogluconate dehydrogenase, decarboxylating | 0.000003 | 0.215 |
| CA1 Carbonic anhydrase 1 | 0.002 | 0.213 |
| CA3 cDNA FLJ52895, highly similar to Carbonic anhydrase 3 | 0.005 | 0.212 |
| HBD Hemoglobin subunit delta | 0.001 | 0.195 |
| HBG2 Hemoglobin subunit gamma-2 | 0.0005 | 0.180 |
| PAFAH1B1 Putative uncharacterized protein PAFAH1B1 (Fragment) | 0.021 | 0.122 |
| ESD S-formylglutathione hydrolase | 0.004 | 0.116 |
| PGM2 Phosphoglucomutase-2 | 0.015 | 0.108 |
| FSCN1 Fascin | 0.015 | 0.101 |
| PGK1 Phosphoglycerate kinase 1 | 0.001 | 0.080 |

### *List of most deregulated proteins in JAK2V617F PV vs JAK2V617F ET*

| **Protein name** | **p-value** | **Ratio** |
|---|---|---|
| IFI35 Isoform 2 of Interferon-induced 35 kDa protein | 0.007 | 4.983 |
| PSMB8 Isoform 2 of Proteasome subunit beta type-8 | 0.028 | 4.884 |
| FLNA Isoform 2 of Filamin-A | 0.008 | 0.500 |
| IQGAP2 Isoform 1 of Ras GTPase-activating-like protein IQGAP2 | 0.006 | 0.483 |
| BAG5 Isoform 2 of BAG family molecular chaperone regulator 5 | 0.003 | 0.447 |
| HDHD2 Isoform 1 of Haloacid dehalogenase-like hydrolase domain-containing protein 2 | 0.011 | 0.427 |
| DAZAP1 Isoform 2 of DAZ-associated protein 1 | 0.023 | 0.425 |
| FLNB Isoform 1 of Filamin-B | 0.014 | 0.408 |
| FGG Putative uncharacterized protein FGG | 0.047 | 0.379 |
| THBS1 Thrombospondin-1 | 0.026 | 0.368 |
| GYG1 cDNA FLJ57427, highly similar to Glycogenin-1 | 0.033 | 0.336 |
| RRM1 Ribonucleoside-diphosphate reductase large subunit | 0.004 | 0.333 |
| RAB11B Ras-related protein Rab-11B | 0.003 | 0.296 |
| PARVB parvin, beta isoform a | 0.007 | 0.283 |
| F13A1 Coagulation factor XIII A chain | 0.012 | 0.252 |
| PLEK Pleckstrin | 0.0004 | 0.247 |

### *List of most deregulated proteins in JAK2V617F PV vs JAK2(-) ET*

| Protein name | p-value | Ratio |
|---|---|---|
| PRIC285 Isoform 2 of Peroxisomal proliferator-activated receptor A-interacting complex 285 kDa protein | 0.008 | 26.445 |
| TRIM58 Tripartite motif-containing protein 58 | 0.039 | 11.182 |
| PSMB8 Isoform 2 of Proteasome subunit beta type-8 | 0.020 | 6.873 |
| IFIT5 Interferon-induced protein with tetratricopeptide repeats 5 | 0.022 | 5.713 |
| IFI35 Isoform 2 of Interferon-induced 35 kDa protein | 0.007 | 5.320 |
| RABGGTA Geranylgeranyl transferase type-2 subunit alpha | 0.017 | 5.305 |
| TARS Threonyl-tRNA synthetase, cytoplasmic | 0.019 | 3.861 |
| MYH10 Isoform 3 of Myosin-10 | 0.049 | 3.359 |
| PPP2R2B Isoform 4 of Serine/threonine-protein phosphatase 2A | 0.020 | 3.157 |
| MYL12B Myosin regulatory light chain 12B | 0.033 | 2.635 |
| MYL4 Myosin light chain 4 | 0.053 | 2.384 |
| PSMA1 Isoform Short of Proteasome subunit alpha type-1 | 0.043 | 2.334 |
| CUTA Isoform B of Protein CutA | 0.040 | 2.258 |
| PFDN2 Prefoldin subunit 2 | 0.035 | 2.232 |
| EEF1A1 Elongation factor 1-alpha 1 | 0.048 | 2.171 |
| MYH9 Isoform 1 of Myosin-9 | 0.034 | 2.143 |
| DCTN3 Isoform 3 of Dynactin subunit 3 | 0.049 | 2.112 |
| PRPS2 Isoform 2 of Ribose-phosphate pyrophosphokinase 2 | 0.026 | 0.485 |
| KRT1 Keratin, type II cytoskeletal 1 | 0.029 | 0.483 |
| RGS10 Isoform 3 of Regulator of G-protein signaling 10 | 0.025 | 0.475 |
| ATG4B Putative uncharacterized protein ATG4B | 0.043 | 0.466 |
| ATG4A Isoform 1 of Cysteine protease ATG4A | 0.014 | 0.465 |
| SEPT2 Putative uncharacterized protein SEPT2 | 0.027 | 0.446 |
| TMOD1 Tropomodulin-1 | 0.036 | 0.400 |
| GAK Cyclin G-associated kinase | 0.032 | 0.394 |
| BAG5 Isoform 2 of BAG family molecular chaperone regulator 5 | 0.012 | 0.380 |
| TBCB Tubulin-folding cofactor B | 0.020 | 0.350 |
| PRKAR2B cAMP-dependent protein kinase type II-beta regulatory subunit | 0.037 | 0.170 |

### *List of most deregulated proteins in JAK2V617F ET vs JAK2(-) ET*

| Protein name | p-value | Ratio |
|---|---|---|
| PDCD5 Programmed cell death protein 5 | 0.042 | 6.463 |
| RABGGTA Geranylgeranyl transferase type-2 subunit alpha | 0.036 | 6.037 |
| ISYNA1 cDNA FLJ57998, highly similar to Homo sapiens myo-inositol 1-phosphate synthase A1 (ISYNA1), mRNA | 0.042 | 3.485 |
| IGBP1 Immunoglobulin-binding protein 1 | 0.004 | 2.770 |
| CASP3 Caspase-3 | 0.024 | 2.640 |
| FADD Protein FADD | 0.017 | 2.524 |
| ARHGDIB Rho GDP-dissociation inhibitor 2 | 0.009 | 2.452 |
| IQGAP2 Isoform 1 of Ras GTPase-activating-like protein IQGAP2 | 0.015 | 2.158 |
| ARHGDIA Rho GDP-dissociation inhibitor 1 | 0.010 | 2.024 |
| PRPS2 Isoform 2 of Ribose-phosphate pyrophosphokinase 2 | 0.027 | 0.493 |
| PARK7 Protein DJ-1 | 0.037 | 0.443 |

## Supplemental Data I-2

Deregulated pathways in MPN erytrhocytes.

### *Deregulated pathways in JAK2V617F PV vs Controls*

List of the significantly deregulated pathways in PV vs controls (p-value < 0.01) ordered in decreasing –log p-value according to *IPA* results. P-value represents the proportion of deregulated proteins from the MS analysis that belong to that pathway. Ratio is made between the number of deregulated proteins and the total number of proteins in that pathway.

| Ingenuity Canonical Pathways | -log(p-value) | Ratio |
|---|---|---|
| RAN Signaling | 8.62 | 0.25 |
| Actin Cytoskeleton Signaling | 8.35 | 0.05 |
| Integrin Signaling | 7.87 | 0.06 |
| Clathrin-mediated Endocytosis Signaling | 5.07 | 0.05 |
| Regulation of Actin-based Motility by Rho | 4.63 | 0.07 |
| Protein Ubiquitination Pathway | 4.50 | 0.04 |
| Ephrin Receptor Signaling | 4.40 | 0.04 |
| VEGF Signaling | 4.23 | 0.06 |
| Rac Signaling | 3.95 | 0.05 |
| RhoA Signaling | 3.95 | 0.05 |
| Axonal Guidance Signaling | 3.84 | 0.03 |
| fMLP Signaling in Neutrophils | 3.75 | 0.05 |
| Signaling by Rho Family GTPases | 3.68 | 0.03 |
| CD28 Signaling in T Helper Cells | 3.63 | 0.05 |
| Corticotropin Releasing Hormone Signaling | 3.57 | 0.04 |
| Synaptic Long Term Potentiation | 3.49 | 0.05 |
| Apoptosis Signaling | 3.37 | 0.05 |
| Cdc42 Signaling | 3.37 | 0.03 |
| ERK/MAPK Signaling | 3.36 | 0.03 |
| Protein Kinase A Signaling | 3.30 | 0.02 |
| CD27 Signaling in Lymphocytes | 3.27 | 0.07 |
| Fcγ Receptor-mediated Phagocytosis in Macrophages and Monocytes | 3.19 | 0.05 |
| Actin Nucleation by ARP-WASP Complex | 3.18 | 0.06 |
| PRPP Biosynthesis I | 3.10 | 0.29 |
| Pyruvate Fermentation to Lactate | 2.96 | 0.20 |
| NGF Signaling | 2.85 | 0.04 |
| RhoGDI Signaling | 2.85 | 0.03 |
| Phospholipase C Signaling | 2.79 | 0.03 |
| Renal Cell Carcinoma Signaling | 2.73 | 0.05 |
| Calcium Signaling | 2.65 | 0.03 |
| Cellular Effects of Sildenafil (Viagra) | 2.45 | 0.03 |
| Role of IL-17F in Allergic Inflammatory Airway Diseases | 2.44 | 0.06 |
| Melanocyte Development and Pigmentation Signaling | 2.43 | 0.04 |
| PAK Signaling | 2.38 | 0.04 |
| α-Adrenergic Signaling | 2.28 | 0.04 |
| CNTF Signaling | 2.28 | 0.05 |
| Cardiac Hypertrophy Signaling | 2.17 | 0.02 |
| HGF Signaling | 2.17 | 0.04 |

| | | |
|---|---|---|
| Role of IL-17A in Arthritis | 2.09 | 0.05 |
| PPARα/RXRα Activation | 2.05 | 0.03 |
| Sertoli Cell-Sertoli Cell Junction Signaling | 2.05 | 0.03 |
| Gα12/13 Signaling | 2.01 | 0.03 |

### *Deregulated pathways in JAK2V617F ET vs Controls*

List of the significantly deregulated pathways in ET vs controls (p-value < 0.01) ordered in decreasing –log p-value according to *IPA* results. P-value represents the proportion of deregulated proteins from the MS analysis that belong to that pathway. Ratio is made between the number of deregulated proteins and the total number of proteins in that pathway.

| **Ingenuity Canonical Pathways** | **-log(p-value)** | **Ratio** |
|---|---|---|
| Actin Cytoskeleton Signaling | 15.80 | 0.10 |
| Integrin Signaling | 9.41 | 0.08 |
| VEGF Signaling | 8.17 | 0.11 |
| Regulation of Actin-based Motility by Rho | 7.77 | 0.11 |
| ILK Signaling | 7.67 | 0.07 |
| RhoA Signaling | 7.65 | 0.10 |
| RAN Signaling | 7.50 | 0.25 |
| Sertoli Cell-Sertoli Cell Junction Signaling | 7.12 | 0.07 |
| Signaling by Rho Family GTPases | 6.74 | 0.06 |
| Germ Cell-Sertoli Cell Junction Signaling | 6.70 | 0.07 |
| Rac Signaling | 6.61 | 0.08 |
| RhoGDI Signaling | 6.40 | 0.06 |
| Tight Junction Signaling | 6.18 | 0.07 |
| Clathrin-mediated Endocytosis Signaling | 5.92 | 0.06 |
| α-Adrenergic Signaling | 5.91 | 0.09 |
| Protein Kinase A Signaling | 5.83 | 0.04 |
| Coagulation System | 5.71 | 0.16 |
| Cellular Effects of Sildenafil (Viagra) | 5.43 | 0.07 |
| Mechanisms of Viral Exit from Host Cells | 5.28 | 0.13 |
| FAK Signaling | 5.21 | 0.08 |
| NRF2-mediated Oxidative Stress Response | 5.20 | 0.06 |
| Fcγ Receptor-mediated Phagocytosis in Macrophages and Monocytes | 4.96 | 0.08 |
| Paxillin Signaling | 4.83 | 0.07 |
| Caveolar-mediated Endocytosis Signaling | 4.67 | 0.08 |
| Acute Phase Response Signaling | 4.66 | 0.06 |
| Extrinsic Prothrombin Activation Pathway | 4.59 | 0.20 |
| Pyruvate Fermentation to Lactate | 4.32 | 0.30 |
| Virus Entry via Endocytic Pathways | 4.00 | 0.07 |
| Gap Junction Signaling | 3.93 | 0.05 |
| Cdc42 Signaling | 3.90 | 0.05 |
| Gluconeogenesis I | 3.83 | 0.10 |
| Intrinsic Prothrombin Activation Pathway | 3.59 | 0.11 |
| Crosstalk between Dendritic Cells and Natural Killer Cells | 3.35 | 0.06 |
| Axonal Guidance Signaling | 3.30 | 0.03 |
| PAK Signaling | 3.29 | 0.06 |
| Glycogen Degradation II | 3.24 | 0.19 |

| | | |
|---|---|---|
| Ephrin Receptor Signaling | 3.12 | 0.04 |
| Glucocorticoid Receptor Signaling | 3.09 | 0.03 |
| Protein Ubiquitination Pathway | 3.09 | 0.04 |
| Glycogen Degradation III | 3.07 | 0.17 |
| Leukocyte Extravasation Signaling | 2.98 | 0.04 |
| Regulation of eIF4 and p70S6K Signaling | 2.98 | 0.04 |
| AMPK Signaling | 2.91 | 0.04 |
| Glycolysis I | 2.90 | 0.09 |
| BMP signaling pathway | 2.88 | 0.06 |
| Role of Tissue Factor in Cancer | 2.85 | 0.05 |
| Breast Cancer Regulation by Stathmin1 | 2.79 | 0.04 |
| D-myo-inositol-5-phosphate Metabolism | 2.79 | 0.08 |
| Melatonin Signaling | 2.78 | 0.06 |
| Neuroprotective Role of THOP1 in Alzheimer's Disease | 2.75 | 0.07 |
| Leptin Signaling in Obesity | 2.73 | 0.06 |
| PRPP Biosynthesis I | 2.73 | 0.29 |
| EIF2 Signaling | 2.63 | 0.03 |
| Corticotropin Releasing Hormone Signaling | 2.60 | 0.04 |
| CD27 Signaling in Lymphocytes | 2.59 | 0.07 |
| Thioredoxin Pathway | 2.59 | 0.25 |
| Melanocyte Development and Pigmentation Signaling | 2.54 | 0.05 |
| Actin Nucleation by ARP-WASP Complex | 2.50 | 0.06 |
| PPARα/RXRα Activation | 2.47 | 0.04 |
| CDK5 Signaling | 2.43 | 0.05 |
| D-myo-inositol (1,4,5,6)-Tetrakisphosphate Biosynthesis | 2.38 | 0.09 |
| D-myo-inositol (3,4,5,6)-tetrakisphosphate Biosynthesis | 2.38 | 0.09 |
| Sonic Hedgehog Signaling | 2.38 | 0.09 |
| Insulin Receptor Signaling | 2.37 | 0.04 |
| Cardiac Hypertrophy Signaling | 2.36 | 0.03 |
| Calcium Signaling | 2.33 | 0.03 |
| ERK/MAPK Signaling | 2.30 | 0.03 |
| IGF-1 Signaling | 2.30 | 0.05 |
| 3-phosphoinositide Biosynthesis | 2.28 | 0.06 |
| Colorectal Cancer Metastasis Signaling | 2.22 | 0.03 |
| Glycogen Biosynthesis II (from UDP-D-Glucose) | 2.11 | 0.17 |
| fMLP Signaling in Neutrophils | 2.06 | 0.04 |
| Gα12/13 Signaling | 2.04 | 0.04 |
| Chemokine Signaling | 2.03 | 0.05 |
| Ephrin B Signaling | 2.01 | 0.05 |

### *Deregulated pathways in JAK2V617F PV vs JAK2V617F ET*

List of the significantly deregulated pathways in PV vs ET (p-value < 0.01) ordered in decreasing –log p-value according to *IPA* results. P-value represents the proportion of deregulated proteins from the MS analysis that belong to that pathway. Ratio is made between the number of deregulated proteins and the total number of proteins in that pathway.

| Ingenuity Canonical Pathways | -log(p-value) | Ratio |
|---|---|---|
| Actin Cytoskeleton Signaling | 15.50 | 0.09 |
| RhoGDI Signaling | 9.74 | 0.08 |
| RhoA Signaling | 9.17 | 0.11 |
| Signaling by Rho Family GTPases | 9.01 | 0.06 |
| Integrin Signaling | 8.98 | 0.07 |
| Fcγ Receptor-mediated Phagocytosis in Macrophages and Monocytes | 8.47 | 0.11 |
| Rac Signaling | 8.04 | 0.09 |
| RAN Signaling | 7.73 | 0.25 |
| Regulation of Actin-based Motility by Rho | 6.97 | 0.10 |
| Protein Ubiquitination Pathway | 6.39 | 0.05 |
| VEGF Signaling | 6.34 | 0.09 |
| FAK Signaling | 5.49 | 0.08 |
| ILK Signaling | 5.47 | 0.06 |
| Germ Cell-Sertoli Cell Junction Signaling | 5.29 | 0.06 |
| Paxillin Signaling | 5.10 | 0.07 |
| Sertoli Cell-Sertoli Cell Junction Signaling | 4.92 | 0.05 |
| Tight Junction Signaling | 4.75 | 0.06 |
| NRF2-mediated Oxidative Stress Response | 4.74 | 0.05 |
| Leukocyte Extravasation Signaling | 4.72 | 0.05 |
| Clathrin-mediated Endocytosis Signaling | 4.66 | 0.05 |
| Pyruvate Fermentation to Lactate | 4.43 | 0.30 |
| Mechanisms of Viral Exit from Host Cells | 4.26 | 0.11 |
| Virus Entry via Endocytic Pathways | 4.24 | 0.07 |
| Cdc42 Signaling | 4.16 | 0.05 |
| Ephrin Receptor Signaling | 4.12 | 0.05 |
| Regulation of eIF4 and p70S6K Signaling | 3.98 | 0.05 |
| Breast Cancer Regulation by Stathmin1 | 3.72 | 0.04 |
| Actin Nucleation by ARP-WASP Complex | 3.63 | 0.08 |
| Gap Junction Signaling | 3.46 | 0.05 |
| α-Adrenergic Signaling | 3.34 | 0.06 |
| Ephrin B Signaling | 3.00 | 0.06 |
| Caveolar-mediated Endocytosis Signaling | 2.97 | 0.06 |
| fMLP Signaling in Neutrophils | 2.96 | 0.05 |
| D-myo-inositol-5-phosphate Metabolism | 2.93 | 0.08 |
| CD28 Signaling in T Helper Cells | 2.85 | 0.05 |
| EIF2 Signaling | 2.84 | 0.03 |
| PRPP Biosynthesis I | 2.81 | 0.29 |
| Adenosine Nucleotides Degradation II | 2.78 | 0.12 |
| CD27 Signaling in Lymphocytes | 2.72 | 0.07 |
| Protein Kinase A Signaling | 2.69 | 0.03 |
| Crosstalk between Dendritic Cells and Natural Killer Cells | 2.68 | 0.05 |
| Thioredoxin Pathway | 2.67 | 0.25 |
| PAK Signaling | 2.64 | 0.05 |
| Axonal Guidance Signaling | 2.60 | 0.03 |
| CDK5 Signaling | 2.60 | 0.05 |
| ERK/MAPK Signaling | 2.50 | 0.03 |
| D-myo-inositol (1,4,5,6)-Tetrakisphosphate Biosynthesis | 2.49 | 0.09 |
| D-myo-inositol (3,4,5,6)-tetrakisphosphate Biosynthesis | 2.49 | 0.09 |

| | | |
|---|---|---|
| 3-phosphoinositide Biosynthesis | 2.41 | 0.06 |
| AMPK Signaling | 2.41 | 0.04 |
| Role of Tissue Factor in Cancer | 2.28 | 0.04 |
| Agrin Interactions at Neuromuscular Junction | 2.25 | 0.06 |
| Glucocorticoid Receptor Signaling | 2.21 | 0.03 |
| BMP signaling pathway | 2.18 | 0.05 |
| Glycogen Biosynthesis II (from UDP-D-Glucose) | 2.18 | 0.17 |
| Chemokine Signaling | 2.16 | 0.05 |
| PTEN Signaling | 2.13 | 0.04 |
| Adenine and Adenosine Salvage III | 2.11 | 0.13 |
| Melatonin Signaling | 2.10 | 0.05 |
| Corticotropin Releasing Hormone Signaling | 2.07 | 0.04 |
| Leptin Signaling in Obesity | 2.06 | 0.05 |
| Purine Ribonucleosides Degradation to Ribose-1-phosphate | 2.05 | 0.12 |
| PI3K/AKT Signaling | 2.00 | 0.03 |

### *Deregulated pathways in JAK2V617F PV vs JAK2(-) ET*

List of the significantly deregulated pathways in PV vs Mut0 (p-value < 0.01) ordered in decreasing –log p-value according to *IPA* results. P-value represents the proportion of deregulated proteins from the MS analysis that belong to that pathway. Ratio is made between the number of deregulated proteins and the total number of proteins in that pathway.

| **Ingenuity Canonical Pathways** | **-log(p-value)** | **Ratio** |
|---|---|---|
| RAN Signaling | 9.33 | 0.29 |
| Actin Cytoskeleton Signaling | 8.94 | 0.07 |
| Protein Ubiquitination Pathway | 7.81 | 0.06 |
| Rac Signaling | 5.73 | 0.07 |
| Regulation of Actin-based Motility by Rho | 5.68 | 0.09 |
| ILK Signaling | 5.25 | 0.06 |
| RhoGDI Signaling | 4.85 | 0.05 |
| RhoA Signaling | 4.78 | 0.07 |
| Protein Kinase A Signaling | 4.74 | 0.04 |
| Tight Junction Signaling | 4.57 | 0.06 |
| Signaling by Rho Family GTPases | 4.56 | 0.04 |
| Pyruvate Fermentation to Lactate | 4.36 | 0.30 |
| PAK Signaling | 4.28 | 0.07 |
| Breast Cancer Regulation by Stathmin1 | 4.27 | 0.05 |
| α-Adrenergic Signaling | 4.10 | 0.07 |
| Regulation of eIF4 and p70S6K Signaling | 3.82 | 0.05 |
| AMPK Signaling | 3.74 | 0.05 |
| Integrin Signaling | 3.65 | 0.04 |
| CDK5 Signaling | 3.32 | 0.06 |
| Sertoli Cell-Sertoli Cell Junction Signaling | 3.22 | 0.04 |
| Cdc42 Signaling | 3.21 | 0.04 |
| IGF-1 Signaling | 3.15 | 0.06 |
| Cellular Effects of Sildenafil (Viagra) | 3.10 | 0.05 |

| | | |
|---|---|---|
| Mechanisms of Viral Exit from Host Cells | 3.04 | 0.09 |
| ERK/MAPK Signaling | 3.01 | 0.04 |
| BMP signaling pathway | 2.95 | 0.06 |
| Axonal Guidance Signaling | 2.91 | 0.03 |
| Ephrin B Signaling | 2.89 | 0.06 |
| D-myo-inositol-5-phosphate Metabolism | 2.84 | 0.08 |
| Melatonin Signaling | 2.84 | 0.06 |
| Gα12/13 Signaling | 2.83 | 0.05 |
| Neuroprotective Role of THOP1 in Alzheimer's Disease | 2.81 | 0.07 |
| Germ Cell-Sertoli Cell Junction Signaling | 2.79 | 0.04 |
| Leptin Signaling in Obesity | 2.79 | 0.06 |
| PRPP Biosynthesis I | 2.76 | 0.29 |
| EIF2 Signaling | 2.71 | 0.03 |
| Corticotropin Releasing Hormone Signaling | 2.68 | 0.04 |
| CD27 Signaling in Lymphocytes | 2.64 | 0.07 |
| Thioredoxin Pathway | 2.62 | 0.25 |
| Melanocyte Development and Pigmentation Signaling | 2.60 | 0.05 |
| Ephrin Receptor Signaling | 2.55 | 0.04 |
| PPARα/RXRα Activation | 2.55 | 0.04 |
| GNRH Signaling | 2.50 | 0.04 |
| VEGF Signaling | 2.48 | 0.05 |
| Cardiac Hypertrophy Signaling | 2.45 | 0.03 |
| Insulin Receptor Signaling | 2.44 | 0.04 |
| NRF2-mediated Oxidative Stress Response | 2.44 | 0.04 |
| D-myo-inositol (1,4,5,6)-Tetrakisphosphate Biosynthesis | 2.42 | 0.09 |
| D-myo-inositol (3,4,5,6)-tetrakisphosphate Biosynthesis | 2.42 | 0.09 |
| Sonic Hedgehog Signaling | 2.42 | 0.09 |
| Virus Entry via Endocytic Pathways | 2.42 | 0.05 |
| Clathrin-mediated Endocytosis Signaling | 2.39 | 0.04 |
| 3-phosphoinositide Biosynthesis | 2.33 | 0.06 |
| Colorectal Cancer Metastasis Signaling | 2.30 | 0.03 |
| Chemokine Signaling | 2.08 | 0.05 |
| PTEN Signaling | 2.04 | 0.04 |
| Renin-Angiotensin Signaling | 2.04 | 0.04 |
| Gap Junction Signaling | 2.00 | 0.03 |

### *Deregulated pathways in JAK2V617F ET vs JAK2(-) ET*

List of the significantly deregulated pathways in ET vs Mut0 (p-value < 0.01) ordered in decreasing –log p-value according to *IPA* results. P-value represents the proportion of deregulated proteins from the MS analysis that belong to that pathway. Ratio is made between the number of deregulated proteins and the total number of proteins in that pathway.

| **Ingenuity Canonical Pathways** | **-log(p-value)** | **Ratio** |
|---|---|---|
| PRPP Biosynthesis I | 4.09 | 0.29 |
| Role of PKR in Interferon Induction and Antiviral Response | 3.94 | 0.07 |
| Parkinson's Signaling | 3.19 | 0.13 |

| | | |
|---|---|---|
| Endoplasmic Reticulum Stress Pathway | 3.09 | 0.11 |
| Tumoricidal Function of Hepatic Natural Killer Cells | 2.84 | 0.08 |
| TWEAK Signaling | 2.56 | 0.05 |
| TNFR1 Signaling | 2.26 | 0.04 |
| Cytotoxic T Lymphocyte-mediated Apoptosis of Target Cells | 2.16 | 0.02 |
| Death Receptor Signaling | 2.08 | 0.03 |
| Myc Mediated Apoptosis Signaling | 2.08 | 0.03 |
| Induction of Apoptosis by HIV1 | 2.07 | 0.03 |
| Retinoic acid Mediated Apoptosis Signaling | 2.03 | 0.03 |

## Supplemental Data I-3

**A**

| | IQGAP1/ actin means | Standard Deviation | N |
|---|---|---|---|
| **PV** | 48.07 | 39.92 | 15 |
| **ET** | 33.35 | 33.95 | 14 |
| **Control set** | 5.76 | 4.70 | 10 |

| T-test analysis | p-value | |
|---|---|---|
| PV vs ET | 0.3030 | |
| PV vs control set | 0.0032 | * |
| ET vs control set | 0.0188 | * |
| ET+PV vs control set | 0.0057 | * |
| Retrospective (PV+ET) vs control set | 0.0313 | * |
| Prospective (PV+ET) vs control set | 0.0012 | * |

**B**

| | IQGAP1/ actin means | Standard Deviation | N |
|---|---|---|---|
| ***JAK2+*** | 32.69 | 30.26 | 25 |
| ***JAK2-*** | 88.78 | 42.35 | 4 |
| **Control set** | 5.76 | 4.70 | 10 |

| T-test analysis | p-value | |
|---|---|---|
| *JAK2+* vs *JAK2-* | 0.0310 | * |
| *JAK2+* vs Control set | 0.0091 | * |
| *JAK2-* vs Control set | 0.0001 | * |

**Supplemental Data I-3.** IQGAP1/ß-actin ratios, means and T-test assays. **A)** It shows IQGAP1/ ß-actin ratios derived from western blot assays in MPNs and control patients which correspond to figure 1. First table contains information about IQGAP1/ß-actin ratio means. standard deviations and number of subjects (N). Second table shows the p-value of student's t test analysis. **B)** IQGAP1/ß-actin ratio means and T-test assays according to patients' genotype. First table contains information about IQGAP1/ß-actin ratio means. standard deviations and number of subjects (N). Second table shows the p-value of student's t test analysis. Patients: Retrospective set: PV1. PV2. PV3. PV4. PV5. PV6 and ET1. ET2. ET3. ET5. ET6 and ET7. Prospective set: *JAK2+*: PV8. PV9. PV10. PV11. PV12. PV13. PV14. ET9. ET10. ET12. ET13. *JAK2-*: ET8. ET11. ET14 and PV15. Control set: C1. C2. C3. C4. C5. C6. C7. C8. C9. and C10.

## Supplemental Data I-4

| | Calreticulin/ actin means | Standard Deviation | N |
|---|---|---|---|
| **PV** | 15.07 | 23.32 | 8 |
| **ET** | 4.15 | 4.57 | 7 |
| **MPNs (PV+ET)** | 9.97 | 17.68 | 15 |
| **Calreticulin+ set** | 16.77 | 14.93 | 6 |
| **Control set** | 11.51 | 9.75 | 10 |
| ***JAK2+*** | 13.10 | 19.93 | 11 |
| ***JAK2-*** | 1.37 | 1.04 | 4 |

| T-test analysis | p-value |
|---|---|
| Calreticulin+ vs Control set | 0.4053 |
| Calreticulin+ vs *JAK2+* | 0.7005 |
| Calreticulin+ vs *JAK2-* | 0.0782 |
| Control vs *JAK2-* | 0.0655 |
| Control vs *JAK2+* | 0.8215 |
| *JAK2+* vs *JAK2-* | 0.2709 |
| PV vs ET | 0.2469 |
| MPNs (PV+ET) vs control | 0.8051 |
| Calreticulin+ vs PV | 0.8790 |
| Calreticulin+ vs ET | 0.0560 |
| Calreticulin+ vs MPNs | 0.4184 |

**Supplemental Data I-4.** Calreticulin/ß-actin ratios, means and T-test assays. First table contains information about Calreticulin/ß-actin ratio means. standard deviations and number of subjects (N). Second table shows the p-value of student's t test analysis. Patients: *JAK2+*: Prospective set: PV8. PV9. PV10. PV11. PV12. PV13. PV14. ET9. ET10. ET12. ET13. *JAK2-*: Prospective set: ET8. ET11. ET14 and PV15. Calreticulin+ set: Calr1. Calr2. Calr3. Calr4. Calr5 and Calr6. Control set: C1. C2. C3. C4. C5. C6. C7. C8. C9. and C10.

## Supplemental Data I-5

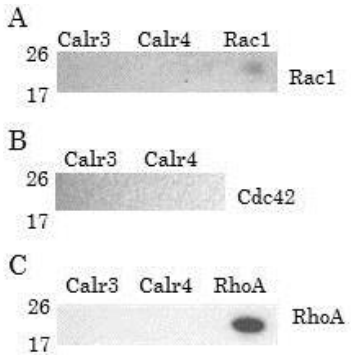


**Supplemental Data I-5.** Pull-down assays of activated proteins of the Rho family. RBC lysates were pulled-down with GST-PAK-PBD or GST-Rhotekin-RBD agarose beads. WBs were developed with Rac1 **(A)**. Cdc42 **(B)** and RhoA **(C)** antibodies. Rac1 and RhoA act as positive controls. Patients: Calreticulin set: Calr3 and Calr4. Molecular weights of targeted proteins: Rac1 21 kDa. Cdc42 21 kDa and RhoA 22kDa.

## Supplemental Data I-6

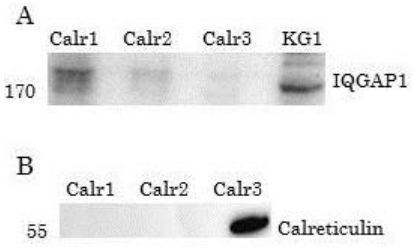


**Supplemental Data I-6.** GTP-Rac1 complexes. Rac1Q61L-GST coupled to Sepharose beads were used to pull-down proteins in *CALR* mutated RBC lysates. **A)** IQGAP1-Rac1 complex was present in all samples. **B)** Calreticulin doesn't form a complex with Rac1-GTP in calreticulin set patients. Patients: Calreticulin+ samples Calr1. Calr2. Calr3. Molecular weights of targeted proteins: IQGAP1 189 kDa. Calreticulin 52 kDa. KG1 was used as positive control.

# SUPPLEMENTAL DATA II

## Supplemental Data II-1

Lists of deregulated proteins in granulocytes among the different subgroups PV, ET, PMF (all *JAK2(+))* and Mut0 (*JAK2(-)* ET and PMF).

### *PV vs Mut0 (JAK2(-) ET and PMF) comparison*

| Protein group | Protein description | Ratio | p-value |
|---|---|---|---|
| REEP5_HUMAN | Receptor expression-enhancing protein 5 | 0.74 | 3.20E-02 |
| LEG10_HUMAN | Galectin-10 | 0.77 | 3.67E-13 |
| ANXA2_HUMAN | Annexin A2 | 0.77 | 3.83E-02 |
| CAP7_HUMAN | Azurocidin | 0.77 | 9.38E-06 |
| EVI2B_HUMAN | Protein EVI2B (CD antigen CD361) | 0.79 | 8.33E-03 |
| LEG1_HUMAN | Galectin-1 | 0.80 | 3.58E-03 |
| CAZA1_HUMAN | F-actin-capping protein subunit alpha-1 | 0.83 | 3.78E-07 |
| B4DV10_HUMAN | cDNA FLJ59142. highly similar to Epididymal secretory protein E1 | 0.84 | 2.75E-03 |
| D3DPU2_HUMAN | Adenylyl cyclase-associated protein | 0.84 | 1.13E-02 |
| BPI_HUMAN | Bactericidal permeability-increasing protein | 0.84 | 1.75E-18 |
| PYGL_HUMAN | Glycogen phosphorylase. liver form | 0.84 | 1.21E-13 |
| COTL1_HUMAN | Coactosin-like protein | 0.84 | 6.85E-03 |
| S10A4_HUMAN | Protein S100-A4 (Calvasculin) | 0.84 | 6.63E-04 |
| B4DVJ0_HUMAN | Glucose-6-phosphate isomerase | 0.85 | 1.35E-02 |
| H2B1O_HUMAN | Histone H2B type 1-O | 0.85 | 2.82E-02 |
| OSTF1_HUMAN | Osteoclast-stimulating factor 1 | 0.85 | 1.46E-02 |
| GDIR2_HUMAN | Rho GDP-dissociation inhibitor 2 | 0.86 | 2.99E-06 |
| MYH9_HUMAN | Myosin-9 | 0.87 | 1.25E-23 |
| ARC1B_HUMAN | Actin-related protein 2/3 complex subunit 1B | 0.87 | 1.44E-02 |
| RB11B_HUMAN | Ras-related protein Rab-11B | 0.88 | 5.96E-04 |
| B2RDE1_HUMAN | cDNA. FLJ96568. highly similar to Homo sapiens tropomyosin 3 | 0.89 | 2.18E-03 |
| TYPH_HUMAN | Thymidine phosphorylase | 0.89 | 2.44E-02 |
| ENOB_HUMAN | Beta-enolase | 0.89 | 1.27E-07 |
| 1433B_HUMAN | 14-3-3 protein beta/alpha | 0.89 | 1.36E-03 |
| COF1_HUMAN | Cofilin-1 | 0.90 | 1.91E-05 |
| S10AC_HUMAN | Protein S100-A12 | 0.90 | 1.24E-07 |
| Q5U077_HUMAN | L-lactate dehydrogenase | 0.90 | 4.38E-02 |
| CATA_HUMAN | Catalase | 0.90 | 1.91E-08 |
| TALDO_HUMAN | Transaldolase | 0.91 | 1.92E-11 |
| Q6IAT1_HUMAN | Epididymis secretory sperm binding protein Li 46e (GDP dissociation inhibitor 2 isoform 1) | 0.92 | 1.72E-02 |
| ECP_HUMAN | Eosinophil cationic protein | 0.92 | 1.43E-02 |
| B2RDW1_HUMAN | Epididymis luminal protein 112 | 0.93 | 1.87E-02 |
| MNDA_HUMAN | Myeloid cell nuclear differentiation antigen | 0.93 | 4.19E-03 |
| PROF1_HUMAN | Profilin-1 | 0.93 | 5.95E-14 |

| | | | |
|---|---|---|---|
| ELNE_HUMAN | Neutrophil elastase | 0.93 | 2.23E-02 |
| Q53EM5_HUMAN | Transketolase | 0.93 | 4.46E-04 |
| G3P_HUMAN | Glyceraldehyde-3-phosphate dehydrogenase (GAPDH) | 0.94 | 4.80E-07 |
| ARP2_HUMAN | Actin-related protein 2 | 0.94 | 4.28E-03 |
| FLNA_HUMAN | Filamin-A | 0.94 | 5.60E-09 |
| PERM_HUMAN | Myeloperoxidase | 0.94 | 1.69E-03 |
| LKHA4_HUMAN | Leukotriene A-4 hydrolase | 0.94 | 4.92E-04 |
| RHOA_HUMAN | Transforming protein Rhoa | 0.94 | 1.55E-03 |
| A4QPB0_HUMAN | IQ motif containing GTPase activating protein 1 | 0.96 | 6.60E-03 |
| GELS_HUMAN | Gelsolin | 0.96 | 8.57E-03 |
| COR1A_HUMAN | Coronin-1A (Coronin-like protein A) | 0.97 | 2.48E-02 |
| TPIS_HUMAN | Triosephosphate isomerase | 0.97 | 2.24E-02 |
| ANXA3_HUMAN | Annexin A3 | 1.04 | 8.40E-03 |
| S10A8_HUMAN | Protein S100-A8 (Calgranulin-A) | 1.05 | 1.27E-05 |
| CAMP_HUMAN | Cathelicidin antimicrobial peptide | 1.08 | 1.91E-05 |
| NAMPT_HUMAN | Nicotinamide phosphoribosyltransferase | 1.08 | 1.90E-02 |
| GSTO1_HUMAN | Glutathione S-transferase omega-1 (GSTO-1) | 1.09 | 2.37E-03 |
| EFHD2_HUMAN | EF-hand domain-containing protein D2 | 1.10 | 1.85E-02 |
| PRG3_HUMAN | Proteoglycan 3 | 1.11 | 2.41E-04 |
| PRTN3_HUMAN | Myeloblastin | 1.12 | 2.52E-06 |
| HXK3_HUMAN | Hexokinase-3 | 1.12 | 3.77E-03 |
| PNCB_HUMAN | Nicotinate phosphoribosyltransferase (NAPRTase) | 1.12 | 2.19E-02 |
| CATD_HUMAN | Cathepsin D | 1.13 | 5.53E-03 |
| HS71A_HUMAN | Heat shock 70 kDa protein 1A | 1.13 | 3.13E-03 |
| CH3L1_HUMAN | Chitinase-3-like protein 1 | 1.14 | 1.09E-03 |
| B3KSM6_HUMAN | cDNA FLJ36606 fis. clone TRACH2015654. highly similar to HEAT SHOCK 70 kDa PROTEIN 6 | 1.14 | 1.40E-02 |
| ACSL1_HUMAN | Long-chain-fatty-acid--CoA ligase 1 | 1.15 | 2.72E-03 |
| Q5CAQ5_HUMAN | Tumor rejection antigen (Gp96) 1 | 1.16 | 5.75E-03 |
| BLVRB_HUMAN | Flavin reductase (NADPH) | 1.18 | 1.49E-04 |
| OLFM4_HUMAN | Olfactomedin-4 | 1.21 | 1.11E-05 |
| GRP78_HUMAN | 78 kDa glucose-regulated protein | 1.22 | 1.09E-15 |
| RETN_HUMAN | Resistin | 1.22 | 6.79E-12 |
| CAH1_HUMAN | Carbonic anhydrase 1 | 1.22 | 1.75E-05 |
| A8K9E4_HUMAN | cDNA FLJ76459. highly similar to Homo sapiens matrix metallopeptidase 8 (neutrophil collagenase) | 1.24 | 7.09E-20 |
| MMP9_HUMAN | Matrix metalloproteinase-9] | 1.26 | 4.75E-13 |
| CALR_HUMAN | Calreticulin (CRP55) (Calregulin) | 1.29 | 4.12E-07 |
| CD44_HUMAN | CD44 antigen (CD antigen CD44) | 1.30 | 1.95E-02 |
| MARCS_HUMAN | Myristoylated alanine-rich C-kinase substrate | 1.32 | 1.12E-02 |
| MCEM1_HUMAN | Mast cell-expressed membrane protein 1 | 1.33 | 1.20E-03 |
| NIBAN_HUMAN | Protein Niban | 1.34 | 5.31E-04 |
| MVP_HUMAN | Major vault protein | 1.38 | 5.02E-04 |
| VAMP8_HUMAN | Vesicle-associated membrane protein 8 | 1.56 | 4.01E-02 |

### *ET vs Mut0 (JAK2(-) ET and PMF) comparison*

| Protein group | Protein description | Ratio | p-value |
|---|---|---|---|
| FOLR3_HUMAN | Folate receptor gamma | 0.36 | 2.66E-05 |
| ITAM_HUMAN | Integrin. alpha M | 0.62 | 1.68E-03 |
| TPM1_HUMAN | Tropomyosin alpha-1 chain | 0.73 | 7.97E-04 |
| RAC2_HUMAN | Ras-related C3 botulinum toxin substrate 2 | 0.74 | 1.47E-02 |

| | | | |
|---|---|---|---|
| B4DVJ0_HUMAN | Glucose-6-phosphate isomerase | 0.76 | 1.37E-02 |
| FCN1_HUMAN | Ficolin-1 | 0.77 | 8.07E-03 |
| LEG10_HUMAN | Galectin-10 | 0.78 | 1.76E-15 |
| B4DV10_HUMAN | cDNA FLJ59142. highly similar to Epididymal secretory protein E1 | 0.79 | 1.33E-03 |
| CAZA1_HUMAN | F-actin-capping protein subunit alpha-1 | 0.80 | 2.53E-05 |
| ARC1B_HUMAN | Actin-related protein 2/3 complex subunit 1B | 0.80 | 7.04E-04 |
| EVI2B_HUMAN | Protein EVI2B (CD antigen CD361) | 0.81 | 4.41E-03 |
| CATG_HUMAN | Cathepsin G | 0.81 | 4.14E-12 |
| BPI_HUMAN | Bactericidal permeability-increasing protein | 0.81 | 4.34E-13 |
| PERE_HUMAN | Eosinophil peroxidase (EPO) | 0.83 | 2.92E-05 |
| RHOG_HUMAN | Rho-related GTP-binding protein RhoG | 0.85 | 7.95E-03 |
| TCPB_HUMAN | T-complex protein 1 subunit beta | 0.86 | 1.47E-04 |
| B2RDE1_HUMAN | cDNA. FLJ96568. highly similar to Homo sapiens tropomyosin 3 | 0.87 | 3.78E-04 |
| Q53GC7_HUMAN | Capping protein | 0.87 | 6.38E-03 |
| LOX15_HUMAN | Arachidonate 15-lipoxygenase | 0.88 | 1.80E-03 |
| CAP7_HUMAN | Azurocidin | 0.88 | 8.23E-05 |
| B2RDW0_HUMAN | cDNA. FLJ96792. highly similar to Homo sapiens calmodulin 2 | 0.88 | 3.89E-04 |
| CBX3_HUMAN | Chromobox protein homolog 3 | 0.88 | 2.75E-02 |
| ARPC2_HUMAN | Actin-related protein 2/3 complex subunit 2 | 0.89 | 1.14E-03 |
| CATD_HUMAN | Cathepsin D | 0.89 | 3.59E-03 |
| TCPE_HUMAN | T-complex protein 1 subunit epsilon | 0.89 | 3.06E-02 |
| PRS8_HUMAN | 26S protease regulatory subunit 8 | 0.90 | 5.00E-02 |
| HXK3_HUMAN | Hexokinase-3 ( | 0.90 | 2.68E-07 |
| ARP2_HUMAN | Actin-related protein 2 | 0.91 | 1.98E-07 |
| S10AC_HUMAN | Protein S100-A12 | 0.91 | 5.61E-06 |
| 1433B_HUMAN | 14-3-3 protein beta/alpha | 0.91 | 1.83E-02 |
| B2RBR9_HUMAN | cDNA. FLJ95650. highly similar to Homo sapiens karyopherin (importin) beta 1 | 0.91 | 7.65E-04 |
| CAN1_HUMAN | Calpain-1 catalytic subunit | 0.91 | 2.74E-03 |
| ILEU_HUMAN | Leukocyte elastase inhibitor | 0.92 | 7.49E-03 |
| ARP3_HUMAN | Actin-related protein 3 | 0.92 | 3.88E-04 |
| RAN_HUMAN | GTP-binding nuclear protein Ran | 0.92 | 2.21E-04 |
| HS90A_HUMAN | Heat shock protein HSP 90-alpha ( | 0.92 | 3.93E-04 |
| URP2_HUMAN | Fermitin family homolog 3 | 0.92 | 2.44E-02 |
| ATPB_HUMAN | ATP synthase subunit beta | 0.92 | 7.66E-04 |
| PYGL_HUMAN | Glycogen phosphorylase. liver form | 0.92 | 3.03E-03 |
| ATPA_HUMAN | ATP synthase subunit alpha. mitochondrial | 0.92 | 1.50E-02 |
| Q53EM5_HUMAN | Transketolase | 0.92 | 6.35E-04 |
| B4DMA2_HUMAN | cDNA FLJ54023. highly similar to Heat shock protein HSP 90-beta | 0.93 | 8.29E-04 |
| MYO1F_HUMAN | Unconventional myosin-If | 0.93 | 3.91E-04 |
| GDIR2_HUMAN | Rho GDP-dissociation inhibitor 2 | 0.93 | 4.90E-03 |
| B4DZT3_HUMAN | cDNA FLJ50934. highly similar to Lamin-B1 | 0.93 | 1.94E-01 |
| GSTP1_HUMAN | Glutathione S-transferase P | 0.94 | 9.37E-04 |
| COF1_HUMAN | Cofilin-1 | 0.94 | 6.92E-03 |
| CALX_HUMAN | Calnexin | 0.94 | 9.13E-03 |
| G3P_HUMAN | Glyceraldehyde-3-phosphate dehydrogenase (GAPDH) | 0.94 | 6.15E-07 |
| FLNA_HUMAN | Filamin-A | 0.94 | 7.10E-09 |
| EF1D_HUMAN | Elongation factor 1-delta | 0.95 | 1.31E-01 |

| | | | |
|---|---|---|---|
| PGK1_HUMAN | Phosphoglycerate kinase 1 | 0.95 | 1.15E-06 |
| PERM_HUMAN | Myeloperoxidase | 0.96 | 8.32E-03 |
| PLSL_HUMAN | Plastin-2 | 0.96 | 5.21E-06 |
| RNAS2_HUMAN | Non-secretory ribonuclease | 0.96 | 9.37E-03 |
| CATA_HUMAN | Catalase | 0.97 | 1.63E-01 |
| PDIA1_HUMAN | Protein disulfide-isomerase ( | 0.99 | 2.11E-01 |
| DOPD_HUMAN | D-dopachrome decarboxylase | 1.00 | 4.55E-03 |
| TLN1_HUMAN | Talin-1 | 1.06 | 2.55E-02 |
| MOES_HUMAN | Moesin | 1.06 | 5.21E-03 |
| ITB2_HUMAN | Integrin beta-2 (CD antigen CD18) | 1.06 | 7.19E-04 |
| RETN_HUMAN | Resistin | 1.07 | 1.75E-04 |
| H15_HUMAN | Histone H1.5 | 1.08 | 4.80E-05 |
| GRP78_HUMAN | 78 kDa glucose-regulated protein (GRP-78) | 1.09 | 1.69E-06 |
| ANXA1_HUMAN | Annexin A1 | 1.09 | 4.43E-09 |
| B2R4C5_HUMAN | Lysozyme | 1.10 | 6.45E-03 |
| APOBR_HUMAN | Apolipoprotein B receptor (Apolipoprotein B-100 ) | 1.12 | 1.17E-01 |
| ANXA3_HUMAN | Annexin A3 | 1.13 | 1.35E-05 |
| A8K9E4_HUMAN | cDNA FLJ76459. highly similar to Homo sapiens matrix metallopeptidase 8 | 1.13 | 6.84E-08 |
| Q5NKU1_HUMAN | Intercellular adhesion molecule 3 | 1.13 | 3.71E-03 |
| BST1_HUMAN | ADP-ribosyl cyclase/cyclic ADP-ribose hydrolase 2 (CD antigen CD157) | 1.13 | 3.92E-02 |
| S10A9_HUMAN | Protein S100-A9 (Calgranulin-B) | 1.13 | 1.45E-02 |
| TERA_HUMAN | Transitional endoplasmic reticulum ATPase | 1.14 | 5.00E-03 |
| 6PGL_HUMAN | 6-phosphogluconolactonase | 1.15 | 1.71E-02 |
| GILT_HUMAN | Gamma-interferon-inducible lysosomal thiol reductase | 1.15 | 6.42E-02 |
| D3DRP5_HUMAN | Chromosome 9 open reading frame 19 | 1.15 | 2.45E-06 |
| ITAM_HUMAN | Integrin alpha-M (CD antigen CD11b) | 1.15 | 1.32E-02 |
| ANXA5_HUMAN | Annexin A5 | 1.16 | 2.33E-04 |
| ACTN1_HUMAN | Alpha-actinin-1 | 1.16 | 1.27E-06 |
| PRTN3_HUMAN | Myeloblastin | 1.16 | 4.05E-22 |
| Q6FHM9_HUMAN | CD59 antigen | 1.17 | 9.85E-03 |
| QSOX1_HUMAN | Sulfhydryl oxidase 1 | 1.17 | 4.96E-03 |
| PSME2_HUMAN | Proteasome activator complex subunit 2 ( | 1.18 | 8.73E-03 |
| CAMP_HUMAN | Cathelicidin antimicrobial peptide | 1.20 | 1.45E-12 |
| Q5TD07_HUMAN | Ribosyldihydronicotinamide dehydrogenase | 1.23 | 1.84E-02 |
| A1AG1_HUMAN | Alpha-1-acid glycoprotein 1 | 1.25 | 1.12E-05 |
| MMP9_HUMAN | Matrix metalloproteinase-9 | 1.27 | 1.11E-08 |
| CALR_HUMAN | Calreticulin (Calregulin) | 1.28 | 9.85E-07 |
| CAH2_HUMAN | Carbonic anhydrase 2 | 1.28 | 6.40E-03 |
| B3AT_HUMAN | Band 3 anion transport protein (CD antigen CD233) | 1.31 | 2.17E-02 |
| BLVRB_HUMAN | Flavin reductase (NADPH) | 1.31 | 2.68E-06 |
| PRG3_HUMAN | Proteoglycan 3 | 1.32 | 7.72E-12 |
| HS71A_HUMAN | Heat shock 70 kDa protein 1A | 1.35 | 3.13E-04 |
| FCG3B_HUMAN | Low affinity immunoglobulin gamma Fc region receptor III-B (CD antigen CD16b) | 1.41 | 1.55E-02 |
| PRDX2_HUMAN | Peroxiredoxin-2 | 1.42 | 7.53E-08 |
| CAH1_HUMAN | Carbonic anhydrase 1 | 1.47 | 3.21E-11 |
| F189B_HUMAN | Protein FAM189B (Protein COTE1) | 1.60 | 3.78E-06 |

### *PMF vs Mut0 (JAK2(-) ET and PMF) comparison*

| Protein group | Protein description | Ratio | p value |
|---|---|---|---|
| FOLR3_HUMAN | Folate receptor gamma (FR-gamma) | 0.63 | 4.64E-04 |
| CAP7_HUMAN | Azurocidin (Cationic antimicrobial protein CAP37) | 0.65 | 3.91E-09 |
| ITA2B_HUMAN | Integrin alpha-IIb | 0.71 | 1.29E-02 |
| CATG_HUMAN | Cathepsin G | 0.74 | 1.32E-13 |
| PERM_HUMAN | Myeloperoxidase (MPO) | 0.80 | 2.53E-15 |
| ELNE_HUMAN | Neutrophil elastase | 0.81 | 3.14E-05 |
| AL5AP_HUMAN | Arachidonate 5-lipoxygenase-activating protein (FLAP) | 0.83 | 4.31E-04 |
| H2B1O_HUMAN | Histone H2B type 1-O | 0.84 | 3.53E-02 |
| Q5U077_HUMAN | L-lactate dehydrogenase | 0.85 | 5.52E-03 |
| RAC2_HUMAN | Ras-related C3 botulinum toxin substrate 2 | 0.85 | 3.86E-02 |
| D3DPE6_HUMAN | Wiskott-Aldrich syndrome protein interacting protein. isoform CRA_a | 0.86 | 2.47E-02 |
| VPS28_HUMAN | Vacuolar protein sorting-associated protein 28 homolog | 0.87 | 1.15E-02 |
| NDRG1_HUMAN | Protein NDRG1 | 0.88 | 3.51E-02 |
| Q4W4Y1_HUMAN | Dopamine receptor interacting protein 4 | 0.88 | 1.53E-04 |
| PYGL_HUMAN | Glycogen phosphorylase. liver form | 0.88 | 4.94E-14 |
| RHOG_HUMAN | Rho-related GTP-binding protein RhoG | 0.88 | 9.30E-05 |
| CHIT1_HUMAN | Chitotriosidase-1 | 0.89 | 8.45E-03 |
| CATS_HUMAN | Cathepsin S | 0.89 | 3.54E-02 |
| Q86VG2_HUMAN | Splicing factor proline/glutamine-rich | 0.89 | 2.33E-02 |
| ILEU_HUMAN | Leukocyte elastase inhibitor | 0.90 | 6.15E-04 |
| 1433B_HUMAN | 14-3-3 protein beta/alpha | 0.90 | 1.40E-03 |
| CAZA1_HUMAN | F-actin-capping protein subunit alpha-1 | 0.90 | 1.41E-05 |
| STK4_HUMAN | Serine/threonine-protein kinase 4 | 0.90 | 3.35E-02 |
| TCTP_HUMAN | Translationally-controlled tumor protein | 0.90 | 3.95E-02 |
| ITAM_HUMAN | Integrin alpha-M (CD11 antigen-like family member B) | 0.90 | 1.85E-02 |
| ODO2_HUMAN | Dihydrolipoyllysine-residue succinyltransferase component of 2-oxoglutarate dehydrogenase complex. mitochondrial | 0.91 | 4.29E-03 |
| GSTP1_HUMAN | Glutathione S-transferase P | 0.91 | 1.04E-07 |
| B3KRM8_HUMAN | Translin. isoform CRA_b | 0.91 | 1.02E-02 |
| B2R4C5_HUMAN | Lysozyme | 0.91 | 1.86E-17 |
| TWF2_HUMAN | Twinfilin-2 | 0.91 | 3.83E-02 |
| KAP0_HUMAN | cAMP-dependent protein kinase type I-alpha regulatory subunit | 0.91 | 4.57E-03 |
| D3DNA1_HUMAN | Integrin beta | 0.91 | 4.85E-02 |
| PRDX3_HUMAN | Thioredoxin-dependent peroxide reductase. mitochondrial | 0.92 | 2.18E-02 |
| B7Z5J7_HUMAN | cDNA FLJ58682. highly similar to Vesicle-fusing ATPase | 0.92 | 1.26E-03 |
| SPCS2_HUMAN | Signal peptidase complex subunit 2 | 0.92 | 7.14E-03 |
| B4DQY1_HUMAN | cDNA FLJ56133. highly similar to Serine/threonine-protein phosphatase 2A 65 kDa regulatory subunit A | 0.93 | 2.11E-03 |
| B2RDW1_HUMAN | Epididymis luminal protein 112 (Ribosomal protein S27a) | 0.93 | 1.05E-03 |
| GMFG_HUMAN | Glia maturation factor gamma (GMF-gamma) | 0.93 | 2.72E-03 |
| GSTO1_HUMAN | Glutathione S-transferase omega-1 | 0.93 | 4.37E-05 |
| GDIR2_HUMAN | Rho GDP-dissociation inhibitor 2 | 0.93 | 6.99E-04 |
| EHD1_HUMAN | EH domain-containing protein 1 | 0.93 | 1.02E-03 |

| | | | |
|---|---|---|---|
| RAB31_HUMAN | Ras-related protein Rab-31 | 0.93 | 4.26E-03 |
| STMN1_HUMAN | Stathmin (Leukemia-associated phosphoprotein p18) (Metablastin) | 0.94 | 2.17E-02 |
| CAMP_HUMAN | Cathelicidin antimicrobial peptide | 0.94 | 2.35E-11 |
| PARK7_HUMAN | Protein deglycase DJ-1 | 0.94 | 1.22E-02 |
| BPI_HUMAN | Bactericidal permeability-increasing protein | 0.94 | 9.34E-07 |
| LKHA4_HUMAN | Leukotriene A-4 hydrolase | 0.94 | 1.84E-04 |
| PYGB_HUMAN | Glycogen phosphorylase. brain form | 0.94 | 4.97E-03 |
| PRDX2_HUMAN | Peroxiredoxin-2 | 0.94 | 9.70E-03 |
| FLNA_HUMAN | Filamin-A | 0.94 | 3.01E-10 |
| Q05DH1_HUMAN | Proteasome subunit alpha type | 0.94 | 1.36E-02 |
| Q6IAT1_HUMAN | Epididymis secretory sperm binding protein Li 46e (GDP dissociation inhibitor 2 isoform 1) | 0.94 | 6.32E-03 |
| CATA_HUMAN | Catalase | 0.94 | 1.55E-06 |
| ARP2_HUMAN | Actin-related protein 2 | 0.94 | 4.52E-04 |
| GDIR1_HUMAN | Rho GDP-dissociation inhibitor 1 | 0.95 | 1.69E-03 |
| PERE_HUMAN | Eosinophil peroxidase (EPO) | 0.95 | 2.17E-02 |
| ANXA4_HUMAN | Annexin A4 | 0.95 | 3.30E-02 |
| MDHC_HUMAN | Malate dehydrogenase. cytoplasmic | 0.95 | 4.48E-02 |
| RAB35_HUMAN | Ras-related protein Rab-35 | 0.95 | 4.11E-03 |
| SURF4_HUMAN | Surfeit locus protein 4 | 0.95 | 2.56E-03 |
| Q59F54_HUMAN | Solute carrier family 2 | 0.95 | 4.51E-02 |
| 1433Z_HUMAN | 14-3-3 protein zeta/delta | 0.95 | 4.43E-02 |
| CAN1_HUMAN | Calpain-1 catalytic subunit | 0.96 | 2.50E-02 |
| B4DMA2_HUMAN | cDNA FLJ54023. highly similar to Heat shock protein HSP 90-beta | 0.96 | 3.53E-02 |
| ARPC5_HUMAN | Actin-related protein 2/3 complex subunit 5 | 0.96 | 2.59E-02 |
| TYPH_HUMAN | Thymidine phosphorylase | 0.96 | 2.08E-02 |
| A4D0U5_HUMAN | Testis derived transcript | 0.96 | 6.38E-03 |
| Q5TZP7_HUMAN | APEX nuclease (Multifunctional DNA repair enzyme) | 0.96 | 4.77E-02 |
| CAPG_HUMAN | Macrophage-capping protein | 0.96 | 2.09E-03 |
| B2RDE1_HUMAN | cDNA. FLJ96568. highly similar to Homo sapiens tropomyosin 3 | 0.96 | 4.84E-02 |
| PRTN3_HUMAN | Myeloblastin | 0.96 | 9.41E-07 |
| MYH9_HUMAN | Myosin-9 | 0.96 | 7.10E-10 |
| CH3L1_HUMAN | Chitinase-3-like protein 1 | 0.96 | 2.24E-02 |
| PA2G4_HUMAN | Proliferation-associated protein 2G4 | 0.96 | 4.21E-02 |
| ATPB_HUMAN | ATP synthase subunit beta. mitochondrial | 0.96 | 3.11E-02 |
| THIO_HUMAN | Thioredoxin | 0.97 | 8.32E-03 |
| ARLY_HUMAN | Argininosuccinate lyase | 0.97 | 1.05E-02 |
| S10AC_HUMAN | Protein S100-A12 | 0.97 | 1.34E-02 |
| SODC_HUMAN | Superoxide dismutase | 0.97 | 1.97E-02 |
| HSP7C_HUMAN | Heat shock cognate 71 kDa protein ( | 0.98 | 4.45E-02 |
| VSTM1_HUMAN | V-set and transmembrane domain-containing protein 1 | 0.98 | 3.49E-03 |
| SC22B_HUMAN | Vesicle-trafficking protein SEC22b | 0.98 | 3.24E-02 |
| VINC_HUMAN | Vinculin | 0.98 | 1.61E-02 |
| G3P_HUMAN | Glyceraldehyde-3-phosphate dehydrogenase (GAPDH) | 0.98 | 2.74E-03 |
| S10A8_HUMAN | Protein S100-A8 (Calgranulin-A) | 1.02 | 1.10E-02 |
| GSHR_HUMAN | Glutathione reductase. mitochondrial | 1.04 | 2.42E-02 |
| TLN1_HUMAN | Talin-1 | 1.06 | 1.29E-03 |
| ANXA1_HUMAN | Annexin A1 | 1.06 | 4.95E-05 |
| ANXA3_HUMAN | Annexin A3 | 1.06 | 2.00E-02 |

| | | | |
|---|---|---|---|
| PPIB_HUMAN | Peptidyl-prolyl cis-trans isomerase B | 1.06 | 6.03E-03 |
| S10A4_HUMAN | Protein S100-A4 (Calvasculin) | 1.06 | 4.62E-02 |
| GDE_HUMAN | Glycogen debranching enzyme | 1.07 | 3.41E-02 |
| DOPD_HUMAN | D-dopachrome decarboxylase | 1.07 | 4.97E-02 |
| Q7Z4X0_HUMAN | MO25-like protein | 1.07 | 2.66E-02 |
| HNRPD_HUMAN | Heterogeneous nuclear ribonucleoprotein D0 | 1.08 | 4.13E-02 |
| PUR6_HUMAN | Multifunctional protein ADE2 | 1.08 | 1.33E-02 |
| CPNE3_HUMAN | Copine-3 | 1.08 | 3.67E-02 |
| B7ZL14_HUMAN | FNBP1 protein (Formin-binding protein 1) | 1.08 | 4.37E-02 |
| GRP78_HUMAN | 78 kDa glucose-regulated protein | 1.08 | 1.96E-10 |
| Q59EL5_HUMAN | Aldo-keto reductase family 1 | 1.08 | 4.50E-03 |
| APOBR_HUMAN | Apolipoprotein B receptor (Apolipoprotein B-100 receptor) | 1.08 | 2.17E-02 |
| GLRX1_HUMAN | Glutaredoxin-1 | 1.08 | 1.24E-02 |
| S10A9_HUMAN | Protein S100-A9 (Calgranulin-B) | 1.09 | 1.53E-06 |
| D3DRP5_HUMAN | Chromosome 9 open reading frame 19. isoform CRA_a | 1.09 | 1.31E-03 |
| PFKAL_HUMAN | ATP-dependent 6-phosphofructokinase. liver type | 1.09 | 2.15E-02 |
| BLVRB_HUMAN | Flavin reductase (NADPH) | 1.09 | 1.97E-02 |
| PSA5_HUMAN | Proteasome subunit alpha type-5 | 1.10 | 1.75E-02 |
| A8K9E4_HUMAN | cDNA FLJ76459. highly similar to Homo sapiens matrix metallopeptidase 8 (neutrophil collagenase) | 1.10 | 2.80E-13 |
| MARCS_HUMAN | Myristoylated alanine-rich C-kinase substrate | 1.11 | 9.83E-03 |
| NAMPT_HUMAN | Nicotinamide phosphoribosyltransferase | 1.11 | 1.42E-03 |
| Q53S24_HUMAN | Prothymosin. alpha | 1.12 | 4.22E-02 |
| Q5SRT3_HUMAN | Chloride intracellular channel protein | 1.12 | 3.73E-02 |
| S10AB_HUMAN | Protein S100-A11 (Calgizzarin) | 1.12 | 2.15E-02 |
| CATD_HUMAN | Cathepsin D | 1.13 | 6.74E-03 |
| B2RB57_HUMAN | cDNA. FLJ95321. highly similar to Homo sapiens ATG7 autophagy related 7 homolog | 1.13 | 4.88E-02 |
| Q53EM5_HUMAN | Transketolase | 1.13 | 2.00E-05 |
| PNCB_HUMAN | Nicotinate phosphoribosyltransferase (NAPRTase) | 1.13 | 1.94E-03 |
| TOLIP_HUMAN | Toll-interacting protein | 1.13 | 2.04E-02 |
| Q32Q12_HUMAN | Nucleoside diphosphate kinase | 1.14 | 2.98E-02 |
| THIC_HUMAN | Acetyl-CoA acetyltransferase. cytosolic | 1.14 | 1.26E-02 |
| Q5CAQ5_HUMAN | Tumor rejection antigen (Gp96) 1 | 1.14 | 5.96E-03 |
| MMP9_HUMAN | Matrix metalloproteinase-9 | 1.14 | 1.57E-09 |
| DEK_HUMAN | Protein DEK | 1.14 | 1.18E-02 |
| NIBAN_HUMAN | Protein Niban | 1.15 | 3.33E-03 |
| RNAS2_HUMAN | Non-secretory ribonuclease | 1.15 | 3.81E-12 |
| ACTN4_HUMAN | Alpha-actinin-4 (Non-muscle alpha-actinin 4) | 1.15 | 2.27E-02 |
| DPP3_HUMAN | Dipeptidyl peptidase 3 | 1.16 | 2.39E-02 |
| LDH6B_HUMAN | L-lactate dehydrogenase A-like 6B | 1.17 | 3.72E-02 |
| SF3B2_HUMAN | Splicing factor 3B subunit 2 | 1.18 | 2.30E-02 |
| MCEM1_HUMAN | Mast cell-expressed membrane protein 1 | 1.20 | 4.31E-03 |
| Q2TU34_HUMAN | Fructose-1.6-bisphosphatase 1 | 1.20 | 3.08E-02 |
| GLYG_HUMAN | Glycogenin-1 | 1.21 | 7.78E-05 |
| PTBP1_HUMAN | Polypyrimidine tract-binding protein 1 | 1.22 | 1.47E-02 |
| LEG10_HUMAN | Galectin-10 | 1.22 | 1.43E-13 |
| B2RDW0_HUMAN | cDNA. FLJ96792. highly similar to Homo sapiens calmodulin (CALM2) | 1.22 | 7.65E-03 |
| ANXA5_HUMAN | Annexin A5 | 1.22 | 3.30E-10 |
| MVP_HUMAN | Major vault protein | 1.22 | 6.68E-03 |

| | | | |
|---|---|---|---|
| CALR_HUMAN | Calreticulin (CRP55) (Calregulin) | 1.22 | 9.34E-07 |
| ECP_HUMAN | Eosinophil cationic protein | 1.26 | 7.74E-21 |
| LEG1_HUMAN | Galectin-1 | 1.30 | 4.29E-02 |
| CYTB_HUMAN | Cystatin-B | 1.32 | 4.50E-02 |
| FCG3B_HUMAN | Low affinity immunoglobulin gamma Fc region receptor III-B (CD antigen CD16b) | 1.38 | 1.27E-03 |
| LOX15_HUMAN | Arachidonate 15-lipoxygenase | 1.39 | 1.33E-06 |
| GILT_HUMAN | Gamma-interferon-inducible lysosomal thiol reductase | 1.41 | 2.02E-02 |
| OLFM4_HUMAN | Olfactomedin-4 | 1.43 | 5.34E-13 |
| PRG3_HUMAN | Proteoglycan 3 | 1.55 | 3.00E-17 |

### *PV vs PMF comparison*

| Protein group | Protein description | Ratio | p value |
|---|---|---|---|
| LEG10_HUMAN | Galectin-10 | 0.64 | 7.28E-17 |
| LEG1_HUMAN | Galectin-1 | 0.64 | 4.05E-03 |
| RUXF_HUMAN | Small nuclear ribonucleoprotein F | 0.70 | 3.45E-02 |
| B7Z466_HUMAN | cDNA FLJ51491. highly similar to Arachidonate 15-lipoxygenase | 0.71 | 1.01E-05 |
| PRG3_HUMAN | Proteoglycan 3 | 0.72 | 1.01E-13 |
| ACTG_HUMAN | Actin. cytoplasmic 2 | 0.72 | 8.35E-03 |
| ECP_HUMAN | Eosinophil cationic protein | 0.75 | 5.45E-29 |
| S10A4_HUMAN | Protein S100-A4 (Calvasculin) | 0.80 | 4.57E-05 |
| B2RDW0_HUMAN | cDNA. FLJ96792. highly similar to Homo sapiens calmodulin 2 (CALM2) | 0.80 | 8.64E-04 |
| B4DVJ0_HUMAN | Glucose-6-phosphate isomerase | 0.81 | 7.51E-03 |
| ANXA5_HUMAN | Annexin A5 | 0.83 | 1.61E-07 |
| COTL1_HUMAN | Coactosin-like protein | 0.84 | 3.89E-03 |
| Q53EM5_HUMAN | Transketolase | 0.84 | 1.43E-10 |
| B4DV10_HUMAN | cDNA FLJ59142. highly similar to Epididymal secretory protein E1 | 0.84 | 6.83E-03 |
| COF1_HUMAN | Cofilin-1 | 0.85 | 4.51E-08 |
| OLFM4_HUMAN | Olfactomedin-4 | 0.85 | 2.83E-06 |
| A4D275_HUMAN | Actin related protein 2/3 complex | 0.86 | 2.18E-02 |
| OSTF1_HUMAN | Osteoclast-stimulating factor 1 | 0.87 | 1.49E-03 |
| Q53S24_HUMAN | Prothymosin. alpha | 0.87 | 6.11E-03 |
| MCTS1_HUMAN | Malignant T-cell-amplified sequence 1 | 0.87 | 7.17E-03 |
| BPI_HUMAN | Bactericidal permeability-increasing protein | 0.90 | 3.18E-11 |
| Q9Y4A1_HUMAN | Talin-related protein | 0.90 | 1.00E-02 |
| TALDO_HUMAN | Transaldolase | 0.90 | 4.76E-11 |
| MYH9_HUMAN | Myosin-9 | 0.90 | 2.43E-15 |
| ENOB_HUMAN | Beta-enolase | 0.90 | 1.08E-06 |
| S10A6_HUMAN | Protein S100-A6 (Calcyclin) | 0.90 | 2.47E-02 |
| GLRX1_HUMAN | Glutaredoxin-1 | 0.91 | 9.49E-03 |
| H15_HUMAN | Histone H1.5 | 0.92 | 4.38E-03 |
| PROF1_HUMAN | Profilin-1 | 0.92 | 1.75E-15 |
| S10AC_HUMAN | Protein S100-A12 | 0.93 | 4.89E-06 |
| A4QPB0_HUMAN | IQ motif containing GTPase activating protein 1 | 0.93 | 1.57E-04 |
| AMPB_HUMAN | Aminopeptidase B | 0.93 | 1.83E-02 |
| PSA5_HUMAN | Proteasome subunit alpha type-5 | 0.93 | 1.84E-02 |
| GDIR2_HUMAN | Rho GDP-dissociation inhibitor 2 | 0.94 | 1.80E-02 |
| RNAS2_HUMAN | Non-secretory ribonuclease | 0.95 | 1.05E-02 |

| | | | |
|---|---|---|---|
| RHOA_HUMAN | Transforming protein RhoA | 0.95 | 5.86E-03 |
| S10A9_HUMAN | Protein S100-A9 (Calgranulin-B) | 0.96 | 2.26E-06 |
| TPIS_HUMAN | Triosephosphate isomerase | 0.97 | 1.07E-02 |
| AL5AP_HUMAN | Arachidonate 5-lipoxygenase-activating protein | 0.97 | 3.18E-02 |
| ANXA1_HUMAN | Annexin A1 | 0.97 | 7.07E-03 |
| COR1A_HUMAN | Coronin-1A | 0.97 | 2.95E-02 |
| PLSL_HUMAN | Plastin-2 | 0.98 | 9.75E-03 |
| TLN1_HUMAN | Talin-1 | 0.98 | 3.07E-03 |
| GSTP1_HUMAN | Glutathione S-transferase P | 1.00 | 1.35E-02 |
| D3DRP5_HUMAN | Chromosome 9 open reading frame 19. isoform CRA | 1.02 | 9.80E-03 |
| S10A8_HUMAN | Protein S100-A8 (Calgranulin-A) | 1.03 | 6.77E-09 |
| IF2A_HUMAN | Eukaryotic translation initiation factor 2 subunit 1 | 1.08 | 2.52E-02 |
| B2R4C5_HUMAN | Lysozyme | 1.08 | 2.23E-02 |
| BLVRB_HUMAN | Flavin reductase (NADPH) | 1.09 | 8.27E-03 |
| HXK3_HUMAN | Hexokinase-3 | 1.09 | 1.05E-02 |
| TERA_HUMAN | Transitional endoplasmic reticulum ATPase | 1.10 | 2.47E-02 |
| MMP9_HUMAN | Matrix metalloproteinase-9 | 1.10 | 3.73E-05 |
| MCEM1_HUMAN | Mast cell-expressed membrane protein 1 | 1.11 | 6.91E-03 |
| ANXA4_HUMAN | Annexin A4 | 1.11 | 4.38E-04 |
| ACSL1_HUMAN | Long-chain-fatty-acid--CoA ligase 1 | 1.11 | 1.36E-02 |
| GRP78_HUMAN | 78 kDa glucose-regulated protein (GRP-78) | 1.13 | 1.94E-10 |
| A8K9E4_HUMAN | cDNA FLJ76459. highly similar to Homo sapiens matrix metallopeptidase 8 (neutrophil collagenase) | 1.13 | 1.82E-08 |
| ELNE_HUMAN | Neutrophil elastase | 1.15 | 6.81E-03 |
| CAMP_HUMAN | Cathelicidin antimicrobial peptide | 1.15 | 2.33E-15 |
| HS71A_HUMAN | Heat shock 70 kDa protein 1A | 1.15 | 2.44E-03 |
| HS71B_HUMAN | Heat shock 70 kDa protein 1B | 1.15 | 2.44E-03 |
| ITAM_HUMAN | Integrin alpha-M (CD11 antigen-like family member B) | 1.16 | 8.58E-03 |
| GSTO1_HUMAN | Glutathione S-transferase omega-1 | 1.17 | 2.99E-05 |
| NIBAN_HUMAN | Protein Niban (Cell growth-inhibiting gene 39 protein) | 1.17 | 6.05E-03 |
| PRTN3_HUMAN | Myeloblastin | 1.18 | 1.42E-14 |
| CH3L1_HUMAN | Chitinase-3-like protein 1 | 1.18 | 3.20E-05 |
| MARCS_HUMAN | Myristoylated alanine-rich C-kinase substrate | 1.19 | 2.05E-02 |
| Q86SR2_HUMAN | AZU1 protein | 1.19 | 1.39E-04 |
| CAH1_HUMAN | Carbonic anhydrase 1 | 1.20 | 3.10E-05 |
| PERM_HUMAN | Myeloperoxidase | 1.21 | 1.69E-09 |
| Q06AH7_HUMAN | Transferrin | 1.22 | 7.75E-03 |
| RETN_HUMAN | Resistin | 1.24 | 2.08E-10 |
| B2R6A3_HUMAN | Na(+)/H(+) exchange regulatory cofactor NHE-RF | 1.31 | 4.14E-02 |
| CATG_HUMAN | Cathepsin G | 1.36 | 2.08E-11 |
| FOLR3_HUMAN | Folate receptor gamma | 1.61 | 4.76E-03 |
| A8K4K0_HUMAN | cDNA FLJ75006. highly similar to Homo sapiens CD177 | 1.69 | 5.18E-03 |

### *ET vs PMFcomparison*

| **Protein group** | **Protein description** | **Ratio** | **p-value** |
|---|---|---|---|
| ITAM_HUMAN | Integrin alpha-M (CD11 antigen-like family member B) | 0.54 | 2.23E-04 |
| FOLR3_HUMAN | Folate receptor gamma (FR-gamma) (Folate receptor 3) | 0.57 | 1.06E-04 |
| LEG10_HUMAN | Galectin-10 | 0.66 | 3.54E-20 |
| B7Z466_HUMAN | cDNA FLJ51491. highly similar to Arachidonate 15-lipoxygenase | 0.66 | 1.24E-06 |
| OLFM4_HUMAN | Olfactomedin-4 | 0.72 | 1.96E-09 |

| | | | |
|---|---|---|---|
| ACTG_HUMAN | Actin. cytoplasmic 2 | 0.72 | 1.86E-02 |
| B4DVJ0_HUMAN | Glucose-6-phosphate isomerase | 0.73 | 1.08E-02 |
| KSYK_HUMAN | Tyrosine-protein kinase SYK | 0.73 | 1.85E-02 |
| FCN1_HUMAN | Ficolin-1 | 0.74 | 1.00E-03 |
| SDCB1_HUMAN | Syntenin-1 | 0.75 | 1.45E-02 |
| B2RDW0_HUMAN | cDNA. FLJ96792. highly similar to Homo sapiens calmodulin 2 | 0.76 | 3.46E-04 |
| LEG1_HUMAN | Galectin-1 | 0.77 | 3.44E-02 |
| Q53GC7_HUMAN | Capping protein | 0.78 | 5.09E-02 |
| Q15657_HUMAN | Tropomyosin isoform | 0.78 | 4.04E-03 |
| CATD_HUMAN | Cathepsin D | 0.80 | 3.19E-04 |
| B4DV10_HUMAN | cDNA FLJ59142. highly similar to Epididymal secretory protein E1 | 0.80 | 1.83E-02 |
| A4D275_HUMAN | Actin related protein 2/3 complex. subunit 1B | 0.80 | 2.04E-03 |
| Q5T5C7_HUMAN | Serine--tRNA ligase. cytoplasmic | 0.81 | 2.10E-02 |
| GILT_HUMAN | Gamma-interferon-inducible lysosomal thiol reductase | 0.82 | 2.98E-02 |
| Q53EM5_HUMAN | Transketolase | 0.83 | 1.10E-11 |
| B5BU52_HUMAN | Non-specific protein-tyrosine kinase | 0.84 | 3.16E-02 |
| TCPB_HUMAN | T-complex protein 1 subunit beta | 0.84 | 1.68E-04 |
| ECP_HUMAN | Eosinophil cationic protein | 0.85 | 1.46E-17 |
| RNAS2_HUMAN | Non-secretory ribonuclease | 0.85 | 1.30E-12 |
| PRG3_HUMAN | Proteoglycan 3 | 0.85 | 2.45E-07 |
| BPI_HUMAN | Bactericidal permeability-increasing protein | 0.87 | 1.33E-07 |
| B2R4D5_HUMAN | Actin-related protein 2/3 complex subunit 3 | 0.87 | 1.81E-03 |
| TCPE_HUMAN | T-complex protein 1 subunit epsilon | 0.87 | 2.28E-02 |
| Q53S24_HUMAN | Prothymosin. alpha | 0.88 | 9.21E-03 |
| LDH6B_HUMAN | L-lactate dehydrogenase A-like 6B | 0.88 | 3.63E-02 |
| CLH1_HUMAN | Clathrin heavy chain 1 | 0.88 | 4.75E-03 |
| PERE_HUMAN | Eosinophil peroxidase (EPO) | 0.88 | 7.90E-04 |
| GLRX1_HUMAN | Glutaredoxin-1 | 0.89 | 5.82E-03 |
| RAN_HUMAN | GTP-binding nuclear protein Ran | 0.89 | 2.23E-04 |
| Q5CAQ5_HUMAN | Tumor rejection antigen (Gp96) 1 | 0.89 | 2.18E-02 |
| CAZA1_HUMAN | F-actin-capping protein subunit alpha-1 | 0.89 | 8.44E-03 |
| PLSI_HUMAN | Plastin-1 | 0.90 | 4.49E-02 |
| GLYG_HUMAN | Glycogenin-1 | 0.90 | 7.91E-03 |
| B2RDE1_HUMAN | cDNA. FLJ96568. highly similar to Homo sapiens tropomyosin 3 | 0.90 | 1.64E-03 |
| PSA5_HUMAN | Proteasome subunit alpha type-5 | 0.90 | 2.85E-02 |
| Q2Q9H2_HUMAN | Glucose-6-phosphate 1-dehydrogenase | 0.91 | 3.40E-02 |
| HXK3_HUMAN | Hexokinase-3 | 0.91 | 1.09E-04 |
| PLIN3_HUMAN | Perilipin-3 | 0.91 | 2.67E-02 |
| B2RBR9_HUMAN | cDNA. FLJ95650. highly similar to Homo sapiens karyopherin (importin) beta 1 | 0.91 | 2.05E-04 |
| Q5SRT3_HUMAN | Chloride intracellular channel protein | 0.92 | 1.43E-02 |
| COF1_HUMAN | Cofilin-1 | 0.92 | 6.12E-03 |
| ARPC2_HUMAN | Actin-related protein 2/3 complex subunit 2 | 0.92 | 4.77E-02 |
| Q6IAM7_HUMAN | Signal peptidase complex catalytic subunit SEC11 | 0.92 | 1.18E-02 |
| Q9Y4A1_HUMAN | Talin-related protein | 0.93 | 2.69E-02 |
| ARP3_HUMAN | Actin-related protein 3 | 0.93 | 2.50E-03 |
| CPNE3_HUMAN | Copine-3 (Copine III) | 0.94 | 2.81E-02 |
| S10AC_HUMAN | Protein S100-A12 | 0.94 | 1.15E-03 |
| A4QPB0_HUMAN | IQ motif containing GTPase activating protein 1 | 0.95 | 3.85E-03 |

| | | | |
|---|---|---|---|
| ANXA5_HUMAN | Annexin A5 | 0.95 | 2.39E-02 |
| PLSL_HUMAN | Plastin-2 | 0.96 | 1.61E-06 |
| PGK1_HUMAN | Phosphoglycerate kinase 1 | 0.97 | 2.06E-04 |
| ALDOA_HUMAN | Fructose-bisphosphate aldolase A | 0.97 | 3.72E-02 |
| G3P_HUMAN | Glyceraldehyde-3-phosphate dehydrogenase (GAPDH) | 0.98 | 2.07E-02 |
| PROF1_HUMAN | Profilin-1 | 0.99 | 1.35E-02 |
| TALDO_HUMAN | Transaldolase | 1.02 | 7.10E-03 |
| ANXA1_HUMAN | Annexin A1 | 1.05 | 2.42E-02 |
| S10A9_HUMAN | Protein S100-A9 (Calgranulin-B) | 1.06 | 1.64E-02 |
| COR1A_HUMAN | Coronin-1A | 1.06 | 1.38E-02 |
| MYH9_HUMAN | Myosin-9 | 1.06 | 2.45E-03 |
| VINC_HUMAN | Vinculin | 1.07 | 2.60E-03 |
| ITB2_HUMAN | Integrin beta-2 | 1.07 | 4.77E-03 |
| GDIA_HUMAN | Rab GDP dissociation inhibitor alpha | 1.09 | 1.92E-02 |
| Q59F54_HUMAN | Solute carrier family 2 | 1.09 | 1.31E-02 |
| SODC_HUMAN | Superoxide dismutase | 1.09 | 8.73E-03 |
| ANXA4_HUMAN | Annexin A4 | 1.09 | 6.41E-03 |
| RETN_HUMAN | Resistin | 1.10 | 6.39E-04 |
| CH3L1_HUMAN | Chitinase-3-like protein 1 | 1.10 | 1.96E-03 |
| GSTO1_HUMAN | Glutathione S-transferase omega-1 | 1.10 | 1.02E-02 |
| ACTN1_HUMAN | Alpha-actinin-1 | 1.10 | 1.07E-03 |
| CATG_HUMAN | Cathepsin G | 1.11 | 1.55E-03 |
| MMP9_HUMAN | Matrix metalloproteinase-9] | 1.11 | 4.63E-04 |
| AL5AP_HUMAN | Arachidonate 5-lipoxygenase-activating protein | 1.12 | 8.69E-04 |
| PPIA_HUMAN | Peptidyl-prolyl cis-trans isomerase A | 1.13 | 4.52E-03 |
| 6PGL_HUMAN | 6-phosphogluconolactonase | 1.16 | 2.03E-02 |
| Q5NKU1_HUMAN | Intercellular adhesion molecule 3 | 1.17 | 3.11E-02 |
| TERA_HUMAN | Transitional endoplasmic reticulum ATPase | 1.17 | 1.45E-03 |
| D3DNA1_HUMAN | Integrin beta | 1.17 | 1.02E-02 |
| A1AG1_HUMAN | Alpha-1-acid glycoprotein 1 | 1.18 | 2.16E-03 |
| BLVRB_HUMAN | Flavin reductase (NADPH) | 1.21 | 1.28E-05 |
| BST1_HUMAN | ADP-ribosyl cyclase/cyclic ADP-ribose hydrolase 2 (CD antigen CD157) | 1.21 | 9.28E-04 |
| CHIT1_HUMAN | Chitotriosidase-1 | 1.21 | 2.86E-02 |
| B2R4C5_HUMAN | Lysozyme | 1.22 | 1.18E-08 |
| PERM_HUMAN | Myeloperoxidase | 1.22 | 1.82E-09 |
| PRTN3_HUMAN | Myeloblastin | 1.23 | 4.88E-31 |
| PSME2_HUMAN | Proteasome activator complex subunit 2 | 1.23 | 1.09E-02 |
| CAH2_HUMAN | Carbonic anhydrase 2 | 1.27 | 4.93E-03 |
| CAMP_HUMAN | Cathelicidin antimicrobial peptide | 1.28 | 2.41E-17 |
| ITAM_HUMAN | Integrin alpha-M (CD11 antigen-like family member B) | 1.31 | 1.16E-03 |
| HS71A_HUMAN y B | Heat shock 70 kDa protein 1A y B | 1.39 | 4.95E-04 |
| Q86SR2_HUMAN | AZU1 protein | 1.41 | 9.30E-08 |
| B3AT_HUMAN | Band 3 anion transport protein | 1.41 | 6.42E-03 |
| CAH1_HUMAN | Carbonic anhydrase 1 | 1.44 | 2.29E-09 |
| PRDX2_HUMAN | Peroxiredoxin-2 | 1.50 | 3.38E-09 |
| A8K4K0_HUMAN | cDNA FLJ75006. highly similar to Homo sapiens CD177 | 1.52 | 2.58E-03 |
| F189B_HUMAN | Protein FAM189B | 1.60 | 9.27E-07 |

### *PV vs ET comparison*

| Protein group | Protein description | Ratio | p-value |
|---|---|---|---|
| F189B_HUMAN | Protein FAM189B | 0.66 | 3.50E-07 |
| PRDX2_HUMAN | Peroxiredoxin-2 | 0.74 | 2.24E-05 |
| S10A4_HUMAN | Protein S100-A4 (Calvasculin) | 0.77 | 4.20E-04 |
| CAH2_HUMAN | Carbonic anhydrase 2 | 0.79 | 4.73E-04 |
| CAH1_HUMAN | Carbonic anhydrase 1 | 0.83 | 1.37E-06 |
| LEG1_HUMAN | Galectin-1 | 0.83 | 6.39E-03 |
| HS71A_HUMAN | Heat shock 70 kDa protein 1A | 0.84 | 1.45E-03 |
| PRG3_HUMAN | Proteoglycan 3 | 0.85 | 1.17E-06 |
| A1AG1_HUMAN | Alpha-1-acid glycoprotein 1 | 0.85 | 1.98E-04 |
| COTL1_HUMAN | Coactosin-like protein | 0.86 | 1.50E-02 |
| MYH9_HUMAN | Myosin-9 | 0.87 | 1.80E-22 |
| ANXA5_HUMAN | Annexin A5 | 0.88 | 1.70E-04 |
| Q86SR2_HUMAN | AZU1 protein | 0.88 | 2.70E-03 |
| H15_HUMAN | Histone H1.5 | 0.89 | 1.47E-02 |
| TALDO_HUMAN | Transaldolase | 0.89 | 1.71E-08 |
| ACTN1_HUMAN | Alpha-actinin-1 | 0.91 | 5.97E-04 |
| PPIA_HUMAN | Peptidyl-prolyl cis-trans isomerase A | 0.91 | 2.85E-05 |
| CAMP_HUMAN | Cathelicidin antimicrobial peptide | 0.92 | 2.98E-04 |
| COR1A_HUMAN | Coronin-1A | 0.92 | 5.68E-05 |
| B2R4C5_HUMAN | Lysozyme (EC 3.2.1.17) | 0.92 | 2.48E-03 |
| PYGL_HUMAN | Glycogen phosphorylase. liver form | 0.92 | 1.12E-02 |
| CATA_HUMAN | Catalase | 0.93 | 7.55E-04 |
| AMPB_HUMAN | Aminopeptidase B | 0.93 | 9.42E-03 |
| ANXA1_HUMAN | Annexin A1 | 0.95 | 3.23E-08 |
| PROF1_HUMAN | Profilin-1 | 0.96 | 5.22E-06 |
| S10A8_HUMAN | Protein S100-A8 (Calgranulin-A) | 1.05 | 9.07E-06 |
| B2RBR9_HUMAN | cDNA. FLJ95650. highly similar to Homo sapiens karyopherin (importin) beta 1 | 1.10 | 1.40E-03 |
| A8K9E4_HUMAN | cDNA FLJ76459. highly similar to Homo sapiens matrix metallopeptidase 8 | 1.11 | 1.75E-05 |
| TCPB_HUMAN | T-complex protein 1 subunit beta | 1.12 | 1.14E-02 |
| GRP78_HUMAN | 78 kDa glucose-regulated protein (GRP-78) heavy chain-binding protein) (BiP) | 1.13 | 1.56E-06 |
| RETN_HUMAN | Resistin | 1.14 | 1.64E-09 |
| MCEM1_HUMAN | Mast cell-expressed membrane protein 1 | 1.14 | 1.39E-02 |
| RNAS2_HUMAN | Non-secretory ribonuclease | 1.14 | 1.31E-04 |
| PDIA6_HUMAN | Protein disulfide-isomerase A6 | 1.17 | 1.08E-02 |
| MVP_HUMAN | Major vault protein (MVP) (Lung resistance-related protein) | 1.20 | 6.67E-03 |
| OLFM4_HUMAN | Olfactomedin-4 | 1.21 | 3.55E-04 |
| NIBAN_HUMAN | Protein Niban | 1.22 | 1.09E-03 |
| CLH1_HUMAN | Clathrin heavy chain 1 | 1.23 | 2.31E-03 |
| CAN1_HUMAN | Calpain-1 catalytic subunit | 1.25 | 8.69E-04 |
| PERE_HUMAN | Eosinophil peroxidase (EPO) | 1.25 | 1.59E-05 |
| CATG_HUMAN | Cathepsin G | 1.25 | 7.68E-09 |
| HXK3_HUMAN | Hexokinase-3 | 1.25 | 5.17E-08 |
| URP2_HUMAN | Fermitin family homolog 3 | 1.27 | 1.43E-02 |
| CATD_HUMAN | Cathepsin D | 1.28 | 2.42E-04 |
| ITAM_HUMAN | Integrin alpha-M (CD antigen CD11b) | 1.68 | 7.50E-03 |

| | | | |
|---|---|---|---|
| FOLR3_HUMAN | Folate receptor gamma | 2.85 | 5.45E-05 |

## Supplemental Data II-2

Lists of deregulated pathways in granulocytes among the different subgroups PV. ET. PMF (all *JAK2(+))* and Mut0 (*JAK2(-)* ET and PMF).

### *PV vs Mut0 (JAK2(-) ET and PMF) comparison*

List of the significantly deregulated pathways in PV vs Mut0 (p-value < 0.05) ordered in increasing p-value according to *reactome* results. P-value represents the proportion of deregulated proteins from the MS analysis that belong to that pathway. Ratio is made between the number of deregulated proteins and the total number of proteins in that pathway.

| Pathway name | Entities found | Entities total | Entities pValue |
|---|---|---|---|
| Glucose metabolism | 6 | 76 | 9.39E-05 |
| Glycolysis | 4 | 33 | 2.99E-04 |
| Nicotinamide salvaging | 2 | 5 | 1.09E-03 |
| EPH-Ephrin signaling | 5 | 94 | 2.12E-03 |
| RHO GTPases activate PKNs | 4 | 60 | 2.69E-03 |
| Gluconeogenesis | 3 | 31 | 3.36E-03 |
| ATF6-alpha activates chaperone genes | 2 | 10 | 4.23E-03 |
| Metabolism of carbohydrates | 8 | 271 | 4.37E-03 |
| Nicotinate metabolism | 2 | 11 | 5.08E-03 |
| ATF6-alpha activates chaperones | 2 | 12 | 6.01E-03 |
| Advanced glycosylation endproduct receptor signaling | 2 | 13 | 7.01E-03 |
| Platelet degranulation | 4 | 79 | 7.07E-03 |
| EPHB-mediated forward signaling | 3 | 41 | 7.26E-03 |
| Response to elevated platelet cytosolic Ca2+ | 4 | 84 | 8.72E-03 |
| Signaling by Rho GTPases | 9 | 379 | 1.01E-02 |
| TGF-beta receptor signaling in EMT (epithelial to mesenchymal transition) | 2 | 16 | 1.04E-02 |
| RHO GTPases Activate ROCKs | 2 | 17 | 1.17E-02 |
| RHO GTPases activate CIT | 2 | 17 | 1.17E-02 |
| RHO GTPase Effectors | 7 | 266 | 1.37E-02 |
| RHO GTPases activate PAKs | 2 | 21 | 1.74E-02 |
| G2/M DNA damage checkpoint | 3 | 58 | 1.83E-02 |
| Insulin effects increased synthesis of Xylulose-5-Phosphate | 1 | 2 | 1.89E-02 |
| Collagen degradation | 3 | 62 | 2.18E-02 |
| Sema4D induced cell migration and growth-cone collapse | 2 | 24 | 2.23E-02 |
| Semaphorin interactions | 3 | 67 | 2.66E-02 |
| Degradation of the extracellular matrix | 4 | 118 | 2.67E-02 |
| Sema4D in semaphorin signaling | 2 | 27 | 2.78E-02 |
| TAK1 activates NFkB by phosphorylation and activation of IKKs complex | 2 | 30 | 3.37E-02 |
| Axonal growth stimulation | 1 | 4 | 3.75E-02 |
| Activation of Matrix Metalloproteinases | 2 | 32 | 3.78E-02 |
| EPHA-mediated growth cone collapse | 2 | 34 | 4.22E-02 |

### *ET vs Mut0 (JAK2(-) ET and PMF) comparison*

List of the significantly deregulated pathways in ET vs Mut0 (p-value < 0.05) ordered in increasing p-value according to *reactome* results. P-value represents the proportion of deregulated proteins from the MS analysis that belong to that pathway. Ratio is made between the number of deregulated proteins and the total number of proteins in that pathway.

| Pathway name | Entities found | Entities total | Entities pValue |
|---|---|---|---|
| O2/CO2 exchange in erythrocytes | 4 | 8 | 4.10E-06 |
| Erythrocytes take up oxygen and release carbon dioxide | 4 | 8 | 4.10E-06 |
| Erythrocytes take up carbon dioxide and release oxygen | 4 | 8 | 4.10E-06 |
| Detoxification of Reactive Oxygen Species | 4 | 29 | 5.76E-04 |
| Platelet degranulation | 6 | 79 | 5.90E-04 |
| Response to elevated platelet cytosolic Ca2+ | 6 | 84 | 8.10E-04 |
| EPH-Ephrin signaling | 6 | 94 | 1.43E-03 |
| Semaphorin interactions | 5 | 67 | 1.84E-03 |
| EPHB-mediated forward signaling | 4 | 41 | 2.05E-03 |
| Scavenging by Class F Receptors | 2 | 7 | 3.80E-03 |
| Assembly of Viral Components at the Budding Site | 2 | 7 | 3.80E-03 |
| Folding of actin by CCT/TriC | 2 | 9 | 6.17E-03 |
| ATF6-alpha activates chaperone genes | 2 | 10 | 7.56E-03 |
| Calnexin/calreticulin cycle | 2 | 11 | 9.07E-03 |
| Virus Assembly and Release | 2 | 11 | 9.07E-03 |
| Glycolysis | 3 | 33 | 9.16E-03 |
| Platelet activation. signaling and aggregation | 8 | 228 | 9.52E-03 |
| Hedgehog ligand biogenesis | 4 | 64 | 9.71E-03 |
| HSF1 activation | 2 | 12 | 1.07E-02 |
| ATF6-alpha activates chaperones | 2 | 12 | 1.07E-02 |
| Reversible hydration of carbon dioxide | 2 | 12 | 1.07E-02 |
| RHO GTPases Activate WASPs and WAVEs | 3 | 35 | 1.07E-02 |
| Advanced glycosylation endproduct receptor signaling | 2 | 13 | 1.25E-02 |
| N-glycan trimming in the ER and Calnexin/Calreticulin cycle | 2 | 13 | 1.25E-02 |
| Glucose metabolism | 4 | 76 | 1.72E-02 |
| Sema3A PAK dependent Axon repulsion | 2 | 16 | 1.84E-02 |
| Metabolism of Angiotensinogen to Angiotensins | 2 | 16 | 1.84E-02 |
| Axon guidance | 13 | 542 | 2.23E-02 |
| Formation of ATP by chemiosmotic coupling | 2 | 18 | 2.29E-02 |
| Cell-extracellular matrix interactions | 2 | 18 | 2.29E-02 |
| Extracellular matrix organization | 8 | 271 | 2.42E-02 |
| Formation of tubulin folding intermediates by CCT/TriC | 2 | 20 | 2.78E-02 |
| Hemostasis | 12 | 515 | 3.36E-02 |
| Hh mutants abrogate ligand secretion | 3 | 55 | 3.47E-02 |
| Hh mutants that don't undergo autocatalytic processing are degraded by ERAD | 3 | 55 | 3.47E-02 |
| BBSome-mediated cargo-targeting to cilium | 2 | 23 | 3.59E-02 |
| Sema4D induced cell migration and growth-cone collapse | 2 | 24 | 3.88E-02 |
| Prefoldin mediated transfer of substrate to CCT/TriC | 2 | 26 | 4.48E-02 |
| Cooperation of Prefoldin and TriC/CCT in actin and tubulin folding | 2 | 27 | 4.79E-02 |
| Smooth Muscle Contraction | 2 | 27 | 4.79E-02 |

| | | | |
|---|---|---|---|
| Sema4D in semaphorin signaling | 2 | 27 | 4.79E-02 |

### *PMF vs Mut0 (JAK2(-) ET and PMF) comparison*

List of the significantly deregulated pathways in PMF vs Mut0 (p-value < 0.05) ordered in increasing p-value according to *reactome* results. P-value represents the proportion of deregulated proteins from the MS analysis that belong to that pathway. Ratio is made between the number of deregulated proteins and the total number of proteins in that pathway.

| **Pathway name** | **Entities found** | **Entities total** | **Entities pValue** |
|---|---|---|---|
| Detoxification of Reactive Oxygen Species | 8 | 29 | 8.54E-08 |
| Platelet degranulation | 8 | 79 | 1.20E-04 |
| Response to elevated platelet cytosolic Ca2+ | 8 | 84 | 1.81E-04 |
| Glycogen breakdown (glycogenolysis) | 4 | 15 | 1.86E-04 |
| Glucose metabolism | 7 | 76 | 5.60E-04 |
| Platelet activation. signaling and aggregation | 11 | 228 | 3.45E-03 |
| Nicotinamide salvaging | 2 | 5 | 3.95E-03 |
| Metabolism of nucleotides | 6 | 81 | 4.06E-03 |
| Synthesis and interconversion of nucleotide di- and triphosphates | 3 | 18 | 4.64E-03 |
| Regulation of mRNA stability by proteins that bind AU-rich elements | 6 | 87 | 5.70E-03 |
| MAP2K and MAPK activation | 4 | 40 | 6.63E-03 |
| Synthesis of Leukotrienes (LT) and Eoxins (EX) | 3 | 21 | 7.08E-03 |
| Sema4D induced cell migration and growth-cone collapse | 3 | 24 | 1.02E-02 |
| Sema4D in semaphorin signaling | 3 | 27 | 1.39E-02 |
| Hemostasis | 17 | 515 | 1.41E-02 |
| GP1b-IX-V activation signalling | 2 | 10 | 1.49E-02 |
| ATF6-alpha activates chaperone genes | 2 | 10 | 1.49E-02 |
| Transcriptional Regulation by TP53 | 5 | 78 | 1.51E-02 |
| TP53 Regulates Metabolic Genes | 5 | 78 | 1.51E-02 |
| Nicotinate metabolism | 2 | 11 | 1.78E-02 |
| AUF1 (hnRNP D0) destabilizes mRNA | 4 | 55 | 1.92E-02 |
| Chk1/Chk2(Cds1) mediated inactivation of Cyclin B:Cdk1 complex | 2 | 12 | 2.09E-02 |
| ATF6-alpha activates chaperones | 2 | 12 | 2.09E-02 |
| Activation of Matrix Metalloproteinases | 3 | 32 | 2.17E-02 |
| Degradation of the extracellular matrix | 6 | 118 | 2.25E-02 |
| Advanced glycosylation endproduct receptor signaling | 2 | 13 | 2.42E-02 |
| RHO GTPases activate PKNs | 4 | 60 | 2.54E-02 |
| p130Cas linkage to MAPK signaling for integrins | 2 | 15 | 3.15E-02 |
| GRB2:SOS provides linkage to MAPK signaling for Integrins | 2 | 15 | 3.15E-02 |
| Activation of BAD and translocation to mitochondria | 2 | 15 | 3.15E-02 |
| Rap1 signalling | 2 | 16 | 3.54E-02 |
| Metabolism of Angiotensinogen to Angiotensins | 2 | 16 | 3.54E-02 |
| Semaphorin interactions | 4 | 67 | 3.58E-02 |

### *PV vs PMF comparison*

List of the significantly deregulated pathways in PV vs PMF (p-value < 0.05) ordered in increasing p-value according to *reactome* results. P-value represents the proportion of deregulated proteins from the MS analysis that belong to that pathway. Ratio is made between the number of deregulated proteins and the total number of proteins in that pathway.

| Pathway name | Entities found | Entities total | Entities pValue |
|---|---|---|---|
| EPH-Ephrin signaling | 5 | 94 | 2.49E-03 |
| Activation of Matrix Metalloproteinases | 3 | 32 | 4.07E-03 |
| Glycolysis | 3 | 33 | 4.43E-03 |
| Semaphorin interactions | 4 | 67 | 4.54E-03 |
| Platelet degranulation | 4 | 79 | 8.03E-03 |
| EPHB-mediated forward signaling | 3 | 41 | 8.03E-03 |
| Response to elevated platelet cytosolic Ca2+ | 4 | 84 | 9.89E-03 |
| RHO GTPases Activate ROCKs | 2 | 17 | 1.25E-02 |
| RHO GTPases activate CIT | 2 | 17 | 1.25E-02 |
| Insulin effects increased synthesis of Xylulose-5-Phosphate | 1 | 2 | 1.96E-02 |
| Sema4D induced cell migration and growth-cone collapse | 2 | 24 | 2.39E-02 |
| Sema4D in semaphorin signaling | 2 | 27 | 2.97E-02 |
| PERK regulates gene expression | 2 | 28 | 3.18E-02 |
| Gluconeogenesis | 2 | 31 | 3.82E-02 |
| Axonal growth stimulation | 1 | 4 | 3.88E-02 |
| Glucose metabolism | 3 | 76 | 4.01E-02 |
| Glutathione conjugation | 2 | 33 | 4.27E-02 |
| EPHA-mediated growth cone collapse | 2 | 34 | 4.51E-02 |

### *ET vs PMF comparison*

List of the significantly deregulated pathways in ET vs PMF (p-value < 0.05) ordered in increasing p-value according to *reactome* results. P-value represents the proportion of deregulated proteins from the MS analysis that belong to that pathway. Ratio is made between the number of deregulated proteins and the total number of proteins in that pathway.

| Pathway name | Entities found | Entities total | Entities pValue |
|---|---|---|---|
| Platelet degranulation | 8 | 79 | 1.08E-05 |
| Response to elevated platelet cytosolic Ca2+ | 8 | 84 | 1.68E-05 |
| EPH-Ephrin signaling | 8 | 94 | 3.71E-05 |
| O2/CO2 exchange in erythrocytes | 3 | 8 | 1.74E-04 |
| Erythrocytes take up oxygen and release carbon dioxide | 3 | 8 | 1.74E-04 |
| Erythrocytes take up carbon dioxide and release oxygen | 3 | 8 | 1.74E-04 |
| Glycolysis | 4 | 33 | 9.94E-04 |
| EPHB-mediated forward signaling | 4 | 41 | 2.19E-03 |
| Hemostasis | 15 | 515 | 3.05E-03 |
| Platelet activation. signaling and aggregation | 9 | 228 | 3.21E-03 |
| Glucose metabolism | 5 | 76 | 3.41E-03 |
| Pentose phosphate pathway (hexose monophosphate shunt) | 2 | 7 | 3.94E-03 |
| Folding of actin by CCT/TriC | 2 | 9 | 6.40E-03 |

| | | | |
|---|---|---|---|
| Gluconeogenesis | 3 | 31 | 8.13E-03 |
| Formation of annular gap junctions | 2 | 11 | 9.39E-03 |
| Gap junction degradation | 2 | 12 | 1.11E-02 |
| Reversible hydration of carbon dioxide | 2 | 12 | 1.11E-02 |
| RHO GTPases Activate WASPs and WAVEs | 3 | 35 | 1.13E-02 |
| Advanced glycosylation endproduct receptor signaling | 2 | 13 | 1.29E-02 |
| Metabolism of Angiotensinogen to Angiotensins | 2 | 16 | 1.91E-02 |
| Cell-extracellular matrix interactions | 2 | 18 | 2.37E-02 |
| Insulin effects increased synthesis of Xylulose-5-Phosphate | 1 | 2 | 2.59E-02 |
| EPH-ephrin mediated repulsion of cells | 3 | 50 | 2.86E-02 |
| Formation of tubulin folding intermediates by CCT/TriC | 2 | 20 | 2.88E-02 |
| PCP/CE pathway | 4 | 91 | 3.24E-02 |
| Hh mutants abrogate ligand secretion | 3 | 55 | 3.63E-02 |
| Hh mutants that don't undergo autocatalytic processing are degraded by ERAD | 3 | 55 | 3.63E-02 |
| BBSome-mediated cargo-targeting to cilium | 2 | 23 | 3.71E-02 |
| Lysosomal glycogen catabolism | 1 | 3 | 3.86E-02 |
| Prefoldin mediated transfer of substrate to CCT/TriC | 2 | 26 | 4.63E-02 |
| Cooperation of Prefoldin and TriC/CCT in actin and tubulin folding | 2 | 27 | 4.95E-02 |

### *PV vs ET comparison*

List of the significantly deregulated pathways in PV vs ET (p-value < 0.05) ordered in increasing p-value according to *reactome* results. P-value represents the proportion of deregulated proteins from the MS analysis that belong to that pathway. Ratio is made between the number of deregulated proteins and the total number of proteins in that pathway.

| **Pathway name** | **Entities found** | **Entities total** | **Entities pValue** |
|---|---|---|---|
| Platelet degranulation | 5 | 79 | 2.07E-04 |
| Response to elevated platelet cytosolic Ca2+ | 5 | 84 | 2.74E-04 |
| O2/CO2 exchange in erythrocytes | 2 | 8 | 1.40E-03 |
| Erythrocytes take up oxygen and release carbon dioxide | 2 | 8 | 1.40E-03 |
| Erythrocytes take up carbon dioxide and release oxygen | 2 | 8 | 1.40E-03 |
| Reversible hydration of carbon dioxide | 2 | 12 | 3.10E-03 |
| Metabolism of Angiotensinogen to Angiotensins | 2 | 16 | 5.42E-03 |
| Insulin effects increased synthesis of Xylulose-5-Phosphate | 1 | 2 | 1.35E-02 |
| Detoxification of Reactive Oxygen Species | 2 | 29 | 1.68E-02 |
| Platelet activation. signaling and aggregation | 5 | 228 | 1.93E-02 |
| Lysosome Vesicle Biogenesis | 2 | 37 | 2.65E-02 |
| Extracellular matrix organization | 5 | 271 | 3.69E-02 |
| Reverse Transcription of HIV RNA | 1 | 7 | 4.65E-02 |
| Minus-strand DNA synthesis | 1 | 7 | 4.65E-02 |
| Plus-strand DNA synthesis | 1 | 7 | 4.65E-02 |
| Pentose phosphate pathway | 1 | 7 | 4.65E-02 |
| Degradation of the extracellular matrix | 3 | 118 | 4.65E-02 |

## Supplemental Data II-3

Article: Microarray and Proteomic Analyses of Myeloproliferative Neoplasms with a Highlight on the mTOR Signaling Pathway

http://journals.plos.org/plosone/article?id=10.1371/journal.pone.0135463

..\Microarray and Proteomic Analyses of Myeloproliferative Neoplasms with a Highlight on the mTOR Signaling Pathway.pdf

# ABSTRACTS

Besides genetic abnormalities, several studies have reported protein alterations in Ph- Myeloproliferative neoplasms (MPN) which could participate to the clinical phenotype of patients. Nevertheless, little is known about protein alterations in these pathologies. In this context, we used an integrative proteomic approach to decipher the landscape of the erythrocyte and granulocyte proteome abnormalities that could be related to functional cell alterations and to MPN physiopathology. We could identify significant protein deregulations that varied not only according to genetic status *JAK2(+)*, *JAK2(-)* or *CALR(+)* but also among *JAK2(+)* MPNs or depending on the *JAK2V617F* allele burden. These protein deregulations involved pathway alterations such as the IQGAP1/Rho GTPase signaling that could be related to thrombosis via alterations on the membrane integrity by deregulation of PAK1 or the actin cytoskeleton signaling. ROS or mTOR signaling alterations were also identified in granulocytes. Finally, we stress out that CALR protein could have a dual oncogenic role through its up-regulation in *JAK2V617F* MPNs different from its altered function described in *CALR* mutated patients. Altogether, we showed that proteomic deregulations might play an important oncogenic role in MPN physiopathology and could be implicated in complication as thrombotic accidents.

En plus des anomalies génétiques, plusieurs études ont rapporté des altérations des protéines chez les patients atteintes de Syndromes Myéloprolifératifs (SMP) Ph- qui pourraient participer à leurs phénotypes cliniques. Néanmoins, les altérations protéiques dans ces pathologies ne sont pas bien connues. Dans ce contexte, nous avons utilisé une approche protéomique par spectrométrie de masse pour nous aider à déchiffrer le paysage des anomalies des protéomes érythrocytaire et granulocytaire qui pourraient être liées à des altérations cellulaires fonctionnelles et à la physiopathologie des SMP. Nous avons ainsi pu identifier des dérégulations importantes de protéines qui varient selon le statut génétique des patients, [*JAK2(+), JAK2(-)* ou *CALR(+)*], selon la charge allélique de *JAK2V617F*, mais aussi selon le type de SMP *JAK2(+)* ou selon la. Ces dérégulations protéiques perturbent des voies de signalisation comme la voie IQGAP1/Rho GTPase qui pourrait être liée aux thromboses par des modifications de l'intégrité membranaire via la dérégulation de PAK1 ou des protéines du cytosquelette d'actine. Des modifications des voies de signalisation des ROS ou mTOR ont été également identifiées dans les granulocytes. En outre, nous avons montré que la protéine CALR pourrait avoir un double rôle oncogénique grâce à son expression élevée dans les SMP *JAK2V617F,* différent de l'altération de sa fonction décrites dans les patients CALR mutés. En conclusion, nous avons montré que les dérégulations protéomiques pourraient jouer un rôle oncogénique important dans la physiopathologie des SMP Ph- et qu'elles pourraient être impliquées dans certaines complications de ces pathologies telles que les accidents thrombotiques.